Sound transmission through pipe systems and into building structures : a study into the suitability of a simplified SEA model and determination methods for parameters

Please check the document version of this publication:

• A submitted manuscript is the version of the article upon submission and before peer-review. There can be important differences between the submitted version and the official published version of record. People interested in the research are advised to contact the author for the final version of the publication, or visit the DOI to the publisher's website.
• The final author version and the galley proof are versions of the publication after peer review.
• The final published version features the final layout of the paper including the volume, issue and page numbers.

Link to publication

Sound Transmission through Pipe Systems and into Building Structures

**- A study into the suitability of a simplified SEA model
and determination methods for parameters -**

PROEFSCHRIFT

ter verkrijging van de graad van doctor aan de
Technische Universiteit Eindhoven, op gezag van de
Rector Magnificus, prof.dr.ir. C.J. van Duijn, voor een
commissie aangewezen door het College voor
Promoties in het openbaar te verdedigen
op dinsdag 26 juni 2007 om 16.00 uur

door

Geertruida Susanne Bron-van der Jagt

geboren te Wageningen

Dit proefschrift is goedgekeurd door de promotor:

prof.ir. E. Gerretsen

Copromotor:
dr.ir. H.J. Martin

Sound Transmission through Pipe Systems and into Building Structures

**- A study into the suitability of a simplified SEA model
and determination methods for parameters -**

Geertruida Susanne Bron-van der Jagt

Members of the Doctorate Committee

prof.ir. E. Gerretsen, Technische Universiteit Eindhoven (supervisor, core committee)

dr.ir. H.J. Martin, Technische Universiteit Eindhoven (co-supervisor, core committee)

prof.dr. B.M. Gibbs, University of Liverpool (core committee)

prof.dr.ir. G. Vermeir, Katholieke Universiteit Leuven (core committee)

prof.dr.ir. M.H. de Wit, Technische Universiteit Eindhoven (core committee)

prof.dr.ir. J.L.M. Hensen, Technische Universiteit Eindhoven (extended committee)

SUMMARY

Sound Transmission through Pipe Systems and into Building Structures
- A study into the suitability of a simplified SEA model and determination methods for parameters -

In residential and other buildings many people are annoyed by noise due to service equipment. In order to avoid noise annoyance, limits to the maximum allowable sound level in rooms are set in building regulations. However, model based prediction of sound levels is not possible, because no calculation method is available. In this study it has been investigated whether Statistical Energy Analysis (SEA) could be applied in a simplified way as a framework for a prediction model. The study has been focussed on the sound transmission within plastic wastewater pipe systems and between these pipe systems and single, homogeneous plate structures in buildings. The octave bands with centre frequencies 125 Hz to 2000 Hz have been considered, because pipe noise generally concerns this frequency range, i.e. A-weighted sound levels due to pipe noise are generally determined by the sound pressure levels within the octave bands mentioned.

In this study a simplified SEA model has been developed (see chapter 3). Only radial pipe vibrations and out-of-plane plate vibrations as response components are included. This is based on the hypothesis that these types of vibrations are dominant in the sound transmission within pipe systems and between pipe systems and plates, and therefore in the sound radiation to rooms. This hypothesis results from several assumptions regarding (1) the modal properties of pipe system elements and plates, (2) the properties of sources in pipe systems and (3) the energy transmission within pipe systems and between pipe systems and plates. The validity of the assumptions has been tested, based on theoretical, numerical and experimental studies on characteristic pipe system elements and plates, and on a practical source (toilet flushing). The results show that the assumptions are fulfilled in a large part of the frequency range considered, generally from 250 Hz on, often from 125 Hz on (see chapters 4 and 5). The only exception of an assumption which may not be fulfilled in a large part of the frequency range considered is the assumption about excitation of pipe systems (see chapter 6): the results obtained in this study are varying.

To test the validity of the assumptions, various model parameters have been determined with different methods. For the system type studied, the application and accuracy of the methods, in particular some experimental determination techniques for parameters, have been investigated, e.g. by comparing the results obtained with different methods. The

results obtained with the various methods are sufficiently accurate within the scope of this thesis. Generally speaking, for the systems that are subject of this thesis the applied determination methods are usable to obtain parameter data to build a database for example, but they should be developed in more detail (see chapters 4-6).

It is assumed that including only radial pipe vibrations and out-of-plane plate vibrations will result in a model that is sufficiently accurate for engineering applications in building practice. In order to test the validity of this assumption, criteria for the prediction accuracy of the simplified SEA model have been set. The prediction accuracy has been estimated for a characteristic application of the model, i.e. transmission of sound due to toilet flushing from a pipe system to a plate through a pipe clamp. The results show that the criteria are fulfilled (see chapter 7). In the future more (detailed) studies for more cases should be done to come to a final conclusion. Nevertheless, at this moment, the simplified SEA model, specifically the fact that only radial pipe vibrations and out-of-plane plate vibrations are included in the model, seems to be promising as the basis for a design or an engineering tool in building practice, i.e. for predictions.

SAMENVATTING

Geluidoverdracht door leidingsystemen en naar bouwconstructies
- Studie naar de geldigheid van een vereenvoudigd SEA model en bepalingsmethoden voor parameters -

Veel mensen ervaren geluidoverlast door installaties, in woongebouwen, maar ook in gebouwen met een andere gebruiksfunctie. Om geluidoverlast te beperken zijn in de regelgeving voor de bouw eisen gesteld aan maximaal toelaatbare geluidniveaus in ruimten ten gevolge van installaties. Voorspelling van geluidniveaus, bijvoorbeeld op basis van tekeningen in het ontwerpstadium van een gebouw, is echter niet mogelijk omdat geen rekenmethode beschikbaar is. In de onderhavige studie is onderzocht of Statistische Energie Analyse (SEA) op vereenvoudigde wijze toegepast zou kunnen worden als de basis voor een voorspellingsmodel. Hierbij is gefocust op de geluidoverdracht in kunststof afvoerleidingsystemen en van dergelijke systemen naar enkele, homogene vloeren/wanden. De octaafbanden met middenfrequenties 125 Hz tot en met 2000 Hz zijn beschouwd, omdat de geluidniveaus door leidinggeluid doorgaans bepaald worden door de geluiddrukniveaus in de genoemde octaafbanden.

In deze studie is een vereenvoudigd SEA model ontwikkeld (zie hoofdstuk 3). In dit model zijn alleen radiale trillingen in leidingen en trillingen loodrecht op het oppervlak van vloeren/wanden meegenomen. Dit is gedaan op basis van de hypothese dat deze trillingen dominant zijn in de geluidoverdracht tussen verschillende leidingsysteemonderdelen en van leidingsystemen naar vloeren/wanden, en daarmee in de geluidafstraling naar ruimten. Deze hypothese vloeit voort uit verscheidene aannames betreffende (1) de modale eigenschappen (trillingseigenschappen) van leidingsysteemonderdelen en vloeren/wanden, (2) de eigenschappen van bronnen in leidingsystemen en (3) de energieoverdracht tussen leidingen binnen een leidingsysteem en van leidingsystemen naar vloeren/wanden. De geldigheid van deze aannames is getoetst, op basis van theoretische, numerieke en experimentele studies aan in de (bouw)praktijk gebruikelijke leidingsysteemonderdelen en vloeren/wanden, en aan een karakteristieke bron (het doortrekken van een toilet). De resultaten tonen aan dat de aannames correct zijn in een groot deel van het beschouwde frequentiegebied, doorgaans vanaf 250 Hz, vaak al vanaf 125 Hz (zie de hoofdstukken 4 en 5). De enige uitzondering van een aanname die mogelijk niet correct is in een belangrijk deel van het frequentiegebied, is de aanname betreffende de aanstoting van leidingsystemen

door karakteristieke bronnen: de studieresultaten verschillen voor gelijksoortige bronnen en zijn daarom niet eenduidig (zie hoofdstuk 6).

Om de aannames te testen zijn verscheidende modelparameters bepaald, met verschillende bepalingsmethoden voor iedere parameter. De toepassingsmogelijkheden en nauwkeurigheid van deze methoden, in het bijzonder van de experimentele methoden, is onderzocht, door resultaten die verkregen zijn met de verschillende methoden met elkaar te vergelijken. De resultaten tonen aan dat de gebruikte methoden voldoende nauwkeurig zijn voor het toetsen van de aannames van het vereenvoudigde SEA model. Daarnaast blijken de methoden geschikt te zijn om voor de verschillende modelparameters in de toekomst data te verzamelen, bijvoorbeeld om een database te bouwen. Hiertoe dienen de methoden echter nog wel doorontwikkeld te worden (zie de hoofdstukken 4-6).

Verondersteld is dat het vereenvoudigde SEA model voldoende nauwkeurig is voor toepassing tijdens het ontwerpen/aanpassen van gebouwen. Vooraf zijn in deze studie criteria voor de voorspellingsnauwkeurigheid van het model opgesteld. De nauwkeurigheid is getoetst door voorspellingen met het model te doen, voor een beoogde toepassing van het model, namelijk door energieniveaus van een wand te voorspellen, die via een leidingbeugel wordt aangestoten door een leidingsysteem dat in trilling wordt gebracht door een erop aangesloten toilet door te trekken. De voorspelde energieniveaus van de wand zijn vergeleken met gemeten energieniveaus. Aan de gestelde nauwkeurigheidscriteria wordt voldaan (zie hoofdstuk 7). Om tot een definitieve eindconclusie betreffende de toepasbaarheid van het model in de (bouw)praktijk te kunnen komen, dienen in de toekomst voor meerdere toepassingen (detail)studies te worden gedaan. Op basis van de resultaten in deze studie wordt geconcludeerd dat het vereenvoudigde SEA model, specifiek het feit dat in het model alleen radiale trillingen in leidingen en trillingen loodrecht op het oppervlak van vloeren/wanden worden meegenomen, geschikt is om toe te passen als ontwerpondersteunend hulpmiddel in de (bouw)praktijk.

LIST OF SYMBOLS

Roman:

a	mean radius of the pipe wall or shell cross-section, i.e. internal radius plus half the pipe wall thickness [m], acceleration (r.m.s.) [m/s^2]
a_i	internal shell radius [m]
A	cross-sectional area [m^2]; equivalent absorption area [m^2]
B	bending stiffness per unit width for a flat plate [Nm]
c	propagation velocity of sound [m/s]
$det(x)$	determinant of x
E	vibrational energy [J]; Young's modulus of elasticity [N/m^2]
$E_i/\Delta N_i$	modal energy of subsystem i [J]
E_{ij}	vibrational energy of subsystem i when only subsystem j is excited [J]
E^n_{ij}	normalised vibrational energy of subsystem i when only subsystem j is excited [-]
f	frequency [Hz]
f_{centre}	centre frequency of a frequency band [Hz]
f_c	critical frequency [Hz]
$(f_{co})_{pq}$	cut-on frequency of the higher-order acoustic mode (p,q) [Hz]
f_n	resonance frequency [Hz]
f_{ring}	ring frequency [Hz]
F, F_{in}, F_{input}	point force (r.m.s.) [N]
Fl	external normal fluid loading on the pipe wall [-]
G	shear modulus of elasticity [N/m^2]
h	thickness [m]
I	moment of inertia per unit width for a flat plate [m^4]
$Im(x)$	imaginary part of x
k	wave number [1/m]

K	stiffness [N/m]
l, L	length [m]
L_E	energy level [dB re 10^{-12} J]
L_{rc}	term with row number r and column number c in matrix representing equations of motion
L'	total length of all edges of an acoustic volume [m]
L_p	sound pressure level [dB re $2 \cdot 10^{-5}$ Pa]
$L_{p;A}$	A-weighted sound pressure level [dB(A) re $2 \cdot 10^{-5}$ Pa]
$L_{p,rad}$	sound pressure level in a reverberant room due to acoustic radiation from a structure [dB re $2 \cdot 10^{-5}$ Pa]
$L_{\Pi,rad}$	sound power level due to acoustic radiation from a structure [dB re 10^{-12} W]
L_v	velocity level [dB re 10^{-9} m/s]
m''	(modal) surface mass [kg/m^2]
Ma	Mach-number [-]
M	modal overlap [-]; (modal) mass [kg]
n	modal density [1/Hz]
N	mode count or number of modes up to a given frequency [-]
N_{lower}	mode count up to the lower frequency limit of a frequency band [-]
N_{upper}	mode count up to the upper frequency limit of a frequency band [-]
p	sound pressure (r.m.s.) [Pa]
P	perimeter [m]
r, R	radius [m]
$Re(x)$	real part of x
$s_{(x)}$	standard deviation of x
$s^2_{(x)}$	variance of x
Sh	Shear-number [-]
S	surface area [m^2]
S'	total area of all surfaces of an acoustic volume [m^2]
$T_{1/2}$	decay time corresponding to a response amplitude decay of ½ [s]
T_{10}	decay time corresponding to a response drop of 10 dB [s]

T	reverberation time of an acoustic volume [s]
T_x	decay time corresponding to a response drop of x dB [s]
U	fluid flow velocity [m/s]
U_{nm}	amplitude of axial shell displacement for the structural mode *(n,m)*
v	velocity (r.m.s.) [m/s]
V_{nm}	amplitude of tangential shell displacement for the structural mode *(n,m)*
V', V	volume [m³]
w	width [m]
W_{nm}	amplitude of radial shell displacement for the structural mode *(n,m)*
Y_c	point admittance (point mobility) of a coupling [m/Ns]
Y, Y_{input}	(driving-)point or input admittance (input mobility) [m/Ns]
z	distance between a point on a pipe and a pipe system discontinuity [m]

Greek:

β_{ij}	modal coupling factor describing the energy flow from subsystem i to subsystem j [-]
β^2	non-dimensional shell thickness parameter [-]
Γ_{BC}	constant between zero and one, representing the boundary conditions of a 2D-subsystem [-]
$\overline{\delta f}$	average frequency spacing between modes [Hz]
δ_{BC}	constant between zero and one, representing the boundary conditions of a 1D-subsystem [-]
Δf	frequency band [Hz]
$\Delta L_{rec.}$	deviation from the 'reciprocity relationship' between two subsystems [dB]
ΔL_v	velocity level difference [dB]
ΔN	number of modes within a frequency band [-]
η_{ii}	damping loss factor of subsystem i [-] (in the literature often written as η_i)
$\eta_{ii,b}$	coupling damping loss factor of subsystem i [-]
$\eta_{ii,rad}, \eta_{i,rad}, \eta_{io}$	acoustic radiation loss factor of subsystem i [-]; coupling loss factor describing energy flow due to acoustic radiation from subsystem i to acoustic volume o [-]

$\eta_{ii,s}$	material or structural loss factor of subsystem i [-]
η_{ij}	coupling loss factor describing the energy flow from subsystem i to subsystem j [-]
$\eta_{i,tot}$	total loss factor of subsystem i [-]
η_{oi}	coupling loss factor describing energy flow due to acoustic coupling from acoustic volume o to subsystem i [-]
η_{oo}	damping loss factor of acoustic volume o [-]
κ	non-dimensional wave number [-]
λ	wavelength [m]
ν	Poisson's ratio [-] (in this thesis values of 0,2 and 0,3 have been applied for calcium-silicate/brick/concrete and PVC/PE respectively); kinematic viscosity [m^2/s]
$\Pi_{i,diss}$	dissipated power in subsystem i [W]
$\Pi_{i,in}$	input power from an external source to subsystem i [W]
Π_{ij}	net transmitted power between the subsystems i and j [W]
$\Pi_{i \rightarrow j}$	power transmitted from subsystem i to subsystem j [W]
$\Pi_{i,rad}$	power radiated from subsystem i to acoustic volume o [W]
Ω	non-dimensional frequency [-]
Ω_{cut-on}	non-dimensional cut-on frequency of a higher-order flexural mode in the pipe wall [-]
ρ	density [kg/m^3]
σ	radiation efficiency [-]

Other symbols:

^	amplitude of a quantity
¯ or <>	mean value of a quantity
| |	modulus of a complex number
[ ]	matrix
1D	referring to one-dimensional
2D	referring to two-dimensional

a	referring to acoustic waves
ax(ial)	referring to the axial vibrational direction
b	referring to (first-order) flexural waves
f	referring to fluid
higher-order	referring to higher-order waves
i, j	referring to subsystem or structure number
k	excitation or response position
l	referring to (quasi-)longitudinal waves; excitation or response position; row or column number in total loss factor matrix
m	referring to axial mode number in a structure; row or column number in total loss factor matrix
n	referring to circumferential mode number in a structure; total number of rows or columns in total loss factor matrix
nm	referring to structural mode
N	total number of excitation or response positions
o	referring to acoustic volume
p	referring to number of plane diametral nodal surfaces of higher-order acoustic waves in a fluid
p,q	referring to higher-order acoustic mode
q	referring to number of cylindrical nodal surfaces concentric with the cylinder axis of higher-order acoustic waves in a fluid
rad(ial)	referring to the radial vibrational direction
s	referring to material
t	referring to torsional or in-plane shear waves
tan(gential)	referring to the tangential vibrational direction

x

CONTENTS

CHAPTER 1
GENERAL INTRODUCTION

1.1 Noise due to service equipment in buildings

Most buildings accommodate service equipment. Various types can be distinguished, like elevators, ventilation, heating and air conditioning installations, sanitary and drinking water installations. Usually service equipment produces sound, which can be experienced by people as noise, i.e. unwanted sound.

In order to avoid noise annoyance by service equipment limits to the maximum allowable sound level in rooms are set in building regulations. Besides, practical guidelines are developed, which give design solutions that meet the limits.

In spite of this, in residential and other buildings many people are annoyed by noise due to service equipment. In the Netherlands inquiries have shown that sanitary noise is in the top-five of the most annoying noise topics in residential buildings [ref 3].

In case of noise annoyance by service equipment often the maximum allowable sound level in a room is exceeded. For old buildings, this can be due to ageing of the equipment or due to the fact that no regulations were available during its construction. Another reason can be that the building has not been built in accordance with the regulations. Finally, for new building and service equipment types practical guidelines are not always available.

In order to investigate whether it is possible to meet limits for noise from service equipment in a certain situation, a model with which predictions of the sound level in a room due to service equipment can be made would be very useful. The predictions could be based on the design of both structures and service equipment. Based on such predictions, decisions about changes in structures and/or service equipment could be made during the design stage of a building.

Another application of such a model could be the prediction of sound levels due to changes in existing situations. This may occur, for example, in situations where people complain about service equipment noise or in situations that need to be changed for other reasons, e.g. replacement of service equipment in case of renovation.

However, currently no prediction model is available for these purposes. Besides, no calculation method is readily available to implement in such a prediction model. For the

development of such a prediction model a description of the sound transmission from service equipment to structures and rooms of buildings is needed.

Basically most types of service equipment can be divided into two types of sound sources, namely the machinery or appliances and the pipe system. Some examples of the first type are pumps, ventilators, washing machines, toilets and taps. Machinery or appliances radiate sound directly and indirectly. Indirect sound radiation occurs due to vibration transmission into plates and into pipe systems, which on their turn will partly radiate and partly transmit sound. Pipe systems contain or transport gas and/or liquid. Besides sound in pipe systems caused by machinery or appliances, the transportation of gas or liquid can produce sound too, especially at high transport velocities. Figure 1-1 shows an example of service equipment with both types of sound sources and some sound transmission paths.
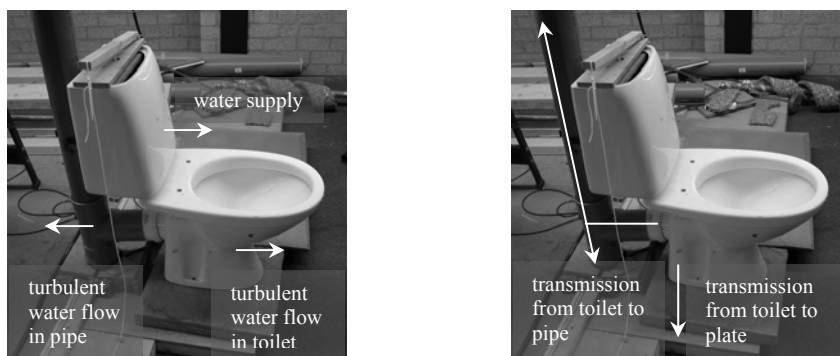
Figure 1-1   Example of service equipment with a subdivision in sound sources (**left side**) and transmission paths (**right side**)

Pipe systems are mostly kept out of sight. However, the sound transmission from pipe systems into plates can be so important that noise annoyance is caused in a room near the installation room or even relatively far away from this room.

Concerning the modelling of the sound production of various types of machinery and appliances a lot of research has been done and is still done. For example, the source characterization of whirlpools, valves and other types of service equipment has been and is still investigated at the University of Liverpool, Great Britain, and at the Fachhochschule in Stuttgart, Germany [90, 91]. In a previous study the source characterization of toilets and washing machines has been investigated at Technische Universiteit Eindhoven, the Netherlands [87, 88]. Also, the European standard EN 12354 Part 5 [92] is under

development. This standard is a first attempt to define prediction models for sound transmission from service equipment to building structures and the related source characterizations for various types of service equipment in buildings.

Concerning the modelling of the sound production of pipe systems, except for ventilation ducts, limited knowledge is available. The development of a calculation method that describes the sound transmission within pipe systems and between pipe systems and plates is important for any prediction model. Therefore and because the development of such a calculation method requires detailed study, this is the main topic of this thesis.

Although there is no calculation method available that describes the sound transmission from pipe systems to plates and rooms, there is a lot of knowledge that could be applied for such a method, for example regarding the vibro-acoustic behaviour of pipe systems and plates. Some parts of this knowledge are implemented in calculation methods. However, the applications differ from the aimed applications in this thesis. For example, calculation methods concerning the vibro-acoustic behaviour of pipe systems have been developed, while focussing on the low frequency range and not on the entire audible frequency range. Furthermore, the models focus on applications in the (automotive, aero-space) industry, ships etc. and are not aimed at buildings and service equipment. Also, the models are meant to be used by researchers and specialists and not as design tools by consultants and other people participating in building processes. Therefore, in this study a calculation method that can be integrated in an easy to handle design tool for building acoustics has been developed.

1.2 Modelling methods

This study has been started with surveying literature on existing theories related to the thesis subject and on modelling and experimental methods more generally. Most theories and experimental methods have been developed for other fields of application than noise due to service equipment, as described in the previous section. This section discusses the choice of a modelling method or a combination of modelling methods as a framework for a prediction model. Therefore, in this section the advantages and disadvantages of the relevant modelling methods are analysed and evaluated.

1.2.1 Deterministic, statistical and hybrid modelling methods

Several modelling techniques that can be useful for sound transmission problems are described in the literature. Roughly, the techniques can be divided into three groups, i.e.

purely deterministic, purely statistical and hybrid modelling methods. This section only contains a brief description of deterministic and statistical modelling methods. The suitability of deterministic and statistical modelling methods depends on the system to be modelled, including dimensions and materials, wave types and frequency range.

Deterministic methods, like the Finite Element Method (FEM) and the Boundary Element Method (BEM), can be applied to predict responses at discrete locations, at discrete frequencies or at discrete moments in time.

A deterministic method is useful in case the natural frequencies[1] of the physical system elements to be modelled are well separated and the responses of corresponding modes in the physical system elements have no (small) spectral overlaps. Besides a deterministic method is only useful in case there is no uncertainty in the system parameters or in case there are statistical data about the (causes of) variation in parameters. Due to these requirements deterministic methods are generally only useful in the low frequency range.

Statistical methods are generally applied to estimate space-averaged responses for entire physical system elements and corresponding variances or standard deviations, based upon known variations in dimensions, materials and other characteristics of ensembles of physical system elements. Often the acoustic and structural vibration responses are values for octave bands or 1/3-octave bands.

A statistical modelling method is useful at higher frequencies, where the number of modes in each frequency band is high and the responses of modes overlap (several modes contribute to the response at each frequency). Generally there is excitation of several natural frequencies in all frequency bands of interest for all physical system elements. These features contribute to smooth response spectra and less spatial variation in responses. Nevertheless, in principle it is possible to apply a statistical model to systems excited by pure tones and to predict responses at discrete frequencies.

Figure 1-2 shows the main difference between deterministic and statistical methods, as derived from figure 1-8 of De Langhe in [ref 7]. In deterministic models averaging (if

---

[1] Natural frequencies or eigenfrequencies are constant frequencies at which a finite system vibrates freely. Natural frequencies are properties of the finite system and are related to its mass and stiffness (inertia and elasticity). At these frequencies standing wave patterns exist, which are called (natural) modes, modes of vibration, eigenmodes or mode shapes. A resonant mode is a (natural) mode with a forced vibration response and is encountered when the natural frequency corresponding to the mode coincides with one of the (external) excitation frequencies.

4

necessary) takes place after the calculation of responses. Statistical models estimate responses based on space- and frequency-averaged parameters.
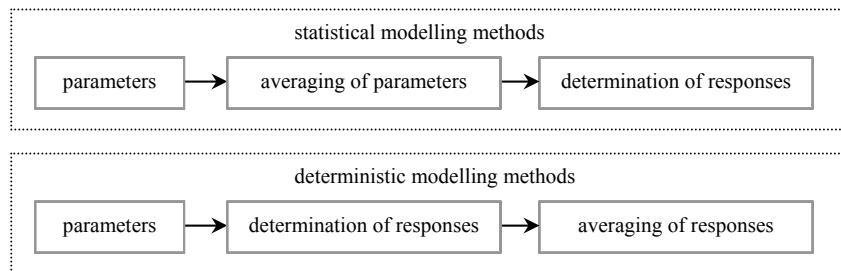
Figure 1-2   Schematic representation of deterministic and statistical modelling methods

The possibility to predict responses at discrete frequencies is an advantage of deterministic modelling methods. For example, to decide about changes of a physical system element, e.g. dimensions or damping, in order to reduce its response it is interesting to know which mode determines the response. Mean response values for frequency bands and for spatial domains give less useful information for this purpose, because then modes are not analysed separately.

However, at higher frequencies the wavelength of all wave types decreases, so, in order to predict the vibration pattern accurately, the size of all model elements has to decrease too. This can result in a huge number of elements in for example a FEM mesh and therefore in huge databases and computational times. Therefore, quick reviews and comparisons of design alternatives can become impossible.

Besides, it is difficult to predict the response for each mode at higher frequencies accurately: small differences between model and the real situation can give responses that are dominated by other modes in the predictions than in reality and can result in huge response differences between model and reality. Besides, in building practice variations occur. More detailed knowledge of all model parameters and often a larger number of parameters are required for deterministic modelling, which results in a more complex description of the system compared to statistical modelling. Besides, calculations need to be repeated with parameter variations to gain insight in the influence of variations on responses. Statistical modelling methods usually estimate averaged response values for frequency bands. These response values are not as sensitive for small differences between model and reality, e.g. variations in nominally equal physical elements.

1.2.1.2 Applicability of deterministic and statistical modelling methods in this study

For many systems the use of both deterministic and statistical methods is necessary to cover the entire frequency range of interest. Regarding the sound transmission through all kinds of pipe systems and from pipe systems into plates, this might be the case.

As an example, Figure 1-3 shows measured A-weighted sound pressure levels [2] generated by sound radiation from a PVC wastewater pipe into an installation room (source room) during toilet flushing. Besides, this figure shows estimated A-weighted sound pressure levels in a receiving room, as calculated from the measured values in the source room and sound insulation values of a 100 mm thick calcium-silicate wall. Only sound transmission due to sound radiation from the pipe to the wall is included. Sound transmission due to structural coupling between pipe and wall, e.g. through pipe clamps, is not included. Structural couplings might result in higher A-weighted sound pressure levels in the receiving room, particularly at low frequencies. The contribution of the low frequencies to the overall A-weighted sound level will strongly depend on the dimensions and materials of pipe, wall and structural couplings. Larger falling heights of the water and walls with less sound insulation will also result in higher A-weighted sound levels in the receiving room.
Figure 1-3 illustrates that noise from wastewater pipes covers a wide frequency range, typically the 1/3-octave bands with centre frequencies 100 Hz to 2500 Hz. The overall A-weighted sound level, which is an indicator for noise annoyance, is determined by the sound pressure levels in this frequency range.

---

[2] Although not common, for each 1/3-octave band the A-weighted sound pressure level instead of the sound pressure level is plotted, in order to illustrate the contribution of each 1/3-octave band to the overall A-weighted sound level.
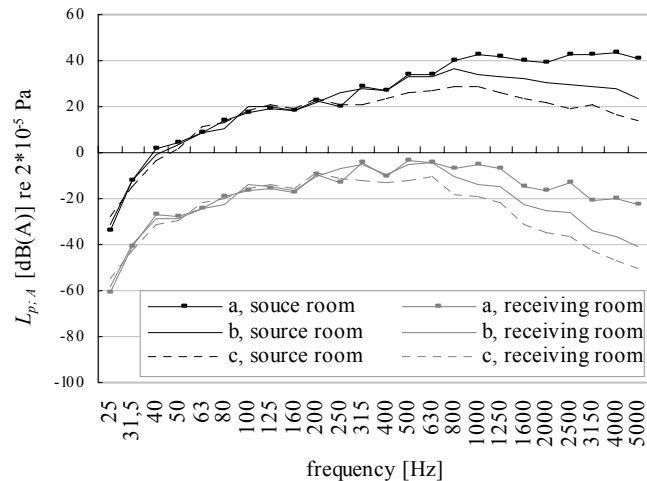
Figure 1-3 <u>Measured</u> A-weighted sound pressure level $L_{p;A}$ in 1/3-octave bands in a room caused by a wastewater pipe in the room considered (<u>source room</u>) during toilet flushing and <u>estimated</u> A-weighted sound pressure level in 1/3-octave bands in a <u>receiving room</u> that is separated from the source room by a 100 mm thick calcium-silicate wall. Three wastewater pipes are considered: (**a**) PVC pipe, wall thickness 3,8 mm, outer shell radius 55 mm, (**b**) pipe (a) with 30 mm thick mineral wool around, (**c**) pipe (a) with 10 mm thick soft foam and a lead layer of about 0,5 mm thickness around.

The reasons why a statistical modelling method is preferable to a deterministic method as a framework for a prediction model concerning pipe noise in buildings are:

- statistical modelling allows for less detailed, and therefore less complex, descriptions of systems;
- quick evaluations of design alternatives are possible;
- results from a statistical model are less sensitive to small variations in pipe systems and plates and to small differences between model and reality; variations are reflected in the model results by presenting mean values, and variances or related variables (e.g. standard deviation or confidence interval);
- pipe noise usually concerns both broadband sound sources and broadband responses;
- the number of natural frequencies and modal overlap per (1/3-)octave band are large in an important part of the frequency range of interest, i.e. the octave bands with centre frequencies 125 Hz to 2000 Hz (see chapter 4).

Hybrid modelling could be an option too, with a statistical modelling method as the framework for the prediction model. Physical system elements that are difficult to model and/or without modes or a limited number of modes (responses corresponding to large

wavelengths compared to the elements dimensions) can be modelled with a deterministic method, e.g. FEM, and implemented in the statistical framework. One example of such a physical system element is a coupling (pipe clamp) between a pipe and a plate. In recent work Langley describes a hybrid analysis method that combines Statistical Energy Analysis (SEA, see section 1.2.2) with Finite Element Analysis and shows good results for an example to which the method has been applied [ref 82].

1.2.2   Statistical Energy Analysis (SEA)

Statistical Energy Analysis (SEA) is a structural-acoustic modelling method that is applied widely, particularly in engineering activities. The development of SEA started about forty years ago with applications in the aerospace industry [ref 6]. Over the past thirty years SEA has been applied, extended and developed for a growing number of applications, e.g. to model sound produced by installations, in cars, in ships and in buildings. Several determination techniques for SEA parameters have been developed.

SEA is more a framework of study, rather than a particular technique. This is emphasised by the word 'analysis' [ref 4].
The word 'statistical' illustrates the assumption that the systems being studied are part of ensembles of similar systems with known distributions of the system parameters.
SEA describes the dynamical behaviour of systems in terms of stored, dissipated and exchanged energies of vibration. 'Energy' in SEA denotes the primary response variable. This variable can be expressed in terms of more common variables for acoustic and structural systems, e.g. pressure or velocity.

In order to model the exchange of vibrational energy within a system properly, it is divided into subsystems. Subsystems represent groups of similar modes associated with physical system elements [ref 4]. Within a subsystem the modes have similar vibro-acoustic characteristics. Usually the vibrational responses of the subsystems are expressed by values averaged over spatial domains and frequency bands and are representative for ensembles of similar physical system elements. Results for octave bands or 1/3-octave bands are most common. Often the variance in response is also of interest. The variance in response is derived from the average values and variances in the model parameters.
Energy distribution over the subsystems is described by power balance equations: incoming power on the one hand and the sum of dissipated and outgoing power on the other hand are equal.

Chapter 2 focuses on a discussion of SEA in general, including the assumptions upon which the SEA method is based. Systems to be modelled with SEA need to fulfil these assumptions.

1.2.2.1 Application of SEA as a framework for a prediction model in this study

This section discusses the most important advantages and disadvantages of the SEA modelling method regarding the subject of this thesis.

Advantages

A model that describes sound transmission within pipe systems and from pipe systems to plates and to rooms contains both acoustic and structural subsystems.

SEA uses only one response variable, i.e. energy, to describe both acoustic and structural systems. Energy losses inside a subsystem and by energy flow from that subsystem to other subsystems are described by parameters related to energy, i.e. damping loss factors and coupling loss factors respectively. Energy distribution over the subsystems is described by power balance equations, while using only a couple of generic parameters.

This makes SEA models transparent and the power balance equations relatively simple and small, even for large systems. Because of the model transparency quick evaluations of design alternatives, e.g. changes in sound transmission paths, are possible. In this way, SEA becomes suitable as a framework for design tools.

Space-, frequency band- and ensemble-averaged responses are generated. Therefore, SEA model results are less sensitive to small variations in subsystems and to small differences between model and reality. More than that, these variations and differences are represented by presenting average values and variances of model parameters and variables (only when enough statistical data are available).

Because of the advantages mentioned SEA seems to be a promising modelling method for noise due to service equipment in buildings and has been applied in this study.

Disadvantages

The accuracy of SEA models depends strongly on the definition of the subsystems. Yet, no well-defined definition methods for all sorts of systems are available.

It is not clear to what extent SEA is useful for modelling systems that do not meet all SEA assumptions, which will often be the case in practice.

Like any modelling technique, SEA predictions are only accurate if reliable parameter data are included in the model. In order to make SEA models suitable as frameworks for design tools, parameter data for numerous subsystems and coupling elements are needed. Such

data can be generated from measurements and from numerical computation, but sometimes also from relations to known parameters from other theoretical analysis models. Example of the latter category are the coupling loss factors for various types of junctions between building structures, which can be derived from textbook data on so-called transmission coefficients. A lot of work concerning parameter data gathering still has to be done. In case no data for SEA parameters for specific subsystems or couplings are available and derivation of these data from measurements or from known parameters (by analytical expressions) is not possible, derivation with other modelling techniques, e.g. FEM, is almost inevitable. For example, coupling loss factors of pipe clamps may be predicted with FEM because of the complex transmission characteristics of these elements, e.g. due to geometrical details, and because the coupling loss factors are partly determined by the vibrational properties of the connected subsystems. This illustrates that SEA parameter data are generally gathered with various methods.

Another possible disadvantage of SEA is that this method has been mainly applied to systems under stationary conditions. Some research concerning non-stationary SEA modelling has been done and it has been shown that SEA definitely can be applied to non-stationary problems, but the application is not common [ref 4]. This is an important aspect within the scope of this thesis, because noise due to service equipment often concerns non-stationary sources such as water flows.

1.3 Objectives of this study

The main objective of this study has been to investigate whether SEA can be applied in a simplified way to describe the sound transmission through pipe systems and from pipe systems into plates, and the sound radiation from these elements to rooms.

Based on various assumptions concerning the vibrational characteristics and excitation of pipe systems, plates and their couplings, a simplified SEA model has been developed. In this study, the validity of these assumptions has been investigated. Also, the prediction accuracy of the model has been estimated and compared with accuracy criteria that have been set in this study.

The application of SEA has been simplified by including only subsystems, which seemed to be most important in the sound transmission. Due to this reduction in subsystems, the system parameters can be determined in a simpler way than in case of inclusion of both important and less important subsystems. The main reason for the simplification is to facilitate the integration of the model in an easy to handle design or engineering tool for building acoustics. In case of satisfying validation results such a tool can be developed successively.

The validity of the proposed simplified SEA model has been tested, based on various analytical models, numerical computations and measurements in experimental set-ups. These set-ups were designed in such a way that they could also be used to determine some of the needed model parameters.

However, the accuracy of some of the (experimental) techniques which are needed for the parameter estimation was not sufficiently well established. Therefore, different techniques were used for the determination of some of the parameters. By evaluating the results a judgement was made on the suitability and the accuracy of a particular technique for parameter estimations needed for a database of the SEA tool in the future. Therefore, the evaluation of (experimental) techniques for determination of parameters is to be considered as a secondary objective of this study.

1.4   Focus on pipe systems, floors and walls in this study

A wide variety in pipe systems, mountings and plates in buildings exists, resulting in various types of sound excitation of and sound transmission in pipe systems and plates. This study focuses on specific types of pipe systems and plates, which is explained below.

Variety in pipe systems, mountings and plates

Drinking water pipes are completely filled with water, while wastewater pipes are partly filled with water and dirt and partly with air. Air ducts are completely filled with air. Characteristic inner diameters of drinking water pipes in buildings range from 10 mm to 60 mm and of wastewater pipes from 40 mm to 160 mm [ref 51]. In the Netherlands, common materials for drinking water pipes in buildings are brass and (crosslinked) PE, for wastewater pipes PVC, ABS, PE, cast iron and laminates of plastics and other, often damping, materials [ref 51]. Other pipes in buildings, e.g. fuel pipes, are usually made of brass, steel or plastic.

The pipe fluid sets the pipe wall into vibration due to its (turbulent) flow, but in drinking water pipes mechanisms like cavitation and water hammer[3] can also be important sound sources. Sometimes, only excitation of the pipe system by the pipe fluid is important. In other cases, excitation of the pipe system by machinery or appliances is important too or even dominant [ref 25], [ref 26].

---

[3] Cavitation causes noise by the implosion of bubbles due to 'boiling' of water caused by pressures, e.g. in a pump, below the vapor pressure. Water hammer causes a banging sound due to (reflecting) shock waves created by a sudden change in flow velocity of a liquid in a pipe, e.g. due to rapid closing or opening of a valve.

In pipes various wave types can propagate (see sections 3.2.2 and 4.2). The vibrations due to different wave types in pipe wall and pipe fluid are coupled[4]. At pipe wall discontinuities, such as bends and joints, wave reflection occurs. Due to reflection and strong coupling of wave types in pipe wall discontinuities, wave type conversion will occur.

Some pipe systems are mounted on plates at discrete points by using pipe hangers, clamps etc. Usually these types of pipe systems are installed above ceilings or in shafts. Other pipe systems are embedded in plates, sometimes with an elastic layer between pipe and plate, and are thus line-connected to plates.

Besides the wide variety in pipe systems and mountings there is a wide variety in plates too. From an acoustic point of view the distinction between massive, stone, relatively heavyweight plates (e.g. of concrete or brick) and lightweight plates (e.g. of wood or gypsum board) is important. Furthermore, also within these two groups different types of plates can be distinguished, e.g. with or without a cavity.
Also in plates various wave types can propagate (see sections 3.2.2 and 4.4).

Focus in this study

This thesis concentrates on plastic wastewater pipe systems for the development and validation of the proposed simplified SEA model. The first reason for this is that within the frequency range of interest (1/3-octave bands with centre frequencies 100 Hz to 2500 Hz) all theoretically possible wave types are really present in these pipe systems due to their dimensions and materials. The second reason is that these pipe systems usually cause more noise in buildings than other types of pipe systems, e.g. water supply pipe systems.
Besides, this thesis concentrates on single, homogeneous, heavyweight floors and walls. The first reason for this is that, in order to avoid noise, in building practice pipe systems are preferably coupled to heavyweight plates, e.g. concrete floors and brick walls. The second reason is that inclusion of the vibrational behaviour of lightweight plates, e.g. gypsumboard walls, would make the modelling much more complicated.
Nevertheless, if after this initial study the proposed simplified SEA model turns out to be promising, wider application could be considered. First of all, other pipe systems than plastic wastewater pipe systems can be investigated. Furthermore, it would be very interesting to include lightweight plates in the model too. In several countries, e.g. in Scandinavia, it is common to use this type of structures. Also for the Netherlands and other countries it is interesting to consider lightweight structures. For example, in the Netherlands

---

[4] For the case of a flexible pipe wall this is necessary in order to fulfil the compatibility condition [ref 25]. For the extreme case of a rigid pipe wall, there is no coupling between vibrations in pipe wall and pipe fluid [ref 26].

12

developments concerning flexible building concepts are going on. These concepts are aimed at the application of lightweight structures, in order to make changes of buildings by removing and replacing plates and service equipment, including pipe systems, relatively easy. In this way it is possible to meet changing needs of people in the future. Therefore, the potential scope of the proposed model may be much wider than the focus in this study might suggest.

1.5   Outline of this thesis

This thesis studies the application of SEA to model the sound transmission through pipe systems and from pipe systems into plates in a simplified way.

Chapter 2 analyses the SEA method in general and applications of SEA in building acoustics. Chapter 3 deals with the application of SEA as a modelling method for the system considered. Both an extensive and a simplified model are developed for the systems of interest in this study. Assumptions for the simplified model and validation criteria are given. Furthermore, criteria for the prediction accuracy of the simplified model are defined.

In the next three chapters the validity of the assumptions of the simplified SEA model is tested. For this purpose, several existing analytical, numerical and experimental methods have been applied. For the system type studied, the suitability and accuracy of the methods have been investigated. Chapter 4 deals with the modal properties of the system elements, chapter 5 with damping and coupling of the system elements and chapter 6 with the excitation of pipe systems in practical building situations. The determination techniques, experimental set-ups and (test) results are described.

Chapter 7 focuses on the prediction accuracy of the simplified SEA model. Based on the results from this study the prediction accuracy is estimated and compared with the accuracy criteria as set in chapter 3.

Chapter 8 concludes with the most important results of this study and perspectives for future work.

CHAPTER 2

STATISTICAL ENERGY ANALYSIS (SEA)

2.1 Introduction

In continuation of section 1.2.2, this chapter gives a more in-depth description of Statistical Energy Analysis (SEA).

To apply SEA properly as a modelling method for a sound transmission problem, the definition of the system to be modelled and the division of the system in so-called subsystems are crucial. This chapter starts with a description of some important aspects related to the definitions of systems and subsystems in general, see sections 2.2 and 2.3.

SEA models the sound transmission in systems by means of power balance equations. Energy is the primary response variable. Section 2.4 gives the basic SEA equations for systems consisting of two and n subsystems. Furthermore, this section describes how SEA can be applied in a predictive scheme.

Sections 2.5 and 2.6 describe some parameters and variables which are in the literature generally referred to as the SEA parameters and primary (response) variables respectively. Besides, section 2.5 gives some references to publications regarding the application of SEA in building acoustics.

Section 2.7 discusses the assumptions on which the SEA method is based.

In the literature many publications deal with the history and fundamentals of SEA, determination techniques for SEA parameters and SEA applications. Probably the most extensive publications are the ones by Lyon and DeJong [ref 4], Craik [ref 5], Fahy [ref 9] and De Langhe [ref 7]. At many places in this thesis is referred to these publications. The description in this chapter is directly related to the application of SEA in this thesis. As far as known to the author, SEA has not been applied in practice to describe the sound transmission through (wastewater) pipe systems and from pipe systems to plates in buildings. For more general information about SEA the reader is referred to one of the publications mentioned.

2.2   System definition

A sound transmission model for noise due to service equipment in buildings always represents the acoustics of a limited part of the complete building, which is designated as 'the system'. The model has to be as extensive as necessary for reliable predictions, but not larger than really necessary in order to limit the complexity and by that the chance of errors, large computational times, etc.

No matter how extensive the model is, at the (artificial) system boundaries always energy is lost, which is not specified separately in the model. In SEA models this energy loss is represented by so-called energy sinks [ref 4]. Another way of including this energy loss into a model is by assigning it to the energy losses of the physical system elements at the boundaries of the system. If this energy loss is not included in the model in some way the power balance equations will be violated.

2.3   Subsystems definition

In SEA each system is divided into physical elements of a suitable size, see the discussion at the end of this section. The modes of each element are combined in groups with similar vibro-acoustic characteristics, e.g. similar values of damping, excitation and coupling parameters. These groups of similar modes are called subsystems [ref 4].

Separate subsystems usually represent groups of modes corresponding to different wave types in a physical system element. For example, in a plate modes due to respectively flexural, in-plane quasi-longitudinal and in-plane shear waves are modelled as separate subsystems. Modes in a reverberant acoustic volume are another example of a subsystem.

The total energy flow between any two subsystems equals the sum of mode-to-mode energy flows evaluated as independent isolated pairs of modes [ref 7]. The responses of the modes within a subsystem are assumed to be incoherent [ref 4].

Only groups of modes that play an important role in the transmission, dissipation and storage of energy, need to be included as subsystems in a model.

One of the assumptions of SEA is that subsystems are weakly coupled (see section 2.7). From a wave point of view, a coupling between two subsystems is generally weak if there is a large impedance mismatch between the subsystems, i.e. substantially reflection of waves at the boundaries of the subsystems. Usually this occurs at connections of physical system elements. Therefore, often the boundaries of physical system elements correspond with the boundaries of subsystems.

However, when subsystems have a relatively high damping there is much decay in waves, which results in large differences in vibrational responses at different positions of a physical system element. Lyon and DeJong [ref 4] suggest to divide highly damped physical system elements in parts represented by different subsystems[5].

The opposite occurs if there is no large impedance mismatch at the boundaries of physical system elements. In that case modes have fairly uniform vibrational responses throughout more than one physical system element or even the whole system (this may differ for different types of modes). These modes are called global modes [ref 4] and often occur in the low frequency range. Global modes have to be represented in a model by separate subsystems.

2.4   Basic SEA equations

2.4.1   System consisting of two subsystems

The principle of SEA is illustrated for a system consisting of two connected subsystems as shown in Figure 2-1.
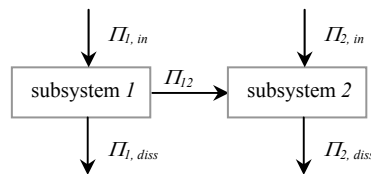
Figure 2-1   Two subsystem SEA model

Energy flows out of a subsystem due to dissipation (conversion of vibrational energy into heat), radiation and transmission to other subsystems. Energy flows into a subsystem due to an external source of excitation or transmission from other subsystems. $\Pi_{1,diss}$ and $\Pi_{2,diss}$ represent the powers dissipated in the subsystems *1* and *2*, $\Pi_{1,in}$ and $\Pi_{2,in}$ the input powers from external sources to the subsystems *1* and *2* and Π_{12} the net transmitted power between the subsystems *1* and *2*.

---

[5] Physical system elements can only be subdivided properly if the important subsystems and some subsystem characteristics are known such as energy group velocity (see section 3.2.2) and damping loss factor (see section 2.5.1). An important question is whether there is weak coupling between different subsystems within a part of a physical system element and between subsystems in different parts of the physical system element. Therefore, subdivision of physical system elements asks for careful deliberation and is surely not fully straightforward.

The dissipated power $\Pi_{1,diss}$ in subsystem *1* is given by

$$\Pi_{1,diss} = 2\pi f \eta_{11} E_1 \qquad (2.1)$$

where η_{11} (often written as η_1) is the damping loss factor and E_1 is the total vibrational energy of the modes at frequency[6] f in subsystem *1*. The damping loss factor is a measure of the rate at which energy is lost out of a subsystem due to energy dissipation.

The dissipated power $\Pi_{2,diss}$ in subsystem *2* is given by

$$\Pi_{2,diss} = 2\pi f \eta_{22} E_2 \qquad (2.2)$$

where η_{22} is the damping loss factor and E_2 is the total vibrational energy of the modes at frequency f in subsystem *2*.

The net transmitted power between the subsystems *1* and *2* Π_{12} is given by

$$\Pi_{12} = 2\pi f \eta_{12} E_1 - 2\pi f \eta_{21} E_2 \qquad (2.3)$$

where η_{12} and η_{21} are coupling loss factors. Each connection between subsystems is characterized by two coupling loss factors, representing a measure of the rate at which energy is transmitted from one subsystem to another subsystem and reverse.

The power balance equations for the two subsystems are

$$\Pi_{1,in} = \Pi_{1,diss} + \Pi_{12} = 2\pi f (\eta_{11} + \eta_{12}) E_1 - 2\pi f \eta_{21} E_2$$
$$\Pi_{2,in} = \Pi_{2,diss} + \Pi_{21} = -2\pi f \eta_{12} E_1 + 2\pi f (\eta_{22} + \eta_{21}) E_2 \qquad (2.4)$$

where $(\eta_{11}+\eta_{12})$ and $(\eta_{22}+\eta_{21})$ equal the total loss factors of the subsystems *1* $(\eta_{1,tot})$ and *2* $(\eta_{2,tot})$ respectively. The total loss factor of a subsystem is the summation of the damping loss factor of the subsystem and the coupling loss factors representing energy transmission from the subsystem to other subsystems.

The power balance equations in matrix notation:

$$\begin{Bmatrix} \Pi_{1,in} \\ \Pi_{2,in} \end{Bmatrix} = 2\pi f \begin{bmatrix} (\eta_{11} + \eta_{12}) & -\eta_{21} \\ -\eta_{12} & (\eta_{22} + \eta_{21}) \end{bmatrix} \begin{Bmatrix} E_1 \\ E_2 \end{Bmatrix} \qquad (2.5)$$

---

[6] In this thesis only frequencies f in hertz or Hz and no angular frequencies ω in rad/s are used.

The following 'reciprocity relationship' or consistency relationship between two connected subsystems *1* and *2* applies [ref 4]:

$$\Delta N_1 \eta_{12} = \Delta N_2 \eta_{21} \tag{2.6}$$

where ΔN_1 and ΔN_2 are the numbers of modes within a frequency band Δf in the subsystems *1* and *2*.

In this thesis the word 'reciprocity relationship' is placed between commas because the relationship can be derived from reciprocity. Strictly speaking, it is not a reciprocity relationship.

When the number of modes per unit frequency, i.e. the modal density, of a subsystem is asymptotically constant[7], $\Delta N = n \cdot \Delta f$, where ΔN the number of modes within a frequency band Δf and n the modal density. Then 'reciprocity relationship' *(2.6)* can be written as

$$n_1 \eta_{12} = n_2 \eta_{21} \tag{2.7}$$

where n_1 and n_2 are the modal densities of the subsystems *1* and *2*.

Substitution of 'reciprocity relationship' *(2.6)* or *(2.7)* in equation *(2.5)* results in a symmetric loss factor matrix. As a consequence, in addition to damping loss factors, coupling loss factor data for only one transmission direction are needed to characterize the energy exchange between the two subsystems. With substitution of equation *(2.7)*, equation *(2.5)* becomes

$$\begin{Bmatrix} \Pi_{1,in} \\ \Pi_{2,in} \end{Bmatrix} = 2\pi f \begin{bmatrix} (\eta_{11} + \eta_{12}) \cdot n_1 & -\eta_{21} \cdot n_2 \\ -\eta_{12} \cdot n_1 & (\eta_{22} + \eta_{21}) \cdot n_2 \end{bmatrix} \begin{Bmatrix} E_1/n_1 \\ E_2/n_2 \end{Bmatrix} \tag{2.8}$$

---

[7] The modal density *n* is given by $n = dN/df$. The modal density can also be defined as the asymptotic limit of the ratio of the number of natural frequencies per unit frequency [ref 7]. *n* will be asymptotically constant in case the modes within a frequency band are evenly distributed (see also the assumption about resonant modes in section 2.7).

2.4.2   System consisting of *n* subsystems

The power balance matrix given by equation *(2.5)* can be generalised to a power balance matrix for *n* subsystems as follows:

$$\begin{Bmatrix} \Pi_{1,in} \\ \Pi_{2,in} \\ \vdots \\ \Pi_{n,in} \end{Bmatrix} = 2\pi f \begin{bmatrix} (\eta_{11} + \sum_{j\neq 1}^{n}\eta_{1j}) & -\eta_{21} & \cdots & -\eta_{n1} \\ -\eta_{12} & (\eta_{22} + \sum_{j\neq 2}^{n}\eta_{2j}) & \ddots & \vdots \\ \vdots & \ddots & \ddots & \vdots \\ -\eta_{1n} & \cdots & \cdots & (\eta_{nn} + \sum_{j\neq n}^{n}\eta_{nj}) \end{bmatrix} \begin{Bmatrix} E_1 \\ E_2 \\ \vdots \\ E_n \end{Bmatrix} \quad (2.9)$$

The power balance equations can also be written as

$$\Pi_{i,in} = 2\pi f \eta_{ii} E_i + \sum_{\substack{j=1 \\ j\neq i}}^{n} 2\pi f (\eta_{ij} E_i - \eta_{ji} E_j) \quad (2.10)$$

or as

$$\{\Pi_{in}\} = 2\pi f \cdot [\eta^0] \cdot \{E\} \qquad \eta_{ij}^0 = -\eta_{ji} \quad and \quad \eta_{ii}^0 = \sum_{j=1}^{n} \eta_{ij} \quad (2.11)$$

2.4.3   Predictive SEA

When SEA is applied for predictions of vibrational responses, the energy distribution over subsystems is calculated from known values of input powers, loss factors and, in case 'reciprocity relationship' *(2.7)* is applied, modal densities:

$$\{E\} = \frac{1}{2\pi f} \cdot [\eta^0]^{-1} \cdot \{\Pi_{in}\} \quad (2.12)$$

In case of weak coupling the coupling loss factor, i.e. off-diagonal, terms in the loss factor matrix are much smaller than the damping loss factor, i.e. diagonal, terms. To be suitable for applying SEA, a system needs to have weak coupling of subsystems. This is an important SEA assumption, as will be discussed in section 2.7. Furthermore, the loss factor matrix contains positive diagonal terms. Therefore, the loss factor matrix can be characterized as positive-definite and diagonally dominant.

In case 'reciprocity relationship' *(2.7)* is applied (see equation *(2.8)*), the matrix becomes symmetric. In most systems, especially large systems, many subsystems are not coupled to each other, resulting in many zero off-diagonal loss factor matrix terms and therefore a sparse matrix. In prediction tools these matrix features can be utilised to speed up computational times and to reduce storage requirements, e.g. by application of Gaussian elimination, Cholesky factorisation or an iterative technique. However, in SEA modelling of many practical systems this is not as much a concern as is the case with FEM models for example. The size of the matrices is relatively small anyhow, given the modern desktop computer memory sizes and speeds.

2.5   SEA parameters

2.5.1   Damping loss factor

The damping loss factor of a subsystem *i* can be written as

$$\eta_{ii} = \eta_{ii,s} + \eta_{ii,rad} + \eta_{ii,b} \qquad (2.13)$$

$\eta_{ii,s}$ is the loss factor associated with structural or material damping in subsystem *i*, i.e. internal conversions of vibrations into heat. The damping is a function of the properties of the materials making up the structural element to which subsystem *i* corresponds.

$\eta_{ii,rad}$ is the loss factor associated with acoustic radiation losses from the surface of the structure of subsystem *i* into the surrounding fluid medium, i.e. conversions of vibrations into sound.
A fluid medium can be modelled as an enclosed reverberant acoustic volume, i.e. a separate subsystem, too. In that case the radiation loss factor term is not part of the damping loss factor, but is represented as a coupling loss factor. Then the sound level in a room caused by a vibrating structure could be predicted.

$\eta_{ii,b}$ is the loss factor associated with coupling damping for subsystem *i*, i.e. damping at the connection between subsystem *i* and other subsystems.
Coupling damping is a non-linear, non-conservative coupling mechanism. One of the assumptions of SEA is that the energy exchange between coupled subsystems is proportional to the difference in modal energy assuming conservative coupling (see section 2.7). In principle non-conservative coupling is not allowed [ref 9]. Fahy and Yao [ref 10] have shown that, in case of coupling damping, the energy exchange depends on both the difference in modal energy and the absolute energy values of the subsystems. However,

they have also shown that, in case of multi-modal subsystems and coupling damping loss factors that are very low compared to the loss factors associated with structural damping and acoustic radiation, the influence of coupling damping on the energy exchange between subsystems is negligible and the coupling damping only increases the damping loss factors of the individual subsystems[8] as described by equation *(2.13)*. Then, the classical power balance equations for conservatively coupled subsystems can be applied.

Generally, when structures are connected rigidly, $\eta_{ii,b} < \eta_{ii,s}$ [ref 6]. In that case the influence of coupling damping on the damping loss factor can be neglected and the damping loss factor is a function of the material damping and acoustic radiation loss factors.

2.5.2   Coupling loss factor

Coupling loss factors depend on the geometry of the connection between subsystems and the vibro-acoustic characteristics of the subsystems, which are determined by their dimensions and materials.

The coupling loss factor is a parameter that is uniquely associated with SEA. It is possible to relate the coupling loss factor to parameters that are known outside the SEA field like radiation efficiencies and transmission coefficients.

Couplings between structural and acoustic subsystems and between acoustic subsystems have been studied extensively in the field of building acoustics. The relations between radiation efficiencies and corresponding coupling loss factors and between transmission efficiencies and corresponding coupling loss factors are described in several handbooks, for example by Cremer and Heckl [ref 12], Lyon and DeJong [ref 4], Craik [ref 5] and Norton [ref 6].

Couplings between structural subsystems are more difficult to evaluate, because the coupling loss factors are dependent on geometrical details of the connection and different wave types can be generated in structures and at connections. Relations between transmission coefficients and corresponding coupling loss factors have been derived for some common structural connections such as beam-beam, beam-plate and plate-plate couplings. Lyon and DeJong [ref 4] and Craik [ref 5] have derived analytical relations between transmission coefficients and corresponding coupling loss factors for all these coupling types. Often the coupling loss factor formulas in the literature concern relatively

---

[8] Since damping loss factors are substantially higher than coupling loss factors (see the assumption about weak coupling between subsystems in section 2.7), this implies that the influence of coupling damping on damping loss factors is also negligible. Strictly speaking, the influence of coupling damping will depend on the ratio of the coupling damping values to the damping loss factor values.

simple couplings, e.g. cross-, T- or L-joints of homogeneous structures, or simplifications of practical couplings, i.e. pure point-, line- or area-couplings. During the last decade more complex couplings have been studied, while focussing on specific application fields, and formulas for coupling loss factors have been derived. For example, Bosmans [ref 38] has described the structure-borne sound transmission through connections between lightweight plates by application of the wave approach and the semi-modal superposition technique. De Langhe [ref 7] describes a general procedure based on the wave approach to derive coupling loss factor formulas for several complex connections. Often connections are so complicated that reliable analytical derivations of coupling loss factors are not possible. Numerical techniques like FEM may be used to determine coupling loss factors for such cases. De Lange [ref 7] has described this application of FEM, for example.

2.5.3 Modal density and related parameters

The modal density n_i of a subsystem i is defined as the number of natural frequencies or modes per unit frequency. There are three other parameters that represent the number of modes within a subsystem. N_i indicates the mode count, i.e. the number of modes below a given frequency. ΔN_i represents the number of modes within a frequency band Δf. $\overline{\delta f_i}$ indicates the average frequency spacing between modes. The relation between the modal parameters is given in equation *(2.14)*.

$$n_i = \frac{\Delta N_i}{\Delta f}$$

$$\overline{\delta f_i} = \frac{1}{n_i}$$

(2.14)

The modes within a subsystem receive, store and transfer energy.

Derivation of the modal parameters of a subsystem is based upon combining geometrical information about the allowed mode shapes of the subsystem[9] with the dispersion relation for free waves in the subsystem [ref 4].

As long as reliable data for the coupling loss factors in both transmission directions are available for all connections between subsystems within a system, knowing the modal density is not essential for predictions with SEA. The modal densities of the subsystems are only needed when 'reciprocity relationship' *(2.7)* between subsystems is used in deriving

coupling loss factors. Besides, the modal density is a subsystem characteristic which determines the suitability of SEA to model the sound transmission within a system, as will be discussed in section 2.7.

2.5.4 Modal overlap

The modal overlap is the ratio of the average half-power bandwidth[10] to the average frequency spacing between modes in a frequency band. It is a measure of the overlap of the responses of modes within a subsystem. The modal overlap M_i of a subsystem i is given by [ref 5]

$$M_i = f\eta_{ii}n_i \qquad (2.15)$$

The modal overlap is not a parameter that is used in predictions with SEA. It is a subsystem characteristic which determines the suitability of SEA to model the sound transmission within a system, as will be discussed in section 2.7.

2.6 Primary SEA variables

2.6.1 Energy

Vibrational energy is the primary response variable of subsystems. This variable can be expressed in terms of more common variables for acoustic and structural systems, e.g. pressure or velocity.

For an acoustic subsystem o (with plane acoustic waves) the energy E_i is given by

$$E_o = \frac{p_o^2 V_o}{\rho_o c_o^2} \qquad (2.16)$$

where p_o is the sound pressure (r.m.s.) averaged over the (air-filled) acoustic volume (room) o. V_o, ρ_o and c_o are the volume of, the density ($\approx 1,2$ kg·m^{-3}) of and the propagation

---

[9] The allowed mode shapes are dependent on the dimensions of the subsystem and on the boundary conditions.

[10] The half-power bandwidth or the modal bandwidth is the frequency spacing between the two magnitude (response) levels that are 3 dB (factor of 2) down from the peak (response) level of a resonance frequency [ref 4].

velocity of sound ($\approx$ 340 m·s^{-1} at 20 ^{0}C) in the (air-filled) acoustic volume (room) o respectively.

For a structural subsystem i the energy E_i is given by

$$E_i = M_i v_i^2 \qquad (2.17)$$

where v_i is the velocity (r.m.s.) averaged over the surface area of the subsystem i with uniformly distributed mass M_i.

2.6.2 Input power

External sources inject energy into one or more subsystems of a system. These sources can be characterized as forces, moments, pressures or motions. The input power is proportional to the real part of the subsystem response function, e.g. the admittance, at the point of excitation. For point force excitations the input power to a subsystem i is given by

$$\Pi_{i,in} = F^2 \, Re(Y_i) \qquad (2.18)$$

where F is the excitation force (r.m.s.) and $Re(Y_i)$ is the real part of the (driving-)point or input admittance of subsystem i in the force direction.

2.7 SEA assumptions

The SEA method is based upon the validity of the following assumptions:

- The flow of vibrational energy between coupled subsystems is proportional to the difference in the average coupled[11] modal energies of the subsystems.

  This is illustrated by the following expression for the net transmitted power between a subsystem i and a subsystem j [ref 4]:

$$\Pi_{ij} = 2\pi\Delta f \beta_{ij} \left(\frac{E_i}{\Delta N_i} - \frac{E_j}{\Delta N_j} \right) \tag{2.19}$$

  where $E_i/\Delta N_i$ and $E_j/\Delta N_j$ are the average modal energies of the subsystems i and j in a frequency band Δf. β_{ij} is a modal coupling factor that depends only on the physical properties of the two coupled subsystems and is given by [ref 4]

$$\beta_{ij} \equiv \frac{\eta_{ij} f}{\overline{\delta f_i}} \tag{2.20}$$

  In addition the vibrational energy that is dissipated in a subsystem is proportional to the subsystem vibrational energy (see equations *(2.1)* and *(2.2)*).

- The subsystems responses are determined by several resonant modes.

  A larger number of resonant modes in a frequency band smoothes the response spectra and the spatial variation in responses, provided that the damping in the subsystems is not too large[12]. This results in more reliable results, e.g. parameters or response predictions.

  The requirement for a certain minimum number of modes within a subsystem determines the lower frequency limit for the application of SEA as a modelling method for a sound

---

[11] Strictly speaking, under weak coupling conditions the flow of vibrational energy between coupled subsystems is proportional to the difference in the average uncoupled modal energies of the subsystems. In order to proceed with the analysis of systems consisting of more than two subsystems, it has been assumed that the uncoupled energies can be replaced by the actual coupled energies (see the assumption about weak coupling between subsystems hereafter in this section). This is justified for weakly coupled subsystems [ref 9].

[12] The vibrational behaviour of a highly damped subsystem is non-resonant (because a wave will be damped before it reaches the subsystem boundaries), which implies that there is no uniform distribution of stored energy over the spatial domain of the subsystem. In that case SEA does not apply [ref 7]. However, the subsystem damping may not be too low either (see the assumption about modal overlap hereafter in this section).

transmission problem, because in general there are more modes in frequency bands at high frequencies.

Clear criteria for the required minimum number of modes are lacking. Craik [ref 5] states that in the literature criteria vary between 2 and 30 modes within each frequency band. Cremer and Heckl [ref 12] mention six modes per frequency band as a minimum value, based on experiences in room acoustics.

Although never completely possible in practical situations, one should try to choose subsystems in such a way that the modes within each subsystem are more or less evenly distributed and the energy is more or less evenly distributed over the modes within the frequency range of interest. As a consequence different wave types are represented by different subsystems, for example. Under these conditions averaging can be expected to provide statistically accurate results.

Although SEA is aimed at resonant transmission between subsystems, modelling of non-resonant transmission can be integrated to some extent in SEA models [ref 4], [ref 5], [ref 7]. This has been done successfully for non-resonant sound transmission between rooms through plates (walls and floors), which is important below the critical frequency[13].

- The subsystems responses have sufficient modal overlap.
  A larger modal overlap in a frequency band smoothes the response spectra and the spatial variation in responses, provided that the damping in the subsystems is not too high (see footnote 12). This results in more reliable results, e.g. parameters or response predictions. As for the number of modes, the requirement for a certain minimum modal overlap also determines the lower frequency limit for the application of SEA, because often the modal overlap in frequency bands is larger at high frequencies, see equation *(2.15)*.
  Although clear criteria for the required range of modal overlap are lacking, various authors have discussed the modal overlap and the related term "damping controlled". Some of the discussion points are given here.
  Lyon and DeJong [ref 4] define responses as "damping controlled" when the responses correspond to frequencies that lie within the half-power bandwidth around a resonance frequency f_n. The lower and upper frequencies f of the half-power bandwidth are given by $f \approx f_n \pm \eta f_n/2$ (for $\eta < 0,3$).

---

[13] The critical frequency is the frequency at which the flexural wavelength of a plate equals the wavelength of acoustic waves in the ambient medium. Below the critical frequency the sound transmission between rooms is not only determined by poorly radiating resonant modes, but also by non-resonant transmission. The mass of the plate is the most important property of the plate that determines the non-resonant transmission.

For one-dimensional subsystems, De Langhe [ref 7] shows that the vibrational behaviour will be non-resonant in case the modal overlap is larger than unity. For two- and three-dimensional subsystems, De Langhe states that these subsystems can have modal overlap values much greater than unity and can still respond highly resonant. De Langhe concludes with the assumption that subsystems with modal overlap values far below unity are not amenable to a SEA approach, see [ref 7] in which is referred to [ref 83].

Craik [ref 5] defines responses as "damping controlled" when the modal overlap is larger than unity. If the modal overlap is smaller than unity, the modal overlap is the fraction of the frequency spectrum that is controlled by resonant modes. For an example of two in-line plates, Craik shows in [ref 5] that the measured coupling loss factors become less than predicted coupling loss factors when the modal overlap falls below unity. The structure was not a typical building structure, but Craik describes that measurements on building structures show a similar trend.

- Sources, which excite the subsystems, are not correlated.
  This allows for linear summation of energies which originate from the individual sources. It is desirable that many modes are excited within each frequency band considered. Broadband random excitation as a source is desirable from these points of view.

- There is weak coupling between subsystems.
  This implies that the ratio of the coupling loss factor η_{ij}, representing the energy transmission from subsystem i to subsystem j, to the total loss factor $\eta_{i,tot}$ of subsystem i minus η_{ij} is substantially smaller than unity (derived from [ref 48]).

Under the weak coupling condition, the flow of vibrational energy in a system which consists of two subsystems, is proportional to the difference in uncoupled modal energies of the subsystems [ref 49], [ref 50]. However, this result cannot simply be generalised for systems consisting of more than two subsystems, as has been discussed by Fahy [ref 9] and Hodges & Woodhouse [ref 8]. Uncoupled modal energies are defined as modal energies of individual subsystems while vibrating by themselves but being driven by the same external sources that would have been applied in a coupled state - if a subsystem has no external source driving it, its uncoupled modal energy is by definition zero [ref 8]. Suppose a system consisting of three subsystems as shown in Figure 2-2.

28
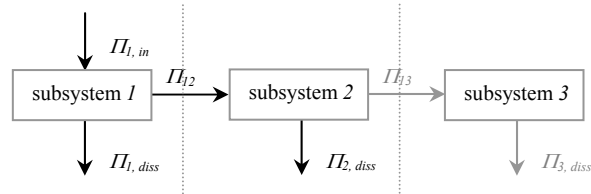
Figure 2-2   Three subsystem SEA model

If there is an input power from an external source to subsystem *1* only, the uncoupled energies in the subsystems *2* and *3* equal zero and hence the energy flow between the subsystems *2* and *3* equals zero in case they are coupled to each other, but not to subsystem *1*. As a result of this the energy in subsystem *3* is zero. Of course the actual (not uncoupled) energy is not zero when all three subsystems are coupled as described above. In order to proceed with the analysis of systems consisting of more than two subsystems, it has been assumed that the uncoupled energies can be replaced by the actual coupled energies [ref 9], as stated under the assumption about proportionality. This is justified for weakly coupled subsystems.

Basically, weak coupling enables that the modal behaviour of the coupled subsystems can be described with the modal properties of the uncoupled subsystems. In general, SEA is suitable for subsystems that are weakly coupled. But how strict this requirement is, is often discussed. Response predictions for some strongly coupled subsystems have shown to be reliable. Nevertheless, the weak coupling condition may at least be applied as a tool for the choice of subsystems. It always seems appropriate to choose subsystems such that there is weak coupling between them.

So, subsystem definitions can be based on expected ratios of coupling loss factors to damping loss factors (weak coupling considered from a modal point of view). But they can also be based on expected impedance mismatches (weak coupling considered from a wave point of view), as described in section 2.3. Both ways are expected to result in the same subsystems definition often.

▪ There is linear, conservative coupling (elastic, inertial or gyrostatic) between subsystems. In spite of this assumption, in section 2.5.1 it has been described how very small coupling damping can be integrated in SEA models.

▪ For each pair of connected subsystems the 'reciprocity relationship' given in equations *(2.6)* and *(2.7)* applies.

In the literature, the 'reciprocity relationship' is not described as a SEA assumption, but as a general principle. Actually this principle is only valid under the condition that the asymptotical values for the modal densities and the coupling loss factor values are accurate within each frequency band considered. This is the reason why the 'reciprocity relationship' is called an assumption in this thesis.

2.8   Conclusions

This chapter has given a general description of SEA without specifically focusing on the subject of this thesis, although at various places has been referred to literature about the application of SEA in the field of building acoustics.

As far as known to the author, SEA has not been applied in practice to describe the sound transmission through (wastewater) pipe systems and from pipe systems to plate structures in buildings. The next chapters focus on this application of SEA.

CHAPTER 3

APPLICATION OF SEA IN THIS STUDY

3.1 Introduction

This chapter describes how SEA is applied in this thesis. The application of SEA is illustrated by means of an example of a practical situation. Based on the vibrational characteristics of pipe systems, plates and couplings, systems and subsystems are defined and a SEA model is developed, see sections 3.2.1 and 3.2.2. Since the subsystems definition in this model is supposed to be quite complete, the model is indicated as "extensive SEA model".

As will be explained in section 3.2.3 determination of the parameters in the extensive SEA model would be complicated. Besides, in section 2.3 it has been stated that only groups of modes that play an important role in the transmission, dissipation and storage of energy, need to be included as subsystems in a SEA model. The question is whether a detailed model as the extensive SEA model is really necessary as the basis for a prediction model. Therefore simplifications of the extensive SEA model are searched for. Based upon a hypothesis and underlying assumptions concerning the sound transmission between subsystems, potential simplifications of the model are defined in section 3.2.3, resulting in a redefinition of the subsystems and a model that is indicated as "simplified SEA model".

The assumptions of the simplified SEA model and corresponding validation criteria are described in section 3.3.

It is assumed that the simplified SEA model is sufficiently accurate for engineering applications in building practice. In order to test the validity of this assumption, criteria for the prediction accuracy of the model are set in section 3.4.

3.2 SEA modelling and potential simplifications

3.2.1 System definition

As mentioned in section 1.4 this thesis focuses on plastic wastewater pipe systems clamped on single, homogeneous, heavyweight floors and walls. In building practice wastewater pipe systems consist of various elements and are coupled to various plates and acoustic volumes, i.e. rooms, either directly or indirectly. The reason for this is that a wastewater

pipe system usually passes by many rooms and plates. Furthermore, practical wastewater pipe systems, especially in apartment buildings, are coupled to various types of appliances, e.g. toilets, bathtubs and water heaters. Sometimes the appliance(s) and the pipe system are coupled to the same plate.

The first step in this study was the definition of the system and its sources. This is illustrated by Figure 3-1 and Figure 3-2. Figure 3-2 shows a schematic representation of Figure 3-1. The physical system elements are represented as blocks and sound transmission paths as lines. The pipe system is represented as one physical system element. Actually the pipe system consists of several elements, see Figure 3-1. In practical situations the wall and floor are coupled to other plates. These plates are not shown separately in Figure 3-2, but are represented as energy sinks.
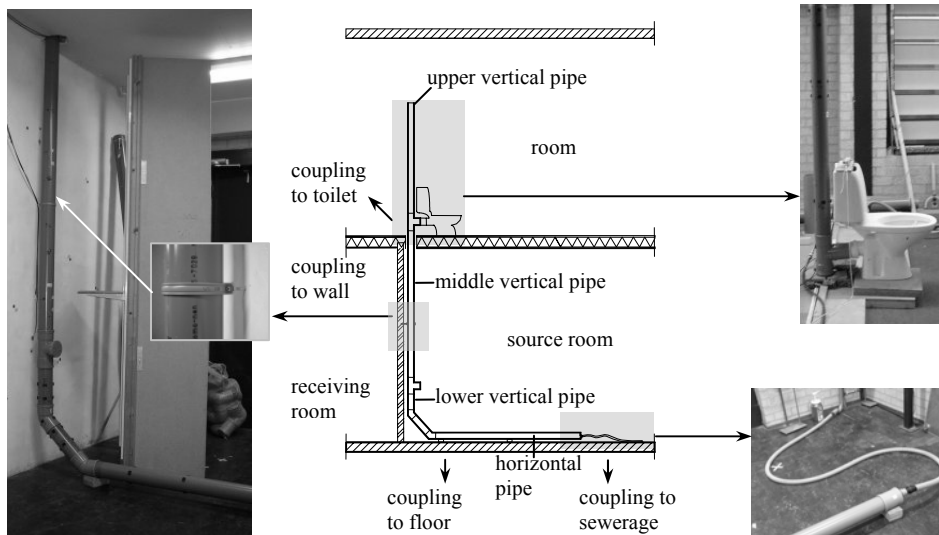
Figure 3-1 A wastewater pipe system coupled to plates, rooms, sewerage and a toilet; **centre**: schematic presentation of a vertical section of the situation
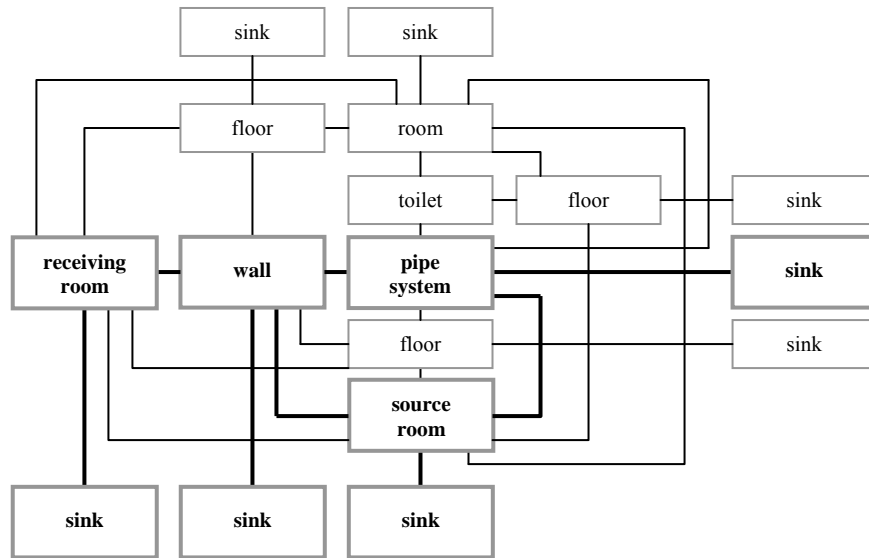
Figure 3-2 Schematic representation of Figure 3-1 (parts printed **in bold** represent the system considered)

Figure 3-2 shows that even a relatively small pipe system can be coupled directly to various plates, rooms and appliances and indirectly to much more of these elements.

The system considered is printed **in bold** in Figure 3-2. The system in the extensive SEA model consists of a wastewater pipe system coupled to one plate and rooms at both sides of the plate (see section 3.2.2). The system in the simplified SEA model consists of a wastewater pipe system coupled to one plate (see section 3.2.3). The toilet is not directly coupled to the same plate, so simultaneous direct excitation of the plate by toilet and pipe system is not investigated. The combined excitation of the pipe system by the water flow from the toilet and the toilet itself is considered as one source. In this case the pipe system is a physical system element. This is one of the possible source definitions. Other source definitions could be that the pipe system itself is modelled as a source or that the clamps are modelled as sources. In the last case the pipe system is not included in the model.

3.2.2   Subsystems definition and extensive SEA model

This section only names the types of modes that can exist in pipes and plates, and their vibrational directions or displacement (response) components. Sections 4.2.1 and 4.4.1 give in-depth descriptions of the different types of these modes in pipes and plates respectively.

For pipes, see Figure 3-3 and Figure 3-4 for illustrations of the various mode types and corresponding shapes.
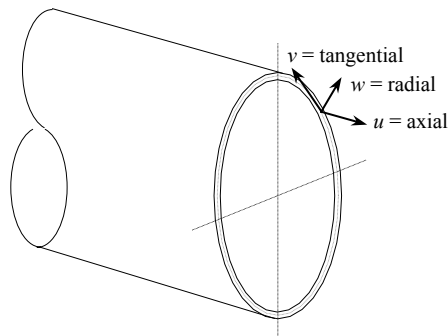
Figure 3-3   Circular cylindrical shell and vibrational directions or response components
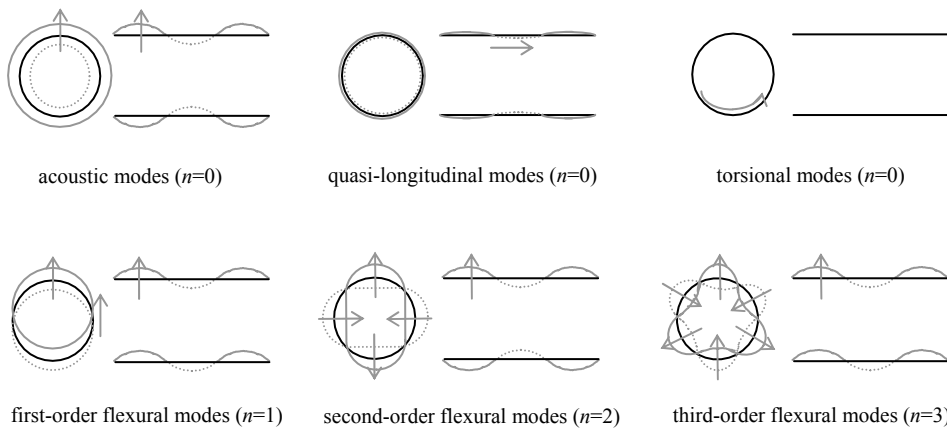
Figure 3-4   Mode shapes without (black lines) and with (grey lines) deformation and main vibrational direction (grey arrows), for the cross-section (**left side**) and the longitudinal section (**right side**) of a pipe due to various wave types

In pipes the following types of modes can exist. Acoustic modes (circumferential mode number $n=0$) originate in the pipe fluid and cause (forced) axial and/or radial vibrations of the pipe wall, i.e. vibrations along the pipe axis and/or perpendicular to the pipe surface. Quasi-longitudinal modes ($n=0$) in the pipe wall cause axial and (limited) radial vibrations of the pipe wall. For both acoustic and quasi-longitudinal modes the ratio of axial to radial vibrations depends on the material and dimensions of the pipe wall and pipe fluid and on

frequency. Torsional modes ($n=0$) cause tangential vibrations of the pipe wall, i.e. circumferential vibrations. First-order flexural modes ($n=1$) cause flexural motions of the pipe. Each pipe cross-section mainly translates transversely and rotates a bit, without cross-section deformation. Due to these flexural motions a point of the pipe wall vibrates primarily in the radial or tangential vibrational direction or equally in both directions, depending on its position on the pipe circumference. Depending on the dimensions and material of the pipe higher-order flexural modes ($n>1$) around the circumference of the pipe wall can exist above so-called cut-on frequencies. The vibrations of these modes are mainly radial. In infinitely long pipes some mode types are coupled, e.g. quasi-longitudinal modes in the pipe wall with acoustic modes in the pipe fluid[14], and some mode types are not coupled, e.g. torsional modes in the pipe wall with acoustic modes in the pipe fluid[15]. In practical pipes (with finite length) all mode types are coupled due to discontinuities (see hereafter).

In 'thin' plates three different types of modes can exist, depending on the dimensions and material of the structure: flexural modes with vibrations mainly perpendicular to the structure surface and quasi-longitudinal and shear modes, both with mainly in-plane vibrations. Due to connections to other plates there is coupling of these mode types within a plate.

In section 2.3 subsystems have been defined as groups of modes with similar vibro-acoustic characteristics. This implies that in a SEA model pipes and plates have to be represented by five and three subsystems respectively, as long as there is weak coupling between the subsystems.

Whether further division of a pipe or a plate into smaller physical system elements is required is determined by their dimensions and damping characteristics. Initially it has been assumed that practical pipes and plates can be represented by one physical system element each. A proper subdivision of a physical system element into smaller parts can be made only if the important subsystems are known, including their energy group velocity[16] and

---

[14] Due to the Poisson effect quasi-longitudinal waves cause radial pipe wall vibrations, which are responsible for the coupling to fluid vibrations.

[15] This is the case when fluid-wall friction is neglected [ref 25].

[16] The energy group velocity is the velocity at which energy in a wave travels. The phase velocity is the velocity at which the wave crest travels. For non-dispersive wave types, such as quasi-longitudinal, torsional and transverse waves, the phase and energy group velocities are equal. For dispersive wave types, i.e. flexural waves, this is not the case [ref 4], [ref 12].

damping loss factor. These issues have been investigated in this study, so a proper subdivision, if necessary, could not have been made beforehand.

In building practice different types of couplings between pipes and plates exist. One type of coupling, i.e. a pipe clamp, has been quantified by coupling loss factors in this study. Initially it has been assumed that weak coupling exists between pipes and plates in building practice. The validity of this assumption has been tested for the pipe clamp considered, see chapter 5.

In building practice pipe systems generally do not consist of only one pipe. Practical pipe system elements can be classified into two types of physical system elements, i.e. (straight) pipes and so-called discontinuities. Examples of discontinuities are bends and joints. Pipe clamps might also be considered as discontinuities within a pipe system. This depends on their influence on the vibrational behaviour of a pipe. In case there is any influence the pipe might have to be divided into separate physical system elements. Initially it has been assumed that the influence is negligible.

An important issue concerns the SEA modelling of pipe system discontinuities. The first possible way of modelling is by representing them as separate physical system elements with their own subsystems and subsystem characteristics. The second way is by treating a discontinuity as a coupling between each pair of subsystems in the connected pipes. At such discontinuities all types of modes are coupled [ref 26]. In a SEA model a discontinuity is represented by coupling loss factors corresponding to different types of subsystems within each individual pipe and by coupling loss factors corresponding to each pair of subsystems within two different pipes. The third way is modelling discontinuities and the connected pipes as one physical system element. This way of modelling is proper if there is no weak coupling between the connected pipes for example. In that case global modes (see section 2.3) in the pipe system exist. This could especially be the case in the low frequency range. Whether the first, second or third way of modelling is proper for a certain pipe system discontinuity depends on its dimensions, material and the frequency range of interest and can differ for different frequencies. Sections 4.3 and 5.4 to 5.6 contain in-depth discussions concerning this issue. Initially the second way of modelling, i.e. representation of discontinuities as couplings, has been applied. In the sections mentioned above it has been tested whether this is a proper way of modelling.

For the system printed **in bold** in Figure 3-2 the physical system elements, subsystems and couplings definitions are illustrated in Figure 3-5. The subsystems are represented as blocks. The *italic*, superscript printed numbers indicate the subsystems numbers. In Figure

3-5 the main vibrational directions[17] of the subsystems (grey printed letters) and input powers (pink arrows) are also shown. The energy losses out of subsystems due to dissipation and unknown transmission paths, i.e. paths that are not specified, are represented by yellow and orange 'energy sinks' respectively. An example of an orange energy sink is the energy transmission from the plate to connected plates. Sound radiation is represented separately by couplings between acoustic volumes and the pipe system or plate (green arrows). The two bends with a short pipe in between are represented as one coupling element between the lower (short) vertical pipe and the horizontal pipe.

Couplings between different modes within a pipe wall or the plate and between modes in different acoustic volumes are represented by black arrows. Red and blue arrows show couplings between modes in the walls of different pipes via the discontinuities and between modes in a pipe wall and the plate via the pipe clamp respectively. Couplings between modes in the pipe fluid and modes in the pipe walls are represented by grey arrows. Green arrows represent couplings between modes in the (source and receiving) rooms and modes in the pipe walls or the plate, as also described above.

---

[17] The main vibrational direction is the vibrational direction or displacement component in which the highest energy of the response of the subsystem is expected. Whether this is correct is investigated in chapter 4.
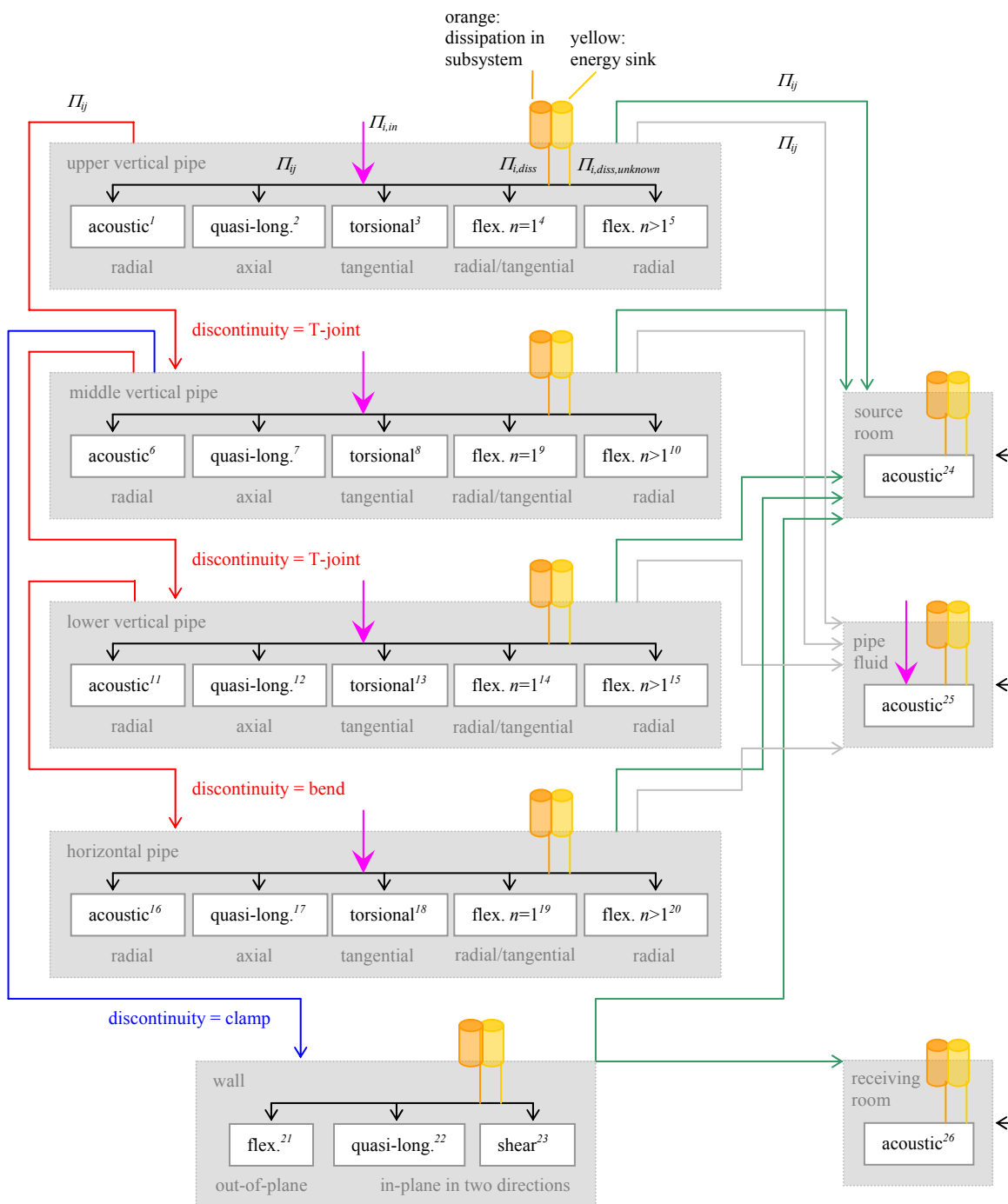
Figure 3-5 Schematic representation of subsystems and couplings for the system printed **in bold** in Figure 3-2 (Figure 3-1 illustrates the system in reality); <u>blocks and arrows</u> represent <u>subsystems and transmission paths/couplings respectively</u> for the <u>three perpendicular vibrational directions or orthogonal displacement components; different parameters</u> are only shown for one physical system element; see text for further explanation

The SEA formulation for the system in Figure 3-5 is given by equation *(3.1)*. The subsystems are represented by the numbers shown in Figure 3-5.

$$\Pi_{i,in} = 2\pi f \eta_{ii} E_i + \sum_{\substack{j=1 \\ j \neq i}}^{26} 2\pi f (\eta_{ij} E_i - \eta_{ji} E_j)$$

$$21 \leq i \leq 26 \; \wedge \; i \neq 25 \qquad\qquad \Rightarrow \Pi_{i,in} = 0$$

$$1 \leq i \leq 5 \; \cap \; 11 \leq j \leq 23 \; \wedge \; j = 26 \qquad \Rightarrow \eta_{ij} = \eta_{ji} = 0$$

$$6 \leq i \leq 10 \; \cap \; 16 \leq j \leq 20 \; \wedge \; j = 26 \qquad \Rightarrow \eta_{ij} = \eta_{ji} = 0$$

$$11 \leq i \leq 15 \; \cap \; 21 \leq j \leq 23 \; \wedge \; j = 26 \qquad \Rightarrow \eta_{ij} = \eta_{ji} = 0$$

$$16 \leq i \leq 20 \; \cap \; 21 \leq j \leq 23 \; \wedge \; j = 26 \qquad \Rightarrow \eta_{ij} = \eta_{ji} = 0$$

$$21 \leq i \leq 23 \; \cap \; j = 25 \qquad\qquad \Rightarrow \eta_{ij} = \eta_{ji} = 0$$

(3.1)

where the sign "∧" means "and" and the sign "∩" means "and at the same time".

Example: $1 \leq i \leq 5 \; \cap \; 11 \leq j \leq 23 \; \wedge \; j = 26 \; \Rightarrow \eta_{ij} = \eta_{ji} = 0$ means that the subsystems *1* to *5* are not coupled to the subsystems *11* to *23* (see Figure 3-5, where there are no lines connecting these subsystems). The subsystems *1* to *5* are also not coupled to subsystem *26*. When subsystems are not coupled to each other, the coupling loss factors equal zero. On the other hand, the subsystems *1* to *5* are coupled to each other. Also, the subsystems *11* to *15* are coupled to each other, and so are the subsystems *16* to *20* and the subsystems *21* to *23*. The subsystems *21* to *23* are also coupled to subsystem *26*. So, the sign "∩" separates groups of subsystems that are not coupled to each other. The subsystems within each group can be coupled to each other. Whether they are really coupled, follows from the other statements in equation *(3.1)*.

3.2.3   Subsystems redefinition and simplified SEA model

For the system considered in section 3.2.2 the subsystems definition as applied in that section is supposed to be quite complete. However, an important disadvantage of the SEA model presented in section 3.2.2 is that obtaining the parameter data for all subsystems and couplings between subsystems is quite complicated.

Theoretical estimations concerning the parameters are not readily available, except those for modal densities. Coupling loss factor data possibly could be obtained numerically by modelling all types of subsystems and couplings, e.g. with FEM. However, in that case data for other parameter types, e.g. mass, stiffness and mechanical resistance for subsystems, are needed, which often are not available either.

For a proper, experimental determination of the parameter data the vibrational behaviour of all separate subsystems has to be analysed. This could be done by exciting all subsystems one by one, which is feasible if a physical system element, e.g. a pipe or a plate, can be isolated from its surroundings. In this way damping loss factors could be obtained experimentally. However, for the determination of input powers and coupling loss factors the physical system elements have to be coupled to each other and their surroundings at all sides as is the case in practice. In that case separate excitation of all subsystems is difficult, e.g. separate excitation of quasi-longitudinal modes in pipes and plates, torsional modes in pipes or shear modes in plates is hardly feasible. An alternative way to analyse the vibrational behaviour of the separate subsystems is by decomposition of the mode types. For plates the different types of modes can be distinguished, because they have different main vibrational directions. As illustrated in Figure 3-5 in pipes several mode types have the same main vibrational directions. Mode (wave) type decomposition techniques[18] have been developed to determine energy flows corresponding to different mode types in straight pipes, see for example [ref 25], [ref 26]. These techniques could possibly be applied to estimate the importance of the various mode types in the energy flows within and between subsystems. However, direct application of these techniques for the derivation of SEA parameter data is not possible.

Application of the preceding determination techniques for parameters is quite complicated, if not impossible, especially in experimental set-ups that are based on practical situations. Instead of trying to determine all parameters corresponding to the model in section 3.2.2, a different approach has been applied in this study. An important question is whether a complicated model as presented in section 3.2.2 is really needed to describe the sound transmission through pipe systems and from pipe systems into plates with sufficient accuracy[19]. In section 2.3 it has been stated that only groups of modes that play an important role in the transmission, dissipation and storage of energy, need to be included as subsystems in a model. Based upon this statement and upon a hypothesis (see hereafter) and

---

[18] For example, for modes with circumferential mode numbers $n \leq 2$ the energy flow of each mode type in the pipe wall or the pipe fluid can be calculated from a two-channel measurement of two equal variables at two different axial positions along a pipe. Depending on the mode type in the pipe wall accelerations in the axial, tangential or radial vibrational direction are measured. In the pipe fluid pressure is the measured variable. Expressions for the calculation of the energy flows from the measurement results by application of this two-channel wave decomposition technique have been found by Verheij [ref 26] en De Jong [ref 25].

[19] Besides, in section 3.2.2 it has been described that all mode types within a physical system element, i.e. a pipe or a plate, are coupled due to connections to other physical system elements. In case these couplings are strong, modelling all mode types within a physical system element as separate subsystems is conflicting with the assumption about weak coupling mentioned in section 2.7.

underlying assumptions concerning the groups of modes as defined in section 3.2.2, potential simplifications of the model are defined in this section, resulting in a redefinition of the subsystems and a simplified SEA model. The subsystems redefinition is illustrated by Figure 3-6. Basically the redefinition consists of two steps, see the explanation below Figure 3-6.
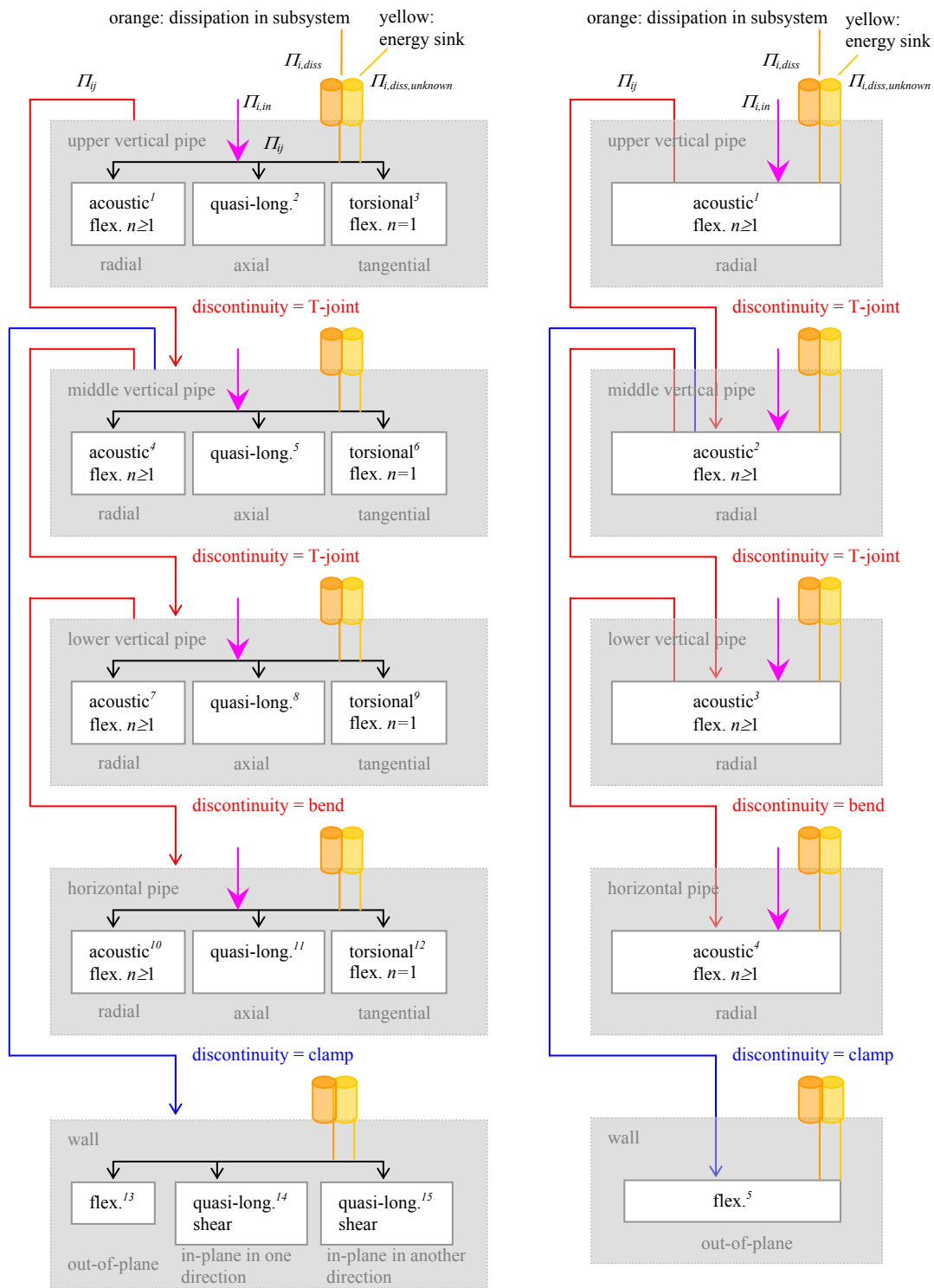
Figure 3-6 Schematic representation of the subsystems and couplings redefinition for the system printed **in bold** in Figure 3-2 (Figure 3-1 illustrates the system in reality); **left side**: redefinition step 1, **right side**: redefinition step 2; blocks and arrows represent subsystems and transmission paths/couplings respectively for the three perpendicular vibrational directions (**left side**) or only radial/out-of-plane vibrations (**right side**); different parameters are only shown for one physical system element; see text for further explanation

The first subsystems redefinition step contains two parts: (1) omission of acoustic volumes, which is explained in section 3.2.3.1 and (2) grouping of mode types with the same main vibrational direction in one subsystem for each physical system element, resulting in three subsystems per element, which is explained here. So, subsystems are classified by vibrational direction, not by mode type. For pipes, the vibrational directions that are distinguished are radial, axial and tangential, see *w*, *u* and *v* respectively in Figure 3-3. For plates, the vibrational directions that are distinguished are out-of-plane and in-plane in two perpendicular directions. For each vibrational direction, the energies corresponding to the vibrational responses of all mode types are summed[20]. Determination of responses in different vibrational directions is quite easy; determination of the contribution of different mode types to the response in one vibrational direction is complicated, as described before. The consequence of this summation is that data for parameters, e.g. damping and coupling loss factors and input powers, which are determined experimentally are only representative for these new subsystems[21]: no distinction between different mode types within the subsystems is made.

The only drawback of this redefinition step is that it might be conflicting with the general SEA assumptions about equal distribution of modes and equal distribution of energy over the modes within each frequency band (see section 2.7).

In the second subsystems redefinition step the three subsystems per physical system element, obtained in the first step, have been reduced to one subsystem per physical system element. This redefinition step is based on the hypothesis that radial pipe vibrations and out-of-plane plate vibrations as response components are dominant in the sound transmission within pipe systems and between pipe systems and plate structures, and therefore in the sound radiation to rooms. This implies that couplings within pipe systems and couplings between pipe systems and plate structures are dominated by radial pipe responses and out-of-plane plate responses. For acoustic couplings, this is correct anyhow,

---

[20] In Figure 3-6 both the radial and tangential vibrational components of the first-order flexural modes in pipes are mentioned, because they are equal. For the other types of modes only the main vibrational component is mentioned. This does not imply that only the energies of the responses of the mode types mentioned are included in the energy of the response in each vibrational direction, i.e. subsystem in the simplified SEA model. Other types of modes also contribute to the energy of the response in a vibrational direction, which is not the main vibrational direction for these types of modes. The main vibrational direction of quasi-longitudinal modes in pipes, for example, is axial. Nevertheless, radial pipe vibrations caused by these modes are included in the energy of the response of the subsystem corresponding to radial pipe vibrations. The same applies for higher-order flexural modes: the axial and tangential vibrations due to these modes are included in the energies of the responses of the corresponding subsystems. Only torsional modes in pipes and shear modes in plates have one vibrational direction.

because sound radiation can only be caused by radial/out-of-plane vibrations. For structural couplings, this implies that axial and tangential pipe responses are assumed to be less effective than radial pipe responses in the sound transmission within pipe systems and from pipe systems through pipe clamps to plate structures for example. Whether this can be made plausible is discussed in section 3.2.3.2.

The hypothesis results from several assumptions concerning the vibro-acoustic characteristics of pipes, plates, couplings between them and sources in pipe systems. These assumptions and corresponding validation criteria are described in section 3.3.

It is assumed that a model which considers only radial pipe vibrations and out-of-plane plate vibrations as response components is sufficiently accurate for our engineering purposes. In order to test the validity of this assumption, accuracy criteria are set in section 3.4.

The SEA formulation for the system according to redefinition step 2 in Figure 3-6 is given by equation *(3.2)*. The subsystems are represented by the numbers shown in Figure 3-6.

$$\Pi_{i,in} = 2\pi f \eta_{ii} E_i + \sum_{\substack{j=1 \\ j \neq i}}^{5} 2\pi f (\eta_{ij} E_i - \eta_{ji} E_j)$$

$$i = 5 \qquad\qquad\qquad \Rightarrow \Pi_{i,in} = 0$$

$$i = 1 \ \cap \ 3 \leq j \leq 5 \quad \Rightarrow \eta_{ij} = \eta_{ji} = 0$$

$$i = 2 \ \cap \ j = 4 \qquad \Rightarrow \eta_{ij} = \eta_{ji} = 0 \qquad\qquad (3.2)$$

$$i = 3 \ \cap \ j = 5 \qquad \Rightarrow \eta_{ij} = \eta_{ji} = 0$$

$$i = 4 \ \cap \ j = 5 \qquad \Rightarrow \eta_{ij} = \eta_{ji} = 0$$

where the sign "∩" means "and at the same time".

Example: $i = 1 \ \cap \ 3 \leq j \leq 5 \quad \Rightarrow \eta_{ij} = \eta_{ji} = 0$ means that subsystem *1* is not coupled to the subsystems *3* to *5* (see Figure 3-6, where there are no lines connecting these subsystems). When subsystems are not coupled to each other, the coupling loss factors equal zero. On the other hand, subsystem *3* is coupled to subsystem *4*. So, the sign "∩" separates groups of subsystems that are not coupled to each other. The subsystems within each group can be coupled to each other. Whether they are really coupled, follows from the other statements in equation *(3.2)*.

---

[21] Actually the parameter values depend on the mode shapes. So the values differ for different modes [ref 6].

3.2.3.1   Energy transmission due to acoustic coupling between subsystems

In the simplified model acoustic volumes are omitted, i.e. sound radiation is not modelled separately. Sound radiation is included in the coupling loss factors or combined with material damping in the damping loss factors. The reason for this is that it has been assumed that in many practical situations where a pipe system is connected to a plate via structural couplings (such as pipe clamps), the transmission of vibrational energy between pipe system and plate caused by the structural couplings will be substantially (at least a factor of 10 or 10 dB[22]) higher than the energy transmission caused by acoustic coupling. [23] Then, the energy transmission due to acoustic coupling is negligibly small in the total energy transmission, which is equal to the energy transmission due to structural coupling. For the coupling between a pipe (system) and a plate this assumption has been investigated in this study and is discussed in sections 5.4.3 and 5.6.4.

In the same way as for the coupling between pipe (system) and plate, it is assumed that for energy transmission between pipe system elements the acoustic path is negligible. Study on this assumption is reported in sections 5.5.3 and 5.6.4.

Appendix IV discusses acoustic couplings and illustrates that it is difficult to predict coupling loss factors and therefore energy flows due to acoustic couplings properly. Therefore, the validity of the assumption has been tested experimentally in this study. It has been shown that the assumption seems to be correct for situations in which relatively rigid structural couplings are applied (the results are described in more detail in the sections mentioned above). In case acoustic coupling might be more important, e.g. in case of relatively flexible structural couplings, it is probably more appropriate to evaluate the sound transmissions due to acoustic coupling and structural coupling separately. Otherwise, acoustic and structural couplings are included in one coupling loss factor. This will not lead to errors. But, in case acoustic coupling is important, separation of both phenomena will result in a model that is more valuable as the basis for a design tool. For example, sound reducing measures can be based upon this.

In case there are no structural couplings between a pipe system and a plate, obviously there is only transmission of vibrational energy due to acoustic couplings. Then the coupling loss factors represent only sound radiation.

In order to predict the sound level in a room due to a pipe system (behind a plate) with the simplified SEA model, the sound radiation characteristics of the plate should be included

---

[22] In this thesis, energies E are presented as $10lg(E/E_{ref})$ re 10^{-12} J.

[23] Whether this is correct depends on the materials and dimensions of the pipe system, on the structural couplings to the plate and on the room or shaft in which the pipe system is situated and is frequency-dependent.

separately in the model. For this reason, in the future the simplified model should be extended again with an extra subsystem (the receiving room) and corresponding parameters. A different approach is to apply plate velocities calculated with the simplified SEA model in another prediction model in order to predict the sound level in a room due to the sound radiation from a plate (then it is necessary that radiation ratios for plates are included in the (second) prediction model).

3.2.3.2 Energy transmission due to structural coupling between subsystems

The hypothesis behind the simplified model is that radial pipe vibrations and out-of-plane plate vibrations as response components are dominant in the sound transmission within pipe systems and between pipe systems and plate structures, and therefore in the sound radiation to rooms.

Sound in a room due to a pipe system may be generated in two ways. In case there is a plate between the pipe system and the room, the sound is radiated from the plate on which the pipe system is mounted, that the pipe system passes or in which the pipe system is embedded. In case there is no plate between the pipe system and the room, there is direct sound radiation to the room from the pipe system itself.

Basically there are four possible configurations of a pipe system, a plate and a room that are important to consider within the context of predictions of the sound level in a room due to a pipe system, see Figure 3-7.
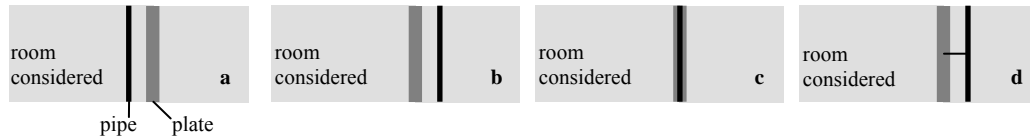
Figure 3-7   Possible configurations of a pipe system, a plate and a room

In case the pipe system is in the room (**a** in Figure 3-7) or in case the pipe system and the room are separated by a plate on which the pipe system is not clamped (**b** in Figure 3-7), there is only acoustic coupling between the pipe system and respectively the room or the plate. In that case only radial vibrations of the pipe system and out-of-plane vibrations of the plate need to be considered[24]. In practical situations where a pipe system is embedded in a plate (**c** in Figure 3-7), it is expected that the conversion from radial pipe wall vibrations into out-of-plane vibrations in the plate and from there into sound is much more effective than from in-plane pipe wall vibrations. So, in that case only radial vibrations of the pipe system and out-of-plane vibrations of the plate need to be considered too. However, for clamped pipe systems (**d** in Figure 3-7) this is uncertain yet. Figure 3-8 illustrates this.

Figure 3-8 shows a pipe that is coupled to a plate with a characteristic pipe clamp. The pipe clamp consists of three parts: a plastic ring, a steel bar with screw thread and a plastic coupling element between ring and bar. The steel bar is screwed in the plate to mount the pipe. It is assumed that a pipe clamp does not exhibit a (multi-)modal vibro-acoustic behaviour (see assumption 3 in section 3.3.1) and that the pipe clamp is a rigid coupling element between pipe and plate.

As discussed in section 3.2.2 various types of modes can occur in pipes. Each mode type has one main vibrational direction, except first-order flexural modes: the responses corresponding to these modes are equal for the radial and tangential vibrational directions, so these modes have two main vibrational directions. For each mode type the main vibrational direction(s) of a pipe is (are) indicated by the grey arrows in Figure 3-8.

The pipe vibrations set the pipe clamp into vibration and subsequently the clamp vibrations set the plate into vibration. The expected predominant vibrational transmission directions into the pipe clamp and into the plate are indicated by respectively red arrows and black arrows in Figure 3-8.

As will be clear from the discussion hereafter, it is difficult to predict which types of modes and vibrational (response) components of the various mode types in pipe systems are dominant in the sound transmission through clamps to plates. The same applies to the sound transmission between different elements within a pipe system, particularly the sound transmission through bends. For structural couplings between pipes and plates, this section discusses qualitatively which plate modes are expected to be caused by the various types of modes and vibrational (response) components in pipes. This section also describes the

---

[24] Only structural vibrations in the direction perpendicular to the surfaces of the physical system elements cause direct sound radiation to rooms (this is a basic physical principle). Structural vibrations in the in-plane directions only can cause sound radiation in an indirect way, i.e. due to conversion into flexural vibrations at structural junctions. In this thesis only plates that are directly coupled to pipe systems are included in the model (see section 3.2.1). Energy losses through non-specified transmission paths are modelled as energy sinks.

simplifications of the SEA model proposed, i.e. the neglected transmissions from pipe to plate, in more detail. The purpose of this section is not to justify the simplifications. The validity of the simplified SEA model is tested based on the validation criteria corresponding to the assumptions in the next sections.

All pictures in Figure 3-8 assume translation of the pipe wall near the pipe clamp. So, it is assumed that there is no node line near the clamp, except for higher-order flexural pipe modes: for these modes it is important to consider the situations without and with node line near the clamp (see the discussion below Figure 3-8). For frequencies where there is a node line in the mode shape of the pipe near the clamp, translation does not occur. Rotation around the node line will result in rotation excitation of the clamp and as a consequence in rotation excitation of the plate, which will result in flexural modes in the plate. Only for first-order flexural pipe modes parallel to the plate, rotation around the node line will result in torsion of the clamp and as a consequence in in-plane torque excitation of the plate, which is not an effective excitation (see the discussion below Figure 3-8).
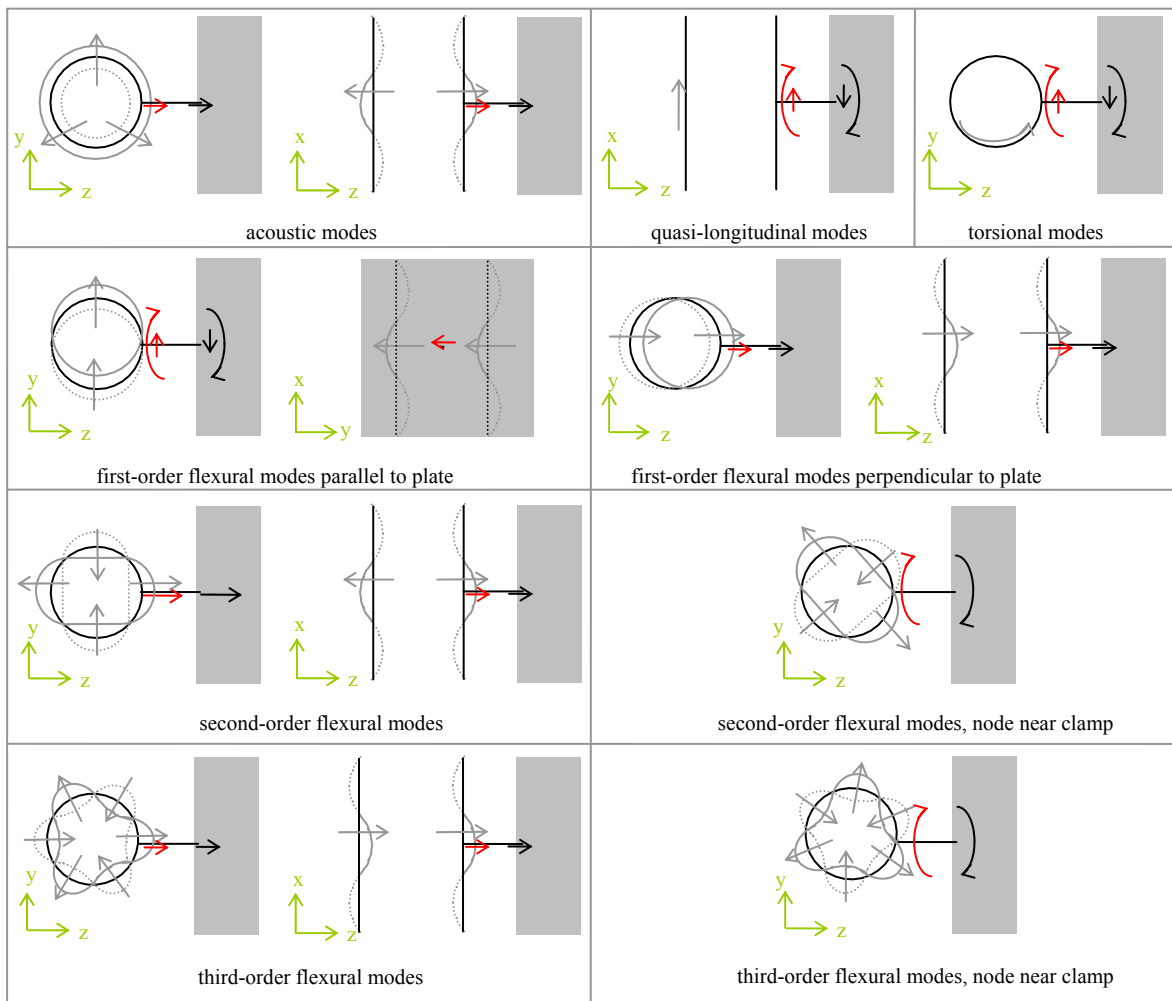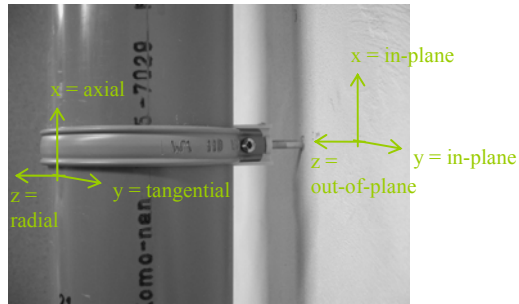
Figure 3-8 Possible modes in a pipe, their main vibrational directions (**grey** arrows) and expected predominant vibrational (sound) transmission directions from the pipe to a characteristic pipe clamp (**red** arrows) and from the pipe clamp to a plate (**black** arrows)

Figure 3-8 illustrates the following expected predominant vibrational (sound) transmissions from pipe to plate:

- acoustic modes in the pipe result in clamp[25] vibrations (translations) perpendicular to the plate and as a consequence in excitation perpendicular into the plate; this 'normal' excitation will result in flexural modes in the plate;
- (1) quasi-longitudinal and torsional modes in the pipe result in clamp vibrations (translations) parallel to the plate and as a consequence in in-plane excitations of the plate; the excitation directions resulting from the quasi-longitudinal and torsional pipe modes are perpendicular to each other; both in-plane excitations will result in quasi-longitudinal modes in the plate; (2) quasi-longitudinal and torsional modes in the pipe also result in two perpendicular rotation excitations of the clamp and as a consequence in two perpendicular rotation excitations of the plate, which will result in flexural modes in the plate;
- (1) first-order flexural modes causing pipe vibrations mainly parallel[26] to the plate result in clamp vibrations (translations) parallel to the plate and as a consequence in in-plane excitation of the plate; the in-plane excitation will result in quasi-longitudinal modes in the plate; (2) these first-order flexural pipe modes also result in rotation excitation of the clamp and as a consequence in rotation excitation of the plate, which will result in flexural modes in the plate;
- first-order flexural modes causing pipe vibrations mainly perpendicular (see footnote 26) to the plate result in clamp vibrations (translations) perpendicular to the plate and as a consequence in excitation perpendicular into the plate; this 'normal' excitation will result in flexural modes in the plate;
- outside nodes, higher-order flexural pipe modes result in clamp vibrations (translations) perpendicular to the plate and as a consequence in excitation perpendicular into the plate; this 'normal' excitation will result in flexural modes in the plate;
- primarily in nodes but also outside nodes, higher-order flexural pipe modes also result in rotation excitation of the clamp and as a consequence in rotation excitation of the plate, which will result in flexural modes in the plate.

Besides the transmissions mentioned above it is expected that the (less important) axial and tangential vibrational components of the first- and higher-order flexural modes in the pipe

---

[25] Actually, the vibrations (translations and rotations) of the clamp bar ends on the pipe and plate side are described.

[26] First-order flexural modes, which cause pipe vibrations that are equally parallel as perpendicular to the plate (pipe rotated over 45 degrees compared to the pictures in Figure 3-8), result in a combination of the described vibrations in clamp and plate.

will result in some in-plane excitation and some rotation excitation of the plate. This will also be the case when the flexural modes in the pipe are not exactly parallel or perpendicular to the plate.

The extent to which the different types of resonant pipe modes are transmitted to a connected plate strongly depends on the effectiveness of sound transmission, or energy losses, from pipe to clamp ring, from clamp ring to clamp bar and from clamp bar to plate. This depends on the dimensions, materials and detailing of the various elements and will be frequency-dependent. Because of the low admittance due to both in-plane and torque excitations of practical plates [ref 43], it is expected that conversions of translations and torsion on a clamp bar into in-plane modes in a plate are not very effective. Conversions of both rotations on the clamp bar end and of axial translations on the clamp bar, i.e. perpendicular to the pipe wall and plate, into flexural modes in the plate are expected to be more effective.

Rotations of the clamp bar end are expected to be mainly due to first-order flexural pipe modes (tangential response component) and to a smaller extent to higher-order flexural (axial and tangential response components), quasi-longitudinal (axial response component), torsional pipe modes and rotations in nodes for all mode types. Axial translations of the clamp bar are expected to be mainly due to first- and higher-order flexural pipe modes (radial response component) and to a smaller extent to quasi-longitudinal (radial response component) pipe modes and forced vibrations of the pipe wall due to acoustic modes in the pipe fluid. [27]

As mentioned in footnote 24 in this section, initially the simplified model considers sound radiation from plates that are directly connected to pipe systems. This is why the model focuses on flexural modes in plates due to excitation by pipe systems. As stated above flexural modes in plates are expected to be mainly a result of first- and higher-order flexural pipe modes.

For the higher-order flexural pipe modes the radial vibrations are expected to be dominant in the vibrational transmission from pipe to plate. However, as described above and shown in Figure 3-8, for the first-order flexural pipe modes the tangential and radial vibrational components are equal. The vibrations in the tangential vibrational direction (pipe vibrations parallel to the plate) result in rotation excitation of the plate and with that in flexural modes in the plate. The vibrations in the radial vibrational direction will also result in flexural modes in the plate. Nevertheless, as a postulated simplification, the simplified SEA model

---

[27] The expectations in this paragraph are mainly based on information about ratios of the responses in the axial, tangential and radial vibrational directions for the various mode types and about ratios of the mode counts of the various mode types. These characteristics are discussed in detail in chapter 4 of this thesis.

ignores the energy transmission into the plate due to the tangential vibrations of the first-order flexural pipe modes.

When first-order flexural pipe modes would be the only modes responsible for the sound transmission within the systems studied and when the sound transmissions due to the tangential and radial vibrational components of these modes would be equally effective, ignoration of the tangential vibrational component would imply ignoration of half of the sound transmission. However, because other mode types with a mainly radial vibrational direction and large mode counts, specifically the higher-order flexural modes, can exist in pipe systems and because the sound transmissions due to the tangential and radial vibrational components might not be equally effective (depending on the rotation stiffness of the clamp), it has been decided that it is valuable to investigate whether it is sufficient to take only radial pipe vibrations into account to predict the sound transmission within the systems studied.

Thus for pipes only vibrations in the radial vibrational direction and for plates only out-of-plane vibrations are included in the simplified SEA model.[28]

3.3   Assumptions of the simplified SEA model and validation criteria

In this thesis the validity of the simplified SEA model is investigated. Basically, three questions need to be answered with a yes, in order to conclude that the simplified SEA model is valid and applicable for predictions in building practice.

These questions are:

1. Are the general SEA assumptions fulfilled?

2. Are radial pipe vibrations and out-of-plane plate vibrations as response components dominant in the sound transmission within pipe systems and between pipe systems and plates, and therefore in the sound radiation to rooms?

3. Is a model which considers only radial pipe vibrations and out-of-plane plate vibrations as response components sufficiently accurate for our engineering purposes?

This study has been aimed at finding the answers to these questions. This section focuses on the first two questions. Section 3.4 deals with the third question, where criteria for the prediction accuracy are set.

---

[28] As a matter of fact, in the measurement results in this thesis vibrations perpendicular to pipe walls and plates due to quasi-longitudinal and acoustic modes are included (see chapter 5), because these vibrations have not been analysed separately from the vibrational components perpendicular to pipe walls and plates due to flexural modes.

In order to find the answers to the first two questions, eight assumptions are defined in sections 3.3.1 and 3.3.2. Whether the simplified SEA model is valid, is determined by the modal properties of typical pipe systems and plates, the properties of typical sources in pipe systems and the properties of the energy transmission within pipe systems and between pipe systems and plates. Some of the assumptions are similar to general SEA assumptions, some are specific for the simplified SEA model. In order to test the validity of the assumptions for the systems that are studied in this thesis, in sections 3.3.1 and 3.3.2 validation criteria[29] are set and reference is made to those parts of this thesis where the validity of the assumptions is studied further.

The validation criteria in sections 3.3.1 and 3.3.2 are set as a starting point for testing the validity of the simplified SEA model, in order to investigate the hypothesis in steps, i.e. for the various model parts. In the end, the prediction accuracy of the complete model determines whether the model is suitable for engineering applications in building practice. Based on the study results among which an estimation of the prediction accuracy of the model, in chapter 7 it is discussed which validation criteria should be reset.

Evaluation of model parts provides information that may be valuable in case the accurateness of predictions with the model would be under discussion. Besides, evaluation of model parts can provide insight in the appropriateness of the model for other types of pipe systems and plate structures in the future.

The validation criteria are set for the octave bands in the frequency range of interest, i.e. for centre frequencies 125 Hz to 2000 Hz. Fulfilling the validation criteria in octave bands seems necessary, because one of the criteria for the prediction accuracy is set for octave bands (see section 3.4). Although the validity of the simplified SEA model is tested based on results in octave bands, this thesis also gives results for 1/3-octave bands in order to present information which might be valuable in the explanation of striking octave band results, e.g. a large peak or jump within a response spectrum.

3.3.1   Assumptions and validation criteria similar to general SEA assumptions

- *Assumption 1:* the subsystems responses in each octave band considered are determined by a sufficiently large number of resonant modes.

  Validation criterion: in this thesis, the assumption is defined to be valid if the number of modes per octave band is at least 6 for each subsystem.

---

[29] Requirements which are to be met to approve the simplified SEA model for the systems studied in this thesis.

Whether this validation criterion is met for practical water supply and wastewater pipes is theoretically investigated in section 4.2.4 and for practical plates in section 4.4.4.

A minimum of 6 modes per octave band has been set as a starting point for testing the validity of the simplified SEA model, based on the values mentioned in the literature (see section 2.7).

▪ *Assumption 2:* the subsystems responses in each octave band considered have sufficient modal overlap.

Validation criterion: in this thesis, this assumption is defined to be valid if the modal overlap in each octave band is at least 1 for each subsystem.

Whether this validation criterion is met for practical water supply and wastewater pipes is theoretically investigated in section 4.2.4 and for practical plates in section 4.4.4.

For the modal overlap, a minimum of 1 per octave band has been set as a starting point for testing the validity of the simplified SEA model, based on the values mentioned in the literature (see section 2.7).

▪ *Assumption 3:* pipe system discontinuities, such as bends, joints or clamps, are no subsystems, but coupling elements.

Basically, in a coupling element the non-resonant sound transmission is dominant, since no or a few resonant modes originate in the coupling element. Resonant modes originating in the coupling element are negligible in the sound transmission between subsystems which are connected to each other by the coupling element. Thus, coupling elements are no subsystems, so based on the validation criterion corresponding to assumption 1 the number of modes per octave band is 5 at most for coupling elements. Another important feature that may determine whether a discontinuity can be modelled as a coupling element is whether it forms a weak coupling between subsystems (see assumption 5).

Validation criterion: in this thesis, this assumption is defined to be valid if the number of modes per octave band is 5 at most for each pipe system discontinuity.

Whether this validation criterion is met for practical pipe system discontinuities is investigated in section 4.3.4.

- *Assumption 4:* the transmission of vibrational energy between subsystems caused by resonant modes is significantly larger (preferably at least a factor of 10) than the energy transmission caused by non-resonant vibrations.[30]

  The validity of this assumption is not tested explicitly in this thesis. Only an implicit indication is obtained by determination of deviations from the 'reciprocity relationship' (see under assumption 8 in section 3.3.2) and of the prediction accuracy of the model (see section 3.4).

- *Assumption 5:* the coupling between subsystems is weak.

  Validation criterion: in this thesis, this assumption is defined to be valid if in each octave band considered the ratio of a coupling loss factor η_{ij}, representing the energy transmission from subsystem i to subsystem j, to the total loss factor $\eta_{i,tot}$ of subsystem i minus η_{ij} is smaller than 0,1 (the total loss factor $\eta_{i,tot}$ minus η_{ij} is at least a factor of 10 (10 dB[31]) higher than the coupling loss factor η_{ij}), e.g. for three subsystems *1*, *2* and *3*, from which subsystem *2* is connected to the subsystems *1* and *3*, but the subsystems *1* and *3* are not coupled with each other:

  $\eta_{12} \leq 0{,}1\,\eta_{11}$, $\eta_{21} \leq 0{,}1(\eta_{22}+\eta_{23})$, $\eta_{23} \leq 0{,}1(\eta_{22}+\eta_{21})$, $\eta_{32} \leq 0{,}1\,\eta_{33}$.

  Whether this validation criterion is met for a practical coupling between a pipe (system) and a plate is investigated in sections 5.4.4 and 5.6.5. For practical couplings within pipe systems, this is investigated in sections 5.5.4 and 5.6.5. Based on this assumption and the validation criterion, possible subdivisions of a pipe system into smaller system elements, e.g. straight pipe elements and discontinuities, are discussed in sections 5.6.2 and 5.6.4.

3.3.2   Assumptions and validation criteria specific for the simplified SEA model

The following assumptions 6 to 8 are specifically related to the hypothesis that radial pipe vibrations and out-of-plane plate vibrations as response components are dominant in the sound transmission within pipe systems and between pipe systems and plates, and therefore in the sound radiation to rooms.

---

[30] When this would not be correct, only the vibrational energy of pipes near clamps should be included in the description of the energy transmission from a pipe system to a plate for example. Then the analysis of the energy transmission would be complicated, because the resonant and non-resonant vibrational behaviour of a pipe part and a part of the plate near a clamp should be analysed separately.

[31] In this thesis, loss factors η are presented as *10lg(η/η_{ref})* [dB] re 10^{-12}.

Whether this hypothesis is correct depends on the following two system properties:

A   the extent to which practical sources in pipe systems cause radial pipe vibrations. This depends on (a) the ratio of the input force components (or input moments) in the radial, axial and tangential vibrational directions and (b) the ratio of the response components of natural modes in pipe systems, i.e. the responses in the radial, axial and tangential vibrational directions under the (theoretical) assumption of equipartition of incoming energy over all natural modes. The combination of (a) and (b) determines how much power is injected in the axial, tangential and radial vibrational directions of pipes;

B   the extent to which the transmission of vibrational energy within pipe systems and between pipe systems and plates is caused by radial pipe vibrations and out-of-plane plate vibrations, i.e. (a) the extent to which out-of-plane plate vibrations are caused by radial vibrations in pipe systems and vice versa, and (b) the extent to which radial vibrations in a pipe are caused by radial vibrations in another pipe that is part of the same pipe system.

The combination of these system properties determines whether the hypothesis is correct. The hypothesis is clearly correct when for example:

-   the radial input force component of a practical source to a pipe and the radial response (energy) component of natural pipe modes are each at least a factor of 10 higher than the sum of the axial and tangential input force components and the sum of the axial and tangential response components respectively, and

-   the energy transmissions corresponding to the transmission from radial pipe vibrations into out-of-plane plate vibrations and vice versa are at least a factor of 10 higher than the sum of the energy transmissions corresponding to other transmissions (from axial/tangential into in-plane vibrations, but also from axial/tangential into out-of-plane vibrations and vice versa).

However, also differences smaller than a factor of 10 might be acceptable. The following situation seems to be acceptable, for example:

-   the radial response (energy) component of natural pipe modes is a factor of 10 (10 dB) higher than the sum of the axial and tangential response components, but

-   the axial, tangential and radial input force components of a practical source to a pipe are equal, and

-   the energy transmissions corresponding to the transmission from radial pipe vibrations into out-of-plane plate vibrations and vice versa are equal to the sum of the energy transmissions corresponding to other transmissions.

Then the energy level of the pipe due to radial pipe responses is expected to be about 10 dB higher than the sum of energy levels of the pipe due to axial and tangential pipe responses. And the energy level of the plate due to out-of-plane plate responses is expected to be about 10 dB higher than the sum of energy levels of the plate due to in-plane plate responses. So, the energy level of the plate due to in-plane responses is negligibly small in the total energy level of the plate, which is approximately equal to the energy level of out-of-plane responses.

The assumptions 6 to 8 focus on the points mentioned above. The numbering of the assumptions does not correspond with the order in which they are dealt with in this thesis.
The response of natural modes in pipe systems (point Ab) has been studied separately. Assumption 6 focuses on point Ab. The excitation by practical sources has been investigated in combination with the response of natural modes in pipe systems. Assumption 7 focuses on point A as a whole. Input force components or input moment components in the three vibrational directions by practical sources have not been determined in this study, so in this thesis point Aa is not dealt with separately.
Assumption 8 focuses on point B.

Section 3.4 gives two criteria for the prediction accuracy of the simplified SEA model. For 99% of the predictions, the difference between predicted and real vibrational energy levels is 2,5 dB at most for A-weighted energy levels and 5 dB at most for energy levels in octave bands (see section 3.4 for an explanation).
For the assumptions in this section, the validation criteria are based on allowed inaccuracies for parts of the model. These inaccuracies are globally balanced with the criteria for the prediction accuracy of the complete model. Whether the validation criteria need to be reset, is discussed in chapter 7, based on results obtained in this study.

- *Assumption 6:* in each octave band considered, the responses of natural modes are predominantly radial for pipes and out-of-plane for plates.

    Validation criteria: in this thesis, for pipes, this assumption is defined to be valid if in each octave band considered the ratio of vibrational energy of radial responses to the sum of energies of axial and tangential responses is at least 1,3. For plates, in each octave band considered the ratio of energy of out-of-plane responses to the sum of energies of in-plane responses is also at least 1,3.

    The background of the criteria is explained for pipes in section 4.2.4 and for plates in section 4.4.4. These criteria are expected to result in an underestimation of the total

energy level (of the pipe and plate responses under the (theoretical) assumption of equipartition of incoming energy over all natural modes) of 2,5 dB at most.

Whether these validation criteria are met for practical water supply and wastewater pipes is theoretically investigated in section 4.2.4 and for practical plates in section 4.4.4.

▪ *Assumption 7:* practical sources in pipe systems, e.g. a water flow or a toilet, cause radial pipe vibrations to be more important as energy-carriers than axial and tangential pipe vibrations.

Validation criterion: in this thesis, this assumption is defined to be valid if in each octave band considered a practical source causes a pipe to vibrate in such a way that the ratio of vibrational energy of radial responses to the sum of energies of axial and tangential responses is at least 1,3.

The criterion is expected to result in an underestimation of the total energy level (of the pipe responses) of 2,5 dB at most (in line with the validation criterion corresponding to assumption 6).

Whether this validation criterion is met for practical excitation of vertical and horizontal pipes due to toilet flushing is investigated in section 6.4.

▪ *Assumption 8:* out-of-plane plate vibrations are predominantly caused by radial vibrations in pipe systems and vice versa. Radial vibrations in a pipe are predominantly caused by radial vibrations in another pipe that is part of the same pipe system.

For acoustical couplings this is correct anyhow, because sound radiation can only be caused by radial/out-of-plane vibrations. For structural couplings, this implies that axial and tangential pipe responses are assumed to be less effective than radial pipe responses in the sound transmission within pipe systems and from pipe systems through pipe clamps to plate structures for example. The reasoning behind this has been explained in more detail in section 3.2.3.2.

In this thesis, 'reciprocity relationship' *(2.7)* between subsystems is applied as a tool to test the validity of this assumption, more generally the subsystems redefinition and the simplified SEA model (and partly the applied parameter determination of coupling loss factors and modal densities).

58

For this purpose, the deviation $\Delta L_{rec.}$ from 'reciprocity relationship' *(2.7)* between two subsystems *1* and *2* is written as:

$$\Delta L_{rec.} = 10\,lg\left(\frac{n_1 \eta_{12}}{n_2 \eta_{21}}\right)$$

(3.3)

Modal densities and coupling loss factors have been determined for several set-ups in this study. Only radial pipe vibrations and out-of-plane plate vibrations have been analysed. The obtained results have been filled in in equation *(3.3)*, see chapter 5 of this thesis. Then, the extent to which the deviation from the 'reciprocity relationship' equals 0 dB [32] is a measure of the accuracy of simplified SEA model concerning energy transmission between subsystems.

The accuracy criterion for octave bands in section 3.4 is applied as a reference for maximal allowed deviations from the 'reciprocity relationship'. Deviations larger than 5 dB are not acceptable. Deviations of 5 dB at most might be acceptable. Might be, because the prediction accuracy of the complete model depends on more factors, e.g. the validity of assumption 7 concerning the excitation of pipe systems. Besides, the accuracy criterion of the complete model for A-weighted energy levels needs to be fulfilled too. When for example only one octave band dominates the A-weighted energy level an inaccuracy of more than 2,5 dB in this octave band is not allowed of course.

Validation criterion: in this thesis, this assumption is defined to be valid if for each pair of connected subsystems, the deviation from the 'reciprocity relationship' (as written in equation *(3.3)*) is 5 dB at most in each octave band considered.

Whether this validation criterion is met for a practical coupling between a pipe (system) and a plate is investigated in sections 5.4.4 and 5.6.5. For practical couplings within pipe systems, this is investigated in sections 5.5.4 and 5.6.5.

3.4   Prediction accuracy of the simplified SEA model

This section deals with the third question in section 3.3, i.e. whether the simplified SEA model is sufficiently accurate for our engineering purposes.
In section 3.3 various validation criteria have been set for parts of the simplified SEA model. However, in the end the prediction accuracy of the complete model determines

---

[32] In this thesis, differences are presented as *10lg(difference)*, so in dB's, in order to relate to the influence these differences have on energy levels.

whether the model is suitable. The prediction accuracy is determined by both the validity of the simplified SEA model and the accuracy of the determination methods for parameters. In this section criteria for the prediction accuracy are set. The criteria are set for the unknown variable, i.e. the vibrational energy in subsystems. The accuracy of the predicted energy level is assumed to be equal to the accuracy of a common variable in building acoustics, i.e. the sound pressure level. This is explained first.

As stated in section 1.1 criteria concerning noise due to service equipment are set in terms of maximum allowable, often A-weighted, sound levels in rooms. In some countries various comfort classes have been defined. Usually, a difference of 5 dB in A-weighted sound level roughly corresponds to a difference of one comfort class [ref 54].

In the simplified SEA model, the subsystem energy is the unknown variable, not the sound pressure level in a room. The relation between the sound pressure level in a room and the vibrational energy of the structure, e.g. a pipe system or a plate that is excited by a pipe system that is responsible for this sound pressure level is described below.

The sound pressure level $L_{p,i,rad}$ (re $2 \cdot 10^{-5}$ Pa) in a reverberant room o due to a radiating structure i can be written as[33]

$$L_{p,i,rad} = L_{\Pi,i,rad} - 10 \lg A_o + 6 dB \qquad (3.4)$$

where $L_{\Pi,i,rad}$ (re 10^{-12} W) is the radiated sound power level from a structure i and A_o is the equivalent absorption area[34] in the room o.

---

[33] The following relation between the radiated sound power and resulting sound pressure exists [ref 12]:

$\Pi_{i,rad} = (13,8 p^2_{i,rad} V_o)/(\rho_o c_o^2 T_o)$

where V_o, ρ_o, c_o and T_o are the volume of, density ($\approx 1,2$ kg·m^{-3}) of, propagation velocity of sound (≈ 340 m·s^{-1} at 20 ^{0}C) in and reverberation time of the (air-filled) acoustic volume (room) o respectively. $\Pi_{i,rad}$ is the radiated sound power from structure i. $p_{i,rad}$ is the average sound pressure (r.m.s.) in room o due to sound radiation from structure i.

[34] The equivalent absorption area A_o is related to the reverberation time T_o and the volume V_o of the room o by [ref 12]

$A_o = 0,16 V_o / T_o$

$L_{\Pi,i,rad}$ is related to the velocity level $L_{v,i}$ of the radiating structure i by[35]

$$L_{\Pi,i,rad} = L_{v,i} + 10 \lg \sigma_i + 10 \lg S_i + 10 \lg \frac{\rho_o c_o S_{ref} v_{ref}^2}{\Pi_{ref}} \qquad (3.5)$$

With $\rho_o \approx 1,2$ kg·m^{-3} and $c_o \approx 340$ m·s^{-1} for an air-filled acoustic volume, $S_{ref} = 1$ m^2, $v_{ref} = 10^{-9}$ m·s^{-1} and $\Pi_{ref} = 10^{-12}$ W, the last term in equation *(3.5)* results in –34 dB.

$L_{v,i}$ is related to the vibrational energy level $L_{E,i}$ of the radiating structure i by [ref 4][36]:

$$L_{v,i} = L_{E,i} - 10 \lg M_i + 10 \lg \frac{E_{ref}}{M_{ref} v_{ref}^2} \qquad (3.6)$$

With $E_{ref} = 10^{-12}$ J, $M_{ref} = 1$ kg and $v_{ref} = 10^{-9}$ m·s^{-1}, the last term in equation *(3.6)* results in +60 dB.

By combining equations *(3.4)* to *(3.6)*, equation *(3.4)* results in:

$$L_{p,i,rad} \approx L_{E,i} - 10 \lg M_i + 10 \lg \sigma_i + 10 \lg S_i - 10 \lg A_o + 32 dB \qquad (3.7)$$

Under the assumption that all parameters in equation *(3.7)* are known (or have negligibly small inaccuracies[37]) except $L_{E,i}$, the accuracy in sound pressure level in the room due to the radiating structure is equal to the accuracy in subsystem energy level.

---

[35] The power radiated from a structure i to an acoustic volume o can be written as [ref 12]

$\Pi_{i,rad} = \rho_o c_o S_i v_i^2 \sigma_i$

where S_i and v_i are the surface area and the average velocity (r.m.s.) of the structure respectively. σ_i represents the radiation efficiency of the structure.

[36] Equation *(3.6)* is derived from the fundamental relation [ref 4]:

$E_i = M_i v_i^2$

where v_i is the velocity (r.m.s.) averaged over the surface area of a structure i with uniformly distributed mass M_i.

[37] This is reasonable for single, homogeneous, heavyweight floors and walls, on which this thesis focuses. For other types of floors or walls the uncertainties in mass and radiation efficiency will be larger. As in all regular standards, sound levels will be normalized on (given for a reference value of) the equivalent absorption area (10 m^2) or reverberation time (0,5 s for residential buildings), so uncertainties in these quantities are not important.

Based on the foregoing the following criteria are set for the prediction accuracy of the simplified SEA model:

- for 99% of the predictions, the difference between the predicted A-weighted energy level of a pipe system or a plate that is excited by a pipe system and the real A-weighted energy level is 2,5 dB at most.

  The background of this criterion is illustrated by an example. Suppose that the simplified SEA model is applied for predictions regarding a future situation in which the energy level may not exceed 30 dB(A). And suppose that an energy level of 27,5 dB(A) is predicted. Because it is a prediction for a future situation, we do not know whether this value is correct. But we know that the value is correct within ± 2,5 dB(A), so that the real energy level (in the future) will lie between 25 dB(A) and 30 dB(A). Based on these results it will be concluded that the criterion of 30 dB(A) is expected to be fulfilled. In this case, one needs to reckon with a 30 dB(A) level, so system changes that might increase the sound level are not allowed for example. However, it is also possible that the real energy level appears to be 25 dB(A). Then, reckoning with a 30 dB(A) level leads to an overestimation of 5 dB(A) and system changes that increase the sound level (with 5 dB(A) at most) are allowed. Naturally, it is not reasonable to expect a prediction model to be exact. A prediction model should be so accurate that course over/underestimations are avoided. This has been taken into account in the foregoing criterion for the prediction accuracy of the simplified SEA model. By setting the criterion as mentioned, over/underestimations of more than 5 dB(A) are avoided and the noise perception corresponding to the predicted and real energy levels is equal (sound level differences of 5 dB and more correspond to clear differences in sound comfort/perception).

- for 99% of the predictions, the difference between predicted and real energy levels in the octave bands with centre frequencies 125 Hz to 2000 Hz is 5 dB at most.

  A criterion in octave bands makes the simplified SEA model useful for engineering. In order to compare and search for design alternatives, generally more detailed predictions than just A-weighted levels, i.e. in octave bands, are needed. Usually, the octave bands mentioned determine the A-weighted sound level. Further detailing, e.g. in 1/3-octave bands, does not seem necessary for engineering in building practice.

  Inaccuracies of 5 dB at most are allowed as a starting point, supposing that inaccuracies in different octave bands might to some extent cancel each other in the calculation of corresponding A-weighted energy levels. Besides, it is possible that an inaccuracy of 5 dB in one octave band is not important at all, because this octave band does not contribute to the A-weighted energy level. On the contrary, it is also possible that an octave band dominates the A-weighted energy level. In that case an inaccuracy of more

than 2,5 dB in this octave band is not allowed of course. These, and more issues related to the accuracy of the simplified SEA model, are discussed in chapter 7, based on results obtained in this study.

3.5   Conclusions

This chapter describes how SEA is applied in this thesis to model the sound transmission through pipe systems and from pipe systems into plates.
In section 3.2.1 a system for this sound transmission problem has been defined.
In section 3.2.2 a so-called "extensive SEA model" has been developed, in which all possible mode types, their excitation and their couplings have been represented separately.

The main focus of this chapter has been the simplified application of SEA to model the system. Based on various assumptions concerning the vibrational characteristics and excitation of pipe systems, plates and their couplings, the number of subsystems per physical system element (pipe or plate) has been reduced to one, resulting in a so-called "simplified SEA model", see section 3.2.3.
The model is based on the hypothesis that radial pipe vibrations and out-of-plane plate vibrations as response components are dominant in the sound transmission. This hypothesis results from several assumptions. Besides, the model is based on several assumptions that are similar to general SEA assumptions. Section 3.3 describes the assumptions and corresponding criteria, which are applied to test the validity of the assumptions in the next chapters of this thesis.
It is assumed that a model which considers only radial pipe vibrations and out-of-plane plate vibrations as response components is sufficiently accurate for engineering purposes. To enable testing the validity of this assumption (as is done in chapter 7), section 3.4 gives criteria for the prediction accuracy of the model. This accuracy depends on the accuracy of the model parameters and on the correctness of the assumptions of the model. For some assumptions, allowed (in)accuracies are mentioned in section 3.3. These (in)accuracies have an important contribution to the prediction accuracy of the model. They are globally balanced with the criteria for the prediction accuracy of the complete model. Whether the validation criteria need to be reset, is discussed in chapter 7, based on results obtained in this study.

CHAPTER 4
MODAL PROPERTIES OF SYSTEM ELEMENTS

4.1   Introduction

This chapter is aimed at testing the validity of the assumptions 1 to 3 and 6 of the simplified SEA model (see section 3.3). These assumptions deal with the modal properties of physical system elements that are subject of this thesis. These are straight pipes, discontinuities in pipe systems and plates (walls and floors) in buildings.

To test the validity of the assumptions, three determination methods for parameters have been applied, namely analytical approximations, the Finite Element Method (FEM) and experiments.

For straight pipes and plates the approximations are preferred for the tests. The disadvantages of FEM compared to the approximations are the huge storage and computational time. The disadvantage of experiments is that in-plane modal properties are difficult, if not impossible, to determine experimentally (see section 3.2.3). However, for some of the pipes and plates studied the validity of the approximations is restricted to the low and mid frequency range (upper frequency limit 500-1250 Hz, see sections 4.2 and 4.4). Therefore, based on comparisons with FEM-results (for straight pipes) and experimental results (for a straight pipe and a plate), it has been determined whether the approximations are sufficiently accurate for testing the validity of the assumptions for other types of pipes and plates.

For discontinuities in pipe systems, the preferred determination method depends on the type of discontinuity. For each type of discontinuity considered the most practical determination method has been applied.

The modal properties and test results for straight pipes, discontinuities in pipe systems and plates are described in sections 4.2, 4.3 and 4.4 respectively.

Each section starts with a description of the vibro-acoustic behaviour of the type of physical system element considered. It is described which types of free waves can exist within the element type. These, together with the dimensions and the boundary conditions of a physical system element, determine at which frequencies which (type of) natural modes can occur. Values for different modal parameters, e.g. numbers of modes and modal overlaps, are presented for various characteristic physical system elements.

For straight pipes and plates, sections 4.2 and 4.4 also contain comparisons of results obtained with the different determination methods for parameters, as mentioned above.

At the end of each section, the validity of the assumptions concerning the modal properties of physical system elements is tested, based on the obtained results. Furthermore, it is concluded for which frequency range SEA is applicable as a modelling method for sound transmission in the systems considered. This thesis focuses on wastewater pipe systems. Nevertheless, the validity of the assumptions is also tested for straight water supply pipes. This is done to illustrate the suitability of SEA as a modelling method for sound transmission in and from pipe systems of service equipment in buildings in general.

4.2   Straight water supply and wastewater pipes

4.2.1   Vibro-acoustic behaviour

The vibro-acoustic behaviour of pipes can be described by solving the equations of motion for the coupled system of shell, i.e. pipe wall, and fluid. The derivation of equations for shell motion can be found in many textbooks, see for example [ref 12], [ref 13] and [ref 14]. During the last century various scientists have given different solutions of the equations of motion. This has resulted in different shell theories. The differences are due to slight differences in simplifying assumptions and/or the exact point in a derivation where a given assumption is used. Various shell theories and the corresponding assumptions have been compared with each other by Leissa [ref 14].

Appendix I of this thesis describes the equations of motion in the frequency domain and the corresponding assumptions. Solving the equations of motion results in the dispersion equations that give the wave number-frequency relationships for different types of free waves in a fluid-filled pipe [ref 25]. For a couple of practical pipes dispersion curves have been calculated, see appendix I.

From the dispersion equations and the pipe length, the numbers of modes corresponding to different types of free waves can be calculated. This has been done for a couple of practical pipes, see sections 4.2.2.1 and 4.2.2.2. From the number of modes and loss factor of these pipes, the modal overlap has been calculated. The number of modes and modal overlap within practical, straight pipes are needed to test the validity of the assumptions 1 and 2 of the simplified SEA model, see section 4.2.4.

Also, for a couple of pipes ratios of the amplitudes of shell displacement[38] in different directions have been calculated for several types of free waves. These ratios give insight in

---

[38] The ratios of the amplitudes describe the three-dimensional motion of shell, i.e. pipe wall, and fluid [ref 25].

the directions in which pipes primarily vibrate. This information is needed to test the validity of assumption 6 of the simplified SEA model, see section 4.2.4.

4.2.1.1 Free waves

Appendix I of this thesis gives approximate dispersion equations derived by Pavic [ref 20] and De Jong [ref 25] from Flügge's shell theory. For some characteristic water supply and wastewater pipes dispersion curves have been calculated using these equations.

The pipe dimensions, pipe wall material and pipe fluid[39] determine which types of free waves can propagate in a pipe within the frequency range of interest. The calculation results in appendix I show that generally only acoustic, quasi-longitudinal, torsional and first-order flexural waves can propagate in practical brass water supply pipes. In practical plastic wastewater pipes also higher-order flexural waves can propagate.

4.2.1.2 Amplitude ratios for different types of free waves

Appendix I of this thesis describes the ratios of the amplitudes of shell displacement at each wave number solution according to Flügge's shell theory, see [ref 25], [ref 20] and [ref 14]. For some characteristic water supply and wastewater pipes amplitude ratios for the different types of free structural waves have been calculated.

The calculation results in appendix I show that the main vibrational direction of acoustic waves is axial at low frequencies for the wastewater pipes considered. Radial vibrations start to dominate above the frequency where the non-dimensional fluid wave number κ_a exceeds Poisson's ratio ν. For the water supply pipe considered (brass pipe with a relatively small diameter) the vibrations are mainly axial in the entire frequency range of interest.
The main vibrational direction of quasi-longitudinal waves is axial. At high frequencies radial vibrations become more important.
The main vibrational direction of torsional waves is tangential.[40]

---

[39] In practice wastewater pipes are partly filled with water and dirt and partly with air. In this study calculations have been done for wastewater pipes completely filled with water or completely filled with air, assuming that the values for properties of practical pipes lie somewhere between the calculated values. This is allowable as long as no exact values are needed, which is the case in this chapter.

[40] Since fluid-wall friction has been neglected in the non-dimensional wave number descriptions of De Jong [ref 25] and Pavic [ref 20] the torsional wave motion is independent of the fluid motion and purely tangential. This is a basic assumption and has not been proved on the basis of calculations in this study.

First-order flexural waves cause flexural motions of pipes. Due to these motions a point of the pipe wall vibrates primarily in the radial or tangential vibrational direction or equally in both directions, depending on its position on the pipe circumference. Therefore, the amplitudes of the radial and tangential vibrational components are approximately equal and larger than the amplitudes of the axial vibrational component. For the higher-order flexural waves the vibrations are more radial than tangential. The amplitudes of the radial and tangential vibrational components are larger than the amplitudes of the axial vibrational component.

4.2.2   Theoretical study of the modal behaviour

4.2.2.1   Derivation of mode count and modal overlap equations

For a uni-axial, prismatic wave-guide subsystem i the mode count N_i up to a certain frequency can be calculated from the wave number k_i for the type of free wave considered, the subsystem length L_i and a constant $\delta_{i,BC}$ [ref 4], [ref 23]:

$$N_{i,1D} = \frac{k_i L_i}{\pi} \pm \delta_{i,BC} \qquad\qquad (4.1)$$

The constant $\delta_{i,BC}$ has a value between zero and one, depending on the boundary conditions of the subsystem. $\delta_{i,BC}$ equals zero if the subsystem is simply supported at both ends. In case other boundary conditions apply the relative error of taking $\delta_{i,BC}$ equal to zero diminishes for large wave-guide systems [ref 23].

As stated, equation *(4.1)* applies to uni-axial, prismatic wave-guide subsystems [ref 23]. For pipes only the mode shapes of acoustic, quasi-longitudinal and torsional modes meet this condition. For first- and higher-order flexural modes there are two modes with equal real wave numbers at each natural frequency, see equation *(I.12)* in appendix I[41]. So for flexural modes the mode count N_i has to be multiplied by a factor of two.

---

[41] The reason for this is that there are two non-vanishing components of displacement V and W that give the system two degrees-of-freedom [ref 52]. In cylindrical shells there is degeneracy of modes: the mode shapes are represented by degenerate mode pairs because of the non-preferential directions available for the mode shapes due to structural axisymmetry [ref 79].

For simply supported pipes $(\delta_{BC}=0)$, equation *(4.2)* [ref 23] gives a summation of the mode counts for the different types of modes up to a certain frequency:

$$N_{pipe} = \frac{1}{\pi} k_a L_{pipe} + \frac{1}{\pi} k_l L_{pipe} + \frac{1}{\pi} k_t L_{pipe} + \frac{2}{\pi} \sum_{n=1}^{n(max)} k_n L_{pipe} \qquad (4.2)$$

where k_a, k_l and k_t represent the wave-numbers for acoustic, quasi-longitudinal and torsional waves respectively. *n* represents the circumferential mode number and *n(max)* the highest circumferential mode number of the modes that can occur within the frequency range of interest.

The number of modes ΔN_i per subsystem *i* and the total number of modes of all subsystems ΔN_{pipe} in a pipe element within (1/3-)octave bands have been calculated with:

$$\Delta N = N_{upper} - N_{lower} \qquad (4.3)$$

where N_{upper} and N_{lower} are the mode counts in integers[42] up to respectively the upper frequency and lower frequency limits of the (1/3-)octave band considered. In the calculations, the approximate wave number equations[43] derived by Pavic and De Jong have been applied, see appendix I.

---

[42] Only when the mode count becomes an integer, a new mode originates. Since this chapter focuses on the determination of the frequency bands in which at least two modes per band originate, N_{upper} and N_{lower} have been rounded down before subtraction. In case of performing calculations with numbers that are not rounded down, a mode could be assigned to the frequency band below or above the frequency band in which the mode originates. The (small) deviations due to performing calculations with non-rounded down numbers decrease at increasing frequency.

However, in most predictions the statistical mode count should be used, because it is the statistical mean property of the subsystem considered. The statistical mode count is not a round number. As the response of a mode to broadband excitation can be spread over a range of frequencies, part of the response may be in one frequency band and part in another. It is therefore physically meaningful to work with non-round numbers for some calculations [ref 5].

[43] The approximate equations are valid far below the so-called ring frequency of a pipe. For the plastic pipes considered the ring frequency is 4406 Hz. So, strictly speaking for these pipes the analytical approximations are only valid below about 500 Hz. Comparisons with FEM and experimental results will show that the approximations give results that are sufficiently accurate for the validity tests in this chapter (see sections 4.2.2.4 and 4.2.3.3). For the brass pipes considered the ring frequency lies above 30000 Hz. So for, these pipes the approximations are valid in the entire frequency range of interest.

The modal overlap M_i within a subsystem i, and M_{pipe} of all subsystems within a pipe element, have been calculated with equation *(2.15)* in section 2.5.4. For this purpose the modal density in 1/3-octave bands has been determined with:

$$n = \frac{N_{upper} - N_{lower}}{0,23 f_{centre}} \qquad (4.4)$$

where *0,23f_{centre}* represents the bandwidth of a 1/3-octave band with centre frequency f_{centre} [ref 4]. For calculations of modal densities in octave bands bandwidths of *0,71f_{centre}* have been applied in equation *(4.4)*. Statistical mode counts have been used to calculate modal densities and modal overlaps (see footnote 42).

4.2.2.2 Results from mode count and modal overlap equations

Number of modes

For practical wastewater and water supply pipes the number of modes has been calculated for each type of mode[44], i.e. the subsystems defined in the extensive SEA model in section 3.2.2. The calculation results for pipe lengths[45] of 3 m and 10 m and for the 1/3-octave bands with centre frequencies 100 Hz to 2500 Hz are presented in Figure 4-1 to Figure 4-3.

The validity testing of the assumptions of the simplified SEA model concerns specific mode types and results in octave bands (see section 4.2.4). This section is aimed at studying the modal characteristics of pipes in more detail. This is why all types of modes are considered and why results for 1/3-octave bands are presented.

---

[44] Since there are 2 modes per natural frequency for first- and higher-order flexural modes the number of first- and higher-order flexural modes is even in all frequency bands.

[45] The considered pipe materials, pipe lenghts and the lengths in between are supposed to cover an important part of the pipes that cause noise complaints in practical situations. In residential buildings in the Netherlands a pipe length of about 3 m is a characteristic length for vertical wastewater pipes, consisting of one element, which are storey-high. In practice wastewater pipes consisting of one element with a length of 10 m do not exist. Water supply pipes can have lengths of 10 m. The calculation results are only valid for 3 m or 10 m long pipes consisting of either one element or more than one element, which vibrate as one continuous element, e.g. two or more wastewater pipes coupled by straight pipe system discontinuities might behave as one element in a part of or in the entire frequency range of interest (in that case the pipes are not weakly coupled).
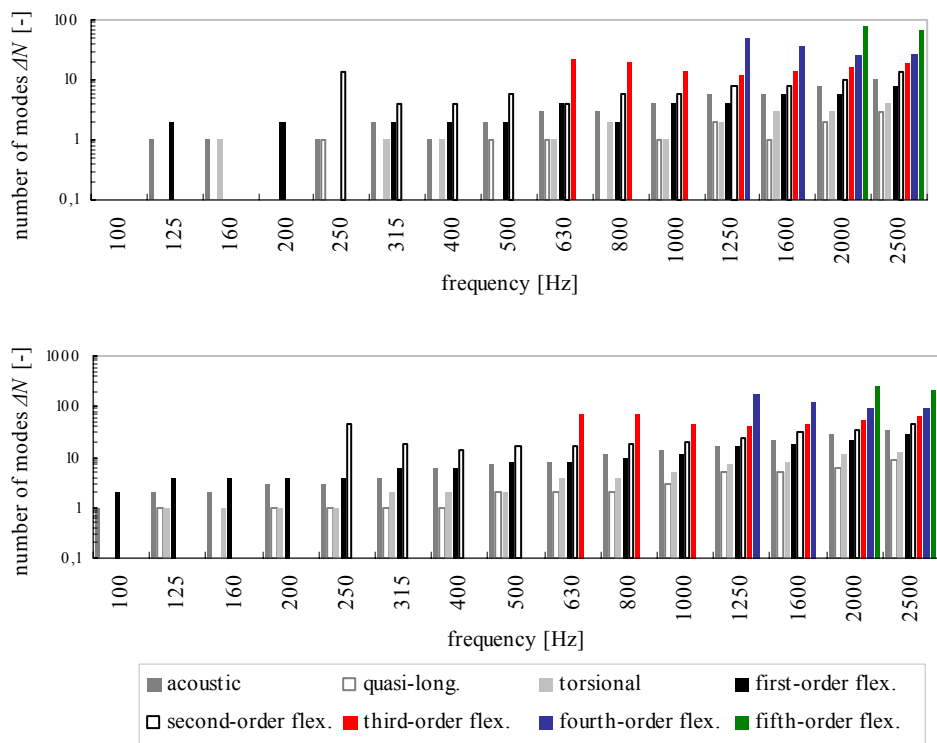
Figure 4-1 Number of modes ΔN in 1/3-octave bands for various mode types in air-filled PVC pipes with 3,8 mm wall thickness and an outer shell radius of 55 mm. Calculation results are for pipe lengths 3,0 m (**upper**) and 10,0 m (**lower**).
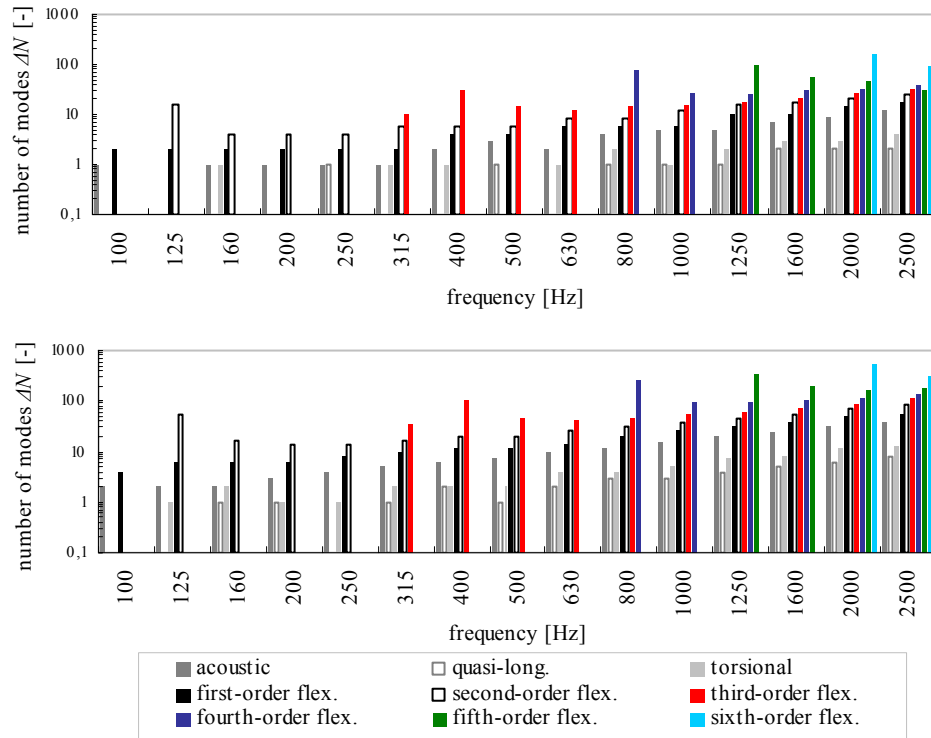
Figure 4-2 Number of modes *ΔN* in 1/3-octave bands for various mode types in <u>water-filled PVC pipes</u> with 3,8 mm wall thickness and an outer shell radius of 55 mm. Calculation results are for pipe lengths 3,0 m (**upper**) and 10,0 m (**lower**).
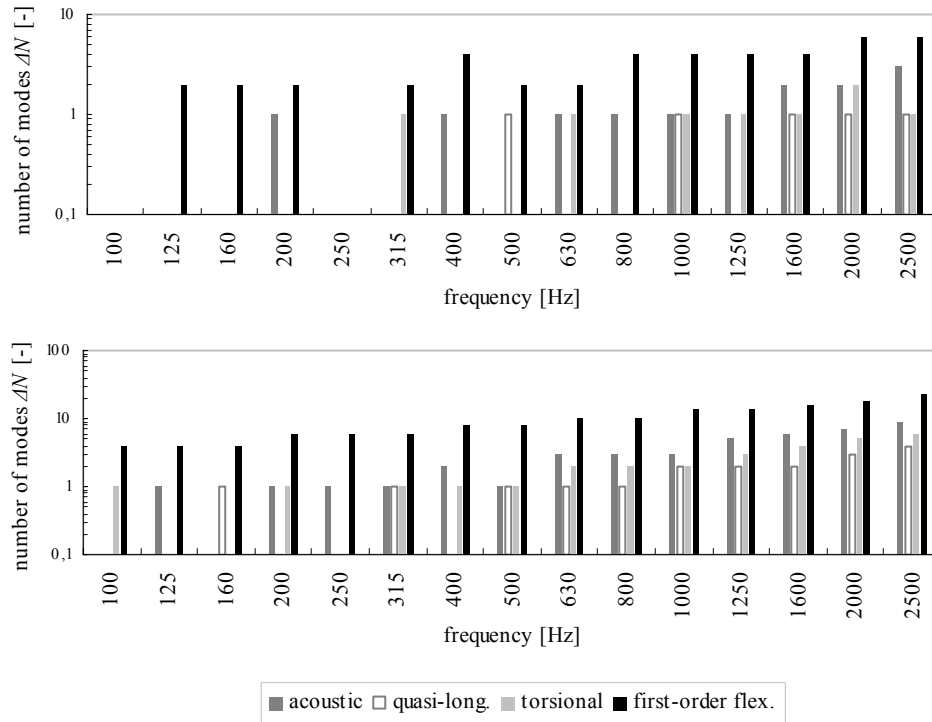
Figure 4-3 Number of modes ΔN in 1/3-octave bands for various mode types in <u>water-filled brass pipes</u> with 2 mm wall thickness and an outer shell radius of 15 mm. Calculation results are for pipe lengths 3,0 m (**upper**) and 10,0 m (**lower**).

The numbers of quasi-longitudinal and torsional modes are the smallest, followed by the numbers of the acoustic and first-order flexural modes. Due to the large phase velocities of higher-order flexural waves, the numbers of higher-order flexural modes are the largest[46]. Generally speaking, for the air- and water-filled wastewater (PVC) pipes in each 1/3-octave band the total number of (first- and higher-order) flexural modes exceeds the numbers of quasi-longitudinal and torsional modes by a factor of at least 5 to 10 from the cut-on frequency for $n=2$ on. For the water-filled brass pipes the number of (first-order) flexural

---

[46] Möser et al. [ref 84] have shown that the phase velocities of higher-order flexural waves are explicitly large at the cut-on frequencies. Therefore, the wave number and consequently the number of higher-order flexural modes are very large at the cut-on frequencies. On the other hand, they also have shown that the group velocities are very small at the cut-on frequencies. The group velocity is the velocity at which energy propagates [ref 12].

modes also exceeds the numbers of quasi-longitudinal and torsional modes, however by a factor of 2 to 5.

In the air-filled PVC wastewater pipe with a pipe length of 3 m first-order flexural modes can exist starting with the 1/3-octave band[47] with centre frequency 315 Hz. Acoustic modes and higher-order flexural modes can exist above 250 Hz. Quasi-longitudinal and torsional modes can exist above 1000 Hz and 630 Hz respectively. For larger pipe lengths the frequencies mentioned are lower, for shorter pipe lengths higher, except for the higher-order flexural modes.

In the water-filled PVC wastewater pipe with a pipe length of 3 m first-order flexural modes can exist starting with the 1/3-octave band with centre frequency 100 Hz. Higher-order flexural modes can exist above 125 Hz. Acoustic modes can exist above 160 Hz. Quasi-longitudinal and torsional modes can exist above 800 Hz and 630 Hz respectively.

In the water-filled brass water supply pipes no higher-order flexural modes can exist in the frequency range of interest[48]. In the brass pipe with a pipe length of 3 m first-order flexural modes can exist starting with the 1/3-octave band with centre frequency 315 Hz. Acoustic, quasi-longitudinal and torsional modes can exist above 630 Hz, 1600 Hz and 1000 Hz respectively.

Modal overlap

For each type of mode in the air-filled PVC pipes the modal overlap has been calculated. In the calculations a damping loss factor value of 0,04 has been applied for the PVC pipe wall, for all mode types, within the entire frequency range of interest. This value has been derived from structural reverberation time measurements (see section 5.3) and is a mean value for the frequency range of interest. In the calculations the centre frequency of each 1/3-octave band has been applied, see equation *(2.15)* in section 2.5.4.

The calculation results for the 1/3-octave bands with centre frequencies 100 Hz to 2500 Hz are presented in Figure 4-4. In case no value is shown for a mode type in a certain 1/3-octave band, then the modal overlap is smaller than 0,1 in that band. For the water-filled PVC and brass pipes the most important calculation results are only described.

---

[47] From the 1/3-octave bands on, mentioned in this text and indicated by their centre frequencies, the number of first-order and higher-order flexural modes per 1/3-octave band is at least 2 and the number of acoustic, quasi-longitudinal and torsional modes per 1/3-octave band is at least 1. In lower 1/3-octave bands sometimes also modes can exist (see the figures). However, between these bands and the bands mentioned there are 1/3-octave bands in which no modes can exist.

[48] In practical brass water supply pipes with a pipe radius of at least about 25 mm second-order flexural modes can exist below 2500 Hz.
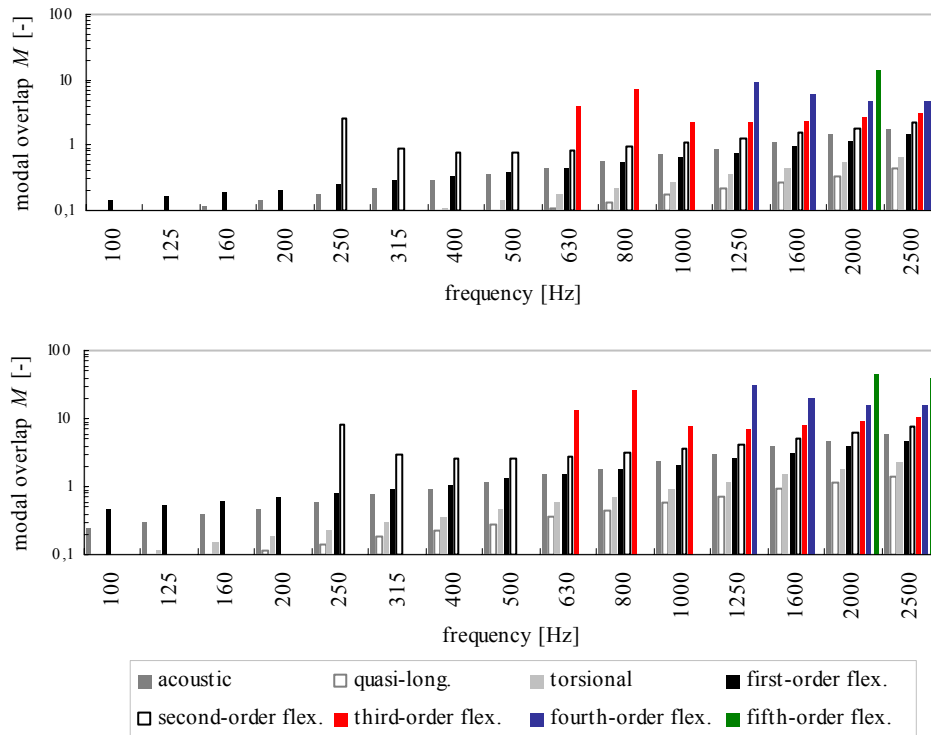
Figure 4-4   Modal overlap M in 1/3-octave bands for various mode types in <u>air-filled PVC pipes</u> with 3,8 mm wall thickness and an outer shell radius of 55 mm. Calculation results are for pipe lengths 3,0 m (**upper**) and 10,0 m (**lower**) and a damping loss factor of 0,04 for the PVC pipe wall.

For the air-filled PVC wastewater pipe with a pipe length of 3 m in each 1/3-octave band the modal overlap becomes larger than 1 above 2500 Hz for the quasi-longitudinal and torsional modes, above 1250 Hz, 1600 Hz and 800 Hz for the acoustic, first-order flexural and second-order flexural modes respectively and above the cut-on frequency for the third-, fourth- and fifth-order flexural modes. For larger pipe lengths the frequencies mentioned are lower, for shorter pipe lengths higher, except for the third-, fourth- and fifth-order flexural modes. Generally speaking, from the cut-on frequency for $n=2$ on the total modal overlap due to (first- and higher-order) flexural modes becomes 1 or larger, while the modal overlaps of the quasi-longitudinal and torsional modes are smaller than 1 in the entire frequency range of interest, except at high frequencies for (very) long pipes.

For the water-filled PVC wastewater pipe with a pipe length of 3 m (results not shown) in each 1/3-octave band the modal overlap becomes larger than 1 above 630 Hz and 400 Hz

for the first- and second-order flexural modes respectively. The modal overlaps for the other mode types become larger than 1 at the same frequencies as mentioned above for the air-filled PVC wastewater pipe.

For the water-filled brass water supply pipes (results not shown) the modal overlaps are much lower than the modal overlaps in the PVC wastewater pipes. The modal overlap is smaller than 0,1, i.e. far below unity, in the entire frequency range of interest. This is mainly due to the low damping loss factor of the pipe wall (a value of 0,001 has been applied in the calculations).

4.2.2.3   Determination of natural frequencies with the Finite Element Method (FEM)

As mentioned in section 4.2.2.1, strictly speaking the approximate dispersion equations applied for the mode number calculations are not valid in the entire frequency range for practical PVC pipes. In order to determine whether the approximations are sufficiently accurate for testing the validity of the model assumptions in this chapter, natural frequencies obtained with the approximations have been compared with natural frequencies obtained with FEM. If the choices of elements, boundary conditions, meshing etc. are appropriate for the system to be modelled, FEM gives results with a high degree of precision. This is an advantage of FEM compared to the approximations. However, disadvantages of FEM are the huge storage and computational time, specifically for relatively large physical elements such as pipes and plates.

Some straight air- and water-filled plastic and steel pipes with a pipe length of 1 m have been modelled in the FEM-package Ansys 5.4 [ref 37]. The FEM models are not described in detail. Appendix II gives the most important characteristics of the models. For a detailed description the reader is referred to [ref 36]. With FEM the natural frequencies and mode shapes of these pipes have been calculated[49].

4.2.2.4   Comparison of results obtained with FEM and approximations

Figure 4-5 shows some of the mode shapes that have been calculated. For several circumferential mode types the mode shape for one corresponding axial mode is presented.

---

[49] The FEM models have been limited to a pipe length of 1 m because of the required storage and computational time. FEM calculations with different boundary conditions have been done, among which boundary conditions that 'simulate' infinitely long pipe vibrational behaviour.

76

acoustic mode
n=0, m=2

torsional mode
n=0, m=3

quasi-longitudinal mode
n=0, m=2

first-order flexural mode
n=1, m=5

second-order flexural mode
n=2, m=1

third-order flexural mode
n=3, m=1
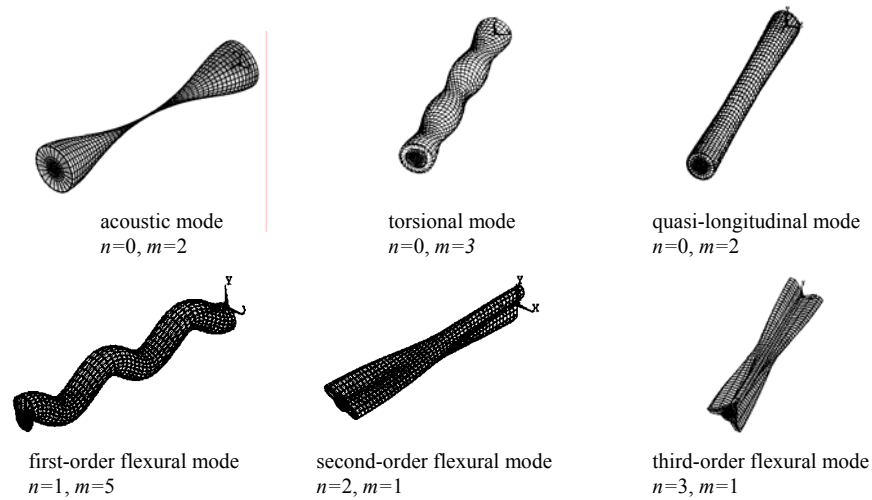
Figure 4-5   Mode shapes for various fluid and structural modes in an air-filled PE pipe with 5 mm wall thickness, mean shell radius 50 mm and pipe length 1,0 m

For a PVC pipe the natural frequencies in the frequency range 100 Hz to 2500 Hz obtained with FEM and with the approximations are plotted in Figure 4-6 and Figure 4-7.[50]

---

[50] In both calculations different values than in all other calculations in this thesis have been applied for the propagation velocity of quasi-longitudinal waves (1627 m/s) and the density (1245 kg/m^3) of PVC. In all other calculations in this thesis values of 1470 m/s and 1393 kg/m^3 have been applied. The FEM calculations have been done in an early stage of the study. Later in the study the values have been determined for commercial PVC pipes (see appendix I). For the comparison in this section, the 'old' values have been used in the approximations, instead of rerunning the FEM calculations, which would have been time-consuming and not necessary within the scope of this section.
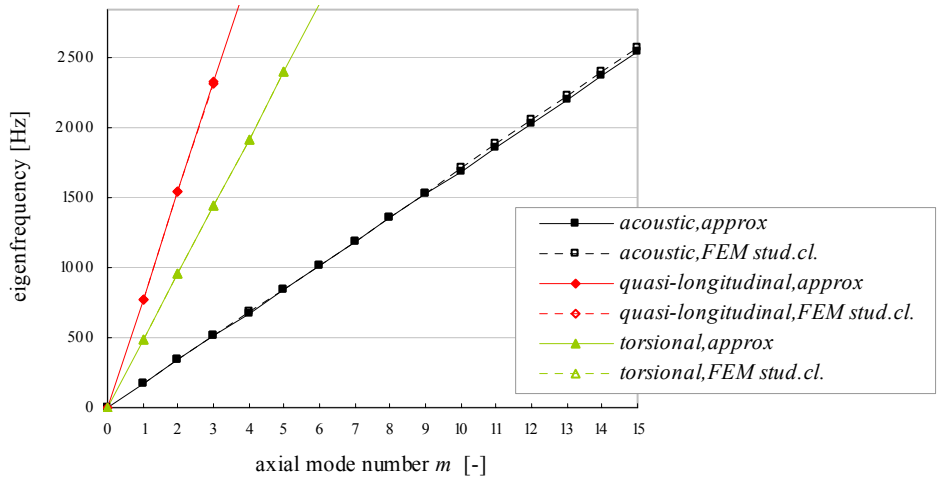
Figure 4-6 Natural frequencies with <u>circumferential mode number *n*=0</u> for an air-filled PVC pipe with 3,8 mm wall thickness, mean shell radius 53 mm and pipe length 1,0 m. Results obtained with <u>FEM</u> (boundary condition "stud clamping", see appendix II for a description of this boundary condition) and obtained with <u>approximations</u>.
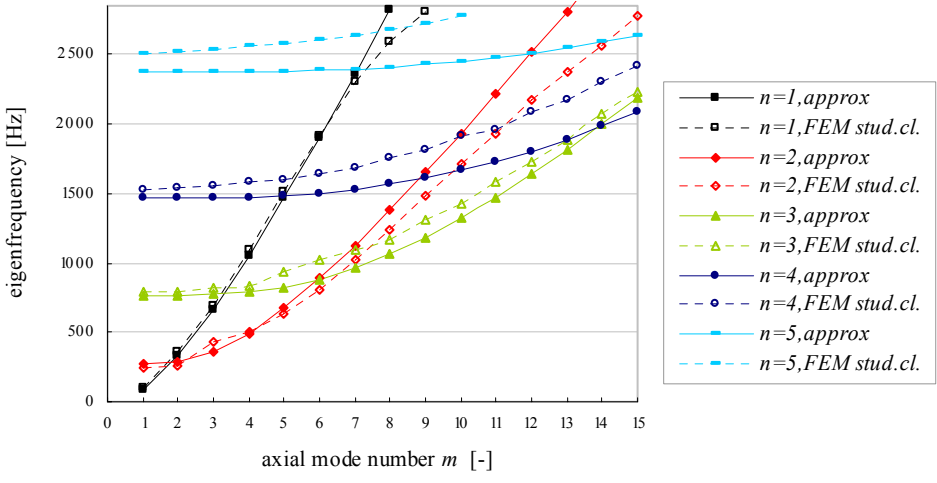
Figure 4-7 Natural frequencies with <u>circumferential mode numbers *n*≥1</u> for an air-filled PVC pipe with 3,8 mm wall thickness, mean shell radius 53 mm and pipe length 1,0 m. Results obtained with <u>FEM</u> (boundary condition "stud clamping", see appendix II for a description of this boundary condition) and obtained with <u>approximations</u>.

Figure 4-6 shows that for circumferential mode number *n=0* the natural frequencies obtained with FEM and with the approximations are almost equal within the frequency range of interest. Figure 4-7 shows that for *n≥1* this is generally also the case for the low and mid frequency range. In the high frequency range the relative differences generally become larger at increasing axial mode number, not at increasing circumferential mode number or at increasing frequency. For each axial mode number, the absolute differences become larger at increasing circumferential mode number. For each circumferential mode number, the absolute differences become larger at increasing axial mode number. In general, the absolute differences increase with increasing frequency. It is not clear whether the differences are due to the fact that the approximations are not valid in the high frequency range or by inappropriate choices of boundary conditions, elements or meshing in the FEM models.

In spite of the differences, the approximations are usable for a quick estimation of numbers of modes: for the given example 13% of the natural frequencies obtained with FEM and with the approximations falls in different 1/3-octave bands, 1% in different octave bands. They are sufficiently accurate for testing the validity of the assumptions concerning the modal properties of physical system elements.

The results for the other modelled pipes are comparable with the results presented [ref 36].

4.2.3 Experimental study of the modal behaviour and comparison of experimental and theoretical results for a wastewater pipe

4.2.3.1 Derivation of numbers of modes from point admittance measurements

The modal density n_i of a subsystem i can be derived from the subsystem mass M_i and the real part of the space-averaged point admittance $Re(Y_i)$ with [ref 5]:

$$n_i = 4M_i \overline{\langle Re(Y_i) \rangle}^{\Delta f} \qquad (4.5)$$

Actually $Re(Y_i)$ represents the point admittance per discrete frequency. In equation *(4.5)* $Re(Y_i)$ represents the point admittance averaged over a frequency band. Averaging is appropriate if the modal overlap within a frequency band is large[51]. Then the point

---

[51] Lyon and DeJong [ref 4] state that averaging is also appropriate if the subsystem is excited with a band of noise.

admittance shows small fluctuations within the frequency band[52], which is expected to provide statistically accurate results. In that case the point admittance becomes less dependent on small variations, which can cause shifting of a natural frequency from a frequency band into an adjacent frequency band for example.

For point excitations the point admittance can be determined from the (complex) excitation force F and the (complex) velocity v at the point of excitation:

$$Y = \frac{v}{F} \qquad\qquad (4.6)$$

Equations *(4.5)* and *(4.6)* can be applied to obtain the modal density in each vibrational direction of a physical system element from point admittance measurements. This implies that the total point admittance of different types of modes in each vibrational direction is determined. No distinction between mode types is made, unless only one mode type determines the point admittance in a vibrational direction.

From the modal density the total number of modes in each 1/3-octave band can be calculated by multiplying the modal density with the bandwidth of the 1/3-octave band considered (see equation *(4.4)*).

4.2.3.2 Experimental set-up and measurement method

For a straight PVC pipe with open ends[53] the total number of modes for mode types with a response component perpendicular to the pipe wall[54] (i.e. the radial vibrational direction) has been determined from point admittance measurements. Figure 4-8 shows the experimental set-up.

---

[52] For a single, homogeneous plate the point admittance in the central area tends to a constant value. This is the same value that would be obtained if the plate was considered to be infinite [ref 5].

[53] Because of the open ends at both sides reflection of the acoustic waves within the pipe occurs, so acoustic modes within the pipe can exist [ref 57].

[54] Practically speaking, these are primarily the first- and higher-order flexural modes and, probably to a lesser degree, quasi-longitudinal and acoustic modes.
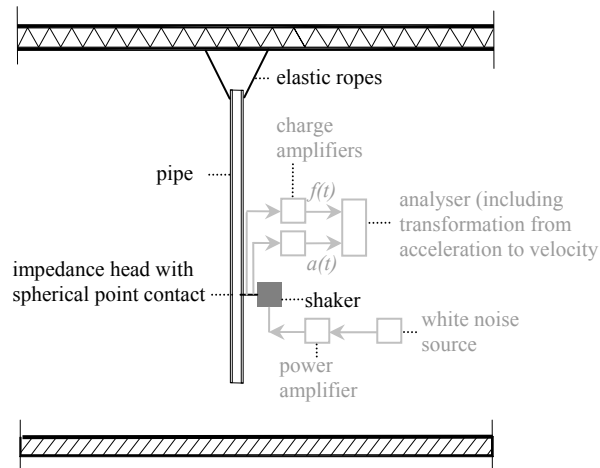
Figure 4-8   Experimental set-up for the determination of the total number of modes with a response component perpendicular to the pipe wall in an air-filled PVC pipe with 3,8 mm wall thickness, outer shell radius 55 mm and pipe length 2,7 m

The pipe was suspended from the ceiling of the measurement room by using elastic ropes. By doing so a mass-spring system was realised with a natural frequency below 10 Hz, i.e. far below the frequency range of interest. So it can be assumed that the pipe vibrated freely. The space-averaged real part of the point admittance has been estimated from force and acceleration[55] measurements at three positions[56] with an impedance head that was mounted between the pipe and a shaker. The measurement equipment is described in appendix V.

4.2.3.3   Experimental results and comparison with theoretical results

Figure 4-9 shows the number of modes in 1/3-octave bands as determined from the point admittance measurements[57] and as obtained from the mode count equations in section 4.2.2.1 with application of approximate wave number equations. The numbers of modes obtained with the two determination methods are compared in order to determine whether

---

[55] The measured accelerations were transformed into velocities in order to calculate the point admittance.

[56] Actually measurements at more than three positions should be done to obtain more accurate mean values (with a smaller variance). Nevertheless, the measurements seem to be sufficiently accurate within the context of this chapter (see the next section).

[57] Because of bad signal-to-noise ratios above 1600 Hz, no values are shown for 1/3-octave bands with centre frequencies above 1600 Hz.

the approximations are sufficiently accurate for testing the validity of the model assumptions in this chapter.

The number of modes calculated from the mode equations concerns the total number of acoustic and (first- and higher-order) flexural modes.[58]
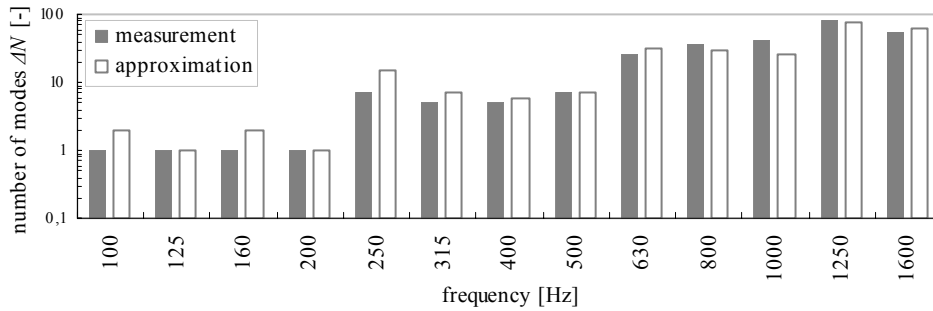
Figure 4-9 Number of modes ΔN in 1/3-octave bands with a vibrational response component perpendicular to the pipe wall in an air-filled PVC pipe with 3,8 mm wall thickness, outer shell radius 55 mm and pipe length 2,7 m. Experimental results and results from approximations.

Figure 4-9 shows a rather good agreement between the numbers of modes obtained from the measurements and from the mode count equations. It has been estimated which error would occur in case the results would be applied to determine coupling loss factors in one direction from coupling loss factors in the opposite direction (with equation *(2.6)* or *(2.7)*) or to determine deviations from the 'reciprocity relationship' (as written in equation *(3.3)*) for example.

In order to express the influence of the error on energy levels, the error has been defined as

$$error = 10\,lg\left(\frac{\Delta N_{meas}}{\Delta N_{approx}}\right) \qquad (4.7)$$

For each (1/3-)octave band within the frequency range of interest the error has been determined. For the 1/3-octave bands this results in errors between 0 dB and 3 dB up to 250 Hz (mean error over this frequency range 2 dB) and errors between 0 dB and 2 dB

---

[58] In order to compare the experimental results with the results from the approximations, the numbers of modes for the mode types mentioned have been summed, because these types of modes mainly cause vibrations perpendicular to the pipe wall. In the experiments no distinction between mode types has been made since the total point admittance of mode types with a vibrational direction perpendicular to the pipe wall has been determined.

from 315 Hz on (mean error 1 dB). For the octave bands this results in errors of 2 dB up to 250 Hz and errors of 1 dB from 500 Hz on.

Because the differences between measurements and approximations become smaller at increasing frequency the differences are not expected to be due to the fact that the approximations are not valid in the high frequency range. Probably the differences are (partly) caused by a limited accuracy of the measurements, e.g. because the number of modes is small below 250 Hz (see section 4.2.3.1), which also limits the accuracy of the mode count equations, and because the measurements have been done at a limited number of points (see footnote 56).

In spite of the differences, both approximations and measurements are sufficiently accurate for testing the validity of the assumptions concerning the modal properties of physical system elements.

4.2.4   Validity of the simplified SEA model for pipes

This section is aimed at testing the validity of the assumptions 1, 2 and 6 of the simplified SEA model concerning the modal properties of subsystems in practical water supply and wastewater pipes. The assumptions and corresponding validation criteria are given below. For the testing, the results obtained for the pipes in section 4.2.2.2 are used. The validation criteria are set for octave bands, but results for both 1/3-octave and octave bands are shown.

Validity of assumption 1

Assumption 1
The subsystems responses in each octave band considered are determined by a sufficiently large number of resonant modes. This assumption is defined to be valid if the number of modes per octave band is at least 6 for each subsystem.

In the simplified SEA model, only vibrations perpendicular to the physical elements surfaces are considered. In pipes, these vibrations are mainly caused by acoustic and (first- and higher-order) flexural modes. Therefore, the numbers of these types of modes are summed to test the validity of assumption 1. Actually, this test is only valid assuming that all natural modes are excited in practice, and therefore become resonant modes. The results are shown in Figure 4-10 to Figure 4-12. Also a value of 6 modes per octave band is shown, to indicate the criterion for a sufficiently large number of modes applied in this thesis. In case for a 1/3-octave band no value is shown, then no mode originates in that band.
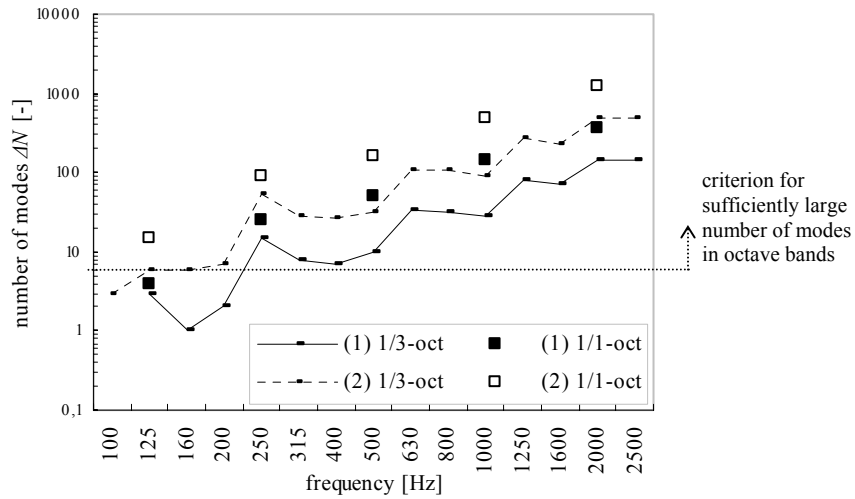
Figure 4-10 Total number of modes *ΔN* in (1/3-)octave bands with a mainly radial vibrational direction in (**1**) an air-filled PVC pipe with 3,8 mm wall thickness, outer shell radius 55 mm and pipe length 3,0 m and (**2**) as (1), but with pipe length 10,0 m. Also the criterion for a sufficiently large number of modes applied in this thesis is shown.
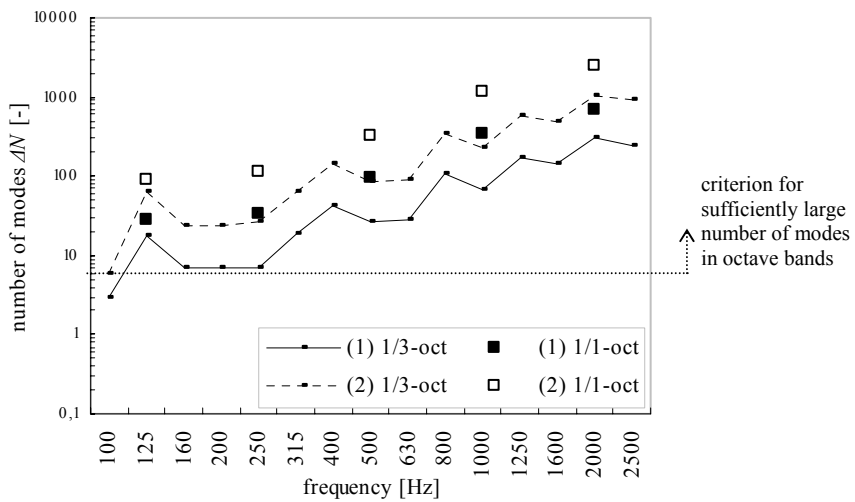
Figure 4-11 Total number of modes *ΔN* in (1/3-)octave bands with a mainly radial vibrational direction in (**1**) a water-filled PVC pipe with 3,8 mm wall thickness, outer shell radius 55 mm and pipe length 3,0 m; (**2**) as (1), but with pipe length 10,0 m. Also the criterion for a sufficiently large number of modes applied in this thesis is shown.
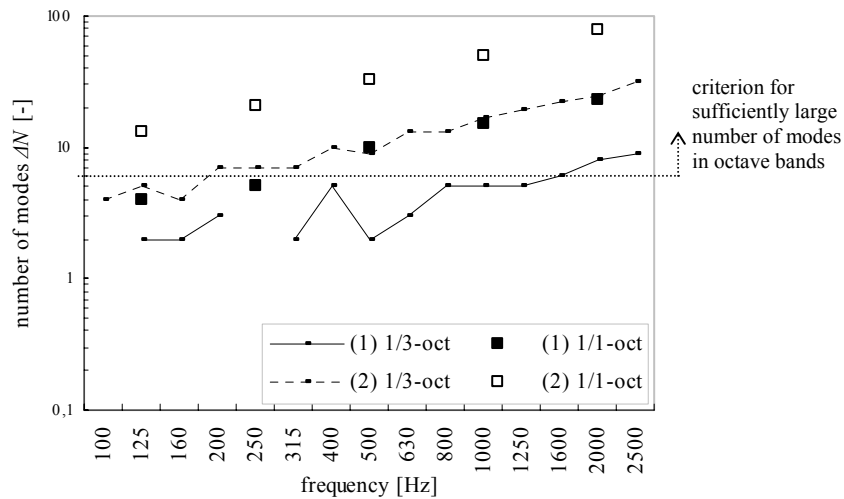
Figure 4-12 Total number of modes *ΔN* in (1/3-)octave bands with a mainly radial vibrational direction in (**1**) a water-filled brass pipe with 2 mm wall thickness, outer shell radius 15 mm and pipe length 3,0 m; (**2**) as (1), but with pipe length 10,0 m. Also the criterion for a sufficiently large number of modes applied in this thesis is shown.

For the air-filled PVC pipe with a pipe length of 3 m Figure 4-10 shows that the number of modes per octave band becomes at least 6 from 250 Hz on. So, assumption 1 is fulfilled from 250 Hz on. For the same pipe with a pipe length of 10 m and the water-filled PVC pipes (see Figure 4-11) with pipe lengths of 3 m and 10 m assumption 1 is fulfilled in the entire frequency range of interest. There are at least 6 modes per octave band.

For the water-filled brass pipe with a pipe length of 3 m Figure 4-12 shows that the number of modes per octave band becomes at least 6 from 500 Hz on. So, assumption 1 is fulfilled from 500 Hz on. For the same pipe with a pipe length of 10 m assumption 1 is fulfilled in the entire frequency range of interest.

Generally speaking, for practical wastewater pipes assumption 1 is fulfilled from 250 Hz on for air-filled pipes and from 125 Hz on for water-filled pipes, so almost in the entire frequency range of interest, although pipes with a smaller shell radius and pipe lengths smaller than 3 m have not been considered here. However, these pipes are expected to cause less noise complaints in practical situations, e.g. because they are applied inside houses and generally not in shafts in apartment buildings. For practical water supply pipes assumption 1 is only fulfilled for relatively long pipes. For shorter pipes the assumption is not fulfilled in the low frequency range.

Validity of assumption 2

Assumption 2

The subsystems responses in each octave band considered have sufficient modal overlap. This assumption is defined to be valid if the modal overlap in each octave band is at least 1 for each subsystem.

For each pipe the modal overlap corresponding to the total number of acoustic and flexural modes has been calculated. Actually, this test is only valid assuming that all natural modes are excited in practice, and therefore become resonant modes (see under Validity of assumption 1). The results are shown in Figure 4-13 to Figure 4-15. Also a value of 1 is shown, to indicate the criterion for sufficient modal overlap applied in this thesis.
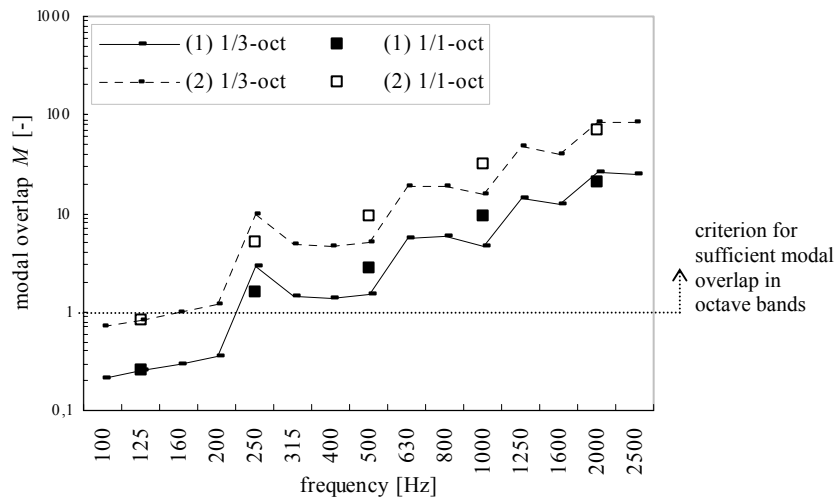
Figure 4-13 Modal overlap *M* in (1/3-)octave bands for modes with a mainly radial vibrational direction in (**1**) an <u>air-filled PVC pipe</u> with 3,8 mm wall thickness, outer shell radius 55 mm and <u>pipe length 3,0 m</u> and (**2**) as (1), but with <u>pipe length 10,0 m</u>. Also the criterion for sufficient modal overlap applied in this thesis is shown.
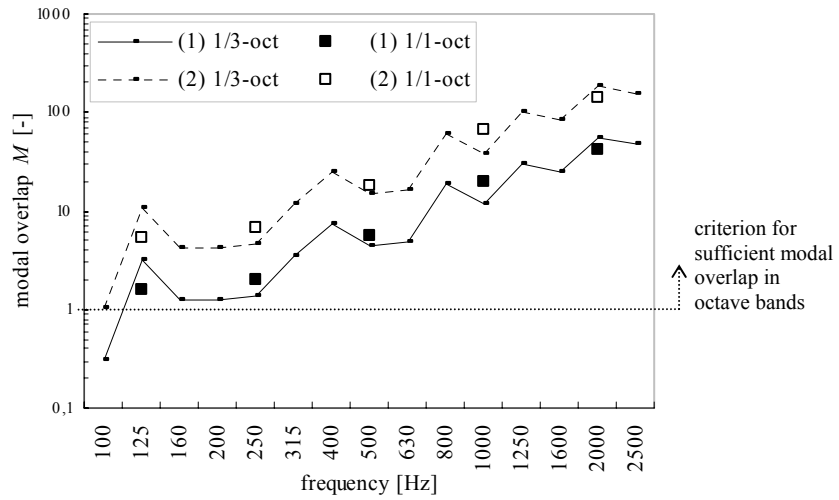
Figure 4-14 Modal overlap M in (1/3-)octave bands for modes with a mainly radial vibrational direction in (**1**) a water-filled PVC pipe with 3,8 mm wall thickness, outer shell radius 55 mm and pipe length 3,0 m and (**2**) as (1), but with pipe length 10,0 m. Also the criterion for sufficient modal overlap applied in this thesis is shown.
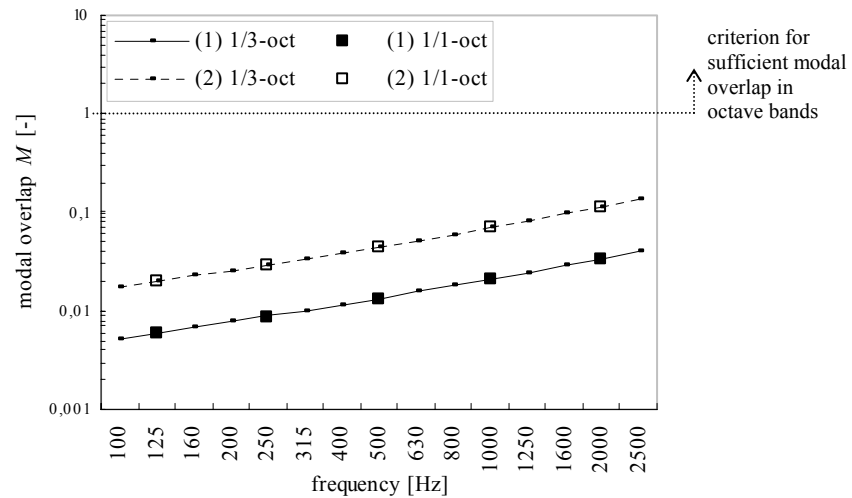
Figure 4-15 Modal overlap M in (1/3-)octave bands for modes with a mainly radial vibrational direction in (**1**) a water-filled brass pipe with 2 mm wall thickness, outer shell radius 15 mm and pipe length 3,0 m and (**2**) as (1), but with pipe length 10,0 m. Also the criterion for sufficient modal overlap applied in this thesis is shown.

For the air-filled PVC pipes with pipe lengths of 3 m and 10 m Figure 4-13 shows that the modal overlap per octave band becomes at least 1 from 250 Hz on. So, assumption 2 is fulfilled from 250 Hz on (for a pipe length of 10 m the modal overlap is nearly 1 at 125 Hz). For the water-filled PVC pipes (see Figure 4-14) with pipe lengths of 3 m and 10 m assumption 2 is fulfilled in the entire frequency range of interest.

For the water-filled brass pipes with pipe lengths of 3 m and 10 m Figure 4-15 shows that the modal overlap is smaller than 1 in the entire frequency range of interest. So, for these pipes assumption 2 is not fulfilled.

Generally speaking, for practical wastewater pipes assumption 2 is fulfilled from 250 Hz on for air-filled pipes and from 125 Hz on for water-filled pipes, so almost in the entire frequency range of interest, although pipes with a smaller shell radius and pipe lengths smaller than 3 m have not been considered here (see under the testing of assumption 1). For practical, metal water supply pipes assumption 2 is not fulfilled.

Validity of assumption 6

Assumption 6
In each octave band considered, the responses of natural modes are predominantly radial for pipes. This assumption is defined to be valid if in each octave band considered the ratio of vibrational energy of radial responses to the sum of energies of axial and tangential responses is at least 1,3.

In order to test the validity of this assumption the ratio of vibrational energies of responses in the three vibrational directions (axial, tangential and radial) has been estimated as described below.

Suppose that vibrational energy is submitted to a pipe and that this energy is equally distributed over all natural modes within the pipe. For the sake of the validity test of assumption 6, the modal energy (i.e. the energy per mode) is taken as $E'_j = 1$ J. In section 4.2.1.2 it has been described that all types of free waves in pipes, except torsional waves, have more than one vibrational direction. Suppose that the modal energy of 1 J is distributed over the different vibrational directions. Because the amplitudes in the three vibrational directions (axial, tangential and radial) differ, the energies of responses in the three vibrational directions will differ, so per mode the energy is not equally distributed over the vibrational directions. The energy distribution per mode is dependent on the mode type (or corresponding wave type) and on the frequency.

In Figure I-14 to Figure I-22 in appendix I the theoretical ratios of the amplitudes of pipe wall displacement in the axial, tangential and radial vibrational directions are shown for the

various wave types. From the ratios of the amplitudes, ratios of the energies of responses in the three vibrational directions have been calculated for each wave type i with:

$$\frac{E_{i,ax}}{E_{i,rad}} = \frac{M_i v_{i,rms,ax}^2}{M_i v_{i,rms,rad}^2} = \frac{(2\pi f)^2 U_{i,rms}^2}{(2\pi f)^2 W_{i,rms}^2} = \frac{\frac{1}{2}|U_i|^2}{\frac{1}{2}|W_i|^2} = \frac{\frac{1}{2}(\hat{U}_i)^2}{\frac{1}{2}(\hat{W}_i)^2} = \left(\frac{\hat{U}_i}{\hat{W}_i}\right)^2$$

(4.8)

$$\frac{E_{i,tan}}{E_{i,rad}} = \frac{M_i v_{i,rms,tan}^2}{M_i v_{i,rms,rad}^2} = \frac{(2\pi f)^2 V_{i,rms}^2}{(2\pi f)^2 W_{i,rms}^2} = \frac{\frac{1}{2}|V_i|^2}{\frac{1}{2}|W_i|^2} = \frac{\frac{1}{2}(\hat{V}_i)^2}{\frac{1}{2}(\hat{W}_i)^2} = \left(\frac{\hat{V}_i}{\hat{W}_i}\right)^2$$

where i represents a wave type and M_i the mass corresponding to this wave type. The mass term differs per wave type, e.g. for torsional waves this is the pipe wall mass, for first-order flexural waves the sum of pipe fluid mass and pipe wall mass. U_i, V_i and W_i represent the complex displacements of wave type i in respectively the axial, tangential and radial vibrational directions. A ^ on top of U_i, V_i and W_i denotes that the amplitudes of these variables are considered.

From the energy ratios in equation (4.8) it has been calculated which part of E'_j (i.e. an energy of 1 J per mode j in this case) results in energy of responses in the axial, tangential and radial vibrational directions respectively with:

$$E'_{j,ax} = \frac{\frac{E'_{j,ax}}{E'_{j,rad}} E'_j}{\left(\frac{E'_{j,ax}}{E'_{j,rad}} + \frac{E'_{j,tan}}{E'_{j,rad}} + \frac{E'_{j,rad}}{E'_{j,rad}}\right)}$$

(4.9)

$$E'_{j,tan} = \frac{\frac{E'_{j,tan}}{E'_{j,rad}} E'_j}{\left(\frac{E'_{j,ax}}{E'_{j,rad}} + \frac{E'_{j,tan}}{E'_{j,rad}} + \frac{E'_{j,rad}}{E'_{j,rad}}\right)}$$

$$E'_{j,rad} = E'_j - E'_{j,ax} - E'_{j,tan} = 1 - E'_{j,ax} - E'_{j,tan}$$

where $E'_{j,ax}$, $E'_{j,tan}$ and $E'_{j,rad}$ represent the energies in mode j in the axial, tangential and radial vibrational directions respectively. $E'_{j,ax}$, $E'_{j,tan}$ and $E'_{j,rad}$ lie between 0 and 1 J for

acoustic, quasi-longitudinal and flexural modes. For torsional modes $E'_{j,tan}$ equals 1 J, $E'_{j,ax}$ and $E'_{j,rad}$ are both 0 J.

Then per frequency band and per vibrational direction (axial, tangential or radial) the total energies of all modes together become[59]:

$$E_{tot,ax} = (E'_{a,ax} \cdot \Delta N_a) + (E'_{l,ax} \cdot \Delta N_l) + \sum_{n=l}^{n(max)} (E'_{n,ax} \cdot \Delta N_n)$$

$$E_{tot,tan} = (E'_{t,tan} \cdot \Delta N_t) + \sum_{n=l}^{n(max)} (E'_{n,tan} \cdot \Delta N_n) \qquad (4.10)$$

$$E_{tot,rad} = (E'_{a,rad} \cdot \Delta N_a) + (E'_{l,rad} \cdot \Delta N_l) + \sum_{n=l}^{n(max)} (E'_{n,rad} \cdot \Delta N_n)$$

where $E_{tot,ax}$, $E_{tot,tan}$ and $E_{tot,rad}$ represent the total energy of all modes together per frequency band in the axial, tangential and radial vibrational directions respectively.

ΔN represents the number of modes corresponding to the indicated mode type in the frequency band considered. The abbreviations a, l, t and n denote acoustic, quasi-longitudinal, torsional and flexural (with circumferential mode number n) modes respectively (were indicated by j in equation *(4.9)*).

$E'_{a,ax}$, $E'_{l,ax}$, $E'_{t,ax}$ and $E'_{n,ax}$ have been determined with the first relation in equation *(4.9)*. $E'_{a,tan}$, $E'_{l,tan}$, $E'_{t,tan}$ and $E'_{n,tan}$ have been determined with the second relation in equation *(4.9)*. $E'_{a,rad}$, $E'_{l,rad}$, $E'_{t,rad}$ and $E'_{n,rad}$ have been determined with the third relation in equation *(4.9)*. ΔN_a, ΔN_l, ΔN_t and ΔN_n have been determined with equation *(4.3)* in section 4.2.2.1. However, statistical mode counts have been applied (see footnote 42).

Per (1/3-)octave band and per vibrational direction the total energies have been estimated. For this purpose the energy ratios in equation *(4.8)* and the energies of responses in the axial, tangential and radial vibrational directions in equation *(4.9)* have been calculated at the centre frequencies of the (1/3-)octave bands. This is expected to give good estimations of the mean values over the (1/3-)octave bands.

Finally, the ratio of vibrational energy of radial responses to the sum of energies of axial and tangential responses has been estimated with:

$$ratio = \frac{E_{tot,rad}}{E_{tot,ax} + E_{tot,tan}} \qquad (4.11)$$

The ratio is independent of pipe length.

---

[59] An important drawback of this estimation method may be that no ratios of amplitudes for different wave types are included, e.g. the ratio of axial displacements for $n=2$ to axial displacements for $n=3$.

A ratio of at least 10 means a difference between the energy level of radial responses and the sum of energy levels of axial and tangential responses of at least 10 dB. The sum of energies of axial and tangential responses is then negligibly small compared to the energy of radial responses. In that case the sum of the energies of responses in the three vibrational directions[60] equals the energy of radial responses and assumption 6 is clearly fulfilled. However, in this study also smaller ratios are allowed. Neglection of vibrations in the axial and tangential vibrational directions results then in an underestimation of the sum of energies of responses in the three vibrational directions. The lower limit for the energy ratio is determined from the first criterion for the prediction accuracy of the simplified SEA model mentioned in section 3.4. Based on this criterion, an underestimation of the sum of energies of responses in the three vibrational directions of 2,5 dB at most seems to be acceptable. This requires a ratio of vibrational energy of radial responses to the sum of energies of axial and tangential responses of at least 1,3. This value has been set as a starting point for testing the validity of assumption 6. Chapter 7 discusses whether this validation criterion should be reset.

For the pipes considered earlier in this section the energy ratio in (1/3-)octave bands is plotted in Figure 4-16 to Figure 4-18. Also a ratio of 1,3 is shown, to indicate the criterion for predominantly radial response applied in this thesis. Because the ratio does not depend on pipe length no results for different pipe lengths are presented.

---

[60] The sum of energies of responses in the three vibrational directions is calculated as $E=10lg(10^{Erad/10}+10^{(Eax+Etan)/10})$.
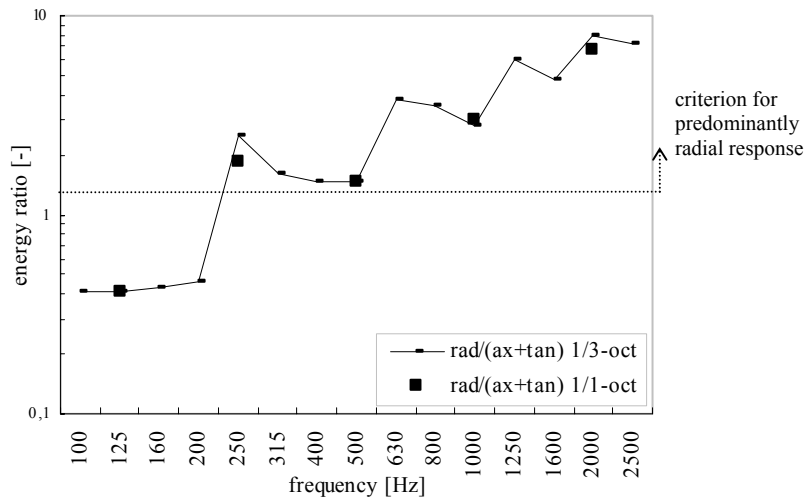
Figure 4-16 Ratio of energy of radial responses to the sum of energies of axial and tangential responses, in (1/3-)octave bands, in <u>air-filled PVC pipes</u> with 3,8 mm wall thickness and outer shell radius 55 mm. Also the criterion for predominantly radial response applied in this thesis is shown.
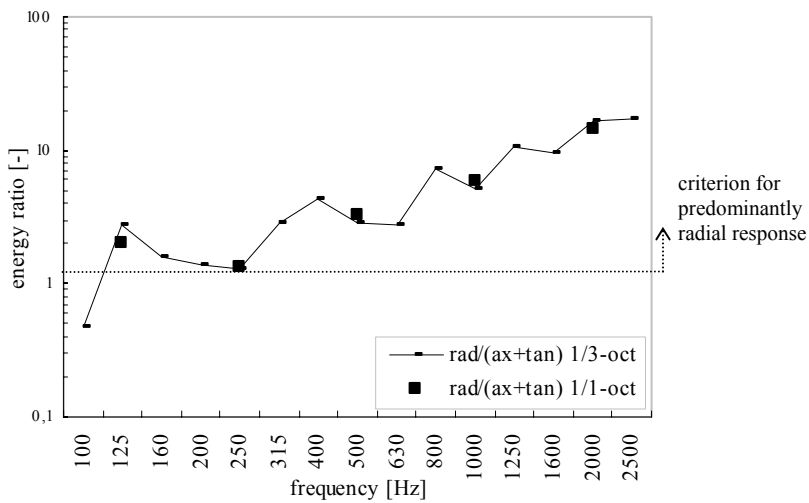
Figure 4-17 Ratio of energy of radial responses to the sum of energies of axial and tangential responses, in (1/3-)octave bands, in <u>water-filled PVC pipes</u> with 3,8 mm wall thickness and outer shell radius 55 mm. Also the criterion for predominantly radial response applied in this thesis is shown.
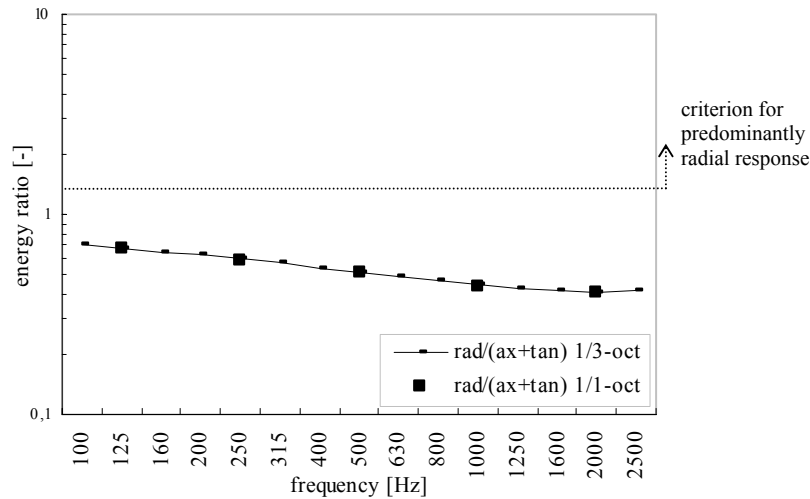
Figure 4-18 Ratio of energy of radial responses to the sum of energies of axial and tangential responses, in (1/3-)octave bands, in <u>water-filled brass pipes</u> with 2 mm wall thickness and outer shell radius 15 mm. Also the criterion for predominantly radial response applied in this thesis is shown.

For the air-filled PVC pipes Figure 4-16 shows for octave bands that the ratio of vibrational energy of radial responses to the sum of energies of axial and tangential responses becomes at least 1,3 from 250 Hz on. So, assumption 6 is fulfilled from 250 Hz on. For the water-filled PVC pipes (see Figure 4-17) assumption 6 is fulfilled in the entire frequency range of interest.

For the water-filled brass pipes Figure 4-18 shows that the energy ratio is smaller than 1,3 in the entire frequency range of interest. So, for these pipes assumption 6 is not fulfilled.

Generally speaking, for practical wastewater pipes assumption 6 is fulfilled from 250 Hz on for air-filled pipes and from 125 Hz on for water-filled pipes, so almost in the entire frequency range of interest, although pipes with a smaller shell radius have not been considered here (see under the testing of assumption 1). For practical, metal water supply pipes assumption 6 is not fulfilled.

4.3   Pipe system discontinuities

4.3.1   Vibro-acoustic behaviour

This section discusses the vibro-acoustic behaviour of discontinuities that are typical for wastewater pipe systems. Two types of discontinuities are distinguished: plastic pipe coupling elements and pipe clamps.

4.3.1.1   Pipe coupling elements

Figure 4-19 shows some examples of pipe coupling elements that are applied in wastewater pipe systems, at least in The Netherlands. Pipe coupling elements connect two or three straight pipes within a pipe system.

Usually coupling elements in pipe systems are made of the same material as the straight pipes. The wall thickness of these elements is about the same too. The most important differences between pipe coupling elements and straight pipes are the length and shape. Besides, pipe coupling elements show small variations in wall thickness and inner and outer radius, as can be seen in Figure 4-19.

T-joint   135º-bend
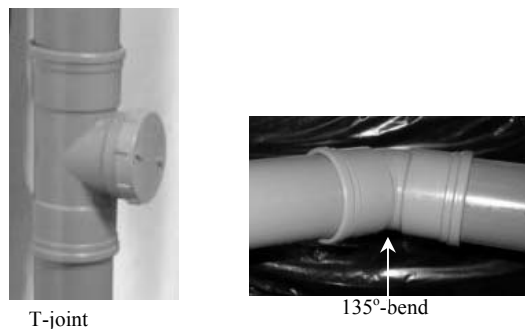
Figure 4-19   Practical pipe coupling elements for plastic wastewater pipe systems (scale ≈ 1:10)

It is assumed that the vibro-acoustic behaviour of straight joints is comparable with the vibro-acoustic behaviour of straight pipes. Therefore, the vibro-acoustic behaviour of these elements has been analysed with the method described for straight pipes in section 4.2.2.1. Section 4.3.2 describes the results.

Other pipe coupling elements, e.g. T-joints and bends, differ that much that the vibro-acoustic behaviour of these elements cannot be described in a similar way. In the literature a description of the vibro-acoustic behaviour of these elements is not available, as far as

known to the author. Therefore, the vibro-acoustic behaviour of these elements has been studied experimentally.[61] Section 4.3.3 describes the results.

Figure 4-19 shows that in building practice pipe coupling elements and the connected pipes partly overlap. This complicates the analysis of the vibro-acoustic behaviour of both the coupling element and the connected pipes. For example, the number of modes within a straight pipe is determined by the pipe length and boundary conditions. Due to the overlap of pipe and coupling element, both features are not exactly known. In the experimental set-ups in this thesis the straight pipes were at least a factor of 10 longer than the coupling elements. Measurements of pipe vibrations were performed at a distance from coupling elements of at least the lengths of the coupling elements. In estimations of modal properties the overlap has been included in the pipe length.

4.3.1.2   Pipe clamps

In building practice there are many different pipe clamps. Figure 4-20 shows some examples of pipe clamps that are applied to mount wastewater pipe systems on plates in buildings, at least in The Netherlands.
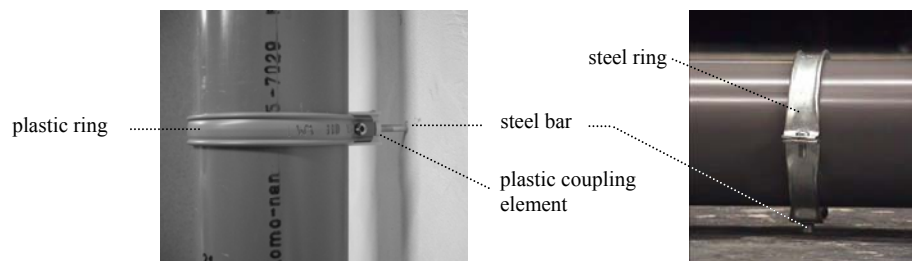
Figure 4-20   Practical pipe clamps for plastic wastewater pipe systems (scale ≈ 1:5)

Figure 4-20 shows that pipe clamps generally consist of two or three parts: a plastic or steel ring, a steel bar with screw thread and possibly a (plastic) coupling element between ring and bar. The steel bar is screwed in a plate to mount a pipe system.

---

[61] The vibro-acoustic behaviour of pipe coupling elements with an irregular shape, and with a 'regular' shape of course, could be studied with FEM. In this study this has not been done, because it is expected that the experiments are sufficiently accurate for testing the validity of assumption 3 of the simplified SEA model concerning the modal properties of pipe system discontinuities.

The vibro-acoustic behaviour of the different parts of pipe clamps has been studied very roughly in this thesis. It is assumed that both the ring and the (plastic) coupling element are too small to exhibit a modal vibro-acoustic behaviour within the frequency range of interest (only some higher-order flexural modes might cut-on, resulting in a "tonal" vibro-acoustic behaviour). Within steel bars theoretically longitudinal, torsional and flexural free waves can propagate. Whether modes can exist in a steel bar within the frequency range of interest depends on the bar length. This has been investigated and is described in the next section.

4.3.2   Theoretical study of the modal behaviour of straight joints and pipe clamps

Straight joints

For each type of mode in some straight plastic joints the number of modes has been calculated according to the method described in section 4.2.2.1. The approximate wave number equations given in appendix I, which originally have been derived for different types of free waves in straight pipes, have been applied in the calculations. Variations in pipe wall diameter and thickness have not been accounted for in the calculations.
The calculation results for characteristic joint lengths of 0,15 m and 0,25 m and for the 1/3-octave bands with centre frequencies 100 Hz to 2500 Hz are presented in Figure 4-21.

The validity testing of the assumption of the simplified SEA model concerning the modal properties of pipe system discontinuities deals with a limited number of types of modes and results in octave bands (see section 4.3.4). This section is aimed at studying the modal characteristics of discontinuities in more detail. This is why all types of modes are considered and why results for 1/3-octave bands are presented.
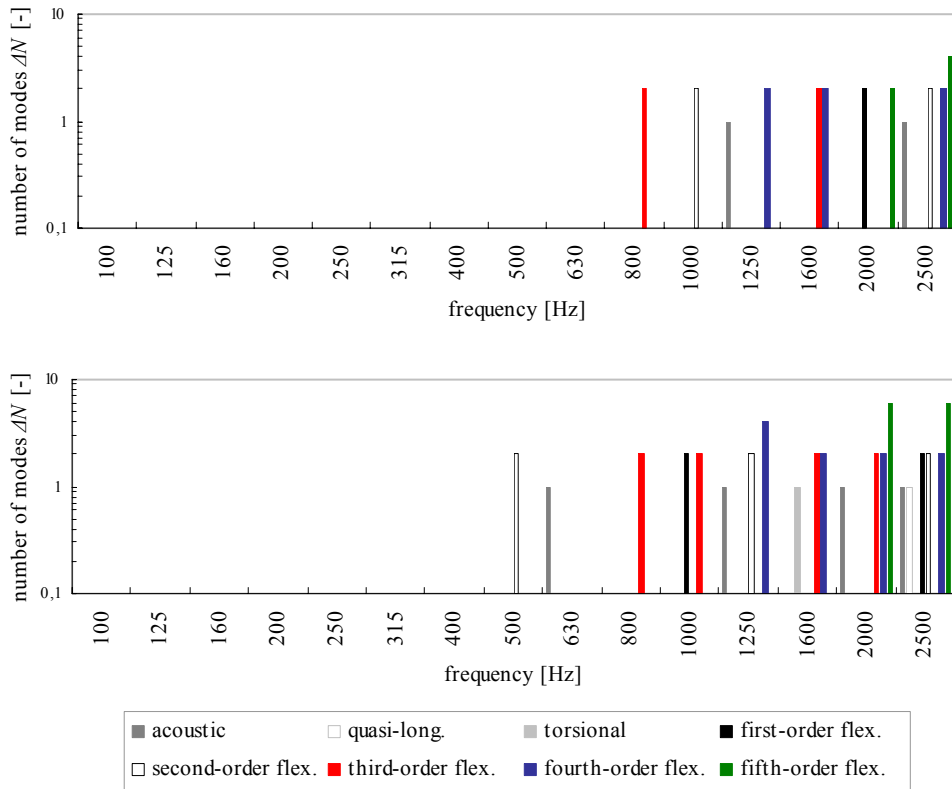
Figure 4-21 Number of modes *ΔN* in 1/3-octave bands for various mode types in <u>straight air-filled PVC joints</u> with 3,8 mm wall thickness and an outer shell radius of 55 mm. Calculation results are for joint lengths of 0,15 m (**upper**) and 0,25 m (**lower**).

Figure 4-21 shows that for the joint with a length of 0,15 m only for fifth-order flexural modes the number of modes per 1/3-octave band becomes at least 2 from 2000 Hz on. For the joint with a length of 0,25 m only for fourth- and fifth-order flexural modes the number of modes per 1/3-octave band becomes at least 2 from 1250 Hz on and from 2000 Hz on respectively. For acoustic modes the number of modes per 1/3-octave band becomes at least 1 from 2000 Hz on.

Steel bars in pipe clamps

For some steel bars the modal densities for longitudinal, torsional and flexural modes have been calculated with the equations given in [ref 4][62]. Subsequently, the number of modes has been calculated with equation *(4.4)* in section 4.2.2.1.

The calculation results are only described here. The number of modes is smaller than 1 in the entire frequency range of interest for two steel bars that are typically applied in pipe clamps, i.e. a steel bar with a radius of 2,5 mm and a length of 70 mm and a steel bar with a radius of 3,5 mm and a length of 100 mm.

4.3.3 Experimental study of the modal behaviour of a T-joint and a bend

For a plastic T-joint and a plastic bend, both with open ends, modes with a vibrational response component perpendicular to the element surface have been estimated from point admittance measurements, by counting peaks in the graphs representing the real part of the point admittance. Figure 4-22 shows the experimental set-up.

---

[62] The modal density of longitudinal modes n_l in a uniform bar with length L_{bar} is given by [ref 4]:

$n_l = (2 \cdot L_{bar})/c_{l,s}$

where $c_{l,s}$ represents the propagation velocity of longitudinal waves in the bar material.

The modal density of torsional modes n_t in a uniform bar with length L_{bar} is given by [ref 4]:

$n_t = (2 \cdot L_{bar})/c_{t,s}$

where $c_{t,s}$ represents the propagation velocity of torsional waves in the bar material and is given by [ref 12]:

$c_{t,s} = \sqrt{(E_s/(2 \cdot \rho_s \cdot (1+v)))}$

where E_s and ρ_s represent respectively the Young's modulus of elasticity and the density of the bar material. v is Poisson's ratio.

The modal density of flexural modes n_b in a uniform bar with length L_{bar} and radius r_{bar} is given by [ref 4]:

$n_b = L_{bar}/(\sqrt{(2\pi f \cdot c_{l,s} \cdot (r_{bar}/\sqrt{12}))})$
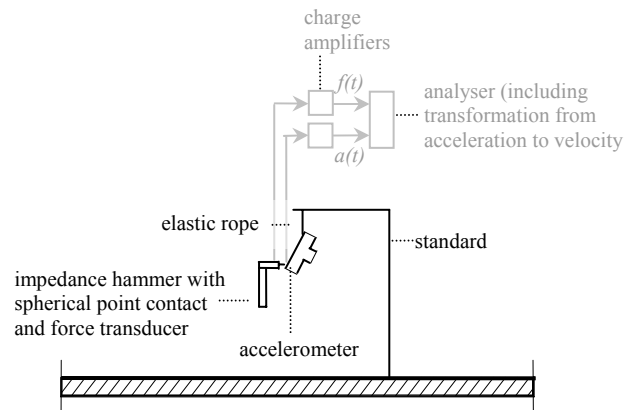
Figure 4-22 Experimental set-up for the estimation of modes in air-filled pipe coupling elements (scale ≈ 1:50)

The T-joint and bend were suspended by using elastic ropes. The space-averaged real part of the point admittance has been estimated from force and acceleration measurements at two positions (see footnote 56). The T-joint and bend were set into vibration with an impedance hammer. The measurement equipment is described in appendix V.

For both the T-joint and the bend, Figure 4-23 shows the modes for the 1/3-octave bands with centre frequencies 100 Hz to 2500 Hz.
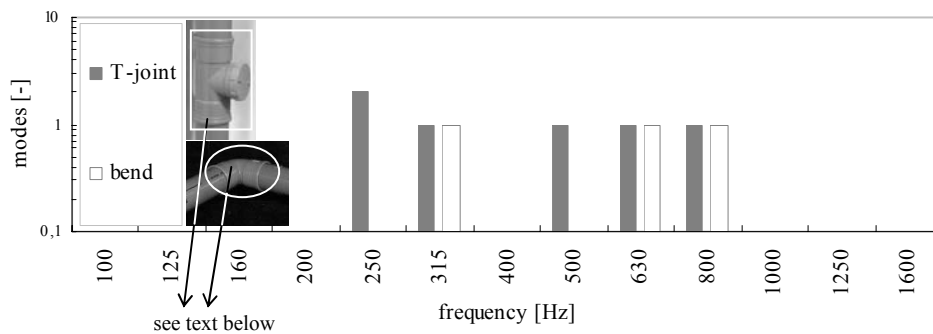
Figure 4-23 Modes in 1/3-octave bands with a vibrational response component perpendicular to the element surface in an air-filled PVC T-joint and an air-filled PVC 90º-bend (only the T-joint and bend have been placed in the experimental set-up, without the straight pipes shown above), determined from point admittance measurements (results above 800 Hz not reliable due to bad signal-to-noise ratios).

The results above 800 Hz are not reliable due to bad signal-to-noise ratios. No modes can be derived from the obtained point admittance curves above 800 Hz, while at least some modes are expected (also in relation to the results in Figure 4-21). Nevertheless, based on the results in Figure 4-23 it is expected that in both T-joints and bends only a very limited number of modes can exist. Because of the small lengths of T-joints and bends, it is assumed that it (mainly) concerns higher-order flexural and acoustic modes.

4.3.4   Validity of the simplified SEA model for pipe system discontinuities

This section is aimed at testing the validity of assumption 3 of the simplified SEA model concerning the modal properties of pipe system discontinuities. The assumption and corresponding validation criterion are given below. For the testing, the results obtained for the discontinuities in the previous sections are used. The validation criteria are set for octave bands, but results for both 1/3-octave and octave bands are shown.

Assumption 3
Pipe system discontinuities, such as bends, joints or clamps, are no subsystems, but coupling elements. This assumption is defined to be valid if the number of modes per octave band is 5 at most for each pipe system discontinuity.

Straight pipe coupling elements

In the simplified SEA model, only vibrations perpendicular to the physical elements surfaces are considered. In straight pipe joints, these vibrations are mainly caused by acoustic and (first- and higher-order) flexural modes. Therefore, the numbers of these types of modes are summed to test the validity of assumption 3. Figure 4-24 shows the results. Also a value of 5 modes per octave band is shown, to indicate the criterion for the maximum allowed number of modes for coupling elements applied in this thesis. In case for a(n) (1/3-)octave band no value is shown, then no mode originates in that band.
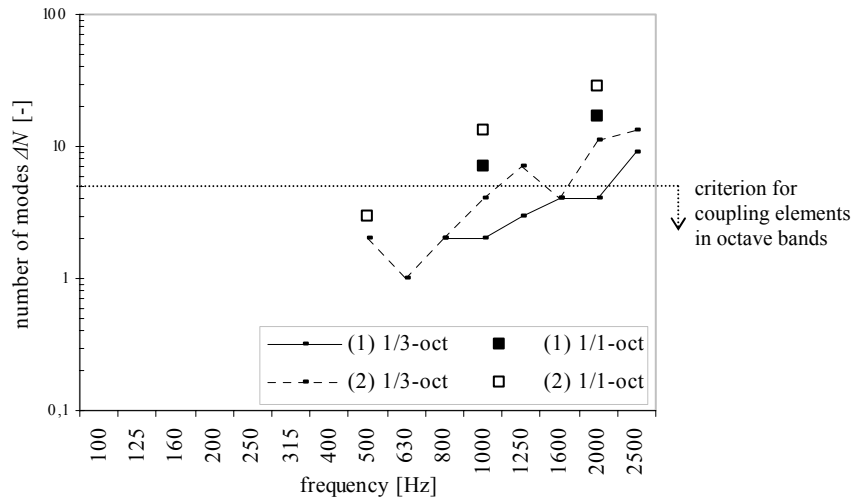
Figure 4-24 Total number of modes *ΔN* in (1/3-)octave bands with a mainly radial vibrational direction in (**1**) an air-filled PVC straight pipe joint with 3,8 mm wall thickness, outer shell radius 55 mm and joint length 0,15 m and (**2**) as (1), but with joint length 0,25 m. Also the criterion for coupling elements applied in this thesis is shown.

For both joint lengths Figure 4-24 shows that the number of modes per octave band becomes larger than 5 from 1000 Hz on. So, assumption 3 is only fulfilled below 1000 Hz.

Pipe clamps, T-joints and bends

From the results obtained for pipe clamps (see section 4.3.2), a T-joint and a bend (see section 4.3.3) it is expected that these discontinuities fulfil assumption 3 in the entire frequency range of interest. The numbers of modes per octave band are smaller than 6.

4.4   Single, homogeneous plates

4.4.1   Vibro-acoustic behaviour

The vibro-acoustic behaviour of single, homogeneous plates can be described by the wave number-frequency relationships for different types of free waves. In practical plates in buildings three types of free waves can propagate: in-plane quasi-longitudinal, in-plane shear and flexural waves. The wave number-frequency relationships can be found in many textbooks, see for example [ref 12], [ref 13] and [ref 15], and are given in appendix III of this thesis.

From the wave number-frequency relationships and the plate dimensions, numbers of modes corresponding to the different types of free waves can be calculated. This has been done for a couple of practical plates, see section 4.4.2. From the number of modes and loss factor of these plates, the modal overlap has been calculated. The number of modes and modal overlap within practical plates are needed to test the validity of the assumptions 1 and 2 of the simplified SEA model, see section 4.4.4.

Both quasi-longitudinal and shear waves cause in-plane vibrations. Quasi-longitudinal waves also cause small vibrations perpendicular to the structure surface. The main vibrational direction of flexural waves is perpendicular to the structure surface. This information is important for testing the validity of assumption 6 of the simplified SEA model, see section 4.4.4.

As described in appendix III, related to the description of the vibro-acoustic behaviour, two types of plates are distinguished in practice: so-called 'thin' plates and so-called 'thick' plates. Practical plates in buildings behave as 'thick' plates in an important part of the frequency range of interest. This implies that the effects of shear deformation and rotatory inertia have to be included in the description of flexural waves. This has been done in the calculations in this thesis.

4.4.2 Theoretical study of the modal behaviour

4.4.2.1 Derivation of mode count and modal overlap equations

For a two-dimensional subsystem[63] i, the mode count N_i up to a certain frequency can be calculated from the wave number k_i for the type of free wave considered, the subsystem dimensions and a constant $\Gamma_{i,BC}$ [ref 4]:

$$N_{i,2D} \approx \frac{S_i k_i^2}{4\pi} + \Gamma_{i,BC} P_i k_i$$

$$S_i = l_i \cdot w_i \qquad\qquad (4.12)$$

$$P_i = 2 \cdot (l_i + w_i)$$

where S_i and P_i are respectively the subsystem surface area and perimeter. l_i and w_i are the subsystem length and width.

---

[63] Generally speaking, practical plates in buildings are supposed to be too thin to behave as an elastic solid (three-dimensional subsystem) within the frequency range of interest.

The constant $\Gamma_{i,BC}$ has a value between zero and one, depending on the boundary conditions of the subsystem[64]. $\Gamma_{i,BC}$ equals zero for plates with simply supported edges. As stated in [ref 5] data from measurements suggest that most practical walls and floors behave like simply supported panels with only a small amount of clamping at the edges. In the calculations in this study a $\Gamma_{i,BC}$-value of zero has been applied.

The number of modes ΔN_i and the modal overlap M_i within a subsystem i have been calculated as described in section 4.2.2.1. Equation *(4.12)* has been applied to calculate N_{upper} and N_{lower}.

4.4.2.2 Results from mode count and modal overlap equations

Number of modes

For practical plates[65] the number of modes has been calculated for each type of mode, i.e. the subsystems defined in the extensive SEA model in section 3.2.2. The calculation results for the 1/3-octave bands with centre frequencies 100 Hz to 2500 Hz are presented in Figure 4-25 and Figure 4-26.

The validity testing of the assumptions of the simplified SEA model concerns a limited number of types of modes and results in octave bands (see section 4.4.4). This section is aimed at studying the modal characteristics of plates in more detail. This is why all types of modes are considered and why results for 1/3-octave bands are presented.

---

[64] Leissa has given solutions for various boundary conditions, see [ref 58] and [ref 15].

[65] The considered plate materials, plate dimensions and the dimensions in between are supposed to cover an important part of the plates on which pipe systems are mounted in buildings. Calculations have been done for plate surface areas of 1x3 m², 4x3 m² and 4x6 m², because these are representative surfaces areas for walls of shafts for service equipment, walls in rooms and floors respectively. Plate thicknesses of 0,1 m and 0,25 m have been considered, because these are characteristic thicknesses of calcium-silicate/brick walls and concrete walls/floors respectively. Of course, the variation in plates in buildings is much larger, but it has been decided to gain insight in the suitability of the simplified SEA model based on calculations for a representative range of practical, single, homogeneous plates.
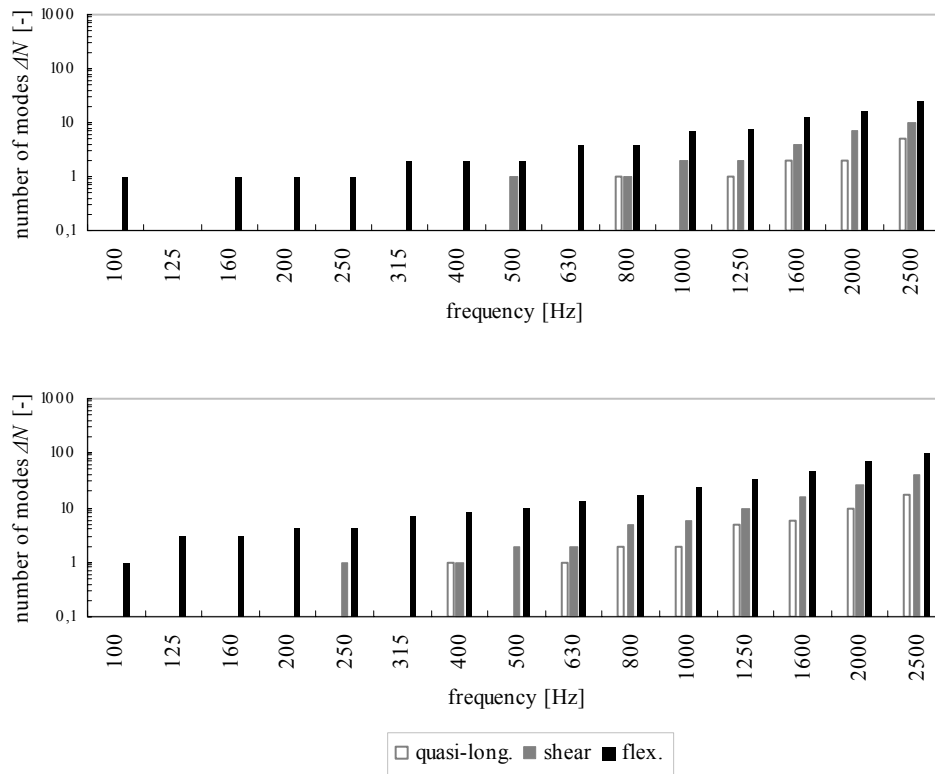
Figure 4-25 Number of modes ΔN in 1/3-octave bands for in-plane quasi-longitudinal, in-plane shear and flexural modes in <u>calcium-silicate plates</u>. Calculation results are for plate dimensions $1{,}0 \times 3{,}0 \times 0{,}1$ m³ (dimensions for a typical shaft wall) (**upper**) and $4{,}0 \times 3{,}0 \times 0{,}1$ m³ (**lower**).
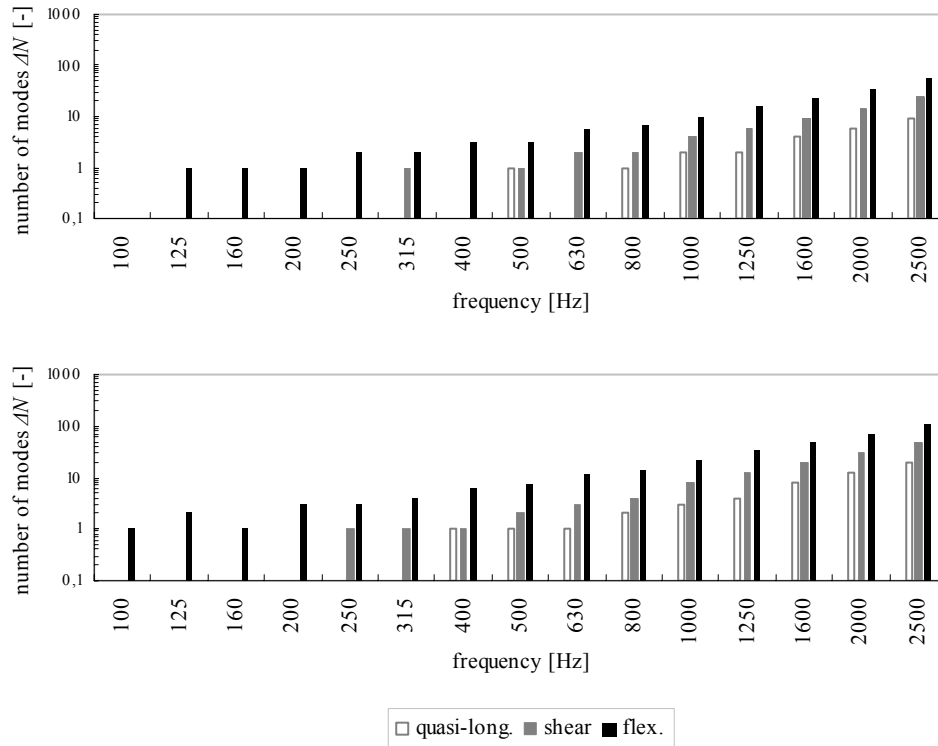
Figure 4-26 Number of modes ΔN in 1/3-octave bands for in-plane quasi-longitudinal, in-plane shear and flexural modes in <u>concrete plates</u>. Calculation results are for plate dimensions 4,0x3,0x0,25 m³ (**upper**) and 4,0x6,0x0,25 m³ (**lower**).

The numbers of quasi-longitudinal modes are the smallest, followed by the numbers of shear modes and then the numbers of flexural modes. At increasing frequency the increase of the numbers of in-plane quasi-longitudinal modes and in-plane shear modes is larger than the increase of the number of flexural modes[66].

Generally speaking, for the plates in each 1/3-octave band the number of flexural modes exceeds the numbers of quasi-longitudinal and shear modes by a factor of 2 to 10.

Figure 4-25 shows that in the large (4x3 m²) calcium-silicate plate flexural modes can exist at low frequencies, i.e. from the 1/3-octave band with centre frequency 100 Hz on. For this

---

[66] This is due to the fact that for quasi-longitudinal and shear modes $k \propto f$, and for flexural modes $k \propto \sqrt{f}$, see section III.1 in appendix III.

plate in-plane shear and in-plane quasi-longitudinal modes can exist from respectively 400 Hz and 630 Hz on.[67]

Figure 4-26 shows that in the large (4x6 m^2) concrete plate flexural modes can exist at low frequencies, i.e. from the 1/3-octave band with centre frequency 100 Hz on. For this plate in-plane shear and in-plane quasi-longitudinal modes can exist from respectively 250 Hz and 400 Hz on.

The frequencies mentioned are higher for smaller surface areas.

Modal overlap

For each type of mode in the plates the modal overlap has been calculated. In the calculations damping loss factor values of 0,015 and 0,006 have been applied for calcium-silicate[68] and concrete[69] respectively, for all mode types, within the entire frequency range of interest. Also some coupling to other structures has been included in the calculations. [70]

The calculation results for the 1/3-octave bands with centre frequencies 100 Hz to 2500 Hz are presented in Figure 4-27 and Figure 4-28. In case no value is shown for a mode type in a certain 1/3-octave band, then the modal overlap is smaller than 0,1 in that band.

---

[67] Since in-plane quasi-longitudinal and in-plane shear modes are often strongly coupled at the boundaries, these mode types are often considered as one mode group [ref 4]. The number of modes of this mode group is equal to the sum of the numbers of in-plane quasi-longitudinal and in-plane shear modes, which results in a higher number of modes and a larger modal overlap.

[68] In [ref 12] damping loss factor values between 10^{-2} and $2 \cdot 10^{-2}$ are given.

[69] In [ref 12] damping loss factor values between $4 \cdot 10^{-3}$ and $8 \cdot 10^{-3}$ are given.

[70] This gives realistic results for practical situations. For masonry type structures in domestic housing Craik has derived the following approximation for the total loss factor of a subsystem i due to damping and coupling [ref 5]:

$\eta_{i,tot} \approx \eta_{ii} + \Sigma(\eta_{ij} - \eta_{ji}) = 0,015 + (1/\sqrt{f})$ with $j=1..n$ and $j \neq i$

This equation shows that the largest differences in total loss factors due to adding coupling losses occur in the low frequency range, resulting in a higher modal overlap in this frequency range compared to a modal overlap in which only damping has been included.
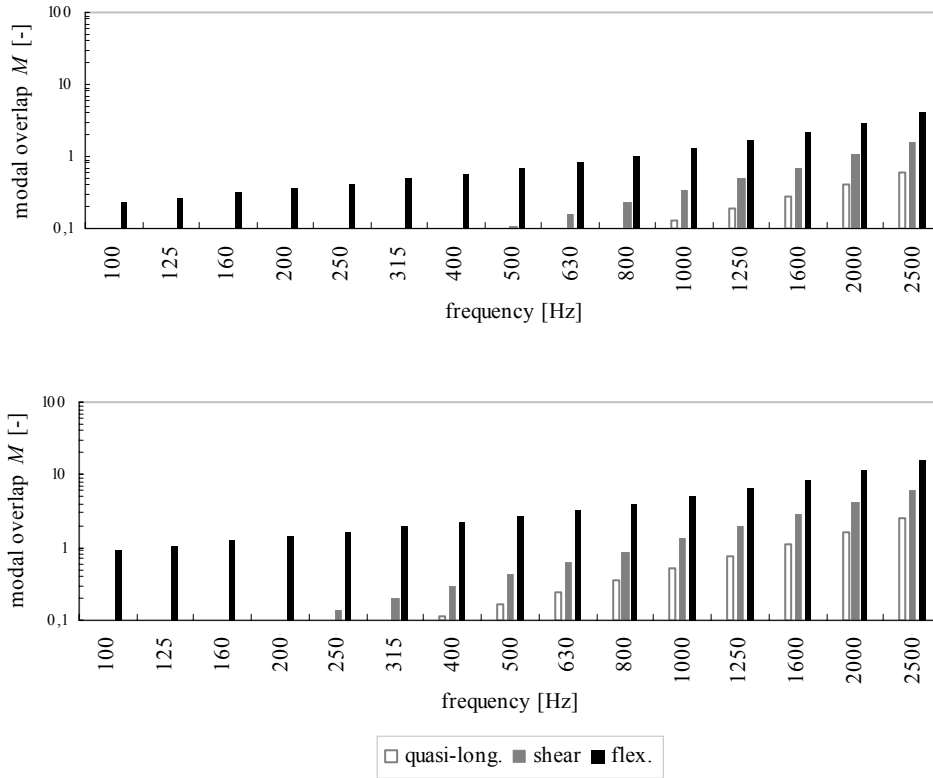
Figure 4-27 Modal overlap M in 1/3-octave bands for in-plane quasi-longitudinal, in-plane shear and flexural modes in <u>calcium-silicate plates</u>. Calculation results are for plate dimensions 1,0x3,0x0,1 m³ (dimensions for a typical shaft wall) (**upper**) and 4,0x3,0x0,1 m³ (**lower**) and a damping loss factor of 0,015 and some coupling to other structures.
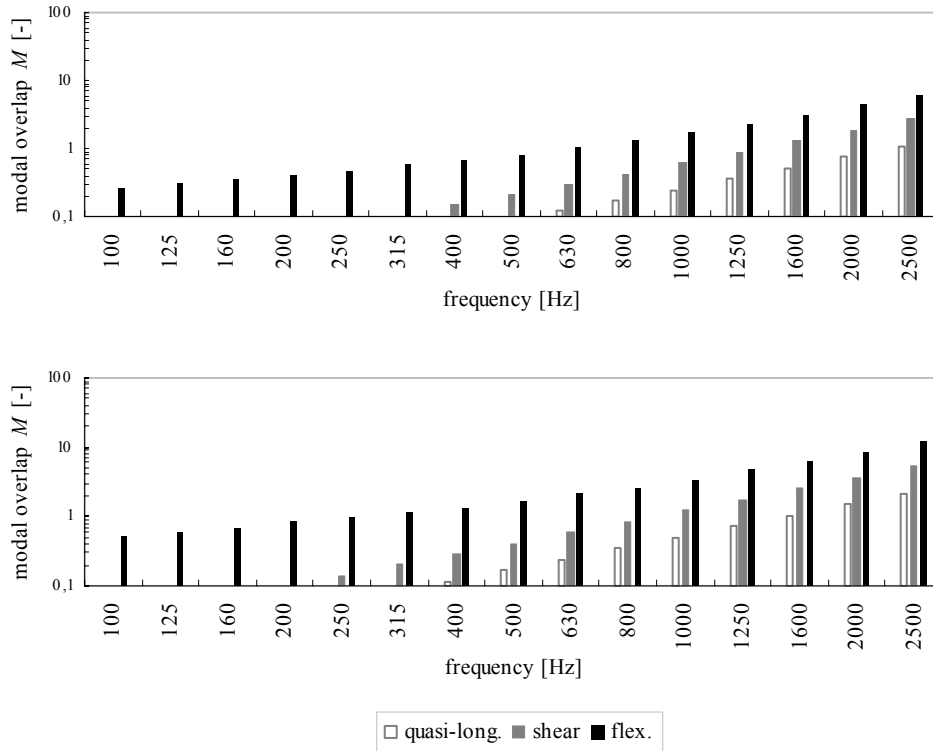
Figure 4-28 Modal overlap M in 1/3-octave bands for in-plane quasi-longitudinal, in-plane shear and flexural modes in <u>concrete plates</u>. Calculation results are for plate dimensions 4,0x3,0x0,25 m^3 (**upper**) and 4,0x6,0x0,25 m^3 (**lower**) and a damping loss factor of 0,006 and some coupling to other structures.

Figure 4-27 shows that for the large (4x3 m^2) calcium-silicate plate the modal overlap of flexural modes becomes larger than 1 at low frequencies, i.e. from the 1/3-octave band with centre frequency 125 Hz on. For this plate the modal overlap of in-plane shear and in-plane quasi-longitudinal modes is larger than 1 from respectively 1000 Hz and 1600 Hz on.

Figure 4-28 shows that for the large (4x6 m^2) concrete plate the modal overlap of flexural modes becomes larger than 1 from the 1/3-octave band with centre frequency 315 Hz on. For this plate the modal overlap of in-plane shear and in-plane quasi-longitudinal modes is larger than 1 from respectively 1000 Hz and 1600 Hz on.

The frequencies mentioned are higher for smaller surface areas.

4.4.3 Experimental study of the modal behaviour and comparison of experimental and theoretical results for a wall

For a calcium-silicate wall the total number of modes that cause out-of-plane vibrations[71] has been determined from point admittance measurements in the same way as described for straight pipes in section 4.2.3. Figure 4-29 shows the experimental set-up.
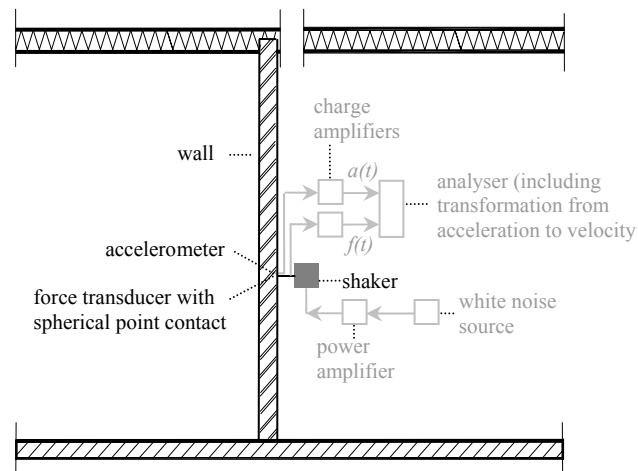
Figure 4-29 Experimental set-up for the determination of the total number of modes that cause out-of-plane vibrations in a calcium-silicate wall with dimensions 4,4x3,4x0,1 m^3 and with a plaster layer of about 10 mm thickness at both sides

The wall was a separation wall between two measurement rooms and was placed on the linoleum floor covering on the concrete floor of the laboratory. At the side and top edges the wall was connected to lightweight structures. For a more extensive description of the structures and joints the reader is referred to section 5.6.1.

The space-averaged real part of the point admittance has been estimated from force and acceleration measurements at three positions (see footnote 56). The force transducer was mounted between the wall and a shaker. The measurement equipment is described in appendix V.

Figure 4-30 shows the number of modes in 1/3-octave bands as determined from the point admittance measurements[72] and as obtained from the mode count equation for flexural modes[73] in section 4.4.2.

The numbers of modes obtained with the two determination methods are compared in order to determine whether numbers of modes obtained with the mode count equation are sufficiently accurate for testing the validity of the model assumptions in this chapter.
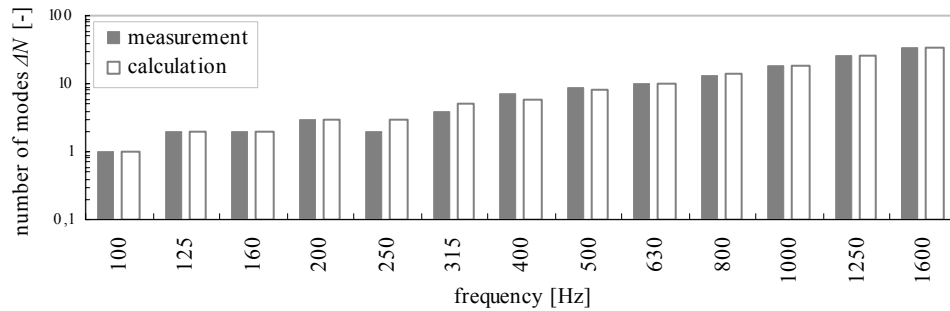
Figure 4-30 Number of modes ΔN in 1/3-octave bands causing out-of-plane vibrations in a calcium-silicate wall with dimensions 4,4x3,4x0,1 m^3 and with a plaster layer of about 10 mm thickness at both sides. Experimental results and results from the mode count equation for flexural modes.

Figure 4-30 shows a good agreement between the numbers of modes obtained from the measurements and from the mode count equation. It has been estimated which error would occur in case the results would be applied to determine coupling loss factors in one direction from coupling loss factors in the opposite direction (with equation *(2.6)* or *(2.7)*) or to determine deviations from the 'reciprocity relationship' (as written in equation *(3.3)*) for example. Ths error has been expressed as presented in equation *(4.7)* in section 4.2.3.3.

For each (1/3-)octave band within the frequency range of interest the error has been determined. For the 1/3-octave bands this results in errors between 0 dB and 2 dB up to 250 Hz (mean error over this frequency range 0,4 dB) and errors between 0 dB and 1 dB

---

[71] Practically speaking, these are primarily flexural modes and, to a lesser degree, quasi-longitudinal modes.

[72] Because of bad signal-to-noise ratios above 1600 Hz, no values are shown for 1/3-octave bands with centre frequencies above 1600 Hz.

[73] Only the number of flexural modes has been used in the comparison, because flexural modes are primarily responsible for out-of-plane plate vibrations. In the experiments no distinction between mode types has been made since the total point admittance of mode types that cause out-of-plane vibrations has been determined, i.e. flexural modes and in-plane quasi-longitudinal modes. The contribution of the in-plane quasi-longitudinal modes to the point admittance has been assumed to be negligibly small compared to the contribution of the flexural modes.

from 315 Hz on (mean error 0,3 dB). For the octave bands this results in errors between 0 dB and 1 dB in the entire frequency range of interest.

In spite of the differences, both approximations and measurements are sufficiently accurate for testing the validity of the assumptions concerning the modal properties of physical system elements.

4.4.4   Validity of the simplified SEA model for plates

This section is aimed at testing the validity of the assumptions 1, 2 and 6 of the simplified SEA model concerning the modal properties of subsystems in practical plates in buildings. The assumptions and corresponding validation criteria are given below. For the testing, the results obtained for the plates in section 4.4.2.2 are used. The validation criteria are set for octave bands, but results for both 1/3-octave and octave bands are shown.

Validity of assumption 1

Assumption 1
The subsystems responses in each octave band considered are determined by a sufficiently large number of resonant modes. This assumption is defined to be valid if the number of modes per octave band is at least 6 for each subsystem.

In the simplified SEA model, only vibrations perpendicular to the physical elements surfaces are considered. In plates, these vibrations are mainly caused by flexural modes. For the plates studied in section 4.4.2 the numbers of flexural modes are plotted in Figure 4-31 and Figure 4-32. Based on these results the validity of assumption 1 is tested. Actually, this test is only valid assuming that all natural modes are excited in practice, and therefore become resonant modes. Also a value of 6 modes per octave band is shown, to indicate the criterion for a sufficiently large number of modes applied in this thesis. In case for a 1/3-octave band no value is shown, then no mode originates in that band.
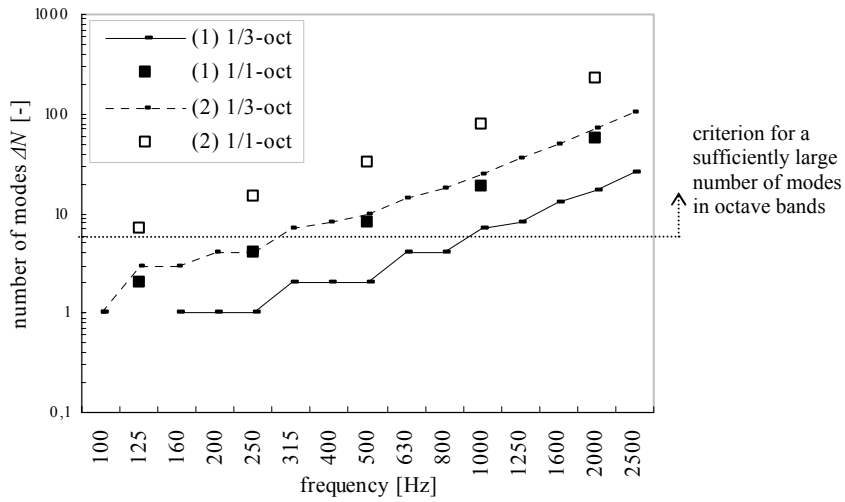
Figure 4-31 Number of flexural modes $\varDelta N$ in (1/3-)octave bands in (**1**) a <u>calcium-silicate plate</u> with dimensions 1,0x3,0x0,1 m³ (dimensions for a typical shaft wall) and (**2**) as (1), but with dimensions 4,0x3,0x0,1 m³. Also the criterion for a sufficiently large number of modes applied in this thesis is shown.
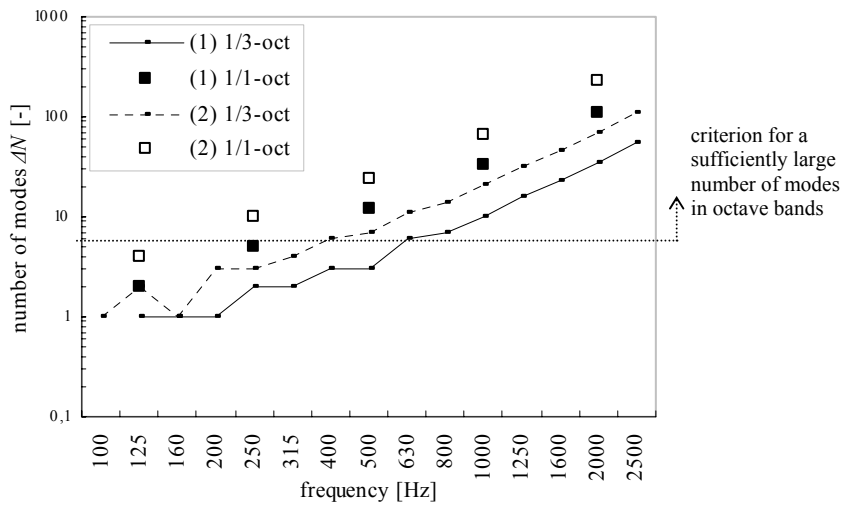
Figure 4-32 Number of flexural modes $\varDelta N$ in (1/3-)octave bands in (**1**) a <u>concrete plate</u> with dimensions 4,0x3,0x0,25 m³ and (**2**) as (1), but with dimensions 4,0x6,0x0,25 m³. Also the criterion for a sufficiently large number of modes applied in this thesis is shown.

For the calcium-silicate plate with surface area 1x3 m^2 (representative for a small shaft wall) Figure 4-31 shows that the number of modes per octave band becomes at least 6 from 500 Hz on. So, assumption 1 is fulfilled from 500 Hz on. For the same plate with surface area 4x3 m^2 (representative for walls in buildings, on which pipe systems are also mounted in building practice) assumption 1 is fulfilled in the entire frequency range of interest. There are at least 6 modes per octave band.

For the concrete plate with surface area 4x3 m^2 (relatively small for this type of structure) Figure 4-32 shows that the number of modes per octave band becomes at least 6 from 500 Hz on (the number of modes is nearly 6 at 250 Hz). So, assumption 1 is fulfilled from 500 Hz on. For the same plate with surface area 4x6 m^2 (representative for walls/floors in buildings) the number of modes per octave band becomes at least 6 from 250 Hz on. So, assumption 1 is fulfilled from 250 Hz on.

Generally speaking, for practical plates with relatively small surface areas assumption 1 is fulfilled from the mid-frequency range on. For larger surface areas the assumption is fulfilled in practically the entire frequency range of interest, depending on plate material and dimensions.

Validity of assumption 2

Assumption 2
The subsystems responses in each octave band considered have sufficient modal overlap. This assumption is defined to be valid if the modal overlap in each octave band is at least 1 for each subsystem.

For each plate the modal overlap corresponding to flexural modes has been calculated. Actually, this test is only valid assuming that all natural modes are excited in practice, and therefore become resonant modes (see under Validity of assumption 1). The results are shown in Figure 4-33 and Figure 4-34. Also a value of 1 is shown, to indicate the criterion for sufficient modal overlap applied in this thesis.
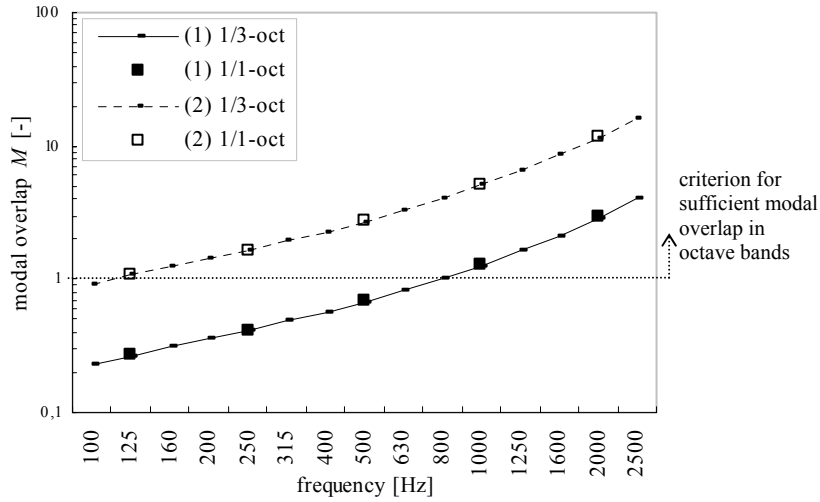
Figure 4-33 Modal overlap M in (1/3-)octave bands for flexural modes in (**1**) a <u>calcium-silicate plate</u> with dimensions 1,0x3,0x0,1 m³ (dimensions for a typical shaft wall) and (**2**) as (1), but with dimensions 4,0x3,0x0,1 m³. Also the criterion for sufficient modal overlap applied in this thesis is shown
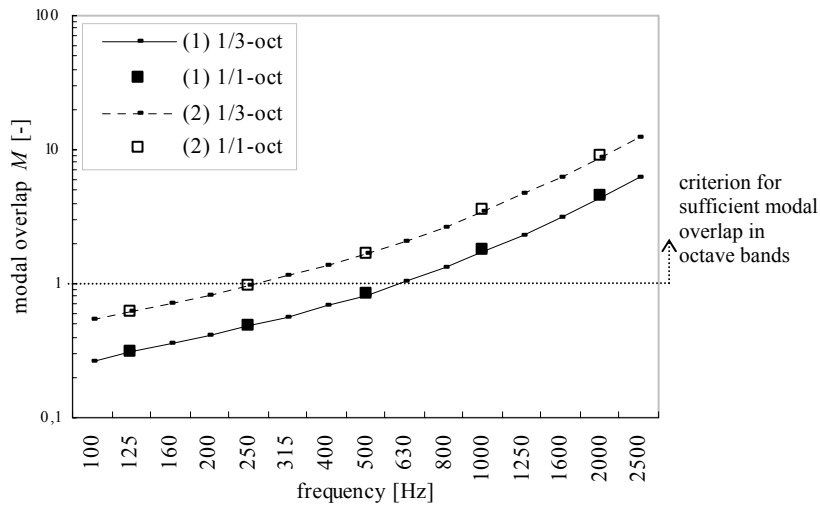
Figure 4-34 Modal overlap M in (1/3-)octave bands for flexural modes in (**1**) a <u>concrete plate</u> with dimensions 4,0x3,0x0,25 m³ and (**2**) as (1), but with dimensions 4,0x6,0x0,25 m³. Also the criterion for sufficient modal overlap applied in this thesis is shown

114

For the calcium-silicate plate with surface area 1x3 m^2 (representative for a small shaft wall) Figure 4-33 shows that the modal overlap per octave band becomes at least 1 from 1000 Hz on. So, assumption 2 is fulfilled from 1000 Hz on. For the same plate with surface area 4x3 m^2 (representative for walls in buildings, on which pipe systems are also mounted in building practice) assumption 2 is fulfilled in the entire frequency range of interest. The modal overlap per octave band is at least 1.

For the concrete plate with surface area 4x3 m^2 (relatively small for this type of structure) Figure 4-34 shows that the modal overlap per octave band becomes at least 1 from 1000 Hz on. So, assumption 2 is fulfilled from 1000 Hz on. For the same plate with surface area 4x6 m^2 (representative for walls/floors in buildings) the modal overlap per octave band becomes at least 1 from 250 Hz on. So, assumption 2 is fulfilled from 250 Hz on.

Generally speaking, for practical plates with relatively small surface areas assumption 2 is only fulfilled in the high-frequency range. For larger surface areas the assumption is fulfilled in practically the entire frequency range of interest, depending on plate material and dimensions.

Validity of assumption 6

Assumption 6

In each octave band considered, the responses of natural modes are predominantly out-of-plane for plates. This assumption is defined to be valid if in each octave band considered the ratio of energy of out-of-plane responses to the sum of energies of in-plane responses is at least 1,3.

In order to test the validity of this assumption the ratio of energy of out-of-plane responses to the sum of energies of in-plane responses has been estimated as described below.

In section 4.4.1 it has been described that in-plane quasi-longitudinal waves in plates cause in-plane vibrations and small out-of-plane vibrations. In-plane shear waves only cause in-plane vibrations. Flexural waves mainly cause out-of-plane vibrations and small in-plane vibrations. So, in-plane quasi-longitudinal and in-plane shear modes are predominantly responsible for in-plane plate vibrations. Flexural modes are predominantly responsible for out-of-plane plate vibrations.

The number of modes within a frequency band is directly related to the modal density in this band, see equation *(4.4)* in section 4.2.2.1. The modal density is directly related to the real part of the point admittance, see equation *(4.5)* in section 4.2.3.1. The real part of the point admittance of a subsystem determines the resulting energy in the subsystem due to excitation by a source, see equation *(2.18)* in section 2.6.2. The real part of the point

admittance differs for the different types of modes. Therefore, when different types of modes are excited by the same source, the resulting energy in the different types of modes differs. The energy ratio is equal to the ratio of the real parts of the point admittances. From the above described relations, it is derived that the ratio of the real parts of the point admittances is equal to the ratio of the numbers of modes.

Based on this information, it has been assumed that the ratio of energy of out-of-plane responses to the sum of energies of in-plane responses for a plate may be well estimated with:

$$ratio = \frac{E_b}{E_l + E_t} = \frac{\Delta N_b}{\Delta N_l + \Delta N_t} \qquad (4.13)$$

where b, l and t represent flexural, in-plane quasi-longitudinal and in-plane shear modes respectively. The ratio is independent of the plate length and width.

Since in-plane quasi-longitudinal and in-plane shear modes are often strongly coupled at the boundaries, these mode types are often considered as one mode group [ref 4].

Analogous to the reasoning for pipes in section 4.2.4, the energy ratio should be at least 1,3 to fulfil assumption 6.

For the plates considered earlier in this section the energy ratio in (1/3-)octave bands is plotted in Figure 4-35. Also a ratio of 1,3 is shown, to indicate the criterion for predominantly out-of-plane response applied in this thesis. Because the ratio does not depend on plate length and width no results for different plate lengths and widths are presented.
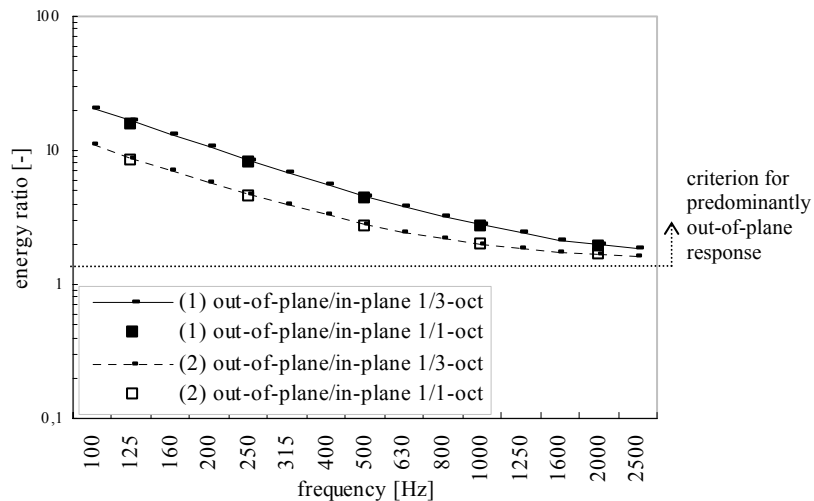
Figure 4-35 Ratio of energy of out-of-plane responses to energy of in-plane responses, in (1/3-)octave bands, in (**1**) 100 mm thick <u>calcium-silicate plates</u> and (**2**) 250 mm thick <u>concrete plates</u>. Also the criterion for predominantly out-of-plane response applied in this thesis is shown.

For both types of plates Figure 4-35 shows for octave bands that the ratio of energy of out-of-plane responses to energy of in-plane responses is at least 1,3 in the entire frequency range of interest. So, assumption 6 is fulfilled in the entire frequency range of interest.

4.5   Conclusions

In this chapter the validity of the assumptions 1 to 3 and 6 of the simplified SEA model (see section 3.3) has been tested. These assumptions deal with the modal properties of the physical system elements that are subject of this thesis. For this purpose values for different modal properties have been estimated for practical straight pipes, plates and discontinuities in pipe systems. The assumptions and test results are summarised below.

Straight pipes and plates

The following assumptions deal with the modal properties of straight pipes and plates.

Assumption 1

The subsystems responses in each octave band considered are determined by a sufficiently large number of resonant modes.

Assumption 2
The subsystems responses in each octave band considered have sufficient modal overlap.
Assumption 6
In each octave band considered, the responses of natural modes are predominantly radial for pipes and out-of-plane for plates.

For testing the validity of these assumptions, numbers of modes, modal overlaps and ratios of vibrational energies of responses in different vibrational directions obtained from analytical approximations have been used. The accuracy of the approximations has been determined based on comparisons with FEM-results (for straight pipes) and experimental results (for a straight pipe and a plate). Although the results of the three determination methods do not correspond exactly with each other (for comparisons see for pipes sections 4.2.2.4 and 4.2.3.3 and for plates section 4.4.3), the results of the approximations are sufficiently accurate for testing the validity of the assumptions.

For pipes the test results are described in detail in section 4.2.4.
For practical (plastic) wastewater pipes these three assumptions are fulfilled from 250 Hz on for air-filled pipes and from 125 Hz on for water-filled pipes, so almost in the entire frequency range of interest, although pipes with a smaller shell radius and pipe lengths smaller than 3 m have not been considered here. However, these pipes are expected to cause less noise complaints in practical situations, e.g. because they are applied inside houses and generally not in shafts in apartment buildings.
For practical (metal) water supply pipes assumption 1 is fulfilled in the entire frequency range of interest for relatively long pipes. For shorter pipes the assumption is only fulfilled in the mid and high frequency range (from 500 Hz on). The other two assumptions are not fulfilled.

For plates the test results are described in detail in section 4.4.4.
For practical plates with relatively small surface areas the assumptions 1 and 2 are only fulfilled in the mid- and/or high-frequency range (from 500 Hz and 1000 Hz on respectively). For larger surface areas the assumptions 1 and 2 are fulfilled from 250 Hz on for concrete plates and from 125 Hz on for calcium-silicate plates, so practically in the entire frequency range of interest, depending on plate material and dimensions. Assumption 6 is fulfilled in the entire frequency range of interest for all practical plates.

So, for the pipe systems and plates on which this thesis focuses, from the results described in this chapter it is concluded that the simplified SEA model is applicable in the entire

frequency range of interest, except for the 125 Hz octave band and for plates with relatively small surface areas below 500-1000 Hz. Whether this becomes a problem depends on the excitation (direction) of practical sources in pipe systems, on the actual modal properties of (partly water-filled) wastewater pipes during flushing (more like air-filled or water-filled pipes?) and on the transmission through couplings between pipe systems and plates and within pipe systems. These issues are discussed in chapters 5 and 6.

Pipe system discontinuities

The following assumption deals with the modal properties of discontinuities in pipe systems.

Assumption 3
Pipe system discontinuities, such as bends, joints or clamps, are no subsystems, but coupling elements.

The validity of the assumption has been tested based on numbers of modes obtained from approximations and experiments.

For pipe system discontinuities the test results are described in detail in section 4.3.4.
For practical, straight, plastic joints this assumption is only fulfilled under 1000 Hz. For practical pipe clamps, plastic T-joints and plastic bends the assumption is expected to be fulfilled in the entire frequency range of interest.

So, for most pipe system discontinuities studied in this thesis, from the results described in this chapter it is concluded that the simplified SEA model is applicable in the entire frequency range of interest. The only exceptions are straight plastic pipe joints from the octave band 1000 Hz on. So, at high frequencies these joints should possibly be modelled as subsystems instead of couplings, or as one subsystem together with the connected straight pipes. In case of weak coupling between pipe joints and connected pipes the first modelling method is more appropriate, in case of strong coupling the second method.

CHAPTER 5

DAMPING AND COUPLING OF SYSTEM ELEMENTS

5.1   Introduction

This chapter is aimed at testing the validity of the assumptions 4, 5 and 8 of the simplified SEA model (see section 3.3). These assumptions deal with damping in and coupling between physical system elements that are subject of this thesis.

The validity of the assumptions mentioned has been tested based on results obtained with the so-called Power Injection Method (PIM). Damping loss factors for straight pipes and plates (walls and floors) and coupling loss factors corresponding to discontinuities in pipe systems (pipe clamps and pipe coupling elements) have been determined. Measurements have been done in various experimental set-ups, which have been designed within the context of this study.

The accuracy of the results obtained with PIM has been estimated based on comparisons with results obtained with other methods for the determination of damping and coupling loss factors. For a description of the various methods the reader is referred to section 5.2. The applied methods are only mentioned here:

- determination of damping loss factors with the decay rate method;
- determination of damping and coupling loss factors with PIM;
- determination of coupling loss factors from subsystems energies, damping loss factors and modal densities;
- determination of coupling loss factors from point admittances of subsystems and coupling element.

In the 80's the first successful experimental determinations of SEA parameters were made. In 1980 Bies and Hamid [ref 59] described successful in-situ determinations of damping and coupling loss factors with the Power Injection Method (PIM). In the following years other successful experimental determinations were reported, especially of modal densities and damping loss factors of fairly simple structures, see for example [ref 60-62]. The next ten years limited progress in the development of experimental determination methods for SEA parameters was made [ref 7]. In 1996 De Langhe [ref 7] reported important developments of PIM.

The determination methods applied in this study are considered as the most promising candidates for the systems that are subject of this thesis. Based on the comparisons of

results, not only the appropriateness of PIM for testing the validity of the assumptions mentioned has been estimated. Also the appropriateness of all four methods for the determination of damping and coupling loss factors has been determined, in order to judge whether the methods are appropriate to build a database for loss factors for example.

Section 5.3 gives damping loss factors for a pipe and two plates obtained with the decay rate method. The section starts with a description of the experimental set-ups and measurement methods. Then the obtained damping loss factors are given. Results obtained with different excitation methods are shown. The results are compared with values mentioned in the literature.

Sections 5.4 to 5.6 give damping and coupling loss factors obtained with PIM in three experimental set-ups. As far as known to the author no coupling loss factor data are available for couplings within wastewater pipe systems and between these pipe systems and plates in buildings. Each section gives the results for one of the experimental set-ups and starts with a description of the set-up, the subsystems definition in accordance with the simplified SEA model and measurement method(s). Then the obtained damping and coupling loss factors are given and discussed. In sections 5.4 and 5.5 coupling loss factor data obtained with the three determination methods are compared. Based on the comparisons, it is discussed whether PIM is an appropriate method for testing the validity of the mentioned assumptions for pipe clamps and pipe coupling elements. For the third set-up, no comparisons have been done: the same types of couplings as in the first two set-ups are used, so conclusions related to the appropriateness of PIM are similar. All sections compare damping loss factors obtained with PIM and the decay rate method. Also, in all sections the contribution of sound radiation to damping and coupling loss factors is discussed. At the end of each section, the validity of the assumptions 4, 5 and 8 of the simplified SEA model is tested, based on the obtained results. Furthermore, it is concluded for which frequency range SEA is applicable as a modelling method for sound transmission in the systems considered.

Two of the experimental set-ups only contained two subsystems and one coupling. The first set-up (see section 5.4) existed of a pipe that was coupled to a plate at one point with a pipe clamp. The second set-up (see section 5.5) existed of two pipes that were connected to each other by a bend. These two set-ups are primarily aimed at the determination of coupling loss factors for wastewater pipe system discontinuities, i.e. clamps, joints and bends, within a well-defined system. Similar set-ups could be applied in the future to obtain data for other pipe systems and corresponding discontinuities. The third set-up (see section 5.6) was built to investigate how well the determination methods for parameters and the simplified SEA

model work in practical situations in buildings. A representative situation was simulated. The set-up consisted of more than two subsystems and was a practical pipe system that existed of several straight pipes and discontinuities, that was mounted on a plate. For this set-up the subsystems definition is not as straightforward as for the first two set-ups. Complications in subsystems definitions for practical situations are discussed in sections 5.6.2 and 5.6.4, based on measurement results in the third set-up.

Based on comparisons of the results obtained in the different experimental set-ups and with the different determination methods, the dependency of loss factors on experimental set-up and determination method is investigated in section 5.7. Some results are already compared in sections 5.4 to 5.6 (see above). In section 5.7 more results are compared. Besides, the results are compared in more detail. The appropriateness of the different methods is discussed within the scope of this study.

5.2   Description of determination methods for damping and coupling loss factors

5.2.1   Determination of damping loss factors with the decay rate method

The two most common methods to obtain frequency band-averaged damping loss factors are the decay rate method and the power balance method. These methods are described, for example, in [ref 4]. Strictly speaking, the methods are only applicable to obtain damping loss factors in case a subsystem is uncoupled from its surroundings (other subsystems). Otherwise, energy loss due to coupling to other subsystems is included.
In this study the decay rate method has been applied. This method was preferred above the power balance method, because the last method uses the same input parameters as PIM. In order to determine the accuracy of results obtained with PIM, comparisons with results obtained with (completely) different determination methods were preferred.

The total loss factor $\eta_{i,tot}$ of a subsystem i can be derived from the half-amplitude decay time $T_{1/2,i}$ of the subsystem with equation *(5.1)* [ref 4].[74]

$$\eta_{i,tot} = \frac{0,22}{fT_{1/2,i}}$$

(5.1)

where $T_{1/2,i}$ is the time required for the subsystem response amplitude to decay by a factor of ½, which corresponds to an energy decay of 6 dB.[75]

In case a subsystem is not connected to other structural subsystems the total loss factor equals the damping loss factor of the subsystem. The connection to acoustic subsystems, i.e. sound radiation, is included in the damping loss factor.
Equation *(5.1)* can be applied to obtain the total loss factor in each vibrational direction of a physical system element: no distinction between mode types is made.

5.2.2 Determination of damping and coupling loss factors with the Power Injection Method (PIM)

The Power Injection Method (PIM) is probably the most common method for determination of damping and coupling loss factors in systems consisting of more than two subsystems. The application fields are diverse, e.g. the aerospace, ship and automotive industries and building acoustics. See for example [ref 4], [ref 5], [ref 6] and [ref 7].
The main advantage of PIM, above other experimental methods[76], is that the loss factors of all subsystems and couplings within a system can be determined without changing the system. All other experimental methods require disconnection or damping of subsystems (which is often not possible from a practical point of view). Then the damping and coupling loss factors are determined one by one.

---

[74] Equation *(5.1)* is based on the transient response of modes with linear damping of which the energy decays in time at a rate proportional to $e^{-2\pi f\eta t}$, where t represents the time interval considered.

[75] In room acoustics the reverberation time T of a room is defined as the time for the sound pressure level to decay 60 dB (see also footnote 86). Then the total loss factor is given by [ref 4]
$\eta = 2,2/(fT)$

[76] Lyon has described various experimental methods to determine either damping or coupling loss factors [ref 4].

The accuracies of loss factors obtained with PIM depend strongly on the accuracies of the determined input powers[77].

In 1996 De Langhe [ref 7] reported important developments of PIM, based on elaborate work regarding experimental and computational determination of SEA parameters, while focussing on applications in the automotive industry. De Langhe has made a valuable contribution in the development of PIM, resulting in less computational time and well-conditioned energy matrices, compared to classical PIM. Furthermore, in [ref 7] De Langhe describes methods to approximate loss factors from a reduced number of elements in the energy matrices[78] and discusses statistical and sensitivity aspects of PIM.

This section gives an outline of basic PIM and approximate PIM, following the work of De Langhe [ref 7]. For detailed descriptions the reader is referred to [ref 7].

5.2.2.1 System consisting of two subsystems

The principle of PIM is illustrated for a system consisting of two connected subsystems as shown in Figure 5-1.
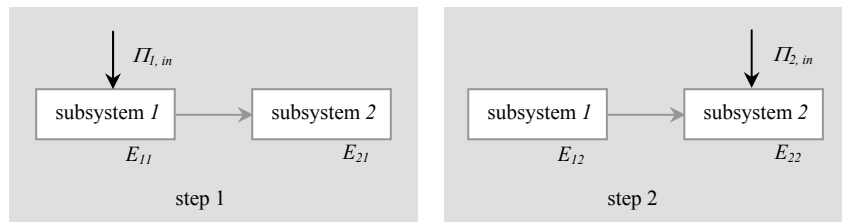
Figure 5-1   Application of PIM and measurement quantities for a system consisting of two subsystems

---

[77] Particularly coupling loss factors are very sensitive to small errors, because they are very small (at least an order of magnitude below the damping loss factors of the corresponding subsystems) and the differences between them are very small.

Accurate determination of the input power is relatively difficult, which is a disadvantage of PIM. Errors in the measurement of force and velocity (or acceleration), due to the mass and stiffness properties of the transducer, due to contact damping, due to the frequency response of the power amplifier and the exciter system and due to exciter-structure feedback interaction, have to be accounted for [ref 6]. The force and velocity transducers have to be calibrated for both magnitude and relative phase. Point contact excitation is required.

[78] The approximate methods are time-saving, especially when only a small part in a large, complex system needs to be considered, for example in case one wants to determine the effectiveness of changes in this part.

Firstly, energy is injected in subsystem *1* only. The input power to subsystem *1* and the response of both subsystems due to this excitation are measured. In this case the power balance equations (analogous to equation *(2.11)* in section 2.4.2) are:

$$\begin{Bmatrix} \Pi_{1,in} \\ 0 \end{Bmatrix} = 2\pi f \begin{bmatrix} \eta_{11}^0 & \eta_{12}^0 \\ \eta_{21}^0 & \eta_{22}^0 \end{bmatrix} \begin{Bmatrix} E_{11} \\ E_{21} \end{Bmatrix} \rightarrow \begin{Bmatrix} 1 \\ 0 \end{Bmatrix} = \begin{bmatrix} \eta_{11}^0 & \eta_{12}^0 \\ \eta_{21}^0 & \eta_{22}^0 \end{bmatrix} \begin{Bmatrix} 2\pi f E_{11}/\Pi_{1,in} \\ 2\pi f E_{21}/\Pi_{1,in} \end{Bmatrix} \rightarrow \begin{Bmatrix} 1 \\ 0 \end{Bmatrix} = \begin{bmatrix} \eta_{11}^0 & \eta_{12}^0 \\ \eta_{21}^0 & \eta_{22}^0 \end{bmatrix} \begin{Bmatrix} E_{11}^n \\ E_{21}^n \end{Bmatrix}$$

$$(5.2)$$

where E^n_{11} and E^n_{21} represent the non-dimensional energies normalised with respect to the input power to subsystem *1* for the subsystems *1* and *2* respectively.

Generally formulated the non-dimensional, normalised, space-averaged energy of subsystem *i* when only subsystem *j* is excited, is defined as:

$$E_{ij}^n = \frac{2\pi f E_{ij}}{\Pi_{j,in}}$$

$$(5.3)$$

Secondly, energy is injected in subsystem *2* only. The input power to subsystem *2* and the response of both subsystems due to this excitation are measured. In this case the power balance equations are:

$$\begin{Bmatrix} 0 \\ \Pi_{2,in} \end{Bmatrix} = 2\pi f \begin{bmatrix} \eta_{11}^0 & \eta_{12}^0 \\ \eta_{21}^0 & \eta_{22}^0 \end{bmatrix} \begin{Bmatrix} E_{12} \\ E_{22} \end{Bmatrix} \rightarrow \begin{Bmatrix} 0 \\ 1 \end{Bmatrix} = \begin{bmatrix} \eta_{11}^0 & \eta_{12}^0 \\ \eta_{21}^0 & \eta_{22}^0 \end{bmatrix} \begin{Bmatrix} 2\pi f E_{12}/\Pi_{2,in} \\ 2\pi f E_{22}/\Pi_{2,in} \end{Bmatrix} \rightarrow \begin{Bmatrix} 0 \\ 1 \end{Bmatrix} = \begin{bmatrix} \eta_{11}^0 & \eta_{12}^0 \\ \eta_{21}^0 & \eta_{22}^0 \end{bmatrix} \begin{Bmatrix} E_{12}^n \\ E_{22}^n \end{Bmatrix}$$

$$(5.4)$$

Combining equations *(5.2)* and *(5.4)* results in:

$$\begin{bmatrix} 1 & 0 \\ 0 & 1 \end{bmatrix} = \begin{bmatrix} \eta_{11}^0 & \eta_{12}^0 \\ \eta_{21}^0 & \eta_{22}^0 \end{bmatrix} \begin{bmatrix} E_{11}^n & E_{12}^n \\ E_{21}^n & E_{22}^n \end{bmatrix}$$

$$(5.5)$$

The loss factor matrix $[\eta^0]$ can be obtained by inverting the normalised energy matrix:

$$\begin{bmatrix} \eta_{11}^0 & \eta_{12}^0 \\ \eta_{21}^0 & \eta_{22}^0 \end{bmatrix} = \begin{bmatrix} E_{11}^n & E_{12}^n \\ E_{21}^n & E_{22}^n \end{bmatrix}^{-1}$$

$$(5.6)$$

By rearranging the terms of the matrix $[\eta^0]$, the loss factors are derived according to:

$$\eta_{11} = \eta_{11}^0 + \eta_{21}^0 \qquad \eta_{12} = -\eta_{21}^0$$
$$\eta_{21} = -\eta_{12}^0 \qquad \eta_{22} = \eta_{22}^0 + \eta_{12}^0$$

$$(5.7)$$

5.2.2.2 System consisting of *n* subsystems

For a system consisting of *n* subsystems the same procedure as for two subsystems is followed. In this case energy is injected in *n* single subsystems successively. Equation *(5.6)* can be generalised for *n* subsystems as follows:

$$
\begin{bmatrix}
\eta_{11}^0 & \eta_{12}^0 & \cdots & \eta_{1n}^0 \\
\eta_{21}^0 & \eta_{22}^0 & \cdots & \vdots \\
\vdots & \vdots & \ddots & \vdots \\
\eta_{n1}^0 & \cdots & \cdots & \eta_{nn}^0
\end{bmatrix}
=
\begin{bmatrix}
E_{11}^n & E_{12}^n & \cdots & E_{1n}^n \\
E_{21}^n & E_{22}^n & \cdots & \vdots \\
\vdots & \vdots & \ddots & \vdots \\
E_{n1}^n & \cdots & \cdots & E_{nn}^n
\end{bmatrix}^{-1}
\tag{5.8}
$$

By rearranging the terms of the matrix $[\eta^0]$, the loss factors are derived according to:

$$
\eta_{ii} = \sum_{j=1}^{n} \eta_{ji}^0 \qquad \eta_{ij} = -\eta_{ji}^0 \ , i \neq j
\tag{5.9}
$$

5.2.2.3 Using sub-sets of the normalised energy matrix

In practical applications damping and coupling loss factors can be approximated by taking only a part of equation *(5.8)* into account. For example, loss factors for two subsystems *i* and *j* and one coupling can be determined from a 2x2 sub-set of the normalised energy matrix:

$$
\begin{bmatrix}
\begin{bmatrix}
\eta_{ii}^0 & \eta_{ij}^0 \\
\eta_{ji}^0 & \eta_{jj}^0
\end{bmatrix}
\end{bmatrix}
=
\begin{bmatrix}
\begin{bmatrix}
E_{ii}^n & E_{ij}^n \\
E_{ji}^n & E_{jj}^n
\end{bmatrix}^{-1}
\end{bmatrix}
\tag{5.10}
$$

The basic assumption behind this is that not all normalised energy terms in equation *(5.8)* equally contribute to the loss factors in equation *(5.10)*. Only terms that primarily contribute to the loss factors are considered. Depending on the desired accuracy 2x2, 3x3, 4x4, … sub-sets can be used.

If the normalised energy matrix is diagonally dominant[79] the loss factors can be approximated by:

$$\eta_{ii}^0 \cong \frac{1}{E_{ii}^n} \qquad \eta_{ij}^0 \cong -\frac{E_{ij}^n}{E_{ii}^n E_{jj}^n}$$

$$\eta_{ji}^0 \cong -\frac{E_{ji}^n}{E_{ii}^n E_{jj}^n} \qquad \eta_{jj}^0 \cong \frac{1}{E_{jj}^n}$$

$$(5.11)$$

Equation *(5.11)* is a first amelioration of an approximate solution of Stimpson and Lalor [ref 65]. In this study, results obtained from equations *(5.8)* and *(5.11)* have been compared based on measurements in the third experimental set-up (see section 5.6.4).

5.2.2.4   Omission of terms in the normalised energy matrix

Damping and coupling loss factors can also be approximated by omitting the energy contribution of some subsystems and accordingly putting the normalised energy terms corresponding to these subsystems in equation *(5.8)* to zero. In [ref 7] De Langhe shows that normalised energy terms can be omitted when they are very small compared to the non-omitted terms. In order to decide about this, clear insight in the model is needed. Small terms do not always correspond to "distant" subsystems, i.e. subsystems that are coupled indirectly to a subsystem considered. "Distant" subsystems can have an energy level that is significant compared to the energy levels of subsystems that are directly coupled to a subsystem considered. In this case these "distant" subsystems cannot be neglected. An example of a "distant" subsystem is a subsystem associated with a physical system element that has a large mass (for example because of a large area in case all subsystems are made of the same material), compared to other physical system elements, and a similar velocity.

Since it was not clear a priori whether "distant subsystems" in pipe systems contribute to the energy transmission between subsystems, e.g. due to acoustic coupling via the pipe fluid, omission of matrix terms has not been applied in this study. Acoustic coupling between indirectly coupled pipe walls[80] in pipe systems might play an important role in the sound transmission, especially when flexible couplings between pipes are applied. Therefore the influence of acoustic coupling, and "distant subsystems", cannot be neglected a priori.

---

[79] This corresponds to the SEA assumption of weak coupling.

[80] There are no structural couplings between these pipe walls. The only coupling is the coupling via the pipe fluid and/or the ambient fluid.

5.2.3 Determination of coupling loss factors from subsystems energies, damping loss factors and modal densities

As mentioned in section 5.2.2 coupling loss factors determined with PIM are very sensitive to small errors in the measured input power data (see footnote 77). For systems consisting of two subsystems only, the coupling loss factors for the connection between the subsystems can also be determined from the difference in subsystems energies, in case the damping loss factors and modal densities of the subsystems are known. Then, no input powers are needed. The subsystems energies are derived from measurements. This method is described below.

Suppose a system consisting of two subsystems of which one subsystem is set into vibration. The power balance equations for this system are given by equation *(2.4)* in section 2.4.1. For this example, in these equations $\Pi_{1,in}$ is the applied input power, $\Pi_{2,in}$ equals zero. The power balance equation for the second subsystem then becomes:

$$0 = -2\pi f \eta_{12} E_1 + 2\pi f (\eta_{22} + \eta_{21}) E_2 \qquad (5.12)$$

From this equation and 'reciprocity relationship' *(2.7)* between the two subsystems the coupling loss factors can be derived. For example, η_{12} can be calculated from:

$$\frac{E_2}{E_1} = \frac{\eta_{12}}{\eta_{22} + \eta_{21}} = \frac{\eta_{12}}{\eta_{22} + \dfrac{n_1}{n_2} \eta_{12}}$$

$$(5.13)$$

$$\eta_{12} = \frac{\eta_{22} E_2}{E_1 - \dfrac{n_1}{n_2} E_2}$$

E_1 and E_2 are derived from measurements. η_{22} is derived either from decay rate measurements (has been done in this study) or from theory. n_1 and n_2 are derived from theory (derivation from frequency response measurements is not preferred because of the chance of errors due to the same reasons as mentioned related to the determination of input powers in footnote 77).

η_{21} can be derived in a similar way or from η_{12} with 'reciprocity relationship' *(2.7)*. In both cases the same result is obtained.

η_{12} and η_{21} can also be derived from the power balance equation for the first subsystem, instead of the second subsystem, with:

$$0 = 2\pi f (\eta_{11} + \eta_{12})E_1 - 2\pi f \eta_{21} E_2 \qquad (5.14)$$

Then, $\Pi_{1,in}$ equals zero and $\Pi_{2,in}$ is the applied input power.

In this study, coupling loss factor values derived from equations *(5.12)* and *(5.14)* have been compared based on measurement results in the first experimental set-up. They are only slightly different, so the mean values of the coupling loss factors obtained with equations *(5.12)* and *(5.14)* are presented in this thesis.

5.2.4 Determination of coupling loss factors from point admittances of subsystems and coupling element

The method described in this section has been applied in this study to investigate whether it is possible to estimate coupling loss factors for a rigid point coupling (e.g. a pipe clamp without flexible interlayer) from the point admittances of the coupling element and of the subsystems on both sides of the coupling.

The sound transmission through a coupling element partly depends on vibrational characteristics of the coupling element, e.g. mass, stiffness and damping, and partly on vibrational characteristics of the connected subsystems, e.g. point admittance and dimensions.
Suppose two subsystems connected at a point (or by an element without modal characteristics: mass or (damped) spring), see Figure 5-2.
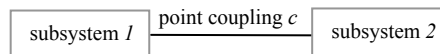
Figure 5-2   Two subsystems connected at a point

The energy flow from subsystem *1* to subsystem *2* equals (see [ref 5] for the derivation of this formula[81])

$$\Pi_{1\to2} = \frac{v_1^2\ Re(Y_2)}{\left|Y_1 + Y_2 + Y_c\right|^2} \qquad (5.15)$$

where Y_1, Y_2 and Y_c represent the point admittances of the subsystems *1* and *2* and of the coupling element respectively.

The energy flow also equals

$$\Pi_{1\to2} = 2\pi f\eta_{12}E_1 = 2\pi f\eta_{12}M_1 v_1^2 \qquad (5.16)$$

From equations *(5.15)* and *(5.16)* the following definition for the coupling loss factor η_{12} can be derived:

$$\eta_{12} = \frac{Re(Y_2)}{2\pi f M_1 \left|Y_1 + Y_2 + Y_c\right|^2} \qquad (5.17)$$

The coupling loss factor η_{21} can be calculated with equation *(5.17)* by transposing *1* and *2* or can be derived from 'reciprocity relationship' *(2.7)* between the subsystems *1* and *2*. The first method is applied in this study. Also deviations from the 'reciprocity relationship' (as written in equation *(3.3)*) are determined. This gives insight in the inaccuracy resulting from the determination method and the fact that only vibrations perpendicular to the pipe and plate surfaces are included (see below). The inaccuracy cannot be determined in case the second method would be applied.

When vibrations in more than one vibrational direction contribute to the sound transmission between two physical system elements, a coupling loss factor for each direction can be determined with equation *(5.17)*. Lyon and DeJong [ref 4] state that, when only translations determine the sound transmission, the coupling loss factors of the different directions can be summed. When both translations and rotations determine the sound transmission, as is the case with flexural vibrations, the total coupling loss factor will be higher than the sum of the separate coupling loss factors due to coupling of the translations and rotations. This might be the case for the coupling considered (a pipe clamp), because flexural vibrations determine the vibrational behaviour of both pipes and plates. Because the simplified SEA

---

[81] In [ref 5] this formula is applied for structural point couplings by wall-ties between cavity walls.

model only considers vibrations perpendicular to pipe walls and plates, only coupling loss factors due to translation in this vibrational direction have been determined for coupling by a pipe clamp in the first experimental set-up (see section 5.4).

An important advantage of this method is that it avoids that a new complete experimental set-up has to be built for each new (not yet considered) situation. Point admittances of subsystems and rigid coupling elements are often known or can be determined rather simply.

5.3   Damping loss factors for a pipe and two plates determined with the decay rate method

5.3.1   Experimental set-ups

For a straight PVC pipe with sound-absorbing elements[82] in the pipe at the ends, the decay time and loss factor of mode types with a response component perpendicular to the pipe wall have been determined. This has also been done for out-of-plane vibrations, i.e. vibrations perpendicular to the structure surface, in two plates. Figure 5-3 to Figure 5-5 show the experimental set-ups.

---

[82] Because of these sound-absorbing elements, made of soft foam, acoustic reflections at the pipe ends were avoided, in order to simulate an infinite pipe fluid, which corresponds to the situation of a practical pipe system of which the pipe considered could be part of. The absorption coefficient of the foam elements varies between 0,7 and 1 from 100 Hz up to 2500 Hz. On one side (in the pipe) the sound-absorbing elements were cone-shaped and their length was 380 mm.
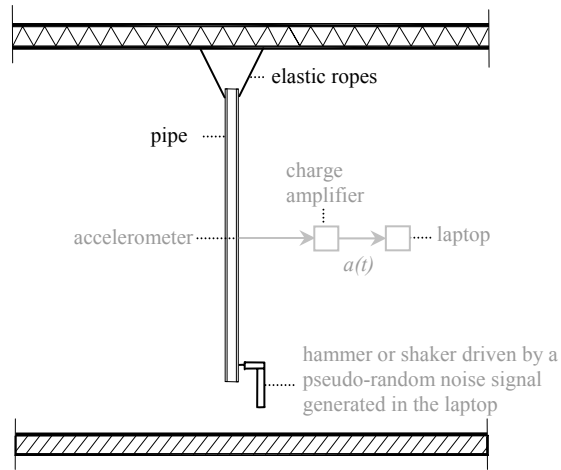
Figure 5-3   Experimental set-up with hammer or shaker excitation for the determination of the decay time and loss factor of an air-filled PVC pipe with 3,8 mm wall thickness, outer shell radius 55 mm and pipe length 2,7 m
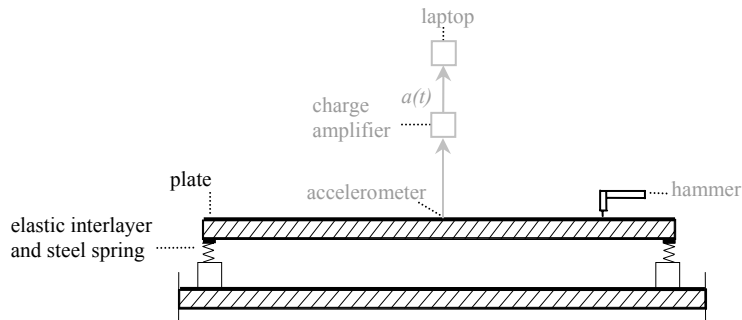
Figure 5-4   Experimental set-up with hammer excitation for the determination of the decay time and loss factor of a concrete plate with dimensions 3,0x2,8x0,12 m^3
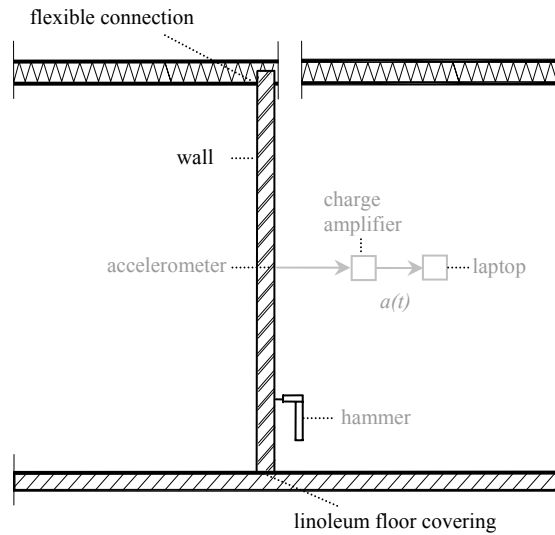
Figure 5-5   Experimental set-up with hammer excitation for the determination of the decay time and loss factor of a calcium-silicate wall with dimensions $4,4 \times 3,4 \times 0,1$ m^3 and with a plaster layer of about 10 mm thickness at both sides

In the first experimental set-up, the pipe was suspended from the ceiling of the measurement room by using elastic ropes. By doing so a mass-spring system with a natural frequency below 10 Hz, i.e. far below the frequency range of interest, was realised.

In the second experimental set-up, the concrete plate was supported on six steel springs with an elastic interlayer between the springs and the plate, resulting in a mass-spring system with a natural frequency for the 'vertical' rigid body mode below 10 Hz.

Since mass-spring-systems were created, there was no vibrational interaction between the subsystems and other structural elements in the frequency range of interest. From the decay time the total loss factor has been determined. Since the subsystems were 'uncoupled' from their surroundings, the total loss factor is essentially equal to the damping loss factor.

In the third experimental set-up, the wall was a separation wall[83] between two measurement rooms and was placed on the linoleum floor covering on the concrete floor of the laboratory. At the side and top edges the wall was flexibly connected to lightweight structures (walls/ceilings). For a more extensive description of the structures and joints the

---

[83] The situation of a practical plate with some coupling at the edges was simulated.

reader is referred to section 5.6. From the decay time the total loss factor has been determined. Since the wall was coupled to other structural elements, the total loss factor represents the damping loss factor of the wall and the coupling loss factors corresponding to couplings of the wall to other elements (walls/ceilings).

5.3.2 Measurement method

The impulse responses[84] of the pipe and the plates have been determined in both 1/3-octave and octave bands. For each element, this has been done for at least eight different combinations of excitation and response positions in the reverberant vibrational field. The responses have been derived from acceleration measurements. The measurement equipment is described in appendix V. The analysis has been done with the software module DIRAC[85] [ref 66] on a laptop.

A hammer has been applied for excitation. Also, a shaker driven with a continuous pseudo-random noise signal has been applied for excitation of the pipe. The impulse responses with shaker excitation are obtained by cross-correlating the excitation signal with the measured response at each position. The pseudo-random noise signal was generated in the laptop with the software module DIRAC and corresponds to a Maximum Length Sequence (MLS), see Schroeder [ref 67].

From the impulse response the space-averaged decay time and loss factor in (1/3-)octave bands have been derived. In order to avoid that decay of the band filter response determines the decay time for the systems considered, which is possible in case of relatively high damping, a time-reversed filtering technique is applied in the software module DIRAC.

5.3.3 Experimental results and comparison with values in the literature

The mean loss factors (space-averaged values) in (1/3-)octave bands of the pipe and the two plates are presented in Figure 5-6 to Figure 5-8. The loss factors have been calculated with the obtained decay times T_{10} [86] with hammer excitation. For the pipe also loss factors have been calculated with the obtained decay times T_{10} with shaker excitation.

---

[84] The so-called Schroeder-plot [ref 47] or decay curve provides the backward integrated squared impulse response.

[85] Software module DIRAC, type 7841 from B&K

[86] With the software module DIRAC so-called T_{10}-values have been calculated. These are extrapolated reverberation times corresponding to a response drop of 60 dB, based on an initial response drop of 10 dB in the decay curve, i.e. the slope from −5 dB to −15 dB response level. Since an extrapolated 60 dB response drop instead of a 6 dB response drop has been calculated, the 0,22 in equation *(5.1)* becomes 2,2 in this case.

Many textbooks contain damping loss factor data, for example [ref 4], [ref 5], [ref 6] and [ref 12]. However, often it is not clear whether only material damping or also acoustic radiation losses are included in the damping loss factor values. The contribution of acoustic radiation losses can be significant, particularly for lightly damped structures. In the text under Figure 5-6 to Figure 5-8 the loss factor values obtained in this study are compared with values found in the literature for material damping. For the plates studied the influence of sound radiation on the loss factor values is expected to be negligibly small, because the loss factor values due to sound radiation (values not presented separately in this thesis) are estimated to be at least 10 dB lower than the loss factor values due to material damping. For the pipe studied sound radiation might have a contribution in the loss factors, because the loss factor values due to sound radiation (see Figure IV-2 in appendix IV) are estimated to be 3 dB to 6 dB lower than the loss factor values in Figure 5-6.
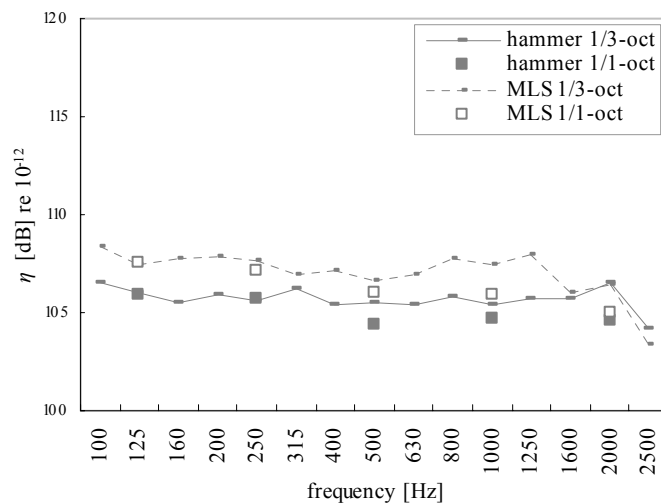
Figure 5-6 Damping loss factors η in (1/3-)octave bands for an <u>air-filled PVC pipe</u> with 3,8 mm wall thickness, outer shell radius 55 mm and pipe length 2,7 m; results are for <u>hammer and shaker (MLS) excitation</u> and are derived from T_{10}-values

Figure 5-6 shows that the damping loss factors in octave bands obtained with shaker excitation are generally higher than the damping loss factors obtained with hammer excitation. The differences and possible causes are discussed in section 5.7, where the loss

---

Generally for structural subsystems it is difficult to achieve a full 60 dB of decay. For plates application of T_{20}-values (i.e. slope from -5 dB to -25 dB response level) is recommended in [ref 45], for example.

factors in Figure 5-6 are also compared with loss factors obtained from PIM and from other experimental set-ups.

Some material damping loss factor data for plastic structures are available in the literature, but the values differ. The material damping of plastics depends on frequency and temperature, but for plastics at practical temperatures in buildings, i.e. between 10^0C and 30^0C, loss factor values due to material damping do not vary much in the frequency range considered. For PVC Norton gives a material damping loss factor value of 0,3 (115 dB re 10^{-12}) [ref 6]. For pure PVC (without plasticizer) Cremer and Heckl give values between 0,025 (104 dB re 10^{-12}) and 0,035 (105 dB re 10^{-12}) for 5^0C and between 0,03 (105 dB re 10^{-12}) and 0,06 (108 dB re 10^{-12}) for 50^0C [ref 12]. Fégeant gives a material damping loss factor value for PVC of 0,05 (107 dB re 10^{-12}) [ref 80]. The loss factors in Figure 5-6 correspond with the values in the literature, except with the values given by Norton. However, Norton gives for PVC a density of 66 kg/m^3 [ref 6], which differs that much from the PVC applied in this study (density about 1393 kg/m^3) that it is concluded that Norton probably considers a much softer PVC and that the results obtained in this study cannot be compared with the values given by Norton.
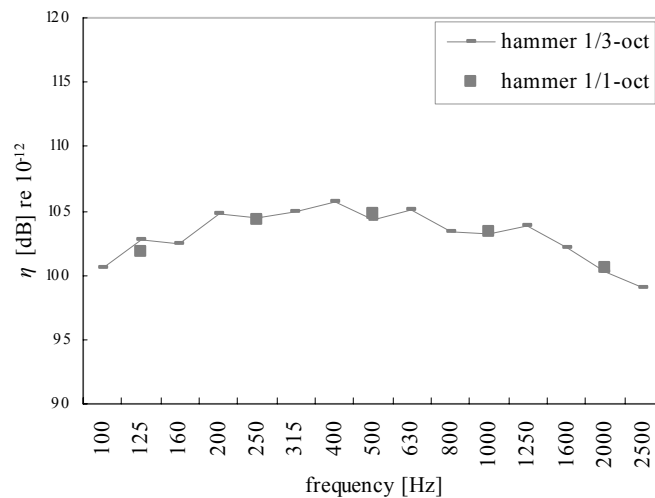
Figure 5-7 Damping loss factors η in (1/3-)octave bands for a <u>concrete plate</u> with dimensions 3,0x2,8x0,12 m^3; results are for hammer excitation and are derived from T_{10}-values

For porous concrete Cremer and Heckl [ref 12] give a material damping loss factor value of 0,01 (100 dB re 10^{-12}). For dense concrete Cremer and Heckl [ref 12] give material damping loss factor values between $4 \cdot 10^{-3}$ (96 dB re 10^{-12}) and $8 \cdot 10^{-3}$ (99 dB re 10^{-12}). For

brick and concrete Norton [ref 6] gives a value of 0,015 (102 dB re 10^{-12}). The loss factors in Figure 5-7 are higher than the values found in the literature in the largest part of the frequency range of interest. The concrete plate considered is poured in a steel framing. Possibly there are some coupling losses from the concrete plate to the steel framing that contribute to the relatively high loss factor values.
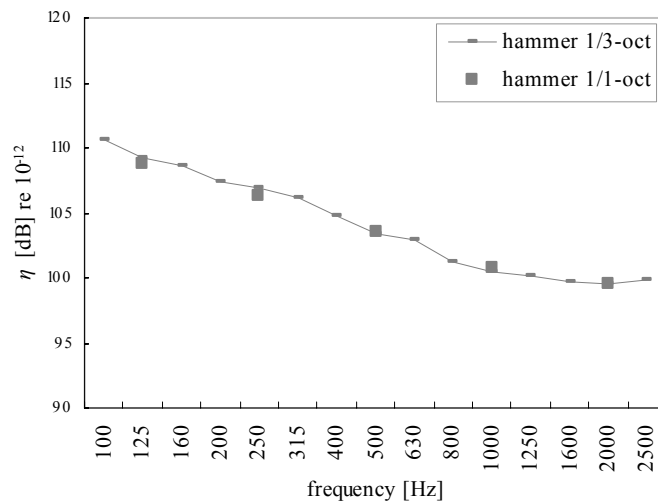
Figure 5-8 Total loss factors η in (1/3-)octave bands for a <u>calcium-silicate wall</u> with dimensions 4,4x3,4x0,1 m^3 and with a plaster layer of about 10 mm thickness at both sides; results are for hammer excitation and are derived from T_{10}-values

For brick Cremer and Heckl [ref 12] give material damping loss factor values between $1 \cdot 10^{-2}$ (100 dB re 10^{-12}) and $2 \cdot 10^{-2}$ (103 dB re 10^{-12}). Norton [ref 6] gives a value of 0,015 (102 dB re 10^{-12}). For plaster Norton [ref 6] gives a value of 0,005 (97 dB re 10^{-12}). At high frequencies, where the influence of coupling to the connected structures is smaller than at low frequencies, the loss factors in Figure 5-8 correspond to the values for material damping found in the literature for brick. At low frequencies coupling losses to the connected structures become more important, which is illustrated by higher loss factors in Figure 5-8. Since the calcium-silicate wall is only indirectly connected to a concrete floor (linoleum layer in between) and the other three edges only have flexible connections to gypsumboard structures, prediction of the coupling losses is difficult.

5.4 Pipe clamps

This section is aimed at testing the validity of the assumptions 4, 5 and 8 of the simplified SEA model for pipe clamps. The test results are described in section 5.4.4. For the testing, results obtained with PIM are used. In order to determine whether the results are sufficiently accurate for the testing, in section 5.4.3 the results are compared with results obtained with the two other methods for the determination of coupling loss factors considered in this study. In section 5.4.3, also the contribution of sound radiation in the coupling loss factors is estimated.

This section primarily concerns coupling loss factors, because coupling loss factors are needed to test the validity of the assumptions. The determination of damping and coupling loss factors in general is discussed in section 5.7.

The results of all three methods are obtained from measurements in the same experimental set-up. In section 5.4.1 the experimental set-up is described, in section 5.4.2 the applied measurement methods. To obtain coupling loss factors from point admittances, various elements in the set-up have been separated.

5.4.1 Experimental set-up and subsystems definition

In the laboratory an experimental set-up has been built, consisting of two subsystems, in accordance with the subsystems definition of the simplified SEA model. A plastic wastewater pipe was mounted at one point on a plate with a pipe clamp. The pipe clamp was the test specimen. Coupling loss factors for all sorts of pipe clamps might be determined in this laboratory set-up.

In order to avoid that specific modes in either the pipe or the plate determine the coupling loss factors, a multi-modal vibrational behaviour of both pipe and plate is desired. The dimensions of the pipe and the plate were chosen in accordance with this.

Figure 5-9 shows the experimental set-up and the corresponding subsystems definition.
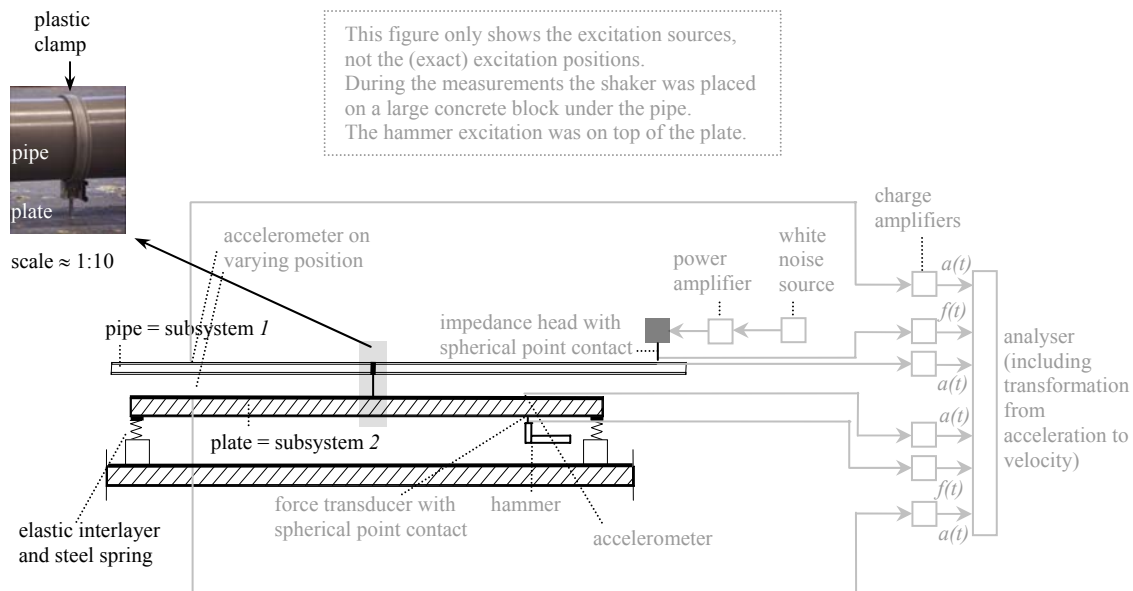
Figure 5-9 Experimental set-up for the determination of damping and coupling loss factors; subsystem *1*: air-filled PVC pipe, wall thickness 3,8 mm, outer shell radius 55 mm, pipe length 2,7 m; subsystem *2*: concrete plate, dimensions 3,0x2,8x0,12 m^3; coupling: a pipe clamp (coupling loss factors for other types of pipe clamps might be determined in this set-up too)

By using springs, there was no vibrational interaction between the test system and other structural elements in the frequency range of interest (see also section 5.3.1).

Coupling loss factors have been determined for a pipe clamp that is often applied in buildings in the Netherlands. The clamp consisted of three parts: a plastic ring, a steel bar with screw thread and a plastic coupling element between ring and bar.

Sound radiation is included in the damping and coupling loss factors, but plays no significant role. This is explained in more detail in section 5.4.3. The subsystems were only connected to each other, so no coupling to other structures is included in the damping loss factors and the coupling loss factors are entirely determined by the pipe clamp between the subsystems.

From measurements in the set-up as shown in Figure 5-9 loss factors have been estimated with PIM and from the subsystems energies, damping loss factors and modal densities, i.e. the methods described in sections 5.2.2 and 5.2.3.

In order to estimate the coupling loss factors from point admittances, i.e. the method described in section 5.2.4, the experimental set-up has been divided in three parts for which theoretical or experimental determination of the real and imaginary parts of the point admittances (see below) is relatively easy, see Figure 5-10.

Actually, the elements 1, 2 and c were separated during the measurements.
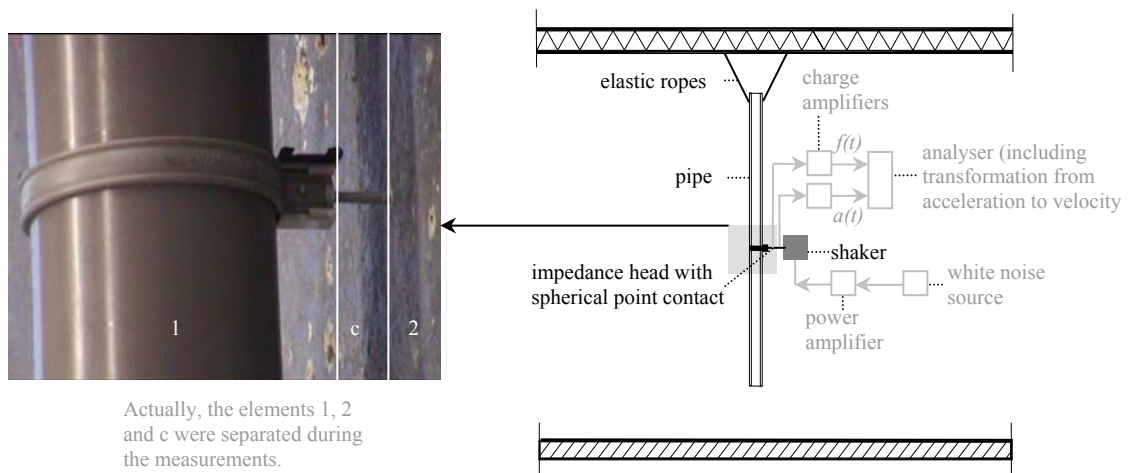
Figure 5-10 Left: separation of pipe, clamp and plate in the experimental set-up for determination of the coupling loss factors for the pipe clamp from point admittances; **Right**: experimental set-up for the determination of the point admittance of the pipe including the plastic ring and coupling element (part indicated as 1 in the left picture)

The plastic ring and coupling element of the pipe clamp were connected to the pipe. The real and imaginary parts of the point admittance have been determined from measurements on the point where the steel bar normally connects the plastic coupling element with a plate[87].

---

[87] Only the point admittance perpendicular to the pipe wall and plate surface can be determined from measurements at the exact point where the steel bar normally is connected to the plastic coupling element. For the other vibrational directions (not considered in this thesis) the point admittances would be determined from measurements on the side surfaces of the plastic coupling element, i.e. not on the exact coupling point, which might result in small errors. By the way, measurements on the plastic coupling element and (directly) on the pipe wall in the vibrational direction perpendicular to the pipe wall and plate surface have shown small differences in point admittance (the results are not shown in this thesis). This illustrates that the coupling

The imaginary part of the point admittance at the ends of the steel bar has been determined theoretically[88].

In this case the imaginary part of the point admittance of the plate and the real part of the point admittance of the steel bar equal zero, so equation *(5.17)* can be written as:

$$\eta_{12} = \frac{Re(Y_2)}{2\pi f M_1 \left\{ (Re(Y_1) + Re(Y_2))^2 + (Im(Y_1) + Im(Y_c))^2 \right\}} \qquad (5.18)$$

The real part of the point admittance of the plate has been determined from measurements. In this study the coupling loss factors η_{21} have been calculated by transposing *1* and *2* in equation *(5.18)* (see the explanation in section 5.2.4).

5.4.2   Measurement methods

The pipe was excited with a shaker driven by a white noise signal[89]. The input power to and point admittance of the pipe have been derived from force and acceleration measurements with an impedance head. For the determination of coupling loss factors from point admittances the plastic coupling element was excited (see Figure 5-10), instead of the pipe. In that case the point admittance of the combination of coupling element, pipe ring and pipe has been determined.

Because of practical reasons, the plate was excited with an impedance hammer (about four hits per second). The input power to and point admittance of the plate have been derived from measurements with a force transducer mounted on the hammer and an accelerometer located on the opposite side of the plate from the excitation position.

---

element behaves like a rigid coupling, without or with only little coupling damping and without or only little influence on the modal vibro-acoustic behaviour of the pipe.

[88] The point admittance of the steel bar equals [ref 5]:

$Y_{bar} = i((2\pi f)/K_{bar})$

where K_{bar} represents the bar stiffness.

The compression stiffness of the bar along the bar axis is assumed to be significantly larger than the compression and flexural stiffness perpendicular to the bar axis. Then the coupling losses through the bar due to vibrations perpendicular to the bar axis are smaller than the coupling losses due to vibrations along the bar axis and the excitation of the plate by the pipe can be modelled as a force. The fact that the in-plane point admittances of both pipe and plate are smaller than the point admittances perpendicular to the pipe and plate surfaces may partly contribute to this. This reasoning illustrates that including only radial pipe vibrations and out-of-plane plate vibrations in predictions of the sound transmission through typical pipe clamps, as is done in the simplified SEA model, may result in predictions that are accurate enough within the scope of this thesis.

[89] This results in a flat force spectrum and therefore in an acceptable weighting of all frequencies within a frequency band.

The reverberant vibrational energies of the pipe and plate have been derived from measurements with accelerometers.

The measurements have been done for two excitation positions and ten response positions [90] on both the pipe and plate. However, the combination of coupling element, pipe ring and pipe has only been excited at one position (ring and coupling element approximately halfway the pipe). The measurement equipment is described in appendix V.

At each excitation position the time-averaged input power to the pipe or plate has been derived from equation *(2.18)* in section 2.6.2.

For each excitation position the space- and time-averaged energies of the pipe and plate have been derived from[91]:

$$E \approx \frac{M}{N} \sum_{k=1}^{N} v_k^2 \qquad\qquad (5.19)$$

where v_k is the velocity (r.m.s.) on response position k, N the total number of response positions and M the pipe or plate mass.

Firstly, the damping and coupling loss factors have been calculated in accordance with the procedure of PIM described in section 5.2.2.1. For each excitation position the normalised energies of pipe and plate have been calculated from the input power and space-averaged energy. The normalised energies for all excitation positions have been averaged.

Secondly, the coupling loss factors have been calculated from the energies of the pipe and the plate according to the method described in section 5.2.3. In that case the damping loss factors given in section 5.3 and theoretically determined modal densities (see chapter 4) have been used.

And thirdly, the coupling loss factors have been calculated from the point admittances of the plate and of the combination of coupling element, pipe ring and pipe, according to the method described in sections 5.2.4 and 5.4.1. The point admittance of the steel bar in the pipe clamp has been determined theoretically.

---

[90] Possibly, a higher number of excitation and response positions could have resulted in more accurate results. Nevertheless, the measurements seem to be sufficiently accurate within the context of this chapter.

[91] Since the subsystems masses are well distributed for the subsystems considered in this thesis, no spatially varying mass correction has been applied [ref 7].

The analysis has been performed in 1/3-octave bands. Damping and coupling loss factors in octave bands have been calculated by averaging (energetic) the 1/3-octave band values of the loss factors.

In agreement with the simplified SEA model, only vibrations perpendicular to the structures surfaces have been considered.

5.4.3 Experimental results and discussion about the appropriateness of PIM for testing the validity of assumptions of the simplified SEA model

Figure 5-11 shows the damping and coupling loss factors derived with PIM[92]. Also the criterion for weak coupling (i.e. validation criterion for assumption 5) applied in this thesis is shown. Figure 5-12 shows the coupling loss factors derived with PIM and the other two discussed determination methods.

Both figures also show deviations from the 'reciprocity relationship' (as written in equation *(3.3)*) in section 3.3. Also the range of deviations from the 'reciprocity relationship' from -5 dB to +5 dB (i.e. validation criterion for assumption 8) as allowed in this thesis is shown. The deviations have been calculated from the 1/3-octave and octave[93] band results obtained with PIM and from point admittances. For the other determination method for coupling loss factors, the deviations equal 0 dB of course. Therefore, for this method no deviations are shown in Figure 5-12.

---

[92] Because of bad signal-to-noise ratios, no η_{12}-values are shown for 1/3-octave bands with centre frequencies above 1250 Hz and no η_{11}-, η_{22}- and η_{21}-values are shown above 1600 Hz.

[93] The coupling loss factors and modal densities have been determined for both 1/3-octave and octave bands. From these results, the deviations from the 'reciprocity relationship' in 1/3-octave and octave bands have been determined.

144
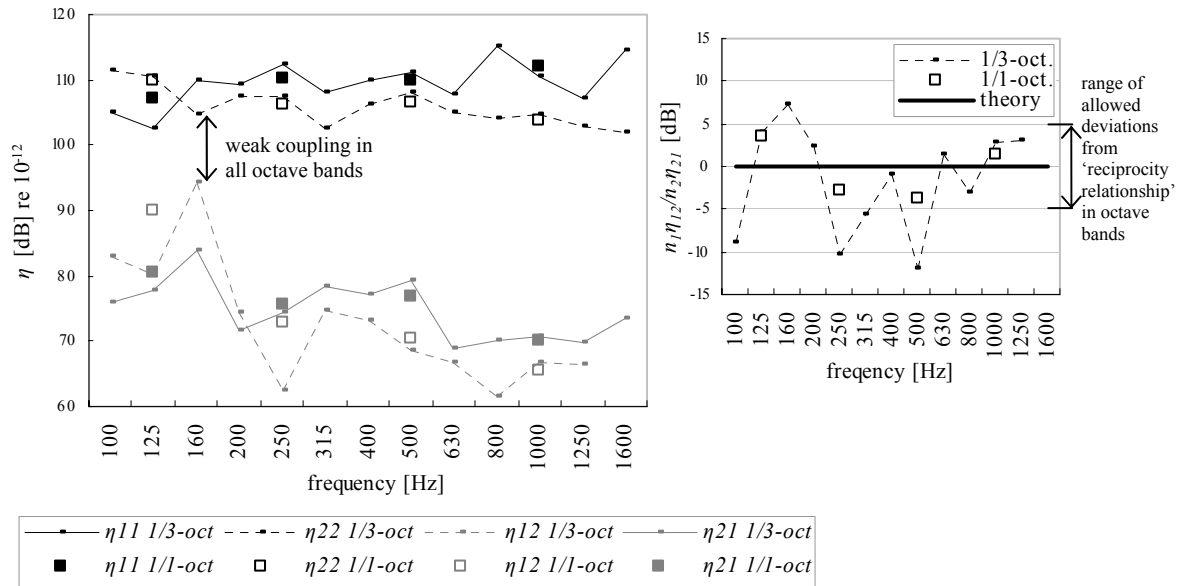
Figure 5-11 Damping and coupling loss factors η in (1/3-)octave bands determined with PIM (**left side**) and corresponding deviations from the 'reciprocity relationship' $\Delta L_{rec.}$ (see equation *(3.3)*) (**right side**); subsystem *1*: air-filled PVC pipe, wall thickness 3,8 mm, outer shell radius 55 mm, pipe length 2,7 m; subsystem *2*: concrete plate, dimensions 3,0x2,8x0,12 m³; coupling: pipe clamp Also the criterion for weak coupling and the range of allowed deviations from the 'reciprocity relationship' applied in this thesis are shown.
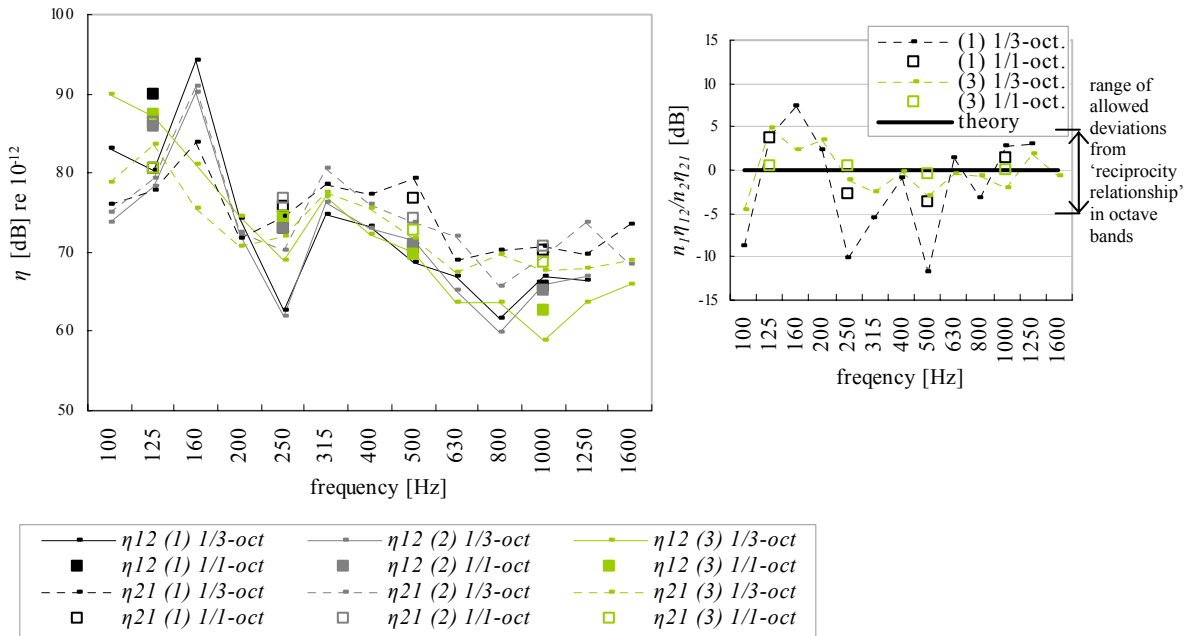
Figure 5-12 Coupling loss factors η in (1/3-)octave bands determined with PIM (indicated as **(1)**), from subsystems energies (indicated as **(2)**) and from point admittances (indicated as **(3)**) (**left side**) and corresponding deviations from the 'reciprocity relationship' $\Delta L_{rec.}$ (see equation *(3.3)*) (**right side**); subsystem *1*: air-filled PVC pipe, wall thickness 3,8 mm, outer shell radius 55 mm, pipe length 2,7 m; subsystem *2*: concrete plate, dimensions 3,0x2,8x0,12 m^3; coupling: pipe clamp. Also the range of allowed deviations from the 'reciprocity relationship' applied in this thesis is shown.

Comparison of damping loss factors obtained with PIM and with the decay rate method

Global comparison of the damping loss factors for the pipe in Figure 5-6 and Figure 5-11 (left) shows that the damping loss factors obtained with PIM are higher than the damping loss factors obtained with the decay rate method. For the plate, comparison of Figure 5-7 and Figure 5-11 (left) also shows higher damping loss factors obtained with PIM, however not for all frequency bands. Besides, for the plate the differences are generally smaller. The differences and possible causes are discussed in section 5.7, where the damping loss factors obtained with both methods are shown in one figure.

Contribution of sound radiation to damping and coupling loss factors

The damping loss factors of both the pipe and the plate are primarily determined by material damping. The damping loss factor values derived in this section are much higher

than the estimated loss factor values due to sound radiation, although for the pipe sound radiation might contribute (for the pipe see Figure IV-2 in appendix IV; for this plate the loss factor due to radiation will be at most approximately $1,5 \cdot 10^{-3}$ (92 dB re 10^{-12}) at the critical frequency of the plate).

In the derived coupling loss factors sound radiation from pipe to plate and reverse is included. The importance of sound radiation has been determined by removing the pipe clamp. The mean velocity level of the plate has been determined for three situations: (1) with the clamp between pipe and plate, and with excitation of the pipe, (2) without the clamp between pipe and plate, and with excitation of the pipe and (3) without excitation of the pipe (velocity level due to background noise). The (arithmetic) difference in velocity level with and without excitation of the pipe has been calculated for the situations with and without clamp. Figure 5-13 shows the results. Also, a difference in velocity level of 3 dB is shown. Only differences larger than 3 dB clearly indicate plate vibrations due to clamping (structural coupling) and/or sound radiation (acoustic coupling). Differences smaller than 3 dB are supposed to indicate (variations in) background noise.
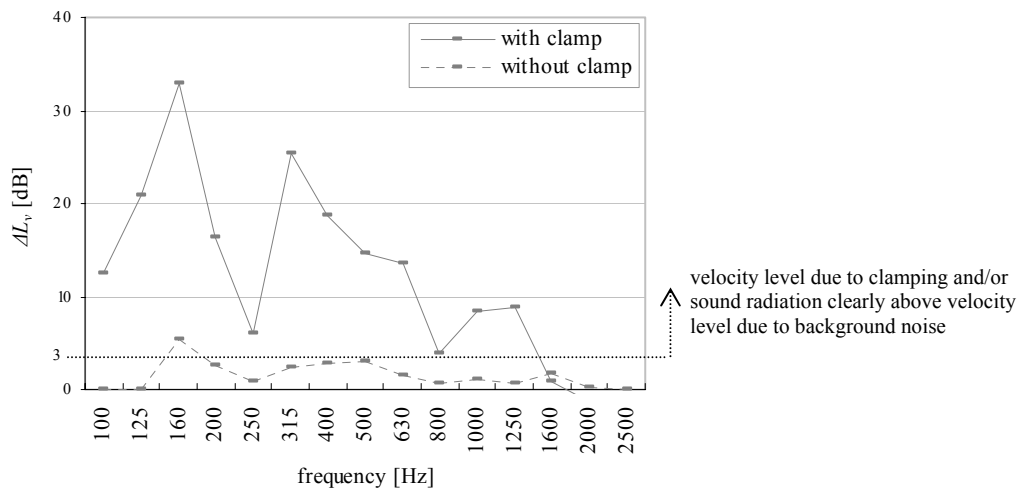
Figure 5-13 (Arithmetic) difference (in 1/3-octave bands) ΔL_v between plate velocity level due to clamping and/or sound radiation and plate velocity level due to background noise for the following situations: (**1**) plastic pipe clamp and (**2**) no pipe clamp between pipe and plate, distance between pipe and plate 70 mm; the source strength is equal for the situations (1) and (2)

Figure 5-13 illustrates that only in the 1/3-octave band with centre frequency 160 Hz[94] there seems to be some sound transmission due to sound radiation from the pipe to the plate: only there the velocity level difference exceeds a value of 3 dB. However, the velocity level difference is much larger with clamping. So, when the pipe clamp considered is applied as a connection between the pipe and the plate, the contribution of sound radiation is negligibly small.

Figure 5-13 also illustrates that the contribution of sound radiation might become more important at increasing frequency, because the differences between the velocity levels due to clamping and due to background noise become smaller at increasing frequency. Especially for more flexible connections between pipes and plates the contribution of sound radiation might become more important. In the future, this could be investigated, but then larger source strengths should be applied. In this study, from 1600 Hz on, the velocity level differences were not large enough to draw conclusions about the contribution of sound radiation, see Figure 5-13.

Similar results as described above were found for another type of pipe clamp (a steel pipe clamp as shown in Figure 4-20), other distances between the pipe and the plate (70 mm in this case, results for distances between 20 mm and 150 mm have been studied) and for the opposite path: sound radiation from the plate to the pipe.

5.4.3.1 Appropriateness of PIM for testing the validity of assumptions

Figure 5-12 (left) shows a rather good agreement between the coupling loss factors in octave bands obtained from the three determination methods applied in this study. Generally speaking, the differences between the loss factors obtained lie between 0 dB and 2 dB, with some exceptions up to 4 dB and one exception of 6 dB at 125 Hz.

In 1/3-octave bands the differences are larger (up to 9 dB from 200 Hz on, below 200 Hz up to 17 dB). The curve trends are similar, although peaks and dips sometimes seem to be shifted.

Figure 5-12 (right) shows differences up to 3 dB in deviations from the 'reciprocity relationship' obtained from the results in octave bands from PIM (first method) and point admittances (third method). The differences are of the same order of magnitude as the differences between the coupling loss factors obtained from these two methods. In 1/3-octave bands the differences are larger.

---

[94] The critical frequency of the plate falls in this frequency band.

It is not clear whether the deviations from the 'reciprocity relationship' for the results obtained from PIM are caused by inaccuracies in the determination method, i.e. the measurements, material data and/or applied modal densities, or by inaccuracy of the simplified SEA model, i.e. the fact that in-plane vibrations are not included but may contribute to the energy transmission between pipe and plate. Furthermore, it is not clear whether the deviations are caused by inaccuracies in the determination of one or both coupling loss factors and/or modal densities. That the applied modal densities can partly be the cause of the deviations also follows from sections 4.2.3.3 and 4.4.3, where inaccuracies in the determination of modal densities are discussed. Literature and other data about deviations from the 'reciprocity relationship' in practical systems are not available, as far as known to the author. So, it is not known what is common for practical systems and the deviations found in this case cannot be compared with other cases. In case the velocity and input power distribution are not uniform and/or the number of excitation and response positions is not large enough, deviations from the 'reciprocity relationship' will occur. From the measurement results in this study it is concluded that the velocity distribution over the subsystems was relatively uniform for each excitation position and that the number of response positions during the measurements was large enough. However, the number of excitation positions was small. Possibly the deviations from the 'reciprocity relationship' would have been smaller in case more excitation positions would have been applied.

Deviations from the 'reciprocity relationship' are smaller for the results obtained from point admittances. The deviations are expected to be caused by inaccuracies in the determination method, i.e. the measurements, material data and/or applied modal densities.

For the second determination method (coupling loss factors from subsystems energies) the deviations equal 0 dB of course (that method is based on reciprocity).

It is not clear which method is the most appropriate one for the determination of coupling loss factors. The second and third methods give no or small deviations from the 'reciprocity relationship'. However, the methods are (more or less) based on reciprocity. The deviations do not represent possible inaccuracies of the simplified SEA model, which results obtained from PIM do. This is discussed in more detail in section 5.7.

Nevertheless, based on the relatively small differences between the results in octave bands from the different determination methods, it is concluded that the results obtained with PIM are sufficiently accurate for testing the validity of the assumptions concerning damping in and coupling between physical system elements.

5.4.4 Validity of the simplified SEA model for pipe clamps

This section is aimed at testing the validity of the assumptions 4, 5 and 8 of the simplified SEA model concerning damping in and coupling (by pipe clamps) between practical wastewater pipes and plates in buildings. The assumptions and corresponding validation criteria are summarised below. See section 3.3 for complete descriptions of assumptions and criteria. For the testing, the results obtained with PIM for the pipe clamp in the previous section are used. The validation criteria are set for octave bands, so only results for octave bands are discussed here.

Validity of assumption 5

Assumption 5
The coupling between subsystems is weak. This assumption is defined to be valid if in each octave band considered the ratio of a coupling loss factor η_{ij}, representing the energy transmission from subsystem i to subsystem j, to the total loss factor $\eta_{i,tot}$ of subsystem i minus η_{ij} is smaller than 0,1 (the total loss factor $\eta_{i,tot}$ minus η_{ij} is at least a factor of 10 (10 dB) higher than the coupling loss factor η_{ij}).

Figure 5-11 shows that for the pipe clamp studied in all octave bands considered the damping loss factors of the pipe and plate are at least 10 dB higher than the coupling loss factors. From the curve trends, it is concluded that this will also be the case in the octave band with centre frequency 2000 Hz. Therefore, assumption 5 is fulfilled in the entire frequency range of interest. This is also the case if damping loss factors obtained from the decay rate method are used (these damping loss factors are 5 dB to 10 dB lower than the damping loss factors obtained from PIM, see the text under Figure 5-12).

An important question is to which extent assumption 5 is fulfilled for other pipes, plates and pipe clamps, i.e. whether the results can be generalised. Some conclusions regarding this are given below, with the corresponding motivation, based on the results obtained in this study.
Assumption 5 is also expected to be fulfilled for:
- other practical pipe and plate dimensions. The damping loss factors are primarily determined by material damping (see the text under Figure 5-12), so not dependent on dimension. For larger pipes and plates, the coupling loss factors become smaller (see equation *(5.18)*, in which *Re(Y)* and *M* become larger), for smaller pipes and plates the opposite occurs. However, in practical situations the range in dimensions is not expected to be that large, that major changes in coupling loss factors occur;

- other practical single, homogeneous plates. For these structures, the damping loss factors are of the same order of magnitude or higher, see for example Figure 5-8;
- other types of pipe clamps. The clamp studied is relatively rigid. For more flexible clamps the coupling will be weaker;
- two clamps instead of one, which also occurs in practice. The coupling loss factors may be 3 dB higher at most (in case the vibro-acoustic behaviour of the clamps is independent which is only correct for a distance between the clamps of at least one wavelength), which still results in weak coupling, except possibly in the octave band 125 Hz (see Figure 5-11), although the differences between damping and coupling loss factors are still expected to be at least 5 dB to 10 dB.

Validity of the assumptions 4 and 8

Assumption 4
The transmission of vibrational energy between subsystems caused by resonant modes is significantly larger (preferably at least a factor of 10) than the energy transmission caused by non-resonant vibrations.

Assumption 8
Out-of-plane plate vibrations are predominantly caused by radial vibrations in pipe systems and vice versa.

These assumptions are defined to be valid if for each pair of connected subsystems, the deviation from the 'reciprocity relationship' (as written in equation *(3.3)*) is 5 dB at most in each octave band considered.

Figure 5-11 shows that for the pipe clamp studied in all octave bands considered the deviation from the 'reciprocity relationship' is 4 dB at most. From the curve trends, it is concluded that this will also be the case in the octave band with centre frequency 2000 Hz. Therefore, the assumptions 4 and 8 are fulfilled in the entire frequency range of interest.
Major changes regarding this are not expected for other pipes, plates and pipe clamps.

The results (loss factors and deviations from 'reciprocity relationship') in 1/3-octave bands show larger fluctuations than the results in octave bands. This is probably caused by the larger number of modes in octave bands, and hence smoother response spectra in octave bands.

5.5   Pipe coupling elements

This section is aimed at testing the validity of the assumptions 4, 5 and 8 of the simplified SEA model for pipe coupling elements. The test results are described in section 5.5.4. For the testing, results obtained with PIM are used. In order to determine whether the results are sufficiently accurate for the testing, in section 5.5.3 the results are compared with results obtained with the two other methods for the determination of coupling loss factors considered in this study. In section 5.5.3, also the contribution of sound radiation in the coupling loss factors is estimated.

This section primarily concerns coupling loss factors, because coupling loss factors are needed to test the validity of the assumptions. The determination of damping and coupling loss factors in general is discussed in section 5.7.

The results of all three methods are obtained from measurements in the same experimental set-up. In section 5.5.1 the experimental set-up is described, in section 5.5.2 the applied measurement methods. To obtain coupling loss factors from point admittances, various elements in the set-up have been considered separately.

5.5.1   Experimental set-up and subsystems definition

In the laboratory an experimental set-up has been built, consisting of two subsystems, in accordance with the subsystems definition of the simplified SEA model. Two plastic wastewater pipes were connected by a discontinuity. The discontinuity was the test specimen. Coupling loss factors for all sorts of discontinuities, i.e. pipe coupling elements such as bends and T-joints[95], might be determined in this laboratory set-up.

In order to avoid that specific modes in the pipes determine the coupling loss factors, a multi-modal vibrational behaviour of the pipes is desired. The dimensions of the pipes were chosen in accordance with this[96].

Figure 5-14 shows the experimental set-up and the corresponding subsystems definition.

---

[95] In order to determine coupling loss factors for a T-joint a similar experimental set-up existing of three pipes should be made.

[96] See the text in section 4.3.1.1 about overlaps of pipe coupling elements and connected pipes.
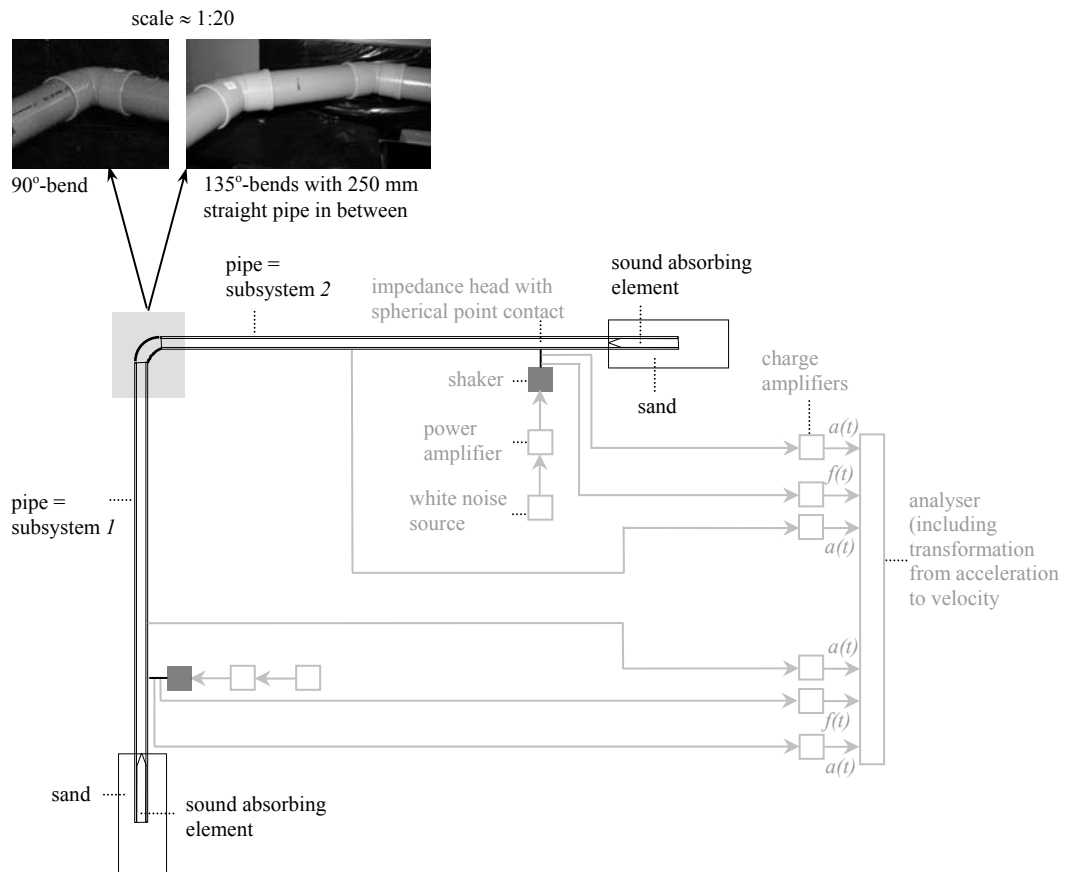
Figure 5-14 Experimental set-up for the determination of damping and coupling loss factors; subsystem *1*: air-filled PVC pipe, wall thickness 3,8 mm, outer shell radius 55 mm, pipe length 3,5 m; subsystem *2*: air-filled PVC pipe, wall thickness 3,8 mm, outer shell radius 55 mm, pipe length 4,0 m; coupling: a bend (the coupling loss factors for two different bends have been determined in this study, but coupling loss factors for other types of bends might be determined in this set-up too)

Coupling loss factors for two discontinuities that are often applied in buildings in the Netherlands, have been determined. The first discontinuity was a 90°-bend. The second discontinuity existed of three parts, i.e. two 135°-bends connected by a 250 mm long straight pipe. In the Netherlands this type of discontinuity is usually applied instead of one 90°-bend in order to avoid the generation of strong turbulent fluid flows.

In the subsystems definition in Figure 5-14, the discontinuity is defined as a coupling. This implies that for the discontinuities studied the number of modes per octave band is assumed to be smaller than six, in accordance with the definition for couplings in this thesis (see

assumption 3 in section 3.3). For the 90°-bend this is correct, see section 4.3.4. However, for the other discontinuity this is only correct below 1000 Hz, see section 4.3.4.

In order to simulate a vibrational behaviour in the pipes as found in infinitely long pipes, reflections at the pipe ends have been avoided as much as possible. This has been achieved by application of sound-absorbing elements[97] in the pipes and sand[98] outside the pipes around the pipe ends. Due to this, extra damping might have been introduced at the pipe ends, resulting in higher total loss factors[99] of the pipes.
In order to avoid sagging of the test system, the pipes were suspended with strings. It is assumed that there was no vibrational interaction between the test system and other structural elements in the frequency range of interest.

From measurements loss factors have been estimated with PIM and from the subsystems energies, damping loss factors and modal densities, i.e. the methods described in sections 5.2.2 and 5.2.3.
Sound radiation is included in the damping and coupling loss factors, but may be negligible, see section 5.5.3. The subsystems were only connected to each other, so no coupling to other structures is included in the damping loss factors and the coupling loss factors are entirely determined by the bend between the subsystems.

In order to estimate the coupling loss factors from point admittances, i.e. the method described in section 5.2.4, equation *(5.17)* has been written as:

$$\eta_{12} = \frac{Re(Y_2)}{2\pi f M_1 \left\{ (Re(Y_1) + Re(Y_2))^2 + (Im(Y_1) + Im(Y_2))^2 \right\}} \qquad (5.20)$$

The real and imaginairy parts of the point admittance of the pipes have been determined from measurements. The bends have not been considered in the estimation. An important question is how this should be done, because there is some overlap of pipes and bends. Besides, the bends are more complicated coupling elements than the pipe clamp in section 5.4 for example. Possibly the coupling loss factors are primarily determined by the fact that two pipes are rigidly coupled under a 90°-angle, and not that much by the connection between pipes and bends (the overlap) and the fact that the second bend considered existed

---

[97] See footnote 82 in section 5.3.1.

[98] The pipe ends have been put into sand along 850 mm, which equals half of the flexural wavelength corresponding to 100 Hz.

[99] The extra damping could also be interpreted as an energy sink.

154

of two bends and a short straight pipe in between. Leaving out the bends makes it a very rough, but simple estimation, just to investigate whether results obtained with PIM seem appropriate for testing the validity of the assumptions.

In this study the coupling loss factors η_{21} have been calculated by transposing *1* and *2* in equation *(5.20)* (see the explanation in section 5.2.4).

5.5.2   Measurement methods

The methods and equipment described in section 5.4.2 and appendix V for the determination of the various needed parameters for pipes have been applied. Measurements have been done for two excitation positions and ten response positions on both pipes (this is not relevant for the determination of coupling loss factors from point admittances).

5.5.3   Experimental results and discussion about the appropriateness of PIM for testing the validity of assumptions of the simplified SEA model

Figure 5-15 and Figure 5-16 show the damping and coupling loss factors derived with PIM for the two bends[100]. Also the criterion for weak coupling (i.e. validation criterion for assumption 5) applied in this thesis is shown. Figure 5-17 and Figure 5-18 show the coupling loss factors for both bends derived with PIM and the other two discussed determination methods. The four figures also show deviations from the 'reciprocity relationship' (as written in equation *(3.3)*) in section 3.3 (see section 5.4.3 for more explanation). Also the range of deviations from the 'reciprocity relationship' from -5 dB to +5 dB (i.e. validation criterion for assumption 8) as allowed in this thesis is shown.

---

[100] Because of bad signal-to-noise ratios, no values are shown for 1/3-octave bands with centre frequencies above 1600 Hz.
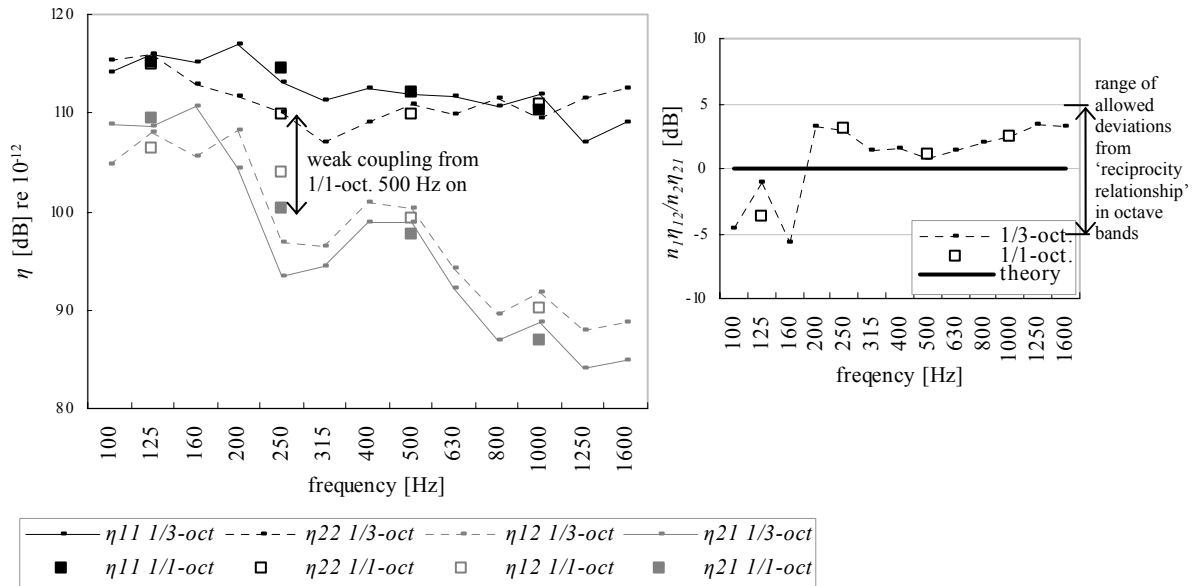
Figure 5-15 Damping and coupling loss factors η in (1/3-)octave bands determined with PIM (**left side**) and corresponding deviations from the 'reciprocity relationship' $\Delta L_{rec.}$ (see equation *(3.3)*) (**right side**); subsystem *1*: air-filled PVC pipe, wall thickness 3,8 mm, outer shell radius 55 mm, pipe length 3,5 m; subsystem *2*: air-filled PVC pipe, wall thickness 3,8 mm, outer shell radius 55 mm, pipe length 4,0 m; <u>coupling: 90°-bend.</u> Also the criterion for weak coupling and the range of allowed deviations from the 'reciprocity relationship' applied in this thesis are shown.
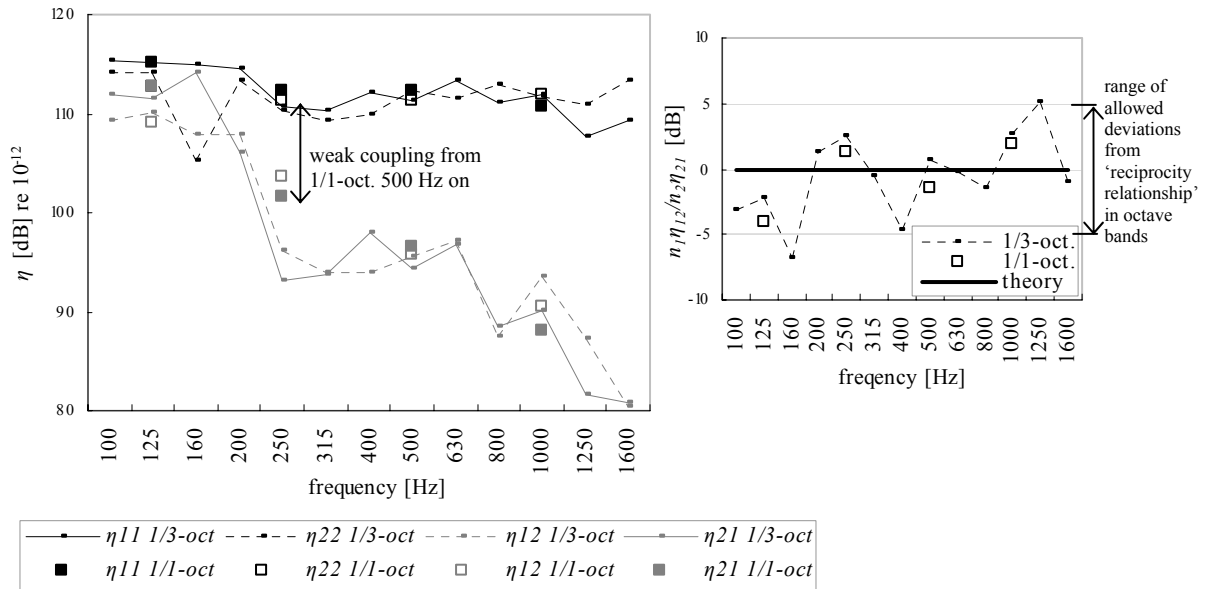
Figure 5-16 Damping and coupling loss factors η in (1/3-)octave bands determined with PIM (**left side**) and corresponding deviations from the 'reciprocity relationship' $\Delta L_{rec.}$ (see equation *(3.3)*) (**right side**); subsystem *1*: air-filled PVC pipe, wall thickness 3,8 mm, outer shell radius 55 mm, pipe length 3,5 m; subsystem *2*: air-filled PVC pipe, wall thickness 3,8 mm, outer shell radius 55 mm, pipe length 4,0 m; coupling: two 135°-bends connected by a 250 mm long straight pipe. Also the criterion for weak coupling and the range of allowed deviations from the 'reciprocity relationship' applied in this thesis are shown.
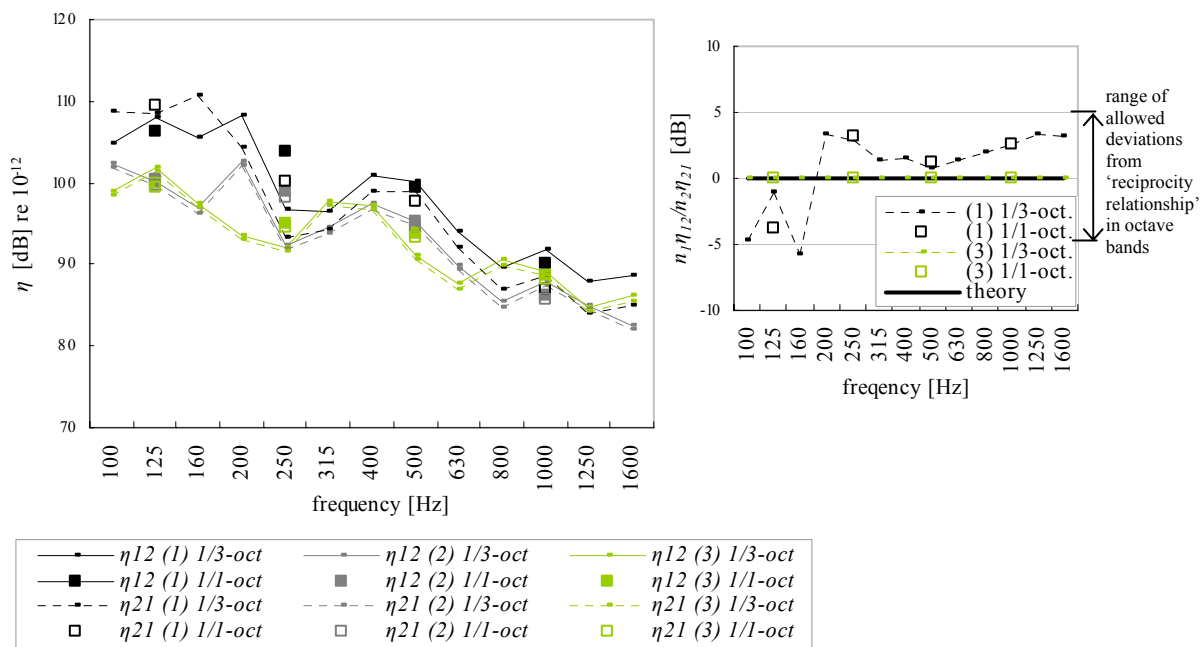
Figure 5-17 Coupling loss factors η in (1/3-)octave bands determined with PIM (indicated as **(1)**), from subsystems energies (indicated as **(2)**) and from point admittances (indicated as **(3)**) (**left side**) and corresponding deviations from the 'reciprocity relationship' $\Delta L_{rec.}$ (see equation *(3.3)*) (**right side**); subsystem *1*: air-filled PVC pipe, wall thickness 3,8 mm, outer shell radius 55 mm, pipe length 3,5 m; subsystem *2*: air-filled PVC pipe, wall thickness 3,8 mm, outer shell radius 55 mm, pipe length 4,0 m; coupling: 90º-bend. Also the range of allowed deviations from the 'reciprocity relationship' applied in this thesis is shown.
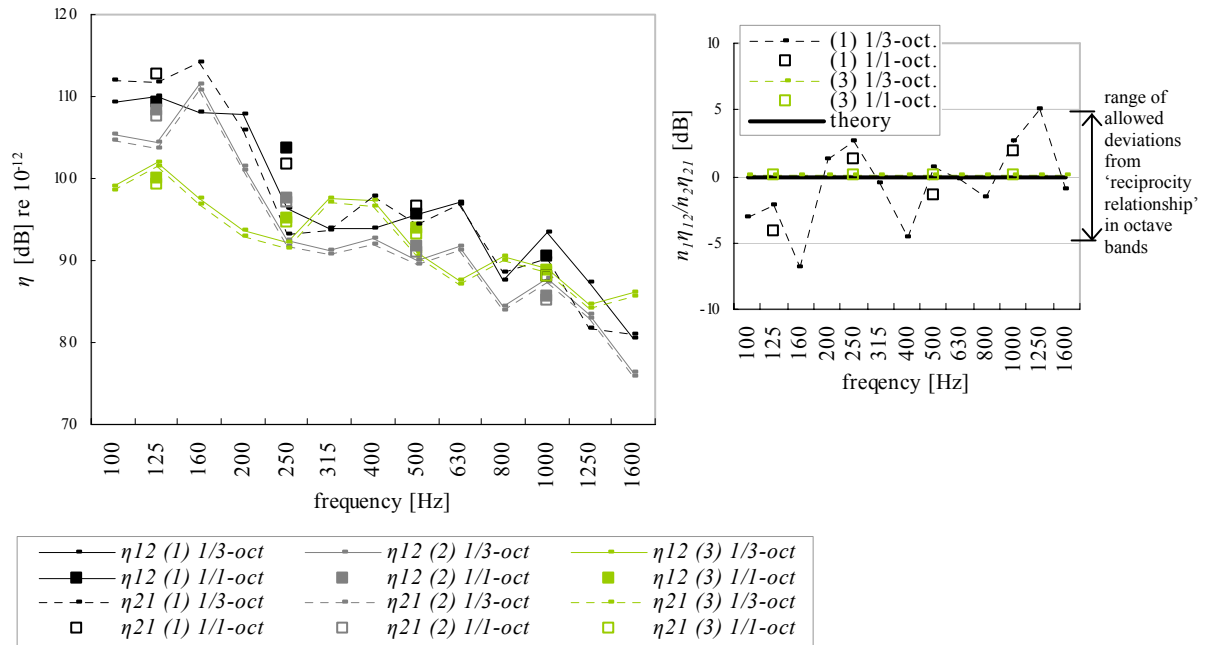
Figure 5-18 Coupling loss factors η in (1/3-)octave bands determined with PIM (indicated as (**1**)), from subsystems energies (indicated as (**2**)) and from point admittances (indicated as (**3**)) (**left side**) and corresponding deviations from the 'reciprocity relationship' $\Delta L_{rec.}$ (see equation *(3.3)*) (**right side**); subsystem *1*: air-filled PVC pipe, wall thickness 3,8 mm, outer shell radius 55 mm, pipe length 3,5 m; subsystem *2*: air-filled PVC pipe, wall thickness 3,8 mm, outer shell radius 55 mm, pipe length 4,0 m; <u>coupling: two 135°-bends connected by a 250 mm long straight pipe.</u> Also the range of allowed deviations from the 'reciprocity relationship' applied in this thesis is shown.

Comparison of damping loss factors obtained with PIM and with the decay rate method

Global comparison of the damping loss factors for the pipes in Figure 5-15 (left) and Figure 5-16 (left) with the damping loss factors for the pipe in Figure 5-6 shows that the damping loss factors obtained with PIM are higher than the damping loss factors obtained with the decay rate method. A full comparison is not possible, because some non-specified damping due to sand around the pipes ends may be included in the damping loss factors in Figure 5-15 (left) and Figure 5-16 (left) (the damping loss factors are generally higher than in Figure 5-11). The differences and possible causes are discussed in section 5.7, where the damping loss factors obtained with both methods are shown in one figure.

159

Contribution of sound radiation to damping and coupling loss factors

The damping loss factors of the pipes are primarily determined by material damping. The damping loss factor values derived in this section are much higher than the estimated loss factor values due to sound radiation, although sound radiation might contribute (see Figure IV-2 in appendix IV).

The coupling loss factors are expected to be primarily determined by the structural coupling of the pipe walls, based on the results described in section 5.6.4 for similar pipe coupling elements. Acoustic coupling between the pipes via the pipe fluid (air) is included in the derived coupling loss factors and is not characterized separately. For more flexible connections of pipe system elements and for high frequencies, the contribution of sound radiation might become more important (see section 5.4.3 where this is explained for pipe clamps).

In the set-up in this section strong acoustic coupling via the ambient medium (air) has been avoided by application of a large amount of sound-absorbing material in the measurement room. This has resulted in a reverberation time that is comparable to reverberation times in practical building situations and in the first and third laboratory set-ups[101].

Comparison of damping loss factors obtained for the two straight pipes in the two set-ups

Figure 5-15 (left) shows large differences in the damping loss factor values for the two straight pipes, especially in the 250 Hz octave band and corresponding 1/3-octave bands. Comparison of Figure 5-15 (left) and Figure 5-16 (left) shows differences in the damping loss factor values for each pipe. Actually, the values should be equal for both pipes in both set-ups. Possibly, there were variations in the application of sand around the pipe ends. This might also be the cause of the differences in the coupling loss factors for each bend (see below).

Comparison of coupling loss factors obtained with PIM for both sound transmission directions

Approximately equal coupling loss factors for both sound transmission directions (from subsystem *1* to subsystem *2* and the opposite direction) are expected. However, not exactly equal. This is explained below.

---

[101] Experimental set-up 1 was situated in one of the rooms of experimental set-up 3. Experimental set-up 2 was situated in a reverberation room.

The pipe lengths differ. So the modal densities and pipe masses differ, both to the same extent. With equation *(4.5)* the following relation for the ratio of the point admittances of the pipes can be derived:

$$\frac{Re(Y_1)}{Re(Y_2)} = \frac{\dfrac{n_1}{4M_1}}{\dfrac{n_2}{4M_2}} = \frac{n_1 M_2}{n_2 M_1} \tag{5.21}$$

Equation *(5.21)* shows that the ratio of the point admittances equals 1.

With equation *(5.17)* in section 5.2.4 the following relation for the ratio of the coupling loss factors for both directions can be derived:

$$\frac{\eta_{12}}{\eta_{21}} = \frac{\dfrac{Re(Y_2)}{2\pi f M_1 |Y_1 + Y_2 + Y_c|^2}}{\dfrac{Re(Y_1)}{2\pi f M_2 |Y_1 + Y_2 + Y_c|^2}} = \frac{Re(Y_2) M_2}{Re(Y_1) M_1} \tag{5.22}$$

Since the ratio of the point admittances equals 1, the ratio of the coupling loss factors is determined by the ratio of the pipe masses. For the experimental set-up in this section, a ratio of approximately 1,14 (0,57 dB) between the coupling loss factors is expected. So, higher η_{12}- than η_{21}-values are expected. Figure 5-15 and Figure 5-16 show higher η_{12}- than η_{21}-values from 200 Hz on, except at 400 Hz and 800 Hz in Figure 5-16. However, the coupling loss factor spectra in Figure 5-15 show larger ratios, from 1,5 (1,8 dB) to 2,5 (4 dB) from 200 Hz on. The differences between the coupling loss factor spectra in Figure 5-16 fluctuate more than in Figure 5-15. However, the average difference is smaller. In both figures the coupling loss factors for both directions clearly show the same trends, but the differences between the coupling loss factors for both directions are larger than expected. The correct differences are obtained if the coupling loss factors are derived with the other two determination methods considered (see Figure 5-17 and Figure 5-18).

A more than assumed role of in-plane vibrations in the vibrational transmission between the pipes, i.e. an incomplete subsystems definition, does not seem the cause of the differences. In case the subsystems definition would be incomplete, the effect should be approximately equal in both directions and therefore for both coupling loss factors. Measurement inaccuracies also seem an illogical explanation for the differences, because the effect is

expected to be the same for both coupling loss factors again. So, an explanation for the differences in coupling loss factors for both directions lacks.

5.5.3.1   Appropriateness of PIM for testing the validity of assumptions

Figure 5-17 (left) and Figure 5-18 (left) show a rather good agreement between the coupling loss factors in octave bands obtained from the three determination methods applied in this study, although the differences are larger than for the pipe clamp in section 5.4. Generally speaking, the differences between the loss factors obtained lie between 0 dB and 5 dB, with some exceptions up to 10 dB and one exception of 14 dB at 125 Hz in Figure 5-18 (left).
In 1/3-octave bands the differences are larger (up to 10 dB from 250 Hz on, below 250 Hz up to 17 dB). From 250 Hz on the curve trends are similar, although peaks and dips sometimes seem to be shifted.

Striking is the good agreement between coupling loss factors in octave bands obtained from the second and third method (differences lie between 0 dB and 3 dB, except for 125 Hz in Figure 5-18). This may imply that these methods are more appropriate for the determination of loss factors than PIM. The larger differences with PIM and higher loss factors obtained with PIM may indicate that the loss factors obtained with PIM are influenced by the fact that the pipes ends were put into sand. However, the higher values may also be caused by the fact that in-plane energy transmission plays a more than assumed role, which is not represented in the values obtained with the second and third method.

The deviations from the 'reciprocity relationship' for the results obtained from PIM are not expected to be caused by inaccuracy of the simplified SEA model, i.e. the fact the in-plane vibrations are not included. The error would be the same for both coupling loss factors, and would therefore not result in deviations from the 'reciprocity relationship' (see also the previous section). The deviations may be due to the fact that the pipes ends were put into sand, in different ways, which may have caused different coupling loss factors and unknown changes of the modal densities of the pipes.

The discussion above illustrates that it is not clear which method is the most appropriate one for the determination of coupling loss factors. The second and third methods give no or small deviations from the 'reciprocity relationship'. However, the methods are (more or less) based on reciprocity. The deviations do not represent possible inaccuracies of the

simplified SEA model, which results obtained from PIM do, although the deviations in this case seem to have other causes (see above).

All in all, it is concluded that the results obtained with PIM are sufficiently accurate for testing the validity of the assumptions concerning damping in and coupling between physical system elements. The obtained loss factors may be too high (4-6 dB difference between results from PIM and the second method for octave bands from 250 Hz on), but the results clearly indicate where there is weak coupling (one of the two assumptions). Besides, the deviations from the 'reciprocity relationship' are expected to be overestimated compared to what is expected for the bends in practical situations (due to the causes mentioned above), and therefore appropriate for testing the validity of the other assumption (maybe pessimistic). However, the loss factors cannot be applied straightforward in predictions for example. For this purpose, it should be clarified which values are the proper ones or new values should be determined (see also section 5.7).

5.5.4 Validity of the simplified SEA model for pipe coupling elements

This section is aimed at testing the validity of the assumptions 4, 5 and 8 of the simplified SEA model concerning damping in and coupling (by pipe coupling elements) between pipes within practical wastewater systems. The assumptions and corresponding validation criteria are summarised below. See section 3.3 for complete descriptions of assumptions and criteria. For the testing, the results obtained with PIM for the bends in the previous section are used. The validation criteria are set for octave bands, so only results for octave bands are discussed here.

Validity of assumption 5

Assumption 5

The coupling between subsystems is weak. This assumption is defined to be valid if in each octave band considered the ratio of a coupling loss factor η_{ij}, representing the energy transmission from subsystem i to subsystem j, to the total loss factor $\eta_{i,tot}$ of subsystem i minus η_{ij} is smaller than 0,1 (the total loss factor $\eta_{i,tot}$ minus η_{ij} is at least a factor of 10 (10 dB) higher than the coupling loss factor η_{ij}).

Figure 5-15 and Figure 5-16 show that for the pipes and bends studied the damping loss factors of the connected pipes are at least 10 dB higher than the coupling loss factors from the octave band with centre frequency 500 Hz on. The coupling between the pipes is almost weak in the octave band 250 Hz (differences between damping and coupling loss factors at

least 7 dB). From the curve trends, it is concluded that the coupling will also be weak in the octave band with centre frequency 2000 Hz. Therefore, assumption 5 is fulfilled from the octave band 500 Hz, possibly 250 Hz, on. This may change to one octave band higher when damping loss factors obtained from the decay rate method are used (these damping loss factors are 5 dB to 10 dB lower than the damping loss factors obtained from PIM, see the text under Figure 5-12).

It is expected that assumption 5 is also fulfilled from the octave band 500 Hz, possibly 250 Hz or lower, for pipes with other dimensions and more flexible pipe bends (motivation analogous to the motivation in section 5.4.4). It is not clear whether the assumption is also fulfilled for other typical pipe system discontinuities, i.e. T-joints and straight joints. For two pipes connected by a T-joint and perpendicular to each other, assumption 5 is expected to be fulfilled to the same extent as described for bends above. For other connections the pipes and coupling element possibly should be modelled as one subsystem. This is probably also an appropriate way of modelling for bends below 250-500 Hz.

Validity of the assumptions 4 and 8

Assumption 4
The transmission of vibrational energy between subsystems caused by resonant modes is significantly larger (preferably at least a factor of 10) than the energy transmission caused by non-resonant vibrations.
Assumption 8
Radial vibrations in a pipe are predominantly caused by radial vibrations in another pipe that is part of the same pipe system.
These assumptions are defined to be valid if for each pair of connected subsystems, the deviation from the 'reciprocity relationship' (as written in equation *(3.3)*) is 5 dB at most in each octave band considered.

Figure 5-15 and Figure 5-16 show that for the bends studied in all octave bands considered the deviation from the 'reciprocity relationship' is 4 dB at most. From the curve trends, it is concluded that this will also be the case in the octave band with centre frequency 2000 Hz. Therefore, the assumptions 4 and 8 are fulfilled in the entire frequency range of interest.
Major changes regarding this are not expected for other pipes and pipe system discontinuities.

The results (loss factors and deviations from 'reciprocity relationship') in 1/3-octave bands show larger fluctuations than the results in octave bands. This is probably caused by the

larger number of modes in octave bands, and hence smoother response spectra in octave bands.

5.6   A pipe system in a practical building situation

This section has two aims. Firstly, it aims to investigate the application of the simplified SEA model in practical situations. For this purpose, a laboratory set-up has been built, in which a practical situation is simulated, as can be found in buildings in the Netherlands, with regard to dimensions and materials. The set-up shows some complicating factors regarding the application of SEA models, specifically the subsystems definition. These complications are typical in building practice and were not found in the two experimental set-ups in the previous sections. This section discusses how to deal with these complications.[102]

Secondly, this section is aimed at testing the validity of the assumptions 4, 5 and 8 of the simplified SEA model for practical building situations.

Section 5.6.1 describes the laboratory set-up. In section 5.6.2 possible subsystems definitions are discussed. Based on some measurements in the set-up, the subsystems definition has been selected, which seemed the most appropriate within a part of the frequency range of interest as large as possible. For this subsystems definition, damping and coupling loss factors have been determined with PIM. Section 5.6.4 describes the results. In this section, also the contribution of sound radiation in the coupling loss factors is estimated. Based on the results, the subsystems definition has been changed. For the changed subsystems definition, section 5.6.4 also gives loss factors. The applied measurement methods are described in 5.6.3. The validity of the assumptions is tested in section 5.6.5.

---

[102] Nevertheless, it has to be emphasised that the set-up was built under laboratory conditions, e.g. there were no unknown or unintentional connections as is often the case in practical situations.

5.6.1 Experimental set-up

Figure 5-19 shows the experimental set-up.
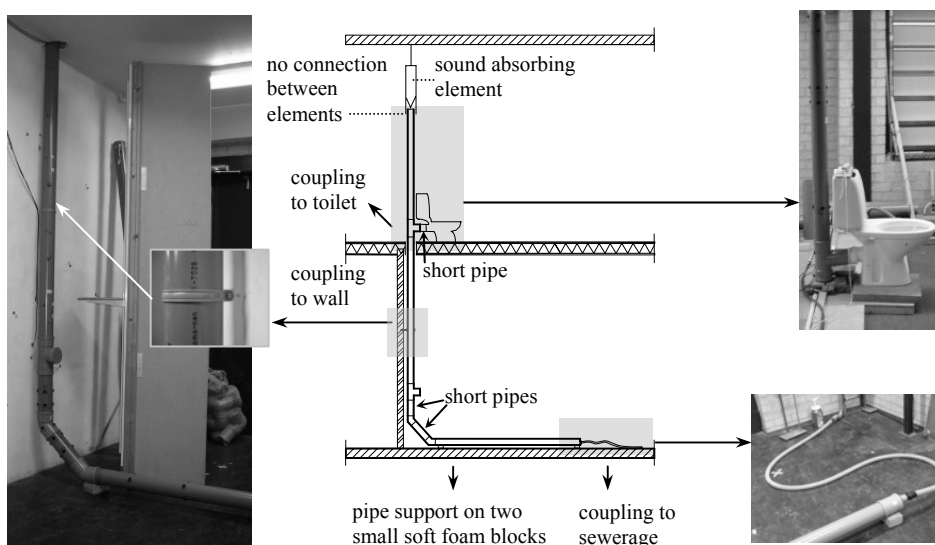
Figure 5-19 Experimental set-up consisting of a wastewater pipe system connected to a toilet, a plate and the sewer system in the laboratory; the pipe system consisted of air-filled PVC pipes, wall thickness 3,8 mm and outer shell radius 55 mm, and various pipe system discontinuities; the plate was a calcium-silicate wall with dimensions 4,4x3,4x0,1 m^3 and with a plaster layer of about 10 mm thickness at both sides; **centre**: schematic presentation of a vertical section of the situation

The set-up consisted of two test rooms that were separated by a wall. The pipe system was mounted on this wall with a pipe clamp. The toilet was placed on a lightweight floating-floor on top of one of the test rooms. There was no direct connection between the pipe system and the floors. Sound transmission between the test rooms via the other walls and ceiling was avoided due to application of lightweight (gypsumboard), double plates and dilatations near the wall. In the set-up the toilet, pipe system, clamp and wall can be replaced.

Examples of physical system elements in practical situations that are difficult to model, are connections at the ends of the system considered. In the set-up in Figure 5-19 elements of

this type are: the connection to the existing sewerage in the laboratory, the connection to the toilet, the required support of the horizontal pipe and the ending of the straight pipe above the toilet.[103] Other examples of elements that are difficult to model, are pipe system elements that are too small to exhibit a multi-modal behaviour in the entire frequency range of interest and are therefore not modelled as subsystems, but can contain some modes at high frequencies. In the set-up in Figure 5-19 elements of this type are the three short pipes.

5.6.1.1 Comparison with the prescribed laboratory set-up for wastewater installations in EN 14366

The European standard document EN 14366 [ref 35] describes an experimental determination method and a laboratory set-up for comparison of sound levels from different wastewater pipe systems, including pipe clamps. Roughly the determination method exists of two parts: determination of the structure-borne sound level due to sound transmission through pipe clamps and determination of the airborne sound level due to sound radiation from the pipe system. The sound levels in a receiving test room due to structure-borne sound and airborne sound are the determination quantities. A test wall[104] separates the receiving room and the test room in which the pipe system is situated. The pipe system is mounted on this wall. In order to obtain similar results for a product, i.e. a certain pipe system, in different laboratories, the standard document prescribes dimensions and materials for a laboratory set-up[105].

The laboratory set-up in this thesis corresponded to the guidelines for set-ups in the standard document, with regard to the dimensions and material of the test wall, the volume and reverberation time of the test rooms, the characteristics and location of the clamp(s), the location of the basement bend and the falling height of the water (a falling height of 5,8 m to 7,5 m is required in accordance with the standard document; in the experimental set-up a falling height up to about 6 m is possible, although this height has not been applied in the measurements described in this section (see Figure 5-19)).

---

[103] Since the couplings to these elements are not separately defined, these elements are energy sinks.

[104] In the standard document it is assumed that a pipe clamp behaves like a force source perpendicular to the test wall. The required surface mass of the test wall is set in accordance with this concept.

[105] Laboratory set-ups in conformity with the standard are presently available at the Fraunhofer Institut in Stuttgart, Germany and at the CSTB in Grenoble, France.

The set-up in this thesis differed from the guidelines for set-ups in the standard document, with regard to the basement bend, the source and flow rate, the inlet configuration and the fixation of the basement bend and horizontal pipe.[106]

5.6.2 Possible subsystems definitions

For the experimental set-up, Figure 5-20 shows four possible subsystems definitions in accordance with the simplified SEA model.

---

[106] In the standard document a basement bend consisting of two 135º-bends, without a straight pipe in between, is prescribed. In this study a basement bend has been applied, which is characteristic for practical Dutch situations.

In the standard document a continuous water flow with a rate of 0,5 l/s, 1 l/s, 2 l/s or 4 l/s is applied as a source. The pipe system is completely filled with water. In this study toilet flushing has been applied.

In the standard document the water inlet consists of a straight pipe with two 90º-bends and then a 90º-T-joint. In this study the water inlet consisted of a practical toilet junction.

The standard document prescribes that the basement bend and horizontal pipe should be fixed rigidly, outside the test room. In the set-up in this study the horizontal pipe has been placed on small soft foam blocks on the floor of the test room, in order to avoid structure-borne sound transmission from the pipe to the floor and from the floor to the test wall.
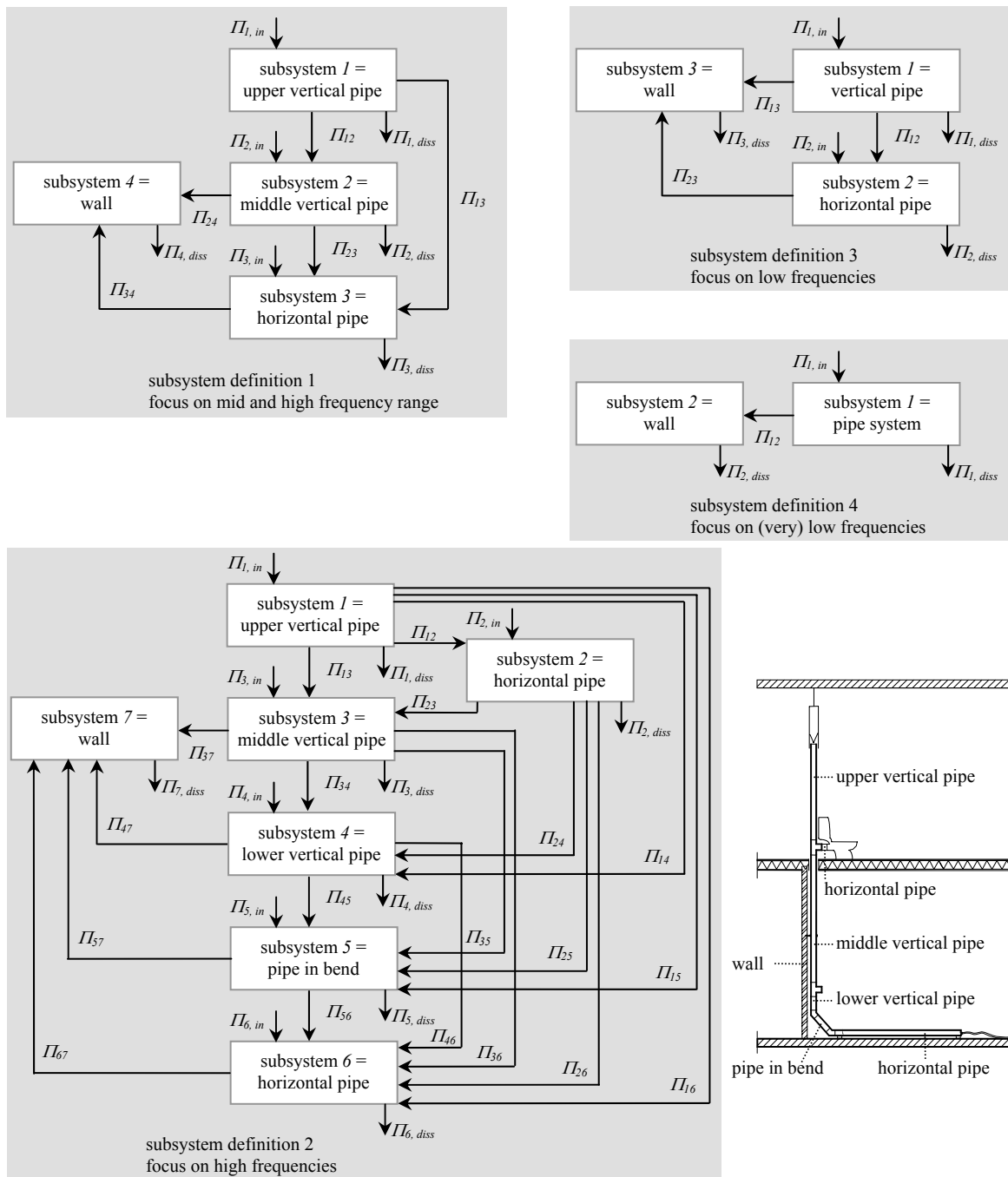
Figure 5-20 Four possible subsystems definitions in accordance with the simplified SEA model for the experimental set-up (energy sinks are not shown)

In the first subsystems definition in Figure 5-20 subsystems are groups of modes with radial/out-of-plane vibrations in the large physical system elements, i.e. the long pipes and wall, which are each expected to exhibit a clear multi-modal behaviour in at least a large part of the frequency range of interest. The T-joints, bends and pipe clamp are defined as couplings between the subsystems. The couplings are assumed to be weak[107]. The two short pipes between the lower T-joint and in the basement bend can only exhibit a clear modal behaviour at high frequencies, i.e. from 1000 Hz on (see Figure 4-24 in section 4.3.4). Therefore, these pipes are not modelled as subsystems, but together with the lower T-joint and two 135°-bends as one large coupling element. The horizontal pipe between the pipe system and toilet is even shorter, so this pipe is not modelled as a subsystem either.

The second subsystems definition concentrates on the high frequency range. Therefore, short pipes are also modelled as separate subsystems.

The third and fourth subsystems definitions concentrate on the low frequency range. Usually, energy differences between subsystems are smaller at lower frequencies. So at low frequencies a coupling can be strong while this coupling is weak at higher frequencies. In the set-up considered, couplings within pipe systems by bends and especially the upper and lower branches of the T-joints are possibly strong in the low frequency range. In that case, modelling the entire pipe system as one subsystem (fourth subsystems definition) or a division in vertical and horizontal subsystems (third subsystems definition) would be more appropriate.

As a starting point, a subsystems definition is selected, which seems to be most appropriate in a part of the frequency range of interest as large as possible. For this purpose, the energy levels of the different pipe system elements have been determined in case of excitation of the upper vertical pipe with a shaker. The energy levels are shown in Figure 5-21. Based on differences in the energy levels, the most appropriate subsystems definition is selected. The criterion for this is: in case of an energy level difference of at least 10 dB between two elements, the elements are defined as separate subsystems.

---

[107] The ends of the T-joints and bends in the pipe system considered contain rubber rings. The application of rubber rings possibly contributes to the energy differences between the subsystems. The energy differences may be smaller for rigid discontinuity ends, resulting in higher coupling loss factors. In that case the subsystems definition should be reviewed.
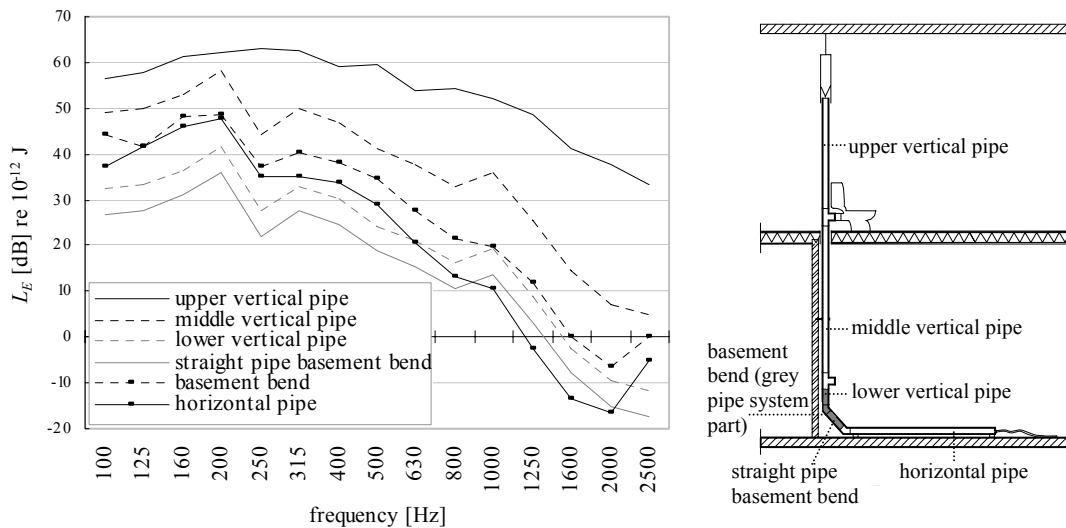
Figure 5-21 Energy levels (in 1/3-octave bands) L_E of different pipe system elements in the experimental set-up shown in Figure 5-19, for excitation of the upper vertical pipe; line indicated as 'basement bend' represents energy level in case the lower vertical pipe, the straight pipe in the basement bend and the 135°-bend in between are considered as one subsystem (grey coloured pipe system part in right-hand figure)

Figure 5-21 shows energy level differences between the upper vertical pipe and the middle vertical pipe of at least 10 dB from 250 Hz on; the differences at 100 Hz to 200 Hz lie between 4 dB and 8 dB. The energy level differences between the middle vertical pipe and horizontal pipe are at least 10 dB in the entire frequency range of interest, except at 125 Hz, 160 Hz and 250 Hz (differences between 7 dB and 9 dB). The energy level differences between the middle vertical pipe and basement bend generally lie between 5 dB and 10 dB up to 500 Hz; from 630 Hz on the differences are at least 10 dB, except at 2500 Hz (difference 5 dB). The energy level differences between the basement bend and horizontal pipe lie between 5 dB and 10 dB from 500 Hz on (at least 10 dB from 1000 Hz on, except at 2500 Hz); below 500 Hz the differences lie between 0 dB and 5 dB (up to 250 Hz no clear difference). In the entire frequency range the energy level differences between the short pipes in the basement bend are about 5 dB. Up to 630-800 Hz and at 2500 Hz the energy of the short pipes in the basement bend is smaller than the energy of the horizontal pipe. The energy of the straight pipe in the basement bend is about 3 dB at 1000 Hz, 5 dB at 1250 Hz and 1600 Hz, and 1 dB at 2000 Hz.

Based on the results, it is concluded that up to 250 Hz the basement bend and horizontal pipe should probably be modelled together as one subsystem and subsystems definition 1 seems to be most appropriate. This subsystems definition also seems to be the most appropriate from 315 Hz on, but with the basement bend as a separate subsystem, which results in subsystems definition 5, as shown in Figure 5-22.
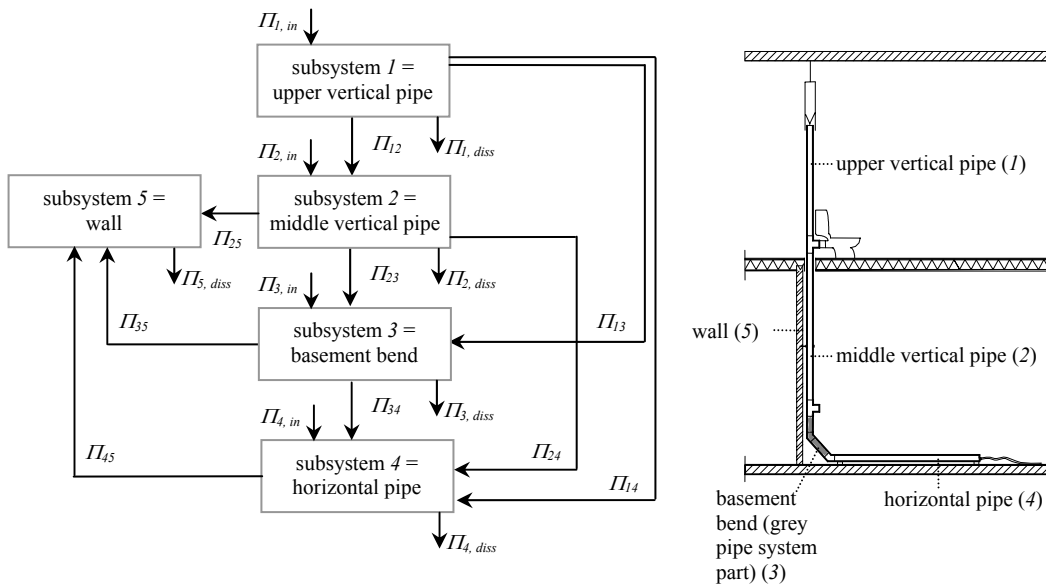
Figure 5-22 Applied subsystems definition 5

Subsystems definition 5 has been applied as a starting point for the determination of damping and coupling loss factors, although the energy level differences between the defined subsystems is not always larger than 10 dB, clearly not below 315 Hz. Based on the results, the subsystems definition is evaluated in section 5.6.4.

The energy loss through the upper T-joint and the short pipe to the toilet has not been quantified separately and is included in the coupling loss factors corresponding to the T-joint. The energy losses due to coupling of the wall to other plates and due to coupling of the horizontal pipe to the sewerage are included in the damping loss factors of respectively the wall and the horizontal pipe.

5.6.3 Measurement method

Damping and coupling loss factors have been determined in accordance with the procedure of PIM. The methods and equipment described in section 5.4.2 and appendix V for the determination of input powers to and reverberant vibrational energies of the pipe system parts and the wall have been applied. For the excitation of both the wall and the pipe system parts a shaker has been applied. The measurements have been done for two excitation positions and ten response positions on the subsystems *2* and *5*, for one excitation position and ten response positions on the subsystems *1* and *4* and for one excitation position and four response positions on subsystem *3*.

5.6.4 Experimental results and discussion about subsystems definition

Figure 5-23 to Figure 5-26 show the damping and coupling loss factors corresponding to subsystems definition 5 in Figure 5-22.[108] Also the criterion for weak coupling (i.e. validation criterion for assumption 5) applied in this thesis is shown. The figures also show deviations from the 'reciprocity relationship' (as written in equation *(3.3)*) in section 3.3 (see section 5.4.3 for more explanation). Also the range of deviations from the 'reciprocity relationship' from -5 dB to +5 dB (i.e. validation criterion for assumption 8) as allowed in this thesis is shown.

---

[108] It was difficult to obtain enough response in all subsystems in the high frequency range without distortion of the excitation signal and lowering the coherence between driving signal and responses. Therefore, only results up to the 1/3-octave band with centre frequency 1600 Hz are presented.
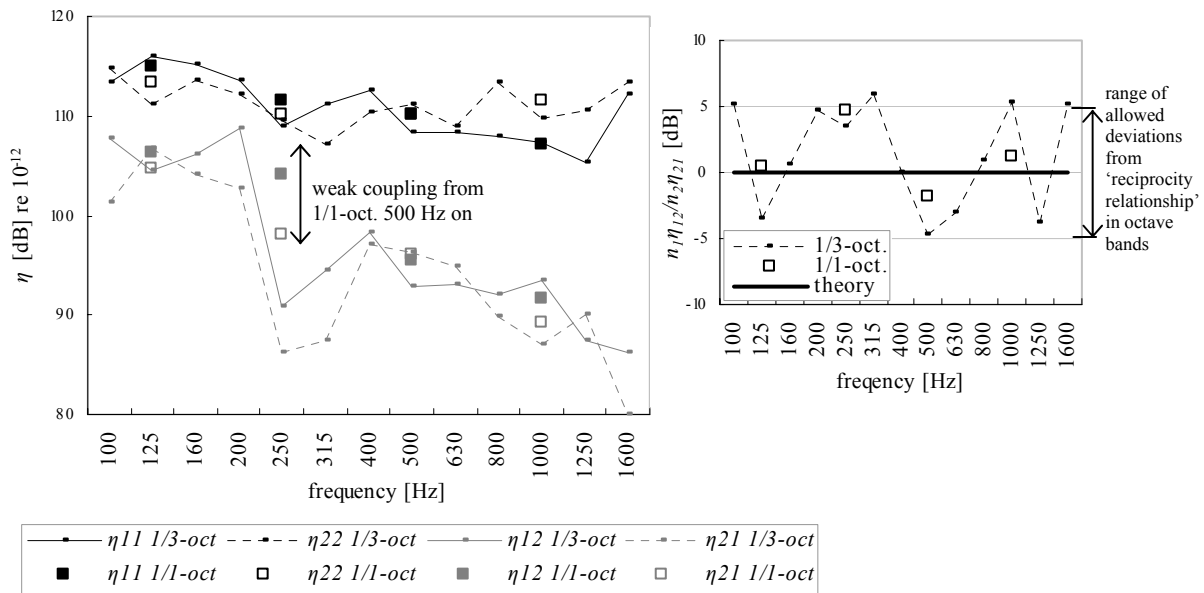
Figure 5-23 Damping and coupling loss factors η in (1/3-)octave bands determined with PIM (**left side**) and corresponding deviations from the 'reciprocity relationship' $\Delta L_{rec.}$ (see equation *(3.3)*) (**right side**); results are for the subsystems *1* (upper vertical pipe) and *2* (middle vertical pipe) and their coupling (subsystems definition 5, according to Figure 5-22). Also the criterion for weak coupling and the range of allowed deviations from the 'reciprocity relationship' applied in this thesis are shown.
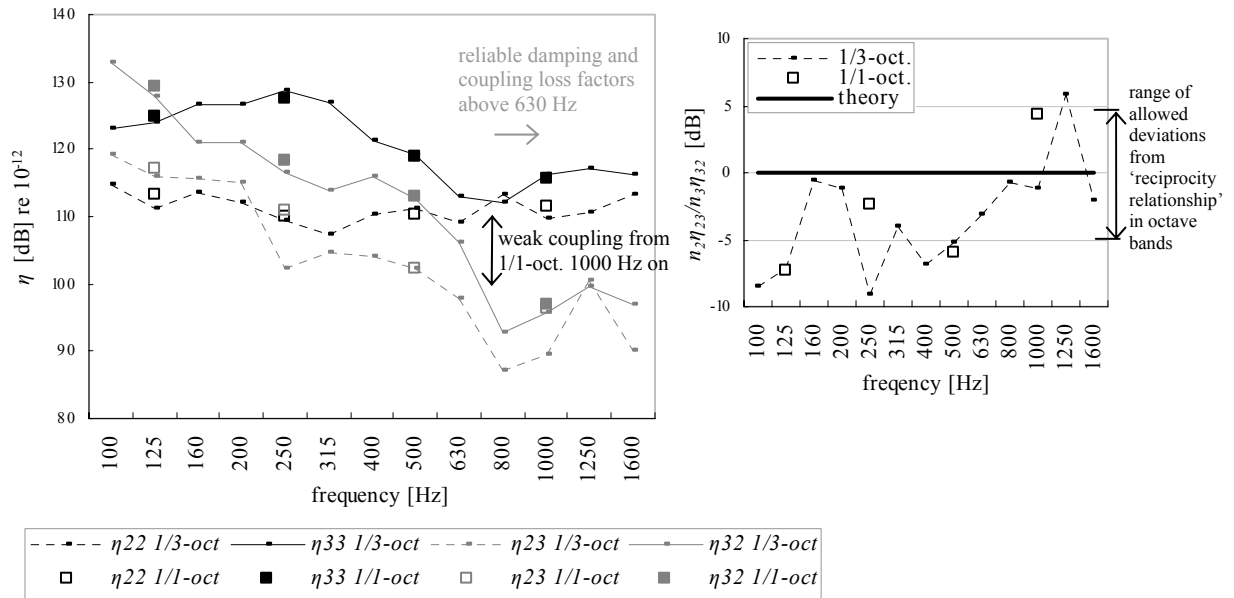
Figure 5-24 Damping and coupling loss factors η in (1/3-)octave bands determined with PIM (**left side**) and corresponding deviations from the 'reciprocity relationship' $\Delta L_{rec.}$ (see equation *(3.3)*) (**right side**); results are for the <u>subsystems *2* (middle vertical pipe) and *3* (basement bend) and their coupling</u> (subsystems definition 5, according to Figure 5-22). Also the criterion for weak coupling and the range of allowed deviations from the 'reciprocity relationship' applied in this thesis are shown.
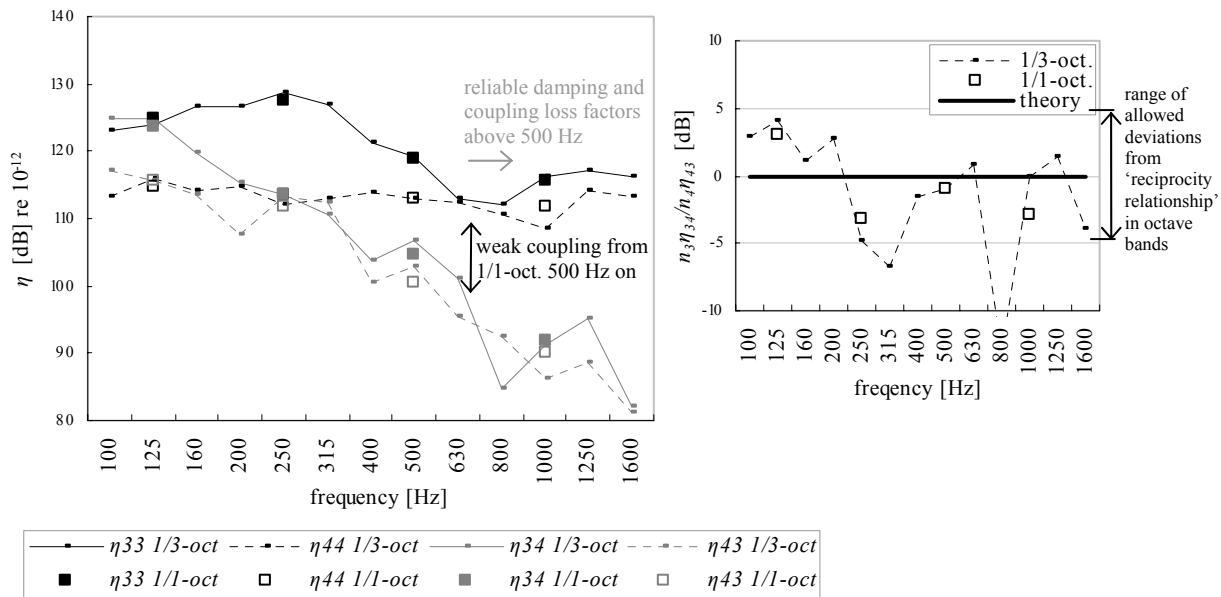
Figure 5-25 Damping and coupling loss factors η in (1/3-)octave bands determined with PIM (**left side**) and corresponding deviations from the 'reciprocity relationship' $\Delta L_{rec.}$ (see equation *(3.3)*) (**right side**); results are for the <u>subsystems *3* (basement bend) and *4* (horizontal pipe) and their coupling</u> (subsystems definition 5, according to Figure 5-22). Also the criterion for weak coupling and the range of allowed deviations from the 'reciprocity relationship' applied in this thesis are shown.

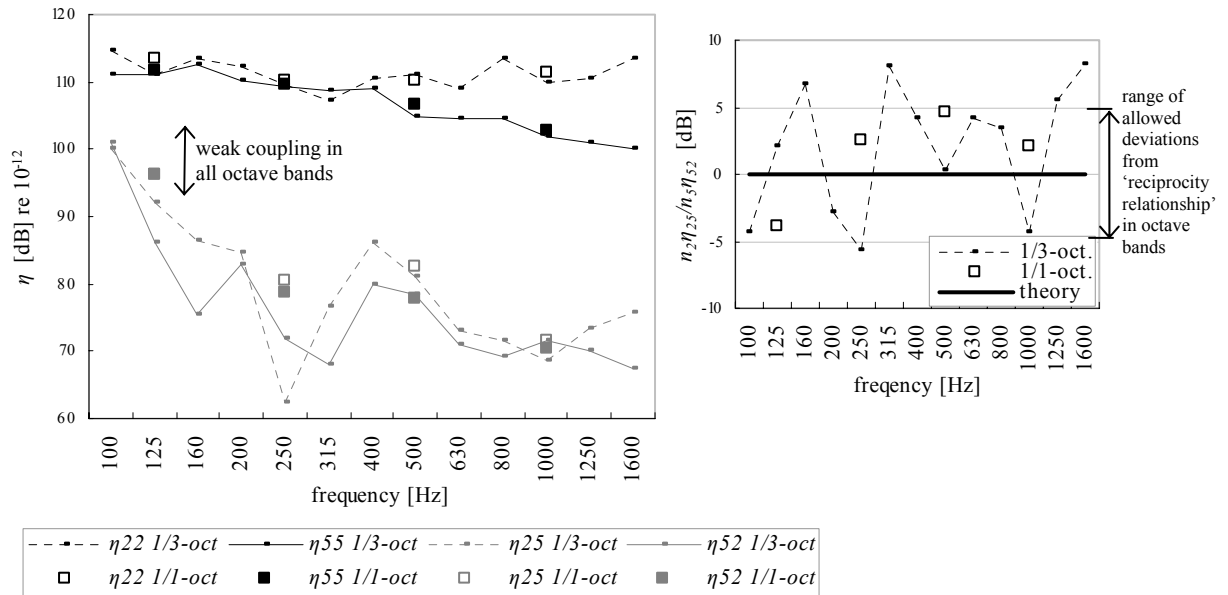**Figure 5-26** Damping and coupling loss factors η in (1/3-)octave bands determined with PIM (**left side**) and corresponding deviations from the 'reciprocity relationship' $\Delta L_{rec.}$ (see equation *(3.3)*) (**right side**); results are for the <u>subsystems 2 (middle vertical pipe) and 5 (wall) and their coupling</u> (subsystems definition 5, according to Figure 5-22). Also the criterion for weak coupling and the range of allowed deviations from the 'reciprocity relationship' applied in this thesis are shown.

From Figure 5-23 to Figure 5-26 the same conclusions can be drawn as in sections 5.4.3 and 5.5.3 regarding the contribution of sound radiation to the damping loss factors and regarding differences between the damping loss factors obtained with PIM and with the decay rate method. Furthermore, from Figure 5-23 the same conclusions can be drawn as in section 5.5.3 regarding the comparison of the damping loss factors of the upper and middle vertical pipes and the coupling loss factors obtained for both sound transmission directions. These issues are not discussed further in this section. This section focuses on the subsystems definition.

Discussion about defining the basement bend as a subsystem

The damping loss factors of the basement bend (subsystem *3*) are (unreliably) high for the 1/3-octave bands with centre frequencies below 630 Hz, compared with the damping loss factors of the other pipe system elements (subsystems *1*, *2* and *4*). The damping loss factors of subsystem *3* exceed a value of 2 (123 dB), which is due to the low number of modes (see

Figure 5-27 below) in subsystem *3*. Oscillations cease at damping loss factor values higher than 2 [ref 4].

The coupling loss factors related to subsystem *3* are (unreliably) high for the 1/3-octave bands with centre frequencies below 630-800 Hz, compared with the coupling loss factors for the coupling between the subsystems *1* and *2*. Obviously, the couplings between subsystem *3* and respectively the subsystems *2* and *4* are strong below 800 Hz (Figure 5-24) or 630 Hz (Figure 5-25).

No multi-modal vibro-acoustic behaviour exists in subsystem *3* in the entire frequency range of interest and the definition of subsystem *3* is not correct in the frequency range below 630 Hz (this was already indicated in section 5.6.2). This also becomes clear from Figure 5-27, which shows the numbers of modes of subsystem *3* derived from point admittance measurements[109] (see section 4.2.3.1 for a description of the determination method).
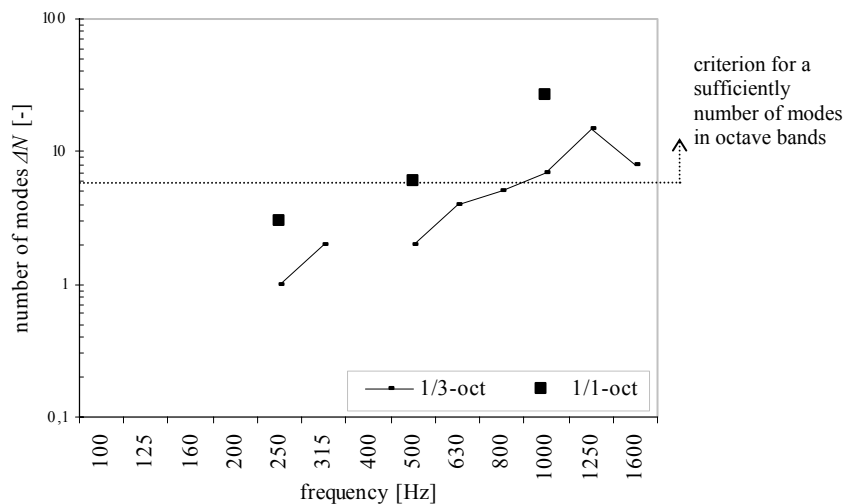
Figure 5-27 Number of modes *ΔN* in (1/3-)octave bands in subsystem *3* derived from measurements. Also the criterion for a sufficiently number of modes applied in this thesis is shown.

---

[109] The measurements have been done in the experimental set-up. The number of modes might be overestimated, because modes corresponding to the entire pipe system are included (particularly at low frequencies, where the rubber rings at the ends of the pipe coupling elements are less effective in "decoupling").

Most appropriate subsystems definitions below 630 Hz and from 630 Hz on

Below 630-800 Hz subsystems definition 1 in Figure 5-20 seems to be most appropriate. This is concluded from the results in Figure 5-24, Figure 5-25 and Figure 5-27 (see above). Whether this is really correct is tested in this section.

For subsystems definition 1 Figure 5-23 and Figure 5-26 also apply. Figure 5-24 and Figure 5-25 do not apply. For subsystem definition 1 derivation of the coupling loss factors between the subsystems *2* (middle vertical pipe) and *4* (horizontal pipe) is relevant. These coupling loss factors and the damping loss factors for the subsystems *2* and *4* are shown in Figure 5-28, together with the corresponding deviations from the 'reciprocity relationship' (as written in equation *(3.3)*) and the coupling loss factors corresponding to the coupling between the subsystems *1* and *2*. Here, number *4* is applied to indicate the horizontal pipe too, as in subsystems definition 5. Actually, in subsystem definition 1 the subsystem number is *3*. Also the criterion for weak coupling (i.e. validation criterion for assumption 5) and the range of allowed deviations from the 'reciprocity relationship' from -5 dB to +5 dB (i.e. validation criterion for assumption 8) applied in this thesis are shown.
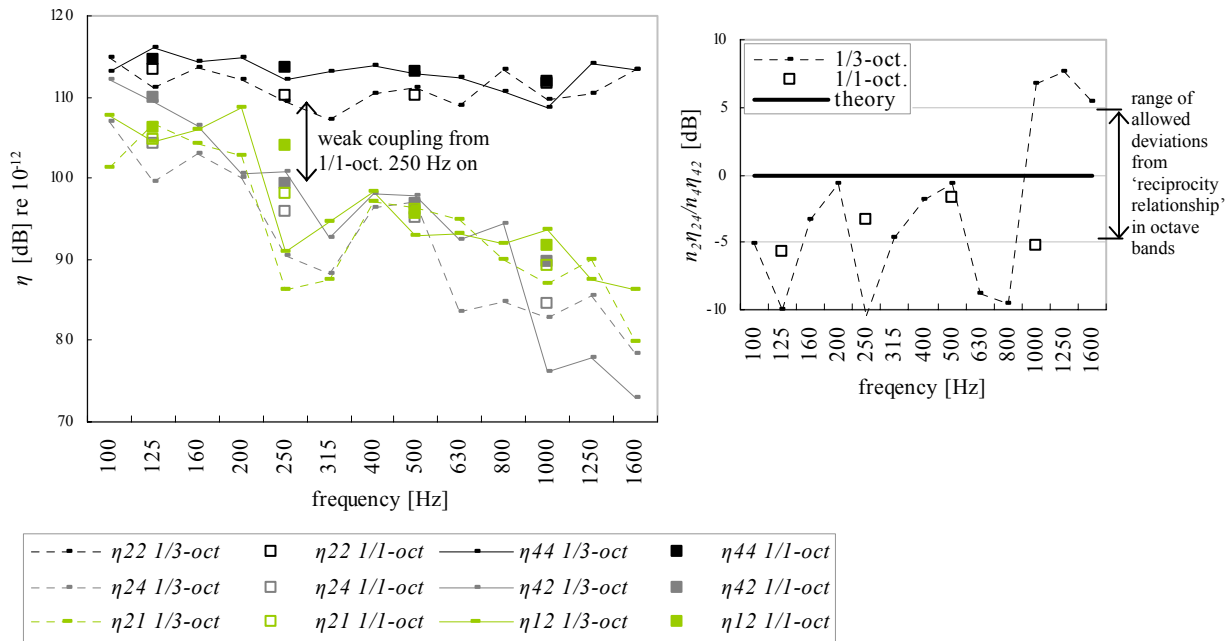
Figure 5-28 Damping and coupling loss factors η in (1/3-)octave bands determined with PIM (**left side**) and corresponding deviations from the 'reciprocity relationship' $\Delta L_{rec.}$ (see equation *(3.3)*) (**right side**); results are for the <u>subsystems *2* (middle vertical pipe) and *4* (horizontal pipe) and their coupling</u> (subsystems definition 1 in Figure 5-20). Also the coupling loss factors corresponding to the <u>coupling between the subsystems *1* (upper vertical pipe) and *2* (middle vertical pipe)</u> are shown. Also the criterion for weak coupling and the range of allowed deviations from the 'reciprocity relationship' applied in this thesis are shown.

Figure 5-28 shows reliable results. Up to 500 Hz the trends of the coupling loss factor curves of η_{21} and η_{24} on the one hand and η_{12} and η_{42} on the other hand are approximately equal. Above 500 Hz the curve trends clearly differ and η_{24} and η_{42} are lower than η_{21} and η_{12} respectively, which seems to be understandable from extra energy losses (compared to the subsystems *1* and *2*) in the pipe system parts between the subsystems *2* and *4* due to material damping, sound radiation and possibly conversion of flexural waves to waves causing mainly in-plane vibrations. Therefore, from 630 Hz on the subsystems definition 5 shown in Figure 5-22 is more appropriate. Below 630 Hz the subsystems definition 1 in Figure 5-20 is more appropriate.[110]

---

[110] Only coupling loss factor η_{32} in the 1/3-octave band with centre frequency 630 Hz remains a problem.

The deviations from the 'reciprocity relationship' (as written in equation *(3.3)*) shown in Figure 5-28 consequently are relatively large in the frequency range from 630 Hz on. The middle vertical pipe and the horizontal pipe have approximately equal lengths, so the modal densities are approximately equal. Therefore, the deviations from the 'reciprocity relationship' are caused by the differences between η_{24} and η_{42}. These results also illustrate that from 630 Hz on the subsystems definition 5 in Figure 5-22 is more appropriate, although it must be realised that measurement inaccuracies may have played a role here and from 1000 Hz the two short pipes in the basement bend possibly should be modelled as separate subsystems (see also section 4.3.4). Below 630 Hz the subsystems definition 1 in Figure 5-20 is more appropriate (see footnote 110).

Sound radiation from pipe system to plate and reverse

Acoustic coupling between the pipe system and the wall is included in the derived coupling loss factors and is not characterized separately. Since a rigid connection between pipe system and wall (pipe clamp without flexible interlayer) was applied, the energy transmission by structural coupling will have been higher than the energy transmission by acoustic coupling, analogous to the results in section 5.4.3. Whether this is also correct for flexible connections and at high frequencies should be investigated in the future.

Sound radiation from a pipe system element to other pipe system elements

Acoustic coupling between the various pipes within the pipe system via the pipe fluid (air) and the ambient medium (air) is included in the derived coupling loss factors and is not characterized separately. It has been investigated whether damping and coupling loss factors determined from sub-sets of the normalised energy matrix, as described in section 5.2.2.3, are sufficiently accurate. Results obtained in this experimental set-up have shown that the damping and coupling loss factors obtained from the entire normalised energy matrix and obtained from sub-sets of the matrix correspond well with each other. Apparently, only inclusion of the subsystems that are connected directly to a pipe system discontinuity is necessary for accurate determination of damping and coupling loss factors. Therefore, the contribution of acoustic coupling seems negligible in the sound transmission between the pipe system elements. For (more) flexible (see footnote 107) connections of pipe system elements and for high frequencies, the contribution of sound radiation might be important anyhow (see section 5.4.3 where this is explained for pipe clamps).

5.6.5 Validity of the simplified SEA model under practical circumstances

This section is aimed at testing the validity of the assumptions 4, 5 and 8 of the simplified SEA model concerning damping in and coupling between pipes within practical wastewater systems and between practical wastewater systems and plates in buildings. The assumptions and corresponding validation criteria are summarised below. See section 3.3 for complete descriptions of assumptions and criteria. Based on the results described in the previous section, it is decided that for the testing up to 500 Hz, the results shown in Figure 5-23, Figure 5-26 and Figure 5-28 are used. This implies that up to 500 Hz the combination of lower T-joint and basement bend is considered as one coupling element. For the testing from 630 Hz on, the results shown in Figure 5-23 to Figure 5-26 are used. This implies that from 630 Hz on the lower T-joint and lower 135°-bend are considered as separate coupling elements. The validation criteria are set for octave bands, so only results for octave bands are discussed here.

Validity of assumption 5

Assumption 5
The coupling between subsystems is weak. This assumption is defined to be valid if in each octave band considered the ratio of a coupling loss factor η_{ij}, representing the energy transmission from subsystem i to subsystem j, to the total loss factor $\eta_{i,tot}$ of subsystem i minus η_{ij} is smaller than 0,1 (the total loss factor $\eta_{i,tot}$ minus η_{ij} is at least a factor of 10 (10 dB) higher than the coupling loss factor η_{ij}).

Figure 5-23 shows that for the upper T-joint the damping loss factors of the connected pipes are at least 10 dB higher than the coupling loss factors from the octave band with centre frequency 500 Hz on. The coupling is almost weak in the octave bands 125 Hz and 250 Hz (differences between damping and coupling loss factors at least 6 dB). Figure 5-24, Figure 5-25 and Figure 5-28 show that for (the combination of) the lower T-joint and basement bend the damping loss factors of the connected pipes are at least 10 dB higher than the coupling loss factors from the octave band with centre frequency 250 Hz on. From the curve trends, it is concluded that the couplings will also be weak in the octave band with centre frequency 2000 Hz. Therefore, for the pipe coupling elements studied assumption 5 is fulfilled from the octave band 125-500 Hz on. This corresponds to the results described in section 5.5. This might change to one octave band higher when damping loss factors obtained from the decay rate method are used (these damping loss factors are 5 dB to 10 dB lower than the damping loss factors obtained from PIM, see the text under Figure 5-12).

Below 125-500 Hz pipes and coupling elements probably should be modelled as one subsystem. Above 800 Hz modelling of short pipes as separate subsystems may be a possibility (see section the discussion in section 5.6.2).

Figure 5-26 shows that for the pipe clamp studied in all octave bands considered the damping loss factors of the pipe and plate are at least 10 dB higher than the coupling loss factors. From the curve trends, it is concluded that this will also be the case in the octave band with centre frequency 2000 Hz. Therefore, for the pipe clamp studied assumption 5 is fulfilled in the entire frequency range of interest. This corresponds to the results described in section 5.4. This is also the case if damping loss factors obtained from the decay rate method are used (these damping loss factors are 5 dB to 10 dB lower than the damping loss factors obtained from PIM, see the text under Figure 5-12).

Validity of the assumptions 4 and 8

Assumption 4
The transmission of vibrational energy between subsystems caused by resonant modes is significantly larger (preferably at least a factor of 10) than the energy transmission caused by non-resonant vibrations.

Assumption 8
Out-of-plane plate vibrations are predominantly caused by radial vibrations in pipe systems and vice versa. Radial vibrations in a pipe are predominantly caused by radial vibrations in another pipe that is part of the same pipe system.

These assumptions are defined to be valid if for each pair of connected subsystems, the deviation from the 'reciprocity relationship' (as written in equation *(3.3)*) is 5 dB at most in each octave band considered.

Figure 5-23 shows that for the upper T-joint in all octave bands considered the deviation from the 'reciprocity relationship' is 5 dB at most. For (the combination of) the lower T-joint and basement bend Figure 5-24, Figure 5-25 and Figure 5-28 show that the deviation from the 'reciprocity relationship' is 5 dB at most for all octave bands considered, except for 125 Hz. From the curve trends, it is not clear whether the deviations from the 'reciprocity relationship' will be 5 dB at most in the octave band with centre frequency 2000 Hz. However, based on the results described in section 5.5.4 this is expected. Therefore, the assumptions 4 and 8 are expected to be fulfilled from the octave band 125-250 Hz on.

Figure 5-26 shows that for the pipe clamp in all octave bands considered the deviation from the 'reciprocity relationship' is 5 dB at most. From the curve trends, it is not clear whether the deviations from the 'reciprocity relationship' will be 5 dB at most in the octave band with centre frequency 2000 Hz. However, based on the results described in section 5.4.4 this is expected. Therefore, the assumptions 4 and 8 are expected to be fulfilled in the entire frequency range of interest. This corresponds to the results described in section 5.4.

The deviations from the 'reciprocity relationship' are generally larger than for the first two experimental set-ups. The larger differences may be due to the fact that the third test system is more complex than the first two systems, which may have resulted in larger inaccuracies in the coupling loss factors.
The results (loss factors and deviations from 'reciprocity relationship') in 1/3-octave bands show larger fluctuations than the results in octave bands. This is probably caused by the larger number of modes in octave bands, and hence smoother response spectra in octave bands.

5.7 Discussion about determination methods for damping and coupling loss factors

In this section the dependency of loss factors on experimental set-ups and determination methods is investigated. Therefore, damping and coupling loss factors obtained with different determination methods and in different experimental set-ups are compared. In case loss factors are not dependent on experimental set-up and determination method, the values obtained in a certain set-up with a certain determination method can be applied in other situations too, which is essential for predictions.

5.7.1 Damping loss factors

Pipes

In the laboratory set-ups described in sections 5.4 to 5.6 damping loss factors have been determined with PIM for straight PVC pipes with different lengths and boundary conditions (see the values for subsystem *1* in Figure 5-11, the subsystems *1* and *2* in Figure 5-15 and Figure 5-16 and the subsystems *1* to *4* in Figure 5-23 to Figure 5-26 and Figure 5-28). For a free-hanging PVC pipe damping loss factors have been determined with the decay rate method (see Figure 5-6 in section 5.3).

184

In the previous sections it has been concluded that damping loss factors of practical plastic wastewater pipes are mainly dependent on material damping, and to a lesser degree on sound radiation. Therefore, the damping loss factors are expected to be independent of pipe length for long pipes, i.e. as far as the vibro-acoustic behaviour is resonant, and to be equal for the various set-ups.

The obtained damping loss factors are shown in Figure 5-29, except for values that may have been determined by other causes than damping in the subsystem itself (sand in set-up 2, see section 5.5, and foam blocks in set-up 3, see section 5.6).
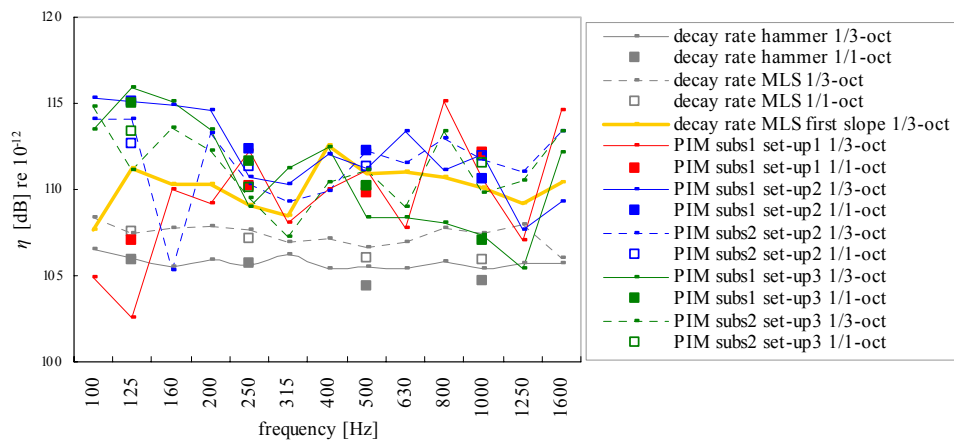
Figure 5-29 Damping loss factors η in (1/3-)octave bands for <u>air-filled PVC pipes</u> determined with PIM in the <u>laboratory set-ups</u> in section 5.4 (set-up numbered as <u>1</u> in this figure), section 5.5 (set-up numbered as <u>2</u> in this figure) and section 5.6 (set-up numbered as <u>3</u> in this figure) and determined with the decay rate method for a <u>free-hanging plastic pipe</u> (see section 5.3). <u>Hammer and shaker</u> (indicated in the legend by "<u>MLS</u>") <u>excitation</u> in case of the <u>decay rate method</u> and <u>shaker excitation</u> in case of <u>PIM</u>. The yellow line indicates damping loss factor values determined from the <u>first slope of a decay curve</u> (for further explanation see the text below).

Figure 5-29 shows differences larger than 10 dB below 250 Hz, which might be due to the low number of modes (see Figure 4-9 in section 4.2.3.3).

From 250 Hz on the damping loss factors values in octave bands obtained with PIM correspond well: the differences lie between 0 dB and 2 dB, except for the loss factor value of subsystem 1 in set-up 3 at 1000 Hz (difference with the other values 5 dB). The differences do not seem dependent on set-up. They are expected to be caused by measurement inaccuracies. In 1/3-octave bands the differences are larger: between 0 dB and 5 dB, except for the 1/3-octave bands with centre frequencies 630 Hz, 800 Hz and 1600 Hz (differences up to 7 dB).

The damping loss factor values obtained with PIM are systematically higher than the values obtained with the decay rate method. In octave bands the differences are generally up to 5 dB, sometimes up to 7 dB, from 250 Hz on. In 1/3-octave bands the differences are generally up to 7 dB, sometimes up to 10 dB, from 200 Hz on.

The pipes for which the damping loss factors have been determined with PIM were coupled to one or more other pipes or a plate. Possibly energy losses in the couplings have increased the damping loss factors. However, the differences are expected to have other causes as well, see below.

The damping loss factor values obtained with the decay rate method vary less in the frequency range (particularly clear for 1/3-octave bands), compared with the values obtained with PIM. The values obtained with the decay rate method seem most reliable from a physical point of view. Besides, they correspond better with most values found in the literature than the values obtained with PIM (see also section 5.3.3).

Figure 5-29 also shows that the damping loss factors obtained with the decay rate method and shaker excitation are higher than the damping loss factors obtained with hammer excitation (for octave bands the differences lies between 0,4 dB and 1,6 dB).

It is not clear whether the differences are caused by the difference in excitation type or by the fact that the shaker might add some extra damping. From measurements on solid, heavy walls Meier and Schmitz [ref 71] and [ref 72] have reported the opposite, i.e. loss factors obtained with hammer excitation are higher than with shaker excitation, probably caused by non-linearities due to strong hammer hits. That effect was not found in this study, also not from experiments on a steel plate, from which the loss factors obtained with shaker excitation were 0,6 dB to 1,9 dB higher than with hammer excitation (different hit strengths) for octave bands 125 Hz to 2000 Hz (results not shown in this thesis). This is discussed in more detail below.

Figure 5-30 shows a typical impulse response and decay curve due to excitation with a hammer for one response position on a pipe. For the plates and excitation with a shaker, the impulse responses and decay curves are similar (not shown in this thesis).
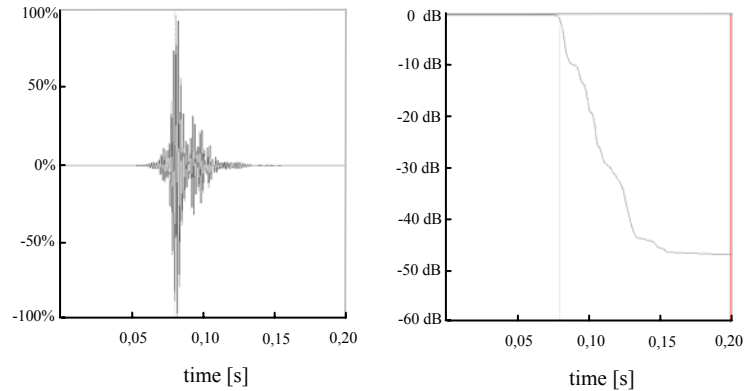
Figure 5-30 Impulse response (**left side**) and decay curve (**right side**) due to hammer excitation for the 1/3-octave band with centre frequency 630 Hz for one measurement position on an <u>air-filled PVC pipe</u> with 3,8 mm wall thickness, outer shell radius 55 mm and pipe length 2,7 m

Figure 5-30 shows multiple slopes in the decay curve, which may correspond to various reflections of (different types of) modes at the pipe's ends.

To illustrate the effect of different slopes in the decay curve, Figure 5-31 gives loss factors in 1/3-octave bands calculated with the decay times for separate slopes and for a number of slopes together (T_{10}). The decay times for separate slopes are indicated as T_x-values where x represents a variable response drop depending on the length of the slope (only straight parts of slopes are considered). For hammer excitation values calculated from the first three successive slopes are shown. For MLS excitation only values calculated from the first slope (initial decay) are shown. Values calculated from other slopes show the same variation for MLS excitation compared to hammer excitation. The loss factors in Figure 5-31 have been calculated from the decay times for only one response and one excitation position. The loss factor values in Figure 5-31 are only meant to illustrate, not to apply in calculations (for that purpose a more accurate determination method should be developed). In this study calculations for other response and excitation positions have been done. The calculation results show the same variation for different parts of the decay curves. In case in a 1/3-octave band no value is shown in Figure 5-31, then the decay corresponding to the straight part of the slope was smaller than 2 dB.
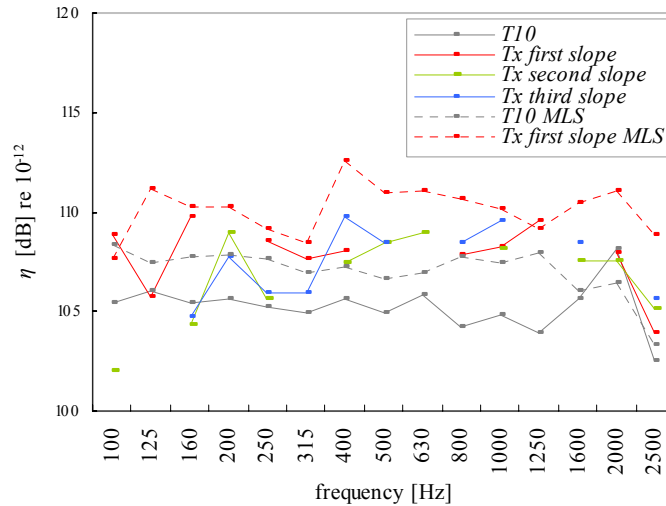
Figure 5-31 Damping loss factors η in 1/3-octave bands for one measurement position on an air-filled PVC pipe with 3,8 mm wall thickness, outer shell radius 55 mm and pipe length 2,7 m; results are for hammer and shaker (indicated in the legend with "MLS") excitation and are derived from T_{10}- and T_x-values

Generally speaking, the loss factors that have been calculated with the decay times for the separate slopes in the decay curve are higher than the loss factors from the decay times for multiple slopes (T_{10}). This might be due to the fact that between the slopes there are small response parts without decay (horizontal) in the decay curves.

For shaker excitation the loss factors from the decay times for multiple slopes are generally higher than for hammer excitation. Also, the loss factors from the decay times for separate slopes are higher.

The largest differences between damping loss factors obtained with PIM and with the decay rate method are observed for loss factors derived from multiple slopes in the decay curve with hammer excitation. The differences are smaller for MLS excitation. The differences for both hammer and MLS excitation are smaller for damping loss factor values derived from the separate slopes in the decay curve. This could indicate that the separate slopes of the decay curve together correspond to a steady state equilibrium of energy, which is also reached during steady state determination methods, e.g. PIM. Crocker and Price [ref 68], Fahy [ref 69], Bies and Hamid [ref 59] and Ranky and Clarkson [ref 70] mention similar findings, based on measurements on thin steel and aluminium plates, and suggest that the initial part of the decay curve corresponds to a steady state equilibrium of energy.

Plates

In the laboratory set-up described in section 5.4 damping loss factors of the concrete plate have been determined with the decay rate method (see Figure 5-7) and PIM (see the values for subsystem *2* in Figure 5-11). Figure 5-32 shows the obtained damping loss factors.

In the laboratory set-up described in section 5.6 total loss factors[111] of the calcium-silicate wall have been determined with the decay rate method (see Figure 5-8) and PIM (see values for subsystem *5* in Figure 5-26). Figure 5-33 shows the obtained damping loss factors.
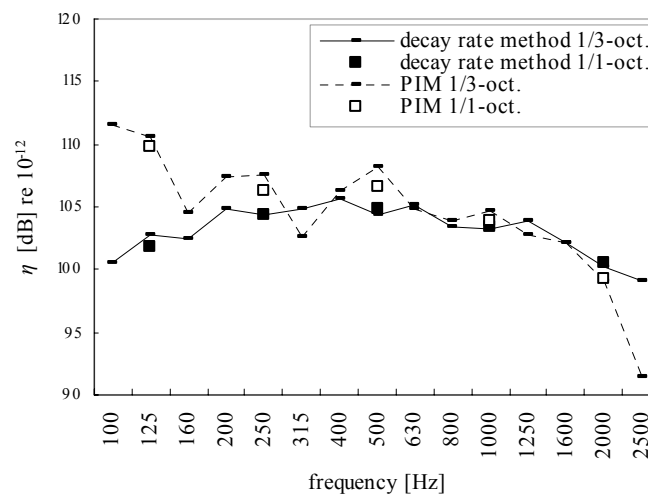
Figure 5-32 Damping loss factors η in (1/3-)octave bands for the concrete plate in laboratory set-up 1 (see section 5.4), determined with the decay rate method and PIM; hammer excitation of the plate in both cases

---

[111] In this set-up there was some coupling of the wall to other structures. Therefore, the term total loss factors instead of damping loss factors is used.
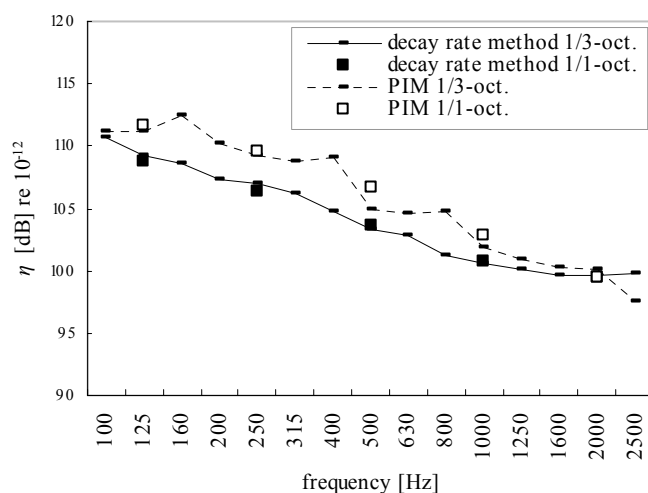
Figure 5-33 Total loss factors η in (1/3-)octave bands for the <u>calcium-silicate wall</u> in laboratory set-up 3 (see section 5.6), determined with the <u>decay rate method and PIM</u>; <u>hammer excitation</u> in case of the decay rate method and <u>shaker excitation</u> in case of PIM

Below 1250 Hz, Figure 5-32 shows higher damping loss factor values obtained with PIM (compared to the decay rate method), except at 315 Hz (value obtained with PIM is lower). Below 2000 Hz, Figure 5-33 also shows systematically higher values obtained with PIM. From 630 Hz on for the concrete plate and 1250 Hz on for the calcium-silicate plate the loss factors obtained with PIM and the decay rate method are approximately equal, except at 2500 Hz, which could be due to distortion of the excitation signal.

Within the frequency range where the number of modes in 1/3-octave bands exceeds a value of 2 (above 160 Hz for the concrete plate and above 100 Hz for the calcium-silicate wall) the differences between the two determination methods vary between 0 dB and 3 dB for octave bands and between 0 dB and 4 dB for 1/3-octave bands, except at 2500 Hz for the concrete plate. Generally speaking, the values obtained with both methods show rather good correspondence.

Nevertheless, higher loss factor values seem characteristic for PIM. The differences seem independent of the excitation type. See Figure 5-32, where hammer excitation has been combined with both the decay rate method (one hammer-hit) and PIM (multiple hammer-hits within the measurement period) and results in higher values obtained with PIM. Based

on this result, it is concluded that the effect of possibly extra damping due to connection to a shaker is negligibly small for (relatively heavy) plates.

Conclusion

From the results described above it is concluded that the damping loss factors do not seem to depend on set-up (see the results obtained with PIM for various pipes), but they do on determination method.

A steady state equilibrium of energy is obtained with PIM and not with the decay rate method. This gives different results for both methods. The (summed) damping effect of separate modes or mode groups (represented by separate slopes in the decay curve) corresponds more to a steady state equilibrium of energy than the damping effect of multiple modes together. The differences between the methods become smaller at higher frequencies. Then, the number of modes is higher and the response spectra are smoother. Probably, this gives smaller differences in the damping effects of separate modes or mode groups and of multiple modes together.

Which of the applied determination methods is most appropriate will depend on the source type and sometimes will not be entirely clear. For example, toilet flushing could be modelled as a transient source that is neither a continuous nor an impulse source. In cases where SEA is applied, a steady state equilibrium of energy is assumed. Otherwise hardly any resonant vibrational behaviour in subsystems exists. From this point of view steady state methods, such as PIM, are preferred for SEA parameter determination.

The influence of the different damping loss factor values on predictions is shown in chapter 7. In order to obtain reliable data for predictions the applied determination methods should be evaluated in more detail and need further development.

5.7.2   Coupling loss factors

Pipe clamps

In the laboratory set-ups 1 and 3 described in respectively sections 5.4 and 5.6 coupling loss factors have been determined for a pipe clamp coupled to different pipes and plates (see Figure 5-12 and Figure 5-26).

Coupling loss factors depend on the vibrational characteristics of the coupling element and of the connected subsystems, see section 5.2.4. Since the subsystems connected by the pipe clamp differed for the set-ups 1 and 3, the coupling loss factors are not expected to be equal. For set-up 3 larger coupling loss factors are expected, because of the larger point admittance and smaller plate mass (see equation *(5.17)*). Nevertheless a comparison is

interesting, in order to determine to which extent coupling loss factors, obtained from measurements in a certain set-up, give an indication for similar elements and situations.

Figure 5-34 shows the coupling loss factors representing the energy transmission from pipe to plate obtained with PIM, from subsystems energies, damping loss factors and modal densities and from point admittances. Figure 5-35 shows the coupling loss factors for the opposite energy transmission direction (from plate to pipe).
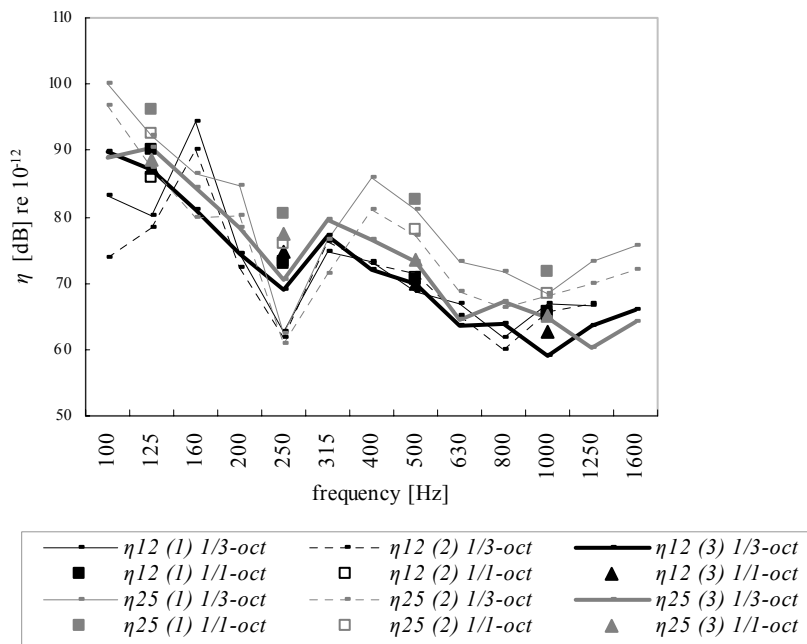
Figure 5-34 Coupling loss factors η in (1/3-)octave bands representing the energy transmission from a plastic wastewater pipe through a plastic pipe clamp to a plate. The loss factors are determined with PIM (indicated as (**1**)), from subsystems energies, damping loss factors and modal densities (indicated as (**2**)) and from point admittances (indicated as (**3**)). The loss factors are determined in laboratory set-up 1 (indicated as **η12**) and in laboratory set-up 3 (indicated as **η25**). In set-up 1 a concrete plate (thickness 0,12 m) was applied, in set-up 3 a calcium-silicate wall (thickness 0,1 m) with a 10 mm thick plaster layer at both sides.
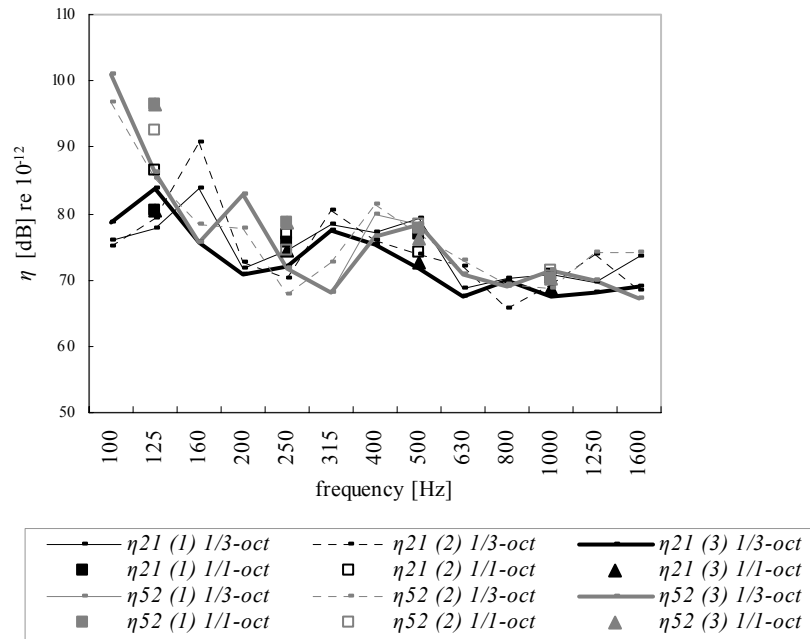
Figure 5-35 Coupling loss factors η in (1/3-)octave bands representing the <u>energy transmission from a plate through a plastic pipe clamp to a plastic wastewater pipe</u>. The loss factors are determined with PIM (indicated as (**1**)), from subsystems energies, damping loss factors and modal densities (indicated as (**2**)) and from point admittances (indicated as (**3**)). The loss factors are determined in laboratory set-up 1 (indicated as **$\eta 21$**) and in laboratory set-up 3 (indicated as **$\eta 52$**). In <u>set-up 1</u> a concrete plate (thickness 0,12 m) was applied, in <u>set-up 3</u> a calcium-silicate wall (thickness 0,1 m) with a 10 mm thick plaster layer at both sides.

From 250 Hz on both Figure 5-34 and Figure 5-35 show good correspondence between the results in octave bands from different set-ups and from different determination methods.

In Figure 5-34 for octave bands the differences between the determination methods generally lie between 0 dB and 2 dB for set-up 1, for set-up 3 between 2 dB and 4 dB. The coupling loss factors obtained with PIM in set-up 3 are systematically larger than the coupling loss factors obtained with the other two determination methods. The differences between the methods are larger than in set-up 1, which might be caused by the fact that set-up 3 is more complex and therefore less accurate results. However, this does not follow from Figure 5-35, where for both set-ups the differences generally lie between 0 dB and 3 dB.

The coupling loss factors obtained from both set-ups differ 2 dB to 4 dB (determined from comparison of loss factors obtained from point admittances).

In 1/3-octave bands the differences are larger. The loss factor curves show similar trends, although peaks and dips sometimes seem to be shifted.

The loss factor spectra, specifically the spectra in Figure 5-34 determined with the first two determination methods, show strong fluctuations[112]. Possibly these fluctuations are caused by different damping characteristics of different types of modes or a strongly fluctuating number of modes and modal overlap in the subsystems.

Pipe coupling elements

In the laboratory set-ups 2 and 3 described in respectively sections 5.5 and 5.6 coupling loss factors have been determined for various pipe coupling elements coupled to different pipes (see Figure 5-15, Figure 5-16, Figure 5-23 to Figure 5-25 and Figure 5-28).

Unfortunately, really good comparisons of coupling loss factors are not possible, because of the small dimensions of the connected subsystem *3* in laboratory set-up 3 (see the discussion in the previous section). Therefore, no detailed comparisons have been made for pipe coupling elements. However, rough comparison of the coupling loss factors in octave bands for all pipe coupling elements generally shows similar curve trends and values.

Conclusion

From the results described above it is concluded that the coupling loss factors depend on determination method, see also sections 5.4.3.1 and 5.5.3.1 where the appropriateness of PIM is discussed. From the results for pipe clamps obtained in set-up 1 it follows that the differences between the determination methods are limited (generally between 0 dB and 2 dB for octave bands). So, all three methods seem appropriate, but it is not clear which one is the most appropriate. The differences may be due to measurement inaccuracies, but may also be inherent in the chosen methods. For example, in the values determined from point admittances no coupling damping is included. Besides, only sound transmission due to vibrations perpendicular to the elements surfaces is included. Both issues correspond to the assumptions of the simplified SEA model. Nevertheless, in the coupling loss factors obtained with the other two methods some coupling damping and sound transmission due to in-plane vibrations may be included. See also the discussions in the sections mentioned above. In order to obtain reliable data for predictions the applied determination methods should be evaluated in more detail and need further development.

---

[112] This effect is also observed in loss factor spectra presented in the literature, for example in [ref 6].

PIM systematically gives higher coupling (and damping) loss factors. However, in predictions the effect of these higher loss factors may be (partly) compensated, because the coupling loss factors in both energy transmission directions are higher. In chapter 7 this is shown.

The coupling loss factors also depend on set-up, which was expected, because they depend on the vibrational characteristics of the connected subsystems, see section 5.2.4. Nevertheless, results obtained in a set-up give a good indication for another (similar) set-up. Besides, derivation of coupling loss factors for a new situation from known coupling loss factors is relatively easy (determined by the differences in point admittance and mass, which are often known, see equation *(5.17)*).

5.8   Conclusions

In this chapter the validity of the assumptions 4, 5 and 8 of the simplified SEA model (see section 3.3) has been tested. These assumptions deal with damping in and coupling between physical system elements that are subject of this thesis. For this purpose damping loss factors for straight pipes and plates (walls and floors) and coupling loss factors corresponding to discontinuities in pipe systems (pipe clamps and pipe coupling elements) have been determined. The assumptions and test results are summarised below.

Assumption 4
The transmission of vibrational energy between subsystems caused by resonant modes is significantly larger (preferably at least a factor of 10) than the energy transmission caused by non-resonant vibrations.
Assumption 5
The coupling between subsystems is weak.
Assumption 8
Out-of-plane plate vibrations are predominantly caused by radial vibrations in pipe systems and vice versa. Radial vibrations in a pipe are predominantly caused by radial vibrations in another pipe that is part of the same pipe system.

For testing the validity of these assumptions, damping and coupling loss factors obtained with the so-called Power Injection Method (PIM) have been used.
The accuracy of the results obtained with PIM has been estimated based on comparisons with results obtained with three other methods:
▪ damping loss factors obtained with the decay rate method;

- coupling loss factors obtained from subsystems energies, damping loss factors (determined with the decay rate method) and modal densities;
- coupling loss factors from point admittances of subsystems and coupling element.

Although the results of the determination methods do not correspond exactly with each other, the results of PIM are sufficiently accurate for testing the validity of the assumptions. For comparisons of coupling loss factors see for pipe clamps section 5.4.3, for pipe coupling elements section 5.5.3 and for both section 5.7. For comparisons of damping loss factors see section 5.7 for both pipes and plates.

Nevertheless, in order to obtain reliable data for predictions the applied determination methods should be evaluated in more detail and need further development. All methods seem appropriate, but it is not clear which method(s) is (are) most appropriate. Differences in results obtained with the different methods in this study may be due to measurement inaccuracies, but may also be inherent to the chosen methods. See section 5.7, where the dependency of loss factors on determination method and on experimental set-up is discussed.

Measurements have been done in three experimental set-ups, which contained different types of subsystems (straight pipes and plates) and couplings and were varying in complexity. The subsystems definition of the simplified SEA model has been applied. The definition of subsystems and couplings has been discussed, especially in section 5.6 for the most complex set-up, i.e. the set-up that was representative for practical situations. The most important conclusions are mentioned below.

Pipe clamps

For pipe clamps the test results are described in detail in sections 5.4.4 and 5.6.5.

From the tests on pipe clamps in this chapter it is concluded that the assumptions are fulfilled, and therefore that the simplified SEA model is applicable, in the entire frequency range of interest. So, the modelling of pipe clamps as coupling elements is correct and makes separate characterization of this type of coupling elements possible in the entire frequency range of interest. Based on the motivation in section 5.4.4 major changes regarding this are not expected for other pipes, plates and pipe clamps.

Pipe coupling elements

For pipe coupling elements the test results are described in detail in sections 5.5.4 and 5.6.5.

From the tests on bends and T-joints in this chapter it is concluded that assumption 5 is fulfilled from the octave band 500 Hz, possibly 125 Hz or 250 Hz, on (depending on type

of coupling element). The assumptions 4 and 8 are fulfilled in the entire frequency range of interest, except for one type of coupling element (combination of a T-joint and basement bend) where these assumptions are fulfilled from 250 Hz on. Major changes regarding this are not expected for other pipes and pipe system discontinuities.

The applicability of the simplified SEA model does not depend on the fact whether or not assumption 5 is fulfilled. The results from the testing of this assumption only determine the subsystems definition. Below 125-500 Hz pipes and coupling elements within a pipe system probably should be modelled as one subsystem. Above 800 Hz modelling of short pipes as separate subsystems may be a possibility (this is consistent with the results described in chapter 4). So, from the results in this chapter it is concluded that the simplified SEA model is generally applicable in the entire frequency range of interest (probably not for more complex coupling elements as described above). But separate characterization of pipe coupling elements is not possible below 125-500 Hz.

CHAPTER 6

EXCITATION OF PIPE SYSTEMS IN PRACTICAL SITUATIONS

6.1   Introduction

This chapter is aimed at testing the validity of assumption 7 of the simplified SEA model (see section 3.3). Assumption 7 deals with the excitation of pipe systems by sources in practical situations, e.g. a water flow or a toilet.
The validity of this assumption has been tested based on results obtained in the experimental set-up as described in section 5.6.1, in which a practical building situation has been simulated. For the tests in this chapter toilet flushing has been applied. The experimental set-up and corresponding sources are described in section 6.2. The validity of assumption 7 has also been tested based on results obtained in a practical situation, i.e. a house.

In order to perform predictions with the simplified SEA model in the future, input powers from sound sources to subsystems in practical pipe systems are needed. Therefore, besides testing the validity of the simplified SEA model, this chapter also gives a first, very rough description of sources in wastewater pipe systems, qualitatively in section 6.2 and quantitatively in section 6.3. A source descriptor that is subsystem-independent, namely the maximum equivalent input force, is proposed in section 6.3. This section also illustrates how subsystem energy levels can be estimated from source data. The source description needs to be elaborated in the future, and then might be the basis for a general characterization method for sources in pipe systems.

In section 6.4 the validity of assumption 7 is tested. In order to get further evidence of the validity of the simplified SEA model, an additional test is described.

6.2   Experimental set-up and qualitative description of sound sources

Figure 6-1 shows the experimental set-up and the subsystems definitions in accordance with the simplified SEA model. For each subsystem, the direct sources are shown. Direct sources are defined as sources that directly excite a subsystem. Each subsystem is also indirectly excited by sources, via connected subsystems (that are directly excited). It is not

expected that the pipe clamp ring around subsystem *2* (middle vertical pipe) changes the water flow in the pipe system. Therefore, the pipe clamp is not defined as a source, even though the pipe clamp is a pipe system discontinuity.

Below 630 Hz, it is not appropriate to model subsystem *3* as a subsystem. Then, it is more appropriate to model subsystem *3* as a coupling element, together with the lower T-joint. This is explained in detail in section 5.6.4. This is the reason why the lower T-joint and subsystem *3* are indicated as one source (2b) in Figure 6-1.
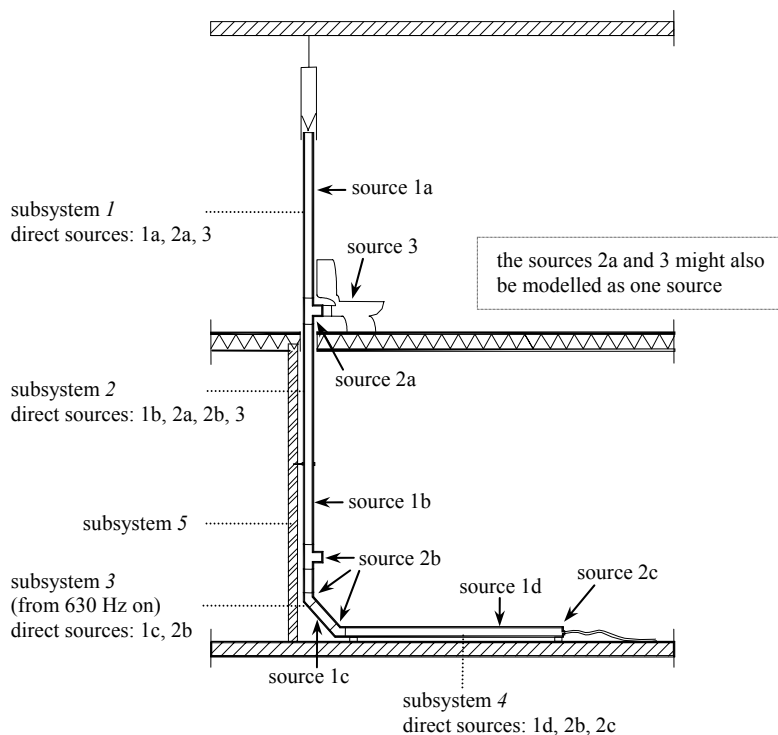
Figure 6-1 Schematic presentation of a vertical section of the experimental set-up (see Figure 5-19 in section 5.6.1 for photographs), subsystems definition and direct sources; source type 1 = water flow, source type 2 = turbulent water flow and falling of water in bends and other pipe system discontinuities and source type 3 = toilet

Roughly three types of sound sources in pipe systems[113] can be distinguished. Firstly, a more or less stationary water (and dirt) flow can occur in long[114] straight pipes. Secondly,

---

[113] This thesis focuses on wastewater pipe systems, but the source types mentioned can be distinguished in other types of pipe systems too.

in practical pipes and near pipe system discontinuities a turbulent water (and dirt) flow exists. Thirdly, a pipe system is set into vibration by machinery or appliances, e.g. a toilet, bathtub, sink or tap.

Generally speaking, machinery or an appliance is connected to only one (pipe) system element and therefore puts energy into one system element. However, a water (and dirt) flow puts energy into all pipe system elements (more or less) simultaneously, except into side branches in a pipe system[115]. In this study, it has been observed that a water flow primarily circles along the pipe circumference in a screw-like motion in vertical wastewater pipe sections. The water partly falls downwards. In horizontal wastewater pipe sections water flows along the lower part of the pipe circumference. Possibly a water (and dirt) flow can cause nearfields and non-resonant sound transmission through pipe couplings into plates[116].

Usually the three types of sound sources are non-stationary. So, a transient SEA model should be made to describe the sound transmission through pipe systems and from pipe systems into plates in detail. However, such a detailed description may not be necessary (see section 6.3).

---

[114] When frequencies above 100 Hz are considered a more or less stationary flow can exist in practical wastewater pipes with a length of at least 6 m, in case of a continuous flow [ref 35].

[115] Side branches are excited by pipe system elements through which water (and dirt) flows. Depending on the flow a pipe system element is excited directly by a water (and dirt) flow the one time, and indirectly by another pipe system element the other time. The pipe system elements on the first storey of a building are always directly excited.

[116] During measurements in this study, it has been observed that excitation of a practical wastewater pipe system due to the falling of water in pipe system discontinuities causes much larger responses of the pipe system than the excitation due to water flow and the excitation by a toilet (the results are not shown in this thesis). The observations have been done by comparing the velocity spectra of straight pipe sections during toilet flushing. The largest velocities were observed during the falling of water in the basement bend of the pipe system. The straight pipe sections considered were located at some distance of the basement bend. Since the responses of these straight pipe sections were dominated by the falling of water in the basement bend and to a lesser degree by water flow in the pipe sections themselves, the sound transmission from one of the pipe sections through a pipe clamp to a plate was expected to be resonant (the other pipe sections were not connected to a plate). The ratio of the sound transmission through pipe clamps due to nearfields and non-resonant transmission to the sound transmission due to resonant transmission is expected to depend on the distance of the pipe clamp to a discontinuity.

6.3 Proposal for a quantitative description of sound sources

6.3.1 Maximum equivalent input force as a source descriptor

The input power $\Pi_{i,in}$ corresponding to a practical source to a subsystem i can be determined from the resulting subsystem energy $E_{i,tot}$ (derived from the subsystem mass and measurements of the reverberant velocity caused by the practical source) and the *in situ* total loss factor of the subsystem $\eta_{i,tot,in\ situ}$:

$$\Pi_{i,in} = 2\pi f \eta_{i,tot,in\ situ} E_{i,tot} \qquad (6.1)$$

Equation *(6.1)* can be rewritten to:

$$2\pi f \eta_{i,tot,in\ situ} M_i = \frac{\Pi_{i,in}}{v_i^2} \qquad (6.2)$$

The term $2\pi f \eta_{i,tot,situ} M_i$ is assumed[117] to be equal for both the known source (shaker) and the unknown source (toilet flushing). So, the term $\Pi_{i,in}/v^2_i$ is assumed to be equal for both the known and the unknown source. Therefore, the (unknown) equivalent input power $\Pi_{i,in}$ corresponding to a practical source to a subsystem i can be determined from a known input power, e.g. from a shaker, and the subsystem velocities corresponding to the known source and the practical source with:

$$\Pi_{i,in} = \Pi_{i,in,known} \cdot \frac{v_{i,unknown}^2}{v_{i,known}^2} \qquad (6.3)$$

Basically, the response due to a known (substitution) source (shaker excitation) is compared with the response due to an unknown source (toilet flushing).

The equivalent input power depends on the subsystem for which it has been determined. In order to make the source description subsystem-independent, equivalent input force may be a good source descriptor. The equivalent input force F_{in} can be determined from the equivalent input power $\Pi_{i,in}$ to a subsystem i and the space-averaged real part of the point admittance $Re(Y_i)$ of the subsystem with:

$$F_{in}^2 = \frac{\Pi_{i,in}}{Re(Y_i)} \qquad (6.4)$$

---

[117] Actually, for the unknown source the term might be slightly larger than for the known source because of a water layer in contact with the pipe wall during toilet flushing.

The equivalent input force can also be determined directly with equation *(6.3)* by transposing $\Pi_{i,in}$ and $\Pi_{i,in,known}$ by F^2_{in} and $F^2_{in,known}$ respectively.

In accordance with the simplified SEA model, only equivalent input powers and forces in the vibrational direction perpendicular to the pipe wall have been determined in this study.

The source description is based on the following assumptions:
- the vibrational energy of radial pipe wall responses due to excitation by practical sources is higher than the sum of the vibrational energies of axial and tangential responses (assumption 7 of the simplified SEA model);
- the vibro-acoustic behaviour of the pipe system section considered is linear for both the known source (shaker) and the unknown source (toilet flushing);
- the terms $2\pi f \eta_{i,tot,situ} M_i$ and $Re(Y_i)$ are assumed to be equal for both sources;
- the pipe system section to which an equivalent input force corresponding to a practical source is determined has a multi-modal vibro-acoustic behaviour with a large modal overlap;
- the vibrational energy of the pipe system section considered is dominated by excitation by the source considered (either the practical source or the shaker) and not by energy flow to or from connected pipe system sections (see the next section).

Because of their variety and non-stationary behaviour, description of practical sources in pipe systems is complicated. A simplified source description has been searched for, in relation to common quantities in regulations aimed at limitation of noise due to service equipment in buildings. In existing regulations, limits are often described in terms of maximum allowable sound levels (max hold values per octave band, time constant 1 s) in rooms, caused by service equipment during one period of operation. Therefore, in this study equivalent input powers/forces and responses of physical system elements have been determined in terms of max hold values.

6.3.2   Measurement method

In the experimental set-up, the maximum equivalent input power to the middle vertical pipe (subsystem *2*) generated by toilet flushing and the corresponding maximum equivalent input force have been determined. The combined excitation of the three source types, as described in section 6.2, is considered. During the measurements is has been observed that the excitation due to the turbulent flow and the falling of water in the basement bend

(indicated as source 2b in Figure 6-1) is dominant in the max hold responses during a period of operation (see footnote 116).

As described in section 6.2, in a pipe system subsystems will partly be excited directly and partly indirectly via other subsystems (that are excited directly). For example, Figure 6-1 shows that subsystem *2* will have been excited directly by[118] the falling of water in the basement bend. Subsystem *2* will also have been excited by subsystem *4* (horizontal pipe) that is excited directly by the falling of water in the basement bend. The last mentioned contribution to the response of subsystem *2* should be subtracted to obtain the real equivalent input power/force to subsystem *2* by the falling of water in the basement bend. This should be done for all subsystems. In this thesis, this has not been done, because proper information to do this was lacking, i.e. no input powers to the subsystems *1* and *4* have been determined. So, the given equivalent input power/force to subsystem *2* may be an overestimation due to the contribution of connected subsystems (particularly subsystem *4*, but possibly also subsystem *1*). Although the contribution of the subsystems *1* and *4* to the energy level of subsystem *2* cannot be determined, the procedure of estimating contributions of connected subsystems to the energy level of a particular subsystem is illustrated by the example in section 6.3.4.

It is desirable to determine equivalent input forces to different subsystems (e.g. vertical and horizontal pipe system parts) for different source types (in case they are not correlated) in the future.

During five toilet flushing cycles space-averaged values of max hold[119] (per octave band, time constant 1 s) radial velocities of subsystem *2* (middle vertical pipe) have been determined in 1/3-octave bands. The mean value over the max hold velocities of the five flushing cycles has been determined. The same has been done for shaker excitation to subsystem *2*. For the shaker excitation also the input power/force to subsystem *2* has been derived. The measurements have been done at the same excitation (shaker)[120] and response

---

[118] Directly, because there are no subsystems between the basement bend and subsystem *2* (only maybe in a part of the frequency range considered), so the turbulent flow and the falling of water in the lower T-joint and the basement bend are considered as one source (2b) exciting subsystem *2* at the pipe's end (see Figure 6-1).

[119] An advantage of max hold values above time-averaged values for a flushing cycle is that the repeatability of the max hold values is larger. This is primarily due to the fact that the representative measurement period for mean values slightly differs for each flushing cycle.

[120] This very rough source characterization is assumed to be reasonably well, because subsystem *2* is assumed to be excited directly at the pipe's end (see footnote 118) and because of the multi-modal vibro-acoustic behaviour of subsystem *2* (see the assumptions in section 6.3.1), making the exact excitation point of the shaker less relevant. However, further elaboration of the source characterization is needed in the future

positions and with the same equipment as described in section 5.6 and appendix V. The maximum equivalent input power/force generated by toilet flushing to subsystem *2* has been derived with equation *(6.3)*. Input powers/forces in octave bands have been calculated by summation of the corresponding 1/3-octave band values.

6.3.3   Experimental results

The maximum equivalent input powers/forces (max hold values) in (1/3-)octave bands to subsystem *2* (middle vertical pipe) are presented in Figure 6-2.
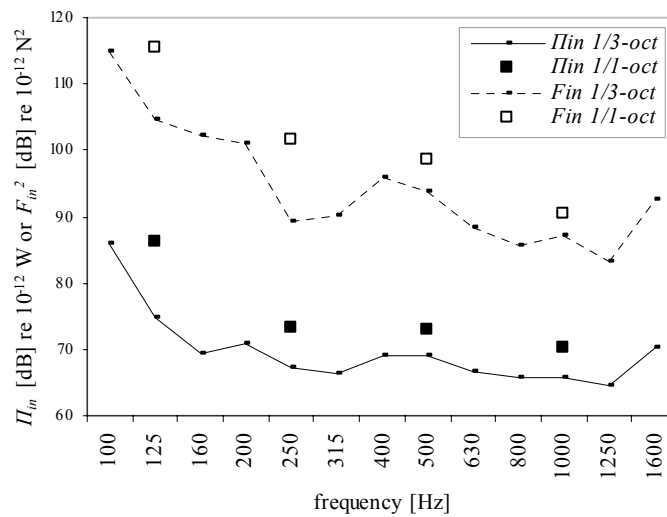
Figure 6-2   Maximum equivalent input power Π_{in} and maximum equivalent input force F_{in}^2 in (1/3-)octave bands due to toilet flushing determined in the experimental set-up from the responses of the middle vertical pipe (subsystem *2*)

6.3.4   Illustration of estimation of subsystem energy levels from source data

This section describes the estimation of the energy level E_1 of subsystem *1* due to excitation by subsystem *2* that is excited by the falling of water in the basement bend (see Figure 6-1). A simplified procedure of estimating is shown by taking only the subsystems *1* and *2* into account in solving the power balance matrix.

---

naturally. An important aspect to study will be the choice of the excitation point of the shaker and the effect of this choice on the results.

The power balance equations for the two subsystems are

$$\Pi_{1,in} = 2\pi f (\eta_{11} + \eta_{12})E_1 - 2\pi f \eta_{21} E_2$$
$$\Pi_{2,in} = -2\pi f \eta_{12} E_1 + 2\pi f (\eta_{22} + \eta_{21})E_2$$

$$(6.5)$$

The input power $\Pi_{1,in}$ to subsystem 1 is set to 0 Watt, because we are interested in E_1 and E_2 due to the falling of water in the basement bend which is characterized by $\Pi_{2,in}$.

Then, by rewriting the first power balance equation E_1 is given by

$$E_1 = \frac{\eta_{21} E_2}{\eta_{11} + \eta_{12}}$$

$$(6.6)$$

And by rewriting the second power balance equation and replacing E_1 by equation *(6.6)*, E_2 is given by

$$E_2 = \frac{\Pi_{2,in}}{\dfrac{-2\pi f \eta_{12}\eta_{21}}{\eta_{11} + \eta_{12}} + 2\pi f (\eta_{22} + \eta_{21})}$$

$$(6.7)$$

By filling in $\Pi_{2,in}$ (see Figure 6-2), η_{11}, η_{22}, η_{12} and η_{21} (see Figure 5-23 for the damping and coupling loss factor values) in equations *(6.6)* and *(6.7)* E_1 and E_2 are found. E_1 and E_2 are shown in Figure 6-3.
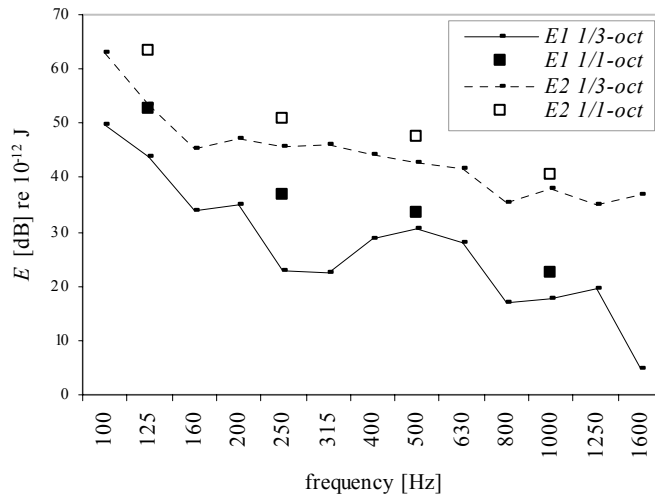
Figure 6-3   Estimated energies E_1 and E_2 in (1/3-)octave bands for the upper vertical pipe (subsystem *1*) and the middle vertical pipe (subsystem *2*) due to toilet flushing, specific the falling of water in the basement bend

Figure 6-3 shows 10 dB to 20 dB lower energy levels at one storey higher (10 dB to 20 dB lower E_1- than E_2-levels due to falling of water in the basement bend). However, the energy level E_1 may be higher when also excitation of subsystem *1* due to the turbulent water flow in the upper T-joint (source 2a) and due to the toilet itself (source 3) is included (see Figure 6-1). Separate characterization of these sources has not been done in this study.

6.4 Validity of the simplified SEA model for practical excitation of pipe systems

6.4.1 Testing the validity of assumption 7

This section is aimed at testing the validity of assumption 7 of the simplified SEA model. The assumption and corresponding validation criterion are summarised below. See section 3.3 for a complete description of the assumption and criterion. The testing is based on measurements, which are described below. The validation criterion is set for octave bands, but results for both 1/3-octave and octave bands are shown.

Assumption 7
Practical sources in pipe systems, e.g. a water flow or a toilet, cause radial pipe vibrations to be more important as energy-carriers than axial and tangential pipe vibrations. This assumption is defined to be valid if in each octave band considered a practical source causes a pipe to vibrate in such a way that the ratio of vibrational energy of radial responses to the sum of energies of axial and tangential responses is at least 1,3.

In the experimental set-up, during five toilet flushing cycles, space-averaged values of max hold (per octave band, time constant 1 s) axial, tangential and radial velocities of the middle vertical pipe (subsystem *2*) and the horizontal pipe (subsystem *4*) have been determined in 1/3-octave bands. The mean value over the max hold velocities of the five flushing cycles has been determined. Velocities in octave bands have been calculated by summation of the corresponding 1/3-octave band values. The measurements have been done at the same response positions and with the same equipment as described in section 5.6 and appendix V.
The same has been done for a vertical PVC pipe (length about 2 m, similar pipe wall thickness and outer shell radius as for the pipes in the experimental set-up) in a practical situation, i.e. a house. There the water flowed into the pipe via a bend consisting of two 135°-bends connected by a short straight pipe. The water flowed out of the pipe into a horizontal pipe via a 90°-bend.

For the pipes in both the experimental set-up and in the practical situation, from the obtained velocity and the corresponding pipe mass, the ratio of vibrational energy of radial responses to the sum of energies of axial and tangential responses in (1/3-)octave bands has been determined with equation *(5.19)* in section 5.4.2 (to calculate the energies of axial, tangential and radial responses) and equation *(4.11)* in section 4.2.4 (to calculate the needed energy ratio).

The results are shown in Figure 6-4 for the vertical pipes and in Figure 6-5 for the horizontal pipe. Also a ratio of 1,3 is shown, to indicate the criterion for predominantly radial response applied in this thesis.
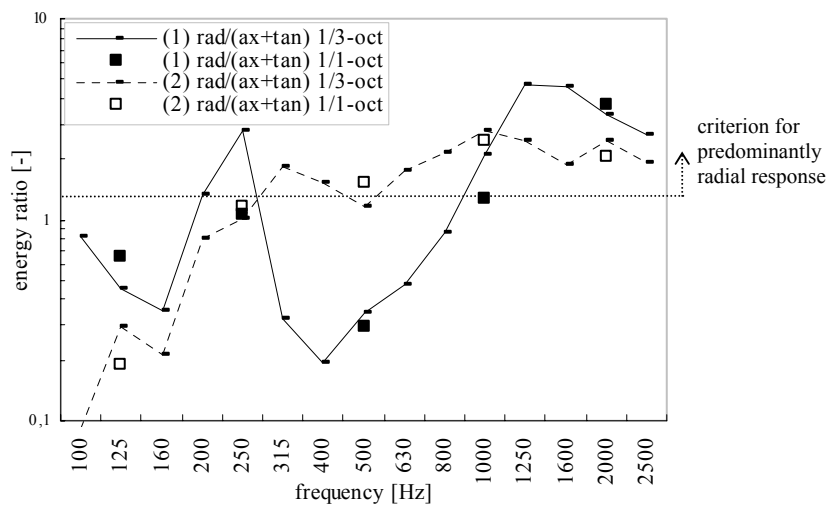
Figure 6-4   Ratio of energy of radial responses to the sum of energies of axial and tangential responses, in (1/3-)octave bands, in **(1)** the middle vertical pipe (subsystem *2*) in the experimental set-up and **(2)** a vertical pipe in a practical situation. Also the criterion for predominantly radial response applied in this thesis is shown.
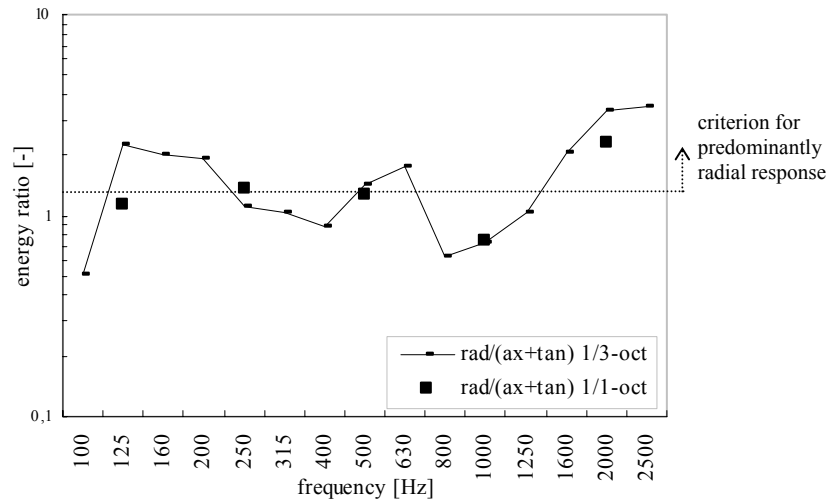
Figure 6-5 Ratio of energy of radial responses to the sum of energies of axial and tangential responses, in (1/3-)octave bands, in the <u>horizontal pipe (subsystem 4)</u> in the <u>experimental set-up</u>. Also the criterion for predominantly radial response applied in this thesis is shown.

Figure 6-4 shows (completely) different results for the vertical pipes, especially in the frequency range 315-800 Hz. For octave bands the ratio of vibrational energy of radial responses to the sum of energies of axial and tangential responses becomes at least 1,3 from 500 Hz on for the pipe in the practical situation and from 1000 Hz on for the pipe in the experimental set-up. For both pipes the ratio is almost 1,3 at 250 Hz. So, assumption 7 is fulfilled from 500-1000 Hz on, for the pipe in the practical situation almost from 250 Hz on.

For the horizontal pipe Figure 6-5 shows for octave bands that the energy ratio becomes (almost) at least 1,3 in the entire frequency range of interest, except at 1000 Hz. So, assumption 7 is (almost) fulfilled in the entire frequency range of interest, except at 1000 Hz.

It is not clear why assumption 7 sometimes is not fulfilled in the middle of the frequency range considered. Because of the cut-on of higher-order flexural modes (with a mainly radial vibrational direction) increasing energy ratios with increasing frequency are expected. The results for the vertical pipe in the practical situation illustrate this, and therefore seem more comprehensible than the results for the vertical pipe in the experimental set-up. Maybe, the energy ratios of the vertical and horizontal pipes in the experimental set-up are partly determined by indirect excitation via the connected subsystems (see section 6.3.2). For example, axial vibrations in a subsystem might be

caused by radial vibrations in a connected subsystem [121]. This point certainly needs further investigation in the future, based on more measurements in various situations.

Whether the fact that assumption 7 is not fulfilled in the entire frequency range becomes a problem depends on the transmission through couplings between pipe systems and plates and within pipe systems. The combined effect of these issues on the prediction accuracy of the simplified SEA model is discussed in chapter 7.

6.4.2   Additional test of the validity of the model

In order to get further evidence of the validity of the simplified SEA model, an additional test has been done. The test is based on measurements, which are described below, and on results described in chapter 5.

The overall accuracy is additionally tested by comparing coupling loss factors representing the energy transmission from pipe to plate, determined with shaker excitation (radial to the pipe, see section 5.6) and with toilet flushing excitation (axial, tangential and radial to the pipe) as described below.

For both sources, the coupling loss factors have been determined from the energy of radial pipe responses and from the energy of out-of-plane plate response.


In the experimental set-up, during five toilet flushing cycles, space-averaged, max hold values (per octave band, time constant 1 s) of the radial velocity component for the middle vertical pipe (subsystem *2*) and of the out-of-plane velocity component for the plate (subsystem *5*) have been determined. The mean value over the five flushing cycles has been determined. The measurements have been done at the same response positions and with the same equipment as described in section 5.6 and appendix V.

From the obtained velocities and the corresponding subsystems masses, the subsystems energies have been calculated with equation *(5.19)* in section 5.4.2. From these energies, the subsystems damping loss factors (given in section 5.3) and theoretically determined modal densities (see chapter 4), coupling loss factors representing the energy transmission from pipe to plate, have been calculated with equation *(5.13)* in section 5.2.3. The analysis has been performed in 1/3-octave bands. Coupling loss factors in octave bands have been calculated by averaging the 1/3-octave band values.

---

[121] At low frequencies axial responses cannot be caused by quasi-longitudinal modes, because the corresponding wave lengths will be about 15 meter, which is too large compared to the subsystems lengths to cause resonant vibrational behaviour in the subsystems. At higher frequencies (from 400 Hz to 800 Hz on) quasi-longitudinal modes can contribute to the axial vibrations.

The results are shown in Figure 6-6, where also the coupling loss factors determined in section 5.6 are presented.
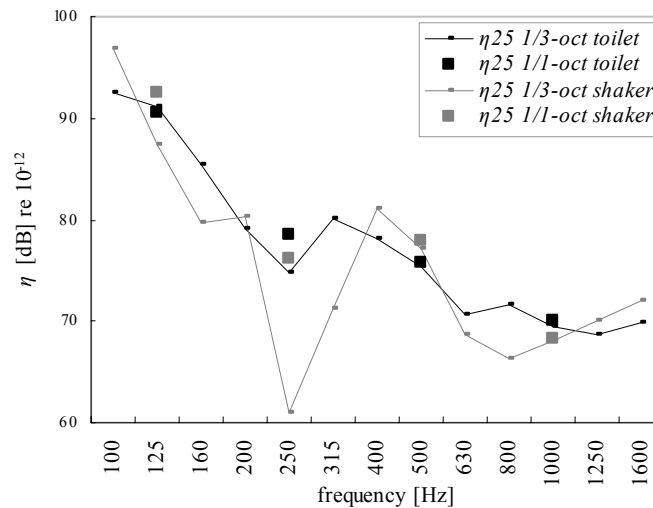
Figure 6-6   Coupling loss factors η, in (1/3-)octave bands, representing the <u>energy transmission from the middle vertical pipe (subsystem 2) via the pipe clamp to the plate (subsystem 5)</u> in the experimental set-up. The coupling loss factors are obtained from subsystems energies of the responses in the radial/out-of-plane vibrational direction, with excitation by a <u>shaker</u> (from <u>time-averaged</u> values) and by <u>toilet flushing</u> (from <u>max hold</u> values).

For octave bands, Figure 6-6 shows differences between the coupling loss factors of 2,4 dB at most. From the curve trends, it is expected that the differences will not be larger in the octave band 2000 Hz. This is (much) lower than the allowed inaccuracies in each octave band considered corresponding to assumption 8, hence 5 dB at most, and to assumption 7, hence 2,5 dB at most. (assumption 8 deals with coupling between physical system elements that are subject of this thesis, i.e. pipes and plates in buildings)

The results in 1/3-octave bands show larger differences, especially at 250 Hz and 315 Hz, where the dip in the coupling loss factor curve obtained with shaker exciation is questionable. This needs further investigation in the future. Might sound radiation from pipe to plate result in larger coupling loss factors obtained from measurements with toilet flushing compared to coupling loss factors obtained with shaker excitation, because a shaker causes less excitation of specific mode types (e.g. with $n=2$ or acoustic modes), for example? The critical frequency, where extra sound radiation is expected, lies around 250 Hz, which might be an explanation for the dip.

The application of max hold values (excitation by toilet flushing) instead of time-averaged values (excitation by shaker) does not seem to have a large influence on the coupling loss factor values, which is striking, but encouraging, related to the discussion about steady-state equilibrium of energy in section 5.7.

6.5   Conclusions

In this chapter the validity of assumption 7 of the simplified SEA model (see section 3.3) has been tested. The assumption and test results are summarised below.

Assumption 7
Practical sources in pipe systems, e.g. a water flow or a toilet, cause radial pipe vibrations to be more important as energy-carriers than axial and tangential pipe vibrations.

The test results are described in detail in section 6.4.
For some vertical and horizontal pipes, the ratio of vibrational energy of radial responses to the sum of energies of axial and tangential responses has been determined during toilet flushing.
For the vertical pipes studied the assumption is fulfilled from 500-1000 Hz on, (possibly) almost from 250 Hz on. For the horizontal pipe studied the assumption is (almost) fulfilled in the entire frequency range of interest, except at 1000 Hz.
Some of the measurement results are not comprehensible. The testing of the validity of the assumption certainly needs to be extended in the future, based on more measurements in various situations.
Whether the fact that the assumption is not fulfilled in the entire frequency range becomes a problem depends on the transmission through couplings between pipe systems and plates and within pipe systems. The combined effect of these issues on the prediction accuracy of the simplified SEA model is discussed in chapter 7.

Additional test
In order to get further evidence of the validity of the simplified SEA model, an additional test has been done.
The overall accuracy is additionally tested by comparing coupling loss factors for a pipe clamp representing the energy transmission from pipe to plate, obtained from max hold responses due to excitation by toilet flushing and obtained from time-averaged responses due to shaker excitation.

The test results are described in detail in section 6.4. For all octave bands considered, the differences between the coupling loss factors are 2,4 dB at most (actually it can be concluded that the combination of the assumptions 7 and 8 (about coupling between physical system elements) is fulfilled in the entire frequency range of interest). This gives some evidence that the simplified SEA model may be sufficiently accurate within the scope of this thesis, in addition to the other test results described in this chapter and in the previous chapters.

Source characterization

This chapter also gives a first, very rough description of practical sources in (wastewater) pipe systems. A source descriptor that is subsystem-independent, namely the maximum equivalent input force, is proposed.

Some first results for maximum equivalent input forces and powers to a wastewater pipe due to toilet flushing have been determined in an experimental set-up in which a practical situation was simulated. Based on this practical example, it is illustrated that the source description is very complex and needs to be elaborated in the future.

CHAPTER 7

PREDICTION ACCURACY OF THE SIMPLIFIED SEA MODEL

7.1   Introduction

In section 3.4 two criteria for the prediction accuracy of the simplified SEA model have been set. In section 7.2 the prediction accuracy is estimated, based on predictions for a practical situation. Section 7.3 discusses whether the criteria are met.

This chapter is not aimed at giving an elaborate probabilistic analysis. For a proper analysis more (detailed) studies for more cases should be done. The results in this chapter are aimed at gaining a first insight in the prediction accuracy of the simplified SEA model, for an example of a characteristic practical situation, in order to decide whether it seems promising enough to develop the model further.

7.2   Estimation of the prediction accuracy for a practical situation

Suppose the system consisting of a pipe system and a plate, which are connected to each other via one of the pipes in the pipe system and a pipe clamp (see Figure 5-19 and Figure 5-22). The prediction accuracy of the simplified SEA model has been estimated by studying only a part of the system, i.e. the pipe mentioned (subsystem *2*), the pipe clamp and the plate (subsystem *5*). We are interested in the energy level E_5 of the out-of-plane plate vibrations due to excitation by the pipe, which on its turn is excited by a real source, i.e. toilet flushing.

By rewriting the second part of equation *(2.4)* for the system part considered ($\Pi_{5,in}$ equals zero), the energy level E_5 of the out-of-plane plate vibrations can be predicted with

$$E_5 = \frac{\eta_{25}E_2}{\eta_{55} + \eta_{52}} \qquad (7.1)$$

For the system mentioned, damping and coupling loss factors have been determined with PIM (method 1) and are presented in Figure 5-26 in section 5.6. Coupling loss factors have also been determined with two other determination methods, i.e. from subsystems energies, damping loss factors (obtained with the decay rate method) and modal densities (method 2) and from point admittances (method 3), and are presented in Figure 5-34 and Figure 5-35 in

section 5.7. The damping loss factors of the pipe and plate corresponding to the methods 2 and 3 are presented in Figure 5-6 and Figure 5-8 respectively in section 5.3.

The energy level E_2 (max hold values) of the pipe during toilet flushing has been determined from measurements as described in section 6.4.

The energy level of the plate has been predicted with equation *(7.1)*, with application of three different sets of damping and coupling loss factors, obtained with the three methods mentioned above. In these cases the energy level of radial pipe vibrations (max hold values) has been applied.

The energy level of the plate has also been predicted with application of the total energy level[122] of the pipe (max hold values) due to axial, tangential and radial vibrations. In this case damping and coupling loss factors obtained from PIM have been applied.

Finally, the energy level of the plate (max hold values) has been determined from velocity measurements and the plate mass.

The various predicted and measured, (1/3-)octave band and A-weighted, energy levels of the plate (max hold values) are presented in Figure 7-1.

---

[122] The total energy is calculated as $E=10lg(10^{Eax/10}+10^{Etan/10}+10^{Erad/10})$.
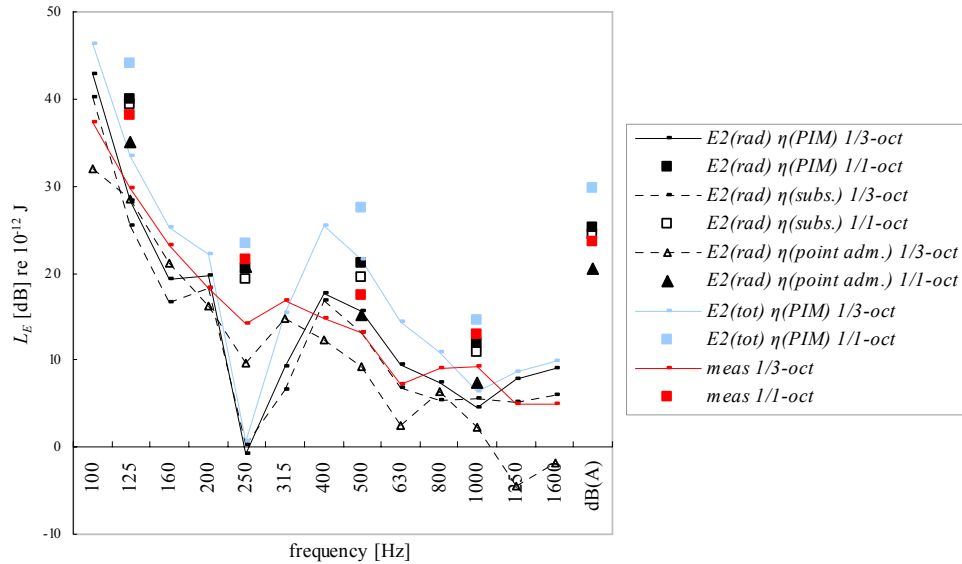
Figure 7-1   Maximum energy levels in (1/3)-octave bands and dB(A) for a plate, predicted with the simplified SEA model from radial and total energy levels due to toilet flushing of a pipe connected with a pipe clamp to the plate (indicated by *E2(rad)* and *E2(tot)* respectively) and from loss factors obtained from PIM (indicated by *η(PIM)*), from subsystems energies, damping loss factors and modal densities (indicated by *η(subs.)*) and from point admittances (indicated by *η(point adm.)*). Also the maximum energy levels of the plate that are directly determined from measurements are shown (indicated by **meas**).

For both the octave bands considered and the A-weighted levels, Figure 7-1 shows differences between the measured (real) energy level of the plate and the energy level of the plate predicted from only the radial pipe vibrations between 1 dB and 3 dB. For the energy level predicted from the axial, tangential and radial pipe vibrations, the differences lie between 2 dB and 10 dB for octave bands; the difference is 6 dB for A-weighted energy levels. For 1/3-octave bands the differences are larger. It is not expected that inclusion of the 2000 Hz octave band will give different results.

From the results it can be concluded that inclusion of only radial pipe vibrations and out-of-plane plate vibrations in a prediction model is more appropriate than inclusion of pipe and plate vibrations in all directions. Application of damping and coupling loss factors obtained with PIM (method 1) or coupling loss factors from subsystems energies, damping loss factors and modal densities (method 2) in predictions is more appropriate than application of coupling loss factors from point admittances (method 3).

The predicted and measured energy levels represent space-averaged values.

The accuracy of the predicted energy values depends on the accuracy by which the values of the model parameters have been determined. Related to this, it has to be remarked that, depending on the accuracy of the determination of input powers, the predicted energy levels of the plate could have been different in case input powers injected into the pipe due to toilet flushing had been applied in the predictions, instead of measured energy levels of the pipe due to toilet flushing.

Apart from this, the correctness of the subsystems definition in the simplified SEA model, i.e. exclusion of in-plane vibrations, determines the prediction accuracy. Assumptions and validation criteria for parts of the model were mentioned in section 3.3. The validity of the assumptions has been tested in the previous three chapters. The extent to which the assumptions are fulfilled contributes to the prediction accuracy of the complete model. This is specifically the case for the assumptions 7 and 8, which becomes clear when we look at equation *(7.1)*. The importance of in-plane pipe vibrations determines the accuracy of E_2. Deviations from the 'reciprocity relationship' determine the accuracy of η_{25} and η_{52}, although inaccuracies in both coupling loss factors might to some extent cancel each other.

Inaccuracies in both the determination methods for the parameters and the simplified SEA model are included in the estimations, however not explicitly.

The accuracy of the determination methods for the parameters has been investigated separately to some extent. See appendix VI for the results.

7.3   Validity of the simplified SEA model

In section 3.4 the following criteria were set for the prediction accuracy of the simplified SEA model:
- for 99% of the predictions, the difference between the predicted A-weighted energy level of a pipe system or a plate that is excited by a pipe system and the real A-weighted energy level is 2,5 dB at most.
- for 99% of the predictions, the difference between predicted and real energy levels in the octave bands with centre frequencies 125 Hz to 2000 Hz is 5 dB at most.

From the results in section 7.2 it is concluded that both criteria are met, maybe with the exception when coupling loss factors obtained from point admittances are applied in the prediction (difference between predicted and measured (real) values 3 dB(A)). So, the simplified SEA model seems to be sufficiently accurate to use it as the basis for a design or an engineering tool in building practice, i.e. for predictions.

Further studies for more cases are needed, in order to perform a probabilistic analysis and to determine 99% confidence levels.

7.4   Conclusions

In this chapter it has been investigated whether the criteria for the prediction accuracy of the simplified SEA model as set in the beginning of this study are met. Based on the results for a characteristic situation (see the previous sections) it is concluded that the criteria are met in the entire frequency range of interest, despite the fact that not all validation criteria corresponding to the separate model assumptions were fulfilled as discussed in chapters 4 to 6. Apparently, the fulfilment of all assumptions might not be that important and/or inaccuracies might to some extent cancel each other. Nevertheless, evaluation of model parts by testing the validity of the assumptions is valuable, and the validation criteria do not need to be reset so far. For example, on the one hand, the differences between predicted and measured energy levels for the octave band with centre frequency 125 Hz are not larger than the differences for the other octave bands considered, although the deviation from the 'reciprocity relationship' for the 125 Hz band was larger than the deviation for the 250 Hz band, for example. Besides, for the pipe, the assumptions concerning the modal properties and concerning excitation of pipe systems are not fulfilled for the 125 Hz band. So, for the 125 Hz band the prediction accuracy is not (clearly) related to the fact that most of the model assumptions are (slightly) not fulfilled. On the other hand, the largest differences between predicted and measured energy levels are observed for the 500 Hz band, which may be related to the fact that for this band the deviations from the 'reciprocity relationship' and from the criterion corresponding to the assumption concerning excitation of pipe systems are the largest. So, in this case the prediction accuracy seems to be related to the fact that some model assumptions are not fulfilled.

The conclusion about fulfilling the criteria for the prediction accuracy is based on the study of only one, though characteristic, situation. In the future more (detailed) studies for more cases should be done to come to a final conclusion. Nevertheless, at this moment, the simplified SEA model, specifically the fact that only radial pipe vibrations and out-of-plane plate vibrations are included in the model, seems to be promising as the basis for a design or an engineering tool in building practice, i.e. for predictions.

CHAPTER 8
CONCLUSIONS AND PERSPECTIVES FOR FURTHER WORK

Simplified SEA model

In this study a simplified SEA model has been developed that describes the sound transmission through pipe systems and between pipe systems and plates in buildings (see section 3.2). The model is based on the hypothesis that radial pipe vibrations and out-of-plane plate vibrations as response components are dominant in the sound transmission, and are therefore dominant in the sound radiation to rooms. In the model, modes with vibrations perpendicular to pipe walls and plates have been grouped in subsystems. Axial and tangential pipe vibrations and in-plane plate vibrations are not included in the model. Pipe clamps and pipe coupling elements, such as joints and bends, have initially been modelled as couplings between pipes and plates and between straight pipes in pipe systems respectively.

The hypothesis mentioned above results from several assumptions. In order to test the validity of these assumptions, validation criteria have been set in section 3.3. It is assumed that including only radial pipe vibrations and out-of-plane plate vibrations will result in a model that is sufficiently accurate for engineering applications in building practice. In order to test the validity of this assumption, criteria for the prediction accuracy of the model have been set in section 3.4.

This study has been aimed at testing the validity of the simplified SEA model, by testing the validity of the model assumptions (see chapters 4-6) and the prediction accuracy (see chapter 7). For this purpose, several model parameters have been determined, while focussing on plastic wastewater pipe systems and single, homogeneous floors and walls in buildings. The octave bands with centre frequencies 125 Hz to 2000 Hz have been considered, because pipe noise generally concerns this frequency range, i.e. A-weighted sound levels due to pipe noise are generally determined by the sound pressure levels within the octave bands mentioned.

In the next table, the model assumptions, corresponding validation criteria and test results are summarised. For detailed descriptions of the test results, the reader is referred to chapters 4-7.

Table

Summary of test results

Assumption	Validation criterion	Tested in section	Tested for	Test result: assumption fulfilled for
Assumptions concerning modal properties of physical system elements				
1. The subsystems responses in each octave band considered are determined by a sufficiently large number of resonant modes.	The number of modes per octave band is at least 6 for each subsystem.	4.2.4 4.4.4	Pipes Plates	$\geq$ 125-250 Hz $\geq$ 125-250, $\geq$ 500 Hz for small surface areas
2. The subsystems responses in each octave band considered have sufficient modal overlap.	The modal overlap in each octave band is at least 1 for each subsystem.	4.2.4 4.4.4	Pipes Plates	$\geq$ 125-250 Hz $\geq$ 125-250, $\geq$ 1000 Hz for small surface areas
3. Pipe system discontinuities, such as bends, joints or clamps, are no subsystems, but coupling elements.	The number of modes per octave band is 5 at most for each pipe system discontinuity.	4.3.4 4.3.4	Straight joints Pipe clamps, T-joints and bends	< 1000 Hz $\geq$ 125 Hz
6. In each octave band considered, the responses of natural modes are predominantly radial for pipes and out-of-plane for plates.	For pipes: in each octave band considered the ratio of vibrational energy of radial responses to the sum of energies of axial and tangential responses is at least 1,3. For plates: in each octave band considered the ratio of energy of out-of-plane responses to the sum of energies of in-plane responses is at least 1,3.	4.2.4 4.4.4	Pipes Plates	$\geq$ 125-250 Hz $\geq$ 125 Hz
Assumptions concerning damping in and coupling between physical system elements				
4. The transmission of vibrational energy between subsystems caused by resonant modes is significantly larger (preferably at least a factor of 10) than the energy transmission caused by non-resonant vibrations.	Testing combined with testing of assumption 8.			

222

5. The coupling between subsystems is weak.	In each octave band considered the ratio of a coupling loss factor η_{ij}, representing the energy transmission from subsystem i to subsystem j, to the total loss factor $\eta_{i,tot}$ of subsystem i minus η_{ij} is smaller than 0,1 (the total loss factor $\eta_{i,tot}$ minus η_{ij} is at least a factor of 10 (10 dB) higher than the coupling loss factor η_{ij}).	5.4.4/5.6.5 5.5.4/5.6.5	Pipe clamps Pipe coupling elements	$\geq$ 125 Hz $\geq$ 125-500 Hz
8. Out-of-plane plate vibrations are predominantly caused by radial vibrations in pipe systems and vice versa. Radial vibrations in a pipe are predominantly caused by radial vibrations in another pipe that is part of the same pipe system.	For each pair of connected subsystems, the deviation from the 'reciprocity relationship' (as written in equation *(3.3)*) is 5 dB at most in each octave band considered.	5.4.4/5.6.5 5.5.4/5.6.5	Pipe clamps Pipe coupling elements	$\geq$ 125 Hz $\geq$ 125-250 Hz
Assumption concerning excitation of pipe systems by practical sources				
7. Practical sources in pipe systems, e.g. a water flow or a toilet, cause radial pipe vibrations to be more important as energy-carriers than axial and tangential pipe vibrations.	In each octave band considered a practical source causes a pipe to vibrate in such a way that the ratio of vibrational energy of radial responses to the sum of energies of axial and tangential responses is at least 1,3.	6.4 6.4	Vertical pipes due to toilet flushing Horizontal pipes due to toilet flushing	$\geq$ 500-1000 Hz $\geq$ 250 Hz, except at 1000 Hz
Prediction accuracy of the model				
The model is sufficiently accurate for engineering applications in building practice.	Criterion 1: for 99% of the predictions, the difference between the predicted A-weighted energy level of a pipe system or a plate that is excited by a pipe system and the real A-weighted energy level is 2,5 dB at most. Criterion 2: for 99% of the predictions, the difference between predicted and real energy levels in the octave bands with centre frequencies 125 Hz to 2000 Hz is 5 dB at most.	7.3 7.3	Sound transmission due to toilet flushing from a pipe system to a plate through a pipe clamp	Fulfilled $\geq$ 125 Hz

The results show that the assumptions are fulfilled in a large part of the frequency range considered, generally from 250 Hz on, often from 125 Hz on (see chapters 4 and 5). The only exception of an assumption which may not be fulfilled in a large part of the frequency range considered is the assumption about excitation of pipe systems (see chapter 6): the results obtained in this study are varying. The excitation of pipe systems by practical sources needs to be investigated in more detail in the future. The modelling of pipe coupling elements, such as joints and bends, needs special attention. These elements are initially modelled as couplings. However, the results show that these elements may rather be modelled as subsystems from 1000 Hz on (see section 4.3.4), below 1000 Hz as one subsystem together with the connected straight pipes (see section 5.6.4). This may be investigated in more detail in the future.

The prediction accuracy has been estimated for a characteristic application of the model, i.e. transmission of sound due to toilet flushing from a pipe system to a plate through a pipe clamp. The results show that both criteria for the prediction accuracy are fulfilled, despite the fact that not all validation criteria corresponding to the separate model assumptions were fulfilled. Apparently, the fulfilment of all assumptions might not be that important and/or inaccuracies might to some extent cancel each other. However, the conclusion is based on the study of only one, though characteristic, situation. In the future more (detailed) studies for more cases should be done to come to a final conclusion. Those studies may also be focussed on other types of pipe systems, such as water supply pipes, and plates, such as lightweight floors and walls. Nevertheless, at this moment, the simplified SEA model, specifically the fact that only radial pipe vibrations and out-of-plane plate vibrations are included in the model, seems to be promising as the basis for a design or an engineering tool in building practice, i.e. for predictions.

Determination methods for parameters

For the testing of the validity of the model assumptions, various model parameters have been determined with different theoretical, numerical and experimental methods. For the system type studied, the application and accuracy of the methods, in particular some experimental determination techniques for parameters, have been investigated, e.g. by comparing the results obtained with different methods.

Modal properties of subsystems have been obtained from (1) analytical approximations, (2) FEM and (3) point admittance measurements. For comparisons of results from the different methods see for pipes sections 4.2.2.4 and 4.2.3.3 and for plates section 4.4.3.

Damping and coupling loss factors have been obtained with the following methods:
- damping loss factors with the decay rate method;
- damping and coupling loss factors with the Power Injection Method (PIM);
- coupling loss factors from subsystems energies, damping loss factors (determined with the decay rate method) and modal densities;
- coupling loss factors from point admittances of subsystems and coupling element. An important advantage of this method is that coupling loss factors can be predicted from parameters that are often known.

For comparisons of coupling loss factors from the different methods see for pipe clamps section 5.4.3, for pipe coupling elements section 5.5.3 and for both section 5.7. For comparisons of damping loss factors see section 5.7 for both pipes and plates. PIM systematically gives higher damping and coupling loss factors. Section 5.7 discusses the dependency of loss factors on determination method and set-up in detail. Damping loss factors do not seem to depend on set-up, but they do on determination method. Coupling loss factors depend on both determination method and set-up, which was expected, because they depend on the vibrational characteristics of the connected subsystems. Nevertheless, results obtained in a set-up give a good indication for another (similar) set-up. Besides, derivation of coupling loss factors for a new situation from known coupling loss factors is relatively easy.

Although the results of the various determination methods do not correspond exactly with each other, it is concluded that the results are sufficiently accurate for testing the validity of the assumptions. Generally speaking, for the systems that are subject of this thesis the applied determination methods are usable, but in order to obtain reliable data for predictions they should be evaluated in more detail and need further development. All methods seem appropriate, but it is not clear which method(s) is (are) most appropriate. Differences in results obtained with the different methods in this study may be due to measurement inaccuracies, but may also be inherent to the chosen methods.

Chapter 6 gives a first, very rough description of practical sources in (wastewater) pipe systems. A source descriptor that is subsystem-independent, namely the maximum equivalent input force, is proposed. Based on some first results for toilet flushing, it is illustrated that the source description is very complex and needs to be elaborated in the future.

226

APPENDIX I

VIBRO-ACOUSTIC BEHAVIOUR OF PIPES

The vibro-acoustic behaviour of straight fluid-filled pipes has been described in detail by many authors. In this appendix the descriptions of Leissa [ref 14], De Jong [ref 25], Pavic ([ref 19] and [ref 20]), Finnveden ([ref 21], [ref 22] and [ref 23]), Fuller and Fahy [ref 17], Fahy [ref 13], Norton [ref 6] and Cremer & Heckl [ref 12] are followed.

The purpose of this appendix is to give a brief outline of the modelling of the vibro-acoustic behaviour, as far as necessary for the understanding of the main text of this thesis. Furthermore, this appendix contains calculation results obtained in this study, while focussing on pipe systems that are subject of this thesis, i.e. water supply and wastewater pipes in buildings.

For a more thorough description of the vibro-acoustic behaviour of straight fluid-filled pipes the reader is referred to one of the publications mentioned above.

I.1 Equations of motion and dispersion equation

The vibro-acoustic behaviour of pipes can be described by solving the equations of motion[123] for the coupled system of pipe shell, i.e. pipe wall, and pipe fluid.

During the past decades various scientists have given different solutions for the equations of motion. This has resulted in different shell theories. The differences are due to slight differences in simplifying assumptions and/or the exact point in a derivation where a given assumption is used. Various shell theories and the corresponding assumptions have been compared with each other, see Leissa [ref 14].

The geometry and the coordinate system for a circular cylindrical shell are shown in Figure I-1.

---

[123] The equations of motion are obtained by rewriting the stress-strain equations for circular cylindrical shells. The derivation of equations for shell motion can be found in many textbooks, see for example [ref 12], [ref 13] and [ref 14].
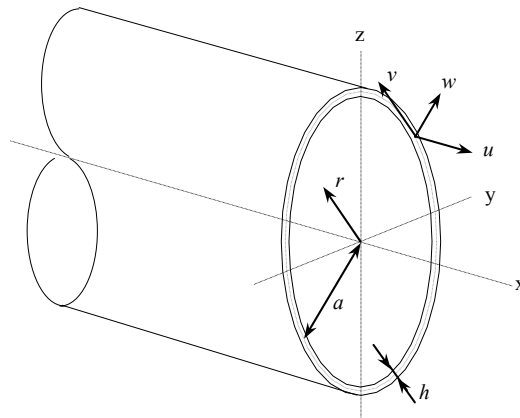
Figure I-1   Geometry and coordinate system for a circular cylindrical shell

Most shell theories are developed under the following assumptions, see for example [ref 14] and [ref 25]:

- the shell thickness is small compared to other shell dimensions, such as the mean radius a of the shell and the axial length of the shell[124,125];
- the deformation of the shell is small compared to its thickness and Kirchhoff's hypothesis applies: normals to the undeformed middle surface remain straight and normal to the deformed middle surface and suffer no extension;
- pipe wall and fluid exhibit a linear elastic behaviour;
- the pipe wall is circular symmetrical;
- pipe wall material and fluid are homogeneous and isotropic;
- the fluid flow velocity is low compared to the propagation velocity of sound in the pipe fluid: the Mach-number is low[126];
- viscosity of the pipe fluid may be neglected: the Shear-number is high[127];
- shear deformation and rotational inertia effects in the pipe wall may be neglected.

---

[124] Generally the following conditions are applied [ref 25]: $h/a \leq 0,1$; $l/a \geq 10$; $l/h \geq 10$, where h is the shell thickness, a the mean radius of the shell and l the axial shell length.

[125] For practical water supply and wastewater pipes this is the case.

[126] Generally the following condition for the Mach-number Ma is applied [ref 25]: $Ma = U/c_f << 1$, where U is the fluid flow velocity and c_f is the propagation velocity of sound in the pipe fluid.

[127] Generally the following condition for the Shear-number Sh is applied [ref 25]: $Sh = a_i(2\pi f/\nu)^{1/2} >> 1$, where a_i is the internal shell radius and ν is the kinematic viscosity.

The free motion of the coupled system of pipe shell and pipe fluid can be solved from the equations of motion in the frequency domain by performing a Fourier transform with respect to time [ref 25].

The equations of motion per structural mode (n,m)[128] can be expressed in a matrix equation, see for example [ref 14] and [ref 17]:

$$\begin{bmatrix} L_{11} & L_{12} & L_{13} \\ L_{21} & L_{22} & L_{23} \\ L_{31} & L_{32} & L_{33} \end{bmatrix} \begin{bmatrix} U_{nm} \\ V_{nm} \\ W_{nm} \end{bmatrix} = \begin{bmatrix} 0 \\ 0 \\ 0 \end{bmatrix} \tag{I.1}$$

where U_{nm}, V_{nm} and W_{nm} represent the amplitudes of axial, tangential and radial shell displacement for each structural mode (n,m) respectively.

The matrix equation gives non-trivial solutions only if [ref 25]:

$$det([L]) = 0 \tag{I.2}$$

Equation $(I.2)$ results in the dispersion equation, i.e. wave number[129]-frequency relationships for free waves in the fluid-filled pipe. The elements of the matrix $[L]$ are different for the different shell theories. For example, according to Flügge's shell theory the elements of the matrix $[L]$ are [ref 20]:

$$\begin{aligned} L_{11} &= \kappa^2 + [(1-\nu)/2](1+\beta^2)n^2 - \Omega^2 \\ L_{12} &= L_{21} = -[(1+\nu)/2]\kappa n \\ L_{13} &= L_{31} = -\nu\kappa - \beta^2\kappa[\kappa^2 - \{(1-\nu)/2\}n^2] \\ L_{22} &= n^2 + [(1-\nu)/2](1+\beta^2)\kappa^2 - \Omega^2 \\ L_{23} &= L_{32} = n + [(3-\nu)/2]\beta^2 n\kappa^2 \\ L_{33} &= 1 - \Omega^2 - Fl + \beta^2[1 - 2n^2 + (\kappa^2+n^2)^2] \end{aligned} \tag{I.3}$$

---

[128] n and m represent the circumferential and axial mode numbers respectively. At structural mode (n,m) the number of nodes around the pipe circumference is $2n$. m corresponds to the number of half wavelengths at structural mode (n,m).

[129] The wave number k is defined as:

$k = 2\pi f/c$

where c represents the propagation velocity of a certain wave type in a structural element or in fluid. At a certain frequency k differs for different types of free waves, because sound propagates with different propagation velocities for different types of free waves.

where the term *Fl* represents the normal fluid loading on the pipe wall, ν Poisson's ratio and κ the non-dimensional wave number[130].

β^2 is a non-dimensional shell thickness parameter, which is defined as:

$$\beta^2 = \frac{h^2}{12a^2} \qquad (I.4)$$

Ω represents the non-dimensional frequency, which is defined as:

$$\Omega = \frac{f}{f_{ring}} = \frac{2\pi f a}{c_{l,s}} \qquad (I.5)$$

where $c_{l,s}$ is the propagation velocity of quasi-longitudinal waves in the shell [ref 12] and f_{ring} is the ring frequency[131].

I.2   Dispersion curves and mode shapes

In fluid-filled pipes several types of free structural and fluid waves can propagate. This section describes these wave types, corresponding mode shapes of the pipe wall and analytical approximations for wave numbers derived from Flügge's shell theory by Pavic ([ref 19] and [ref 20]) and De Jong [ref 25]. This section shows wave numbers that have been calculated with the approximations for various practical pipes. These wave numbers have been used to calculate numbers of modes. The numbers of modes are presented in chapter 4.

The approximations are valid far below the ring frequency. This thesis also considers high frequencies. In order to investigate whether the approximations are sufficiently accurate regarding the applications in this thesis (see footnote 43), the calculation results have been compared with results from FEM calculations and measurements, see chapter 4.

[130] The non-dimensional wave number κ is defined as:

$\kappa = ka$

[131] The ring frequency or breathing frequency is the frequency at which the wavelength of quasi-longitudinal waves in the pipe wall is equal to the pipe's circumference. All wave types cluster at this frequency. [ref 12] The ring frequency f_{ring} is defined as [ref 12]:

$f_{ring} = c_{l,s}/(2\pi a)$

Acoustic waves (n=0)

These are free plane waves in the pipe fluid with a wave propagation direction parallel to the pipe wall, which cause a small (forced) radial displacement of the pipe wall too.
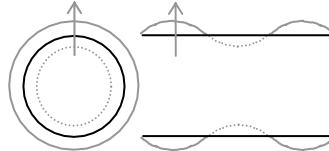
Figure I-2 Mode shape without (black lines) and with (grey lines) deformation and main vibrational direction (grey arrows), for the cross-section (**left side**) and the longitudinal section (**right side**) of a pipe due to acoustic waves (*n*=0)

Approximation for non-dimensional acoustic wave numbers κ_a derived by Pavic [ref 20][132]:

$$\kappa_a = k_a a \approx \zeta_a \Omega ; \quad \zeta_a = \left[\psi + (2\eta + v^2)/(1 - v^2) \right]^{1/2}$$
$$\psi = (c_{l,s} / c_f)^2 \qquad\qquad (I.6)$$
$$\eta = (\rho_f / \rho_s)(a/h)$$

where $c_{l,s}$ and ρ_s are the propagation velocity of quasi-longitudinal waves in and density of the pipe wall material, c_f and ρ_f are the propagation velocity of sound in and density of the pipe fluid. v is Poisson's ratio.

Higher-order acoustic waves

At high frequencies in the pipe fluid higher-order acoustic waves can propagate, i.e. waves in a propagation direction at an angle with the pipe wall, see for example [ref 6].
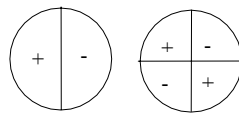
Figure I-3 Acoustic pressure distributions across the cross-section of a pipe fluid due to the first two higher-order acoustic waves

The wave numbers of these waves equal the sum of the 'axial' acoustic wave numbers k_a given by equation *(I.6)* and the acoustic wave numbers associated with the (*p,q*)*th* higher-

---

[132] The approximation is derived from Flügge's shell theory and is valid for low frequencies, $\Omega << 1$.

order acoustic waves κ_{pq}. The non-dimensional higher-order acoustic wave numbers $\kappa_{a,higher-order}$ are given by [ref 6]:

$$\kappa_{a,higher-order} = k_{a,higher-order} a$$

$$k^2_{a,higher-order} = \kappa^2_{pq} + k^2_a = \left(\frac{2\pi f}{c_f}\right)^2 \tag{I.7}$$

$$\kappa_{pq} = \frac{\pi \alpha_{pq}}{a_i}$$

in which the value of $\pi \alpha_{pq}$ for each higher-order acoustic wave is determined from the eigenvalue satisfying the rigid wall boundary condition $J'_p(\kappa_{pq}a_i)=0$, where J' is the first derivative of the Bessel function with respect to r [ref 6]. In [ref 6] the $\pi \alpha_{pq}$ values for the first twelve higher-order acoustic waves are given. These values have been applied in the calculations in this study.

As equation *(I.7)* shows, for higher-order acoustic waves the propagation velocity of sound in the fluid varies with frequency.

Each higher-order acoustic wave can propagate above it's cut-on frequency $(f_{co})_{pq}$ only, which is given by [ref 6]:

$$\left(f_{co}\right)_{pq} = \frac{\kappa_{pq}c_f}{2\pi} = \frac{\pi \alpha_{pq}c_f}{2\pi a_i} \tag{I.8}$$

Quasi-longitudinal waves (n=0)

These are free axial waves causing axial motions and a small cross-sectional contraction.
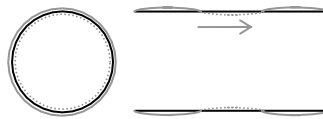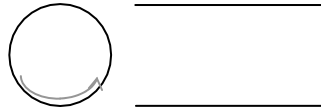

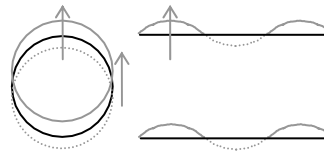**Figure I-4**   Mode shape without (black lines) and with (grey lines) deformation and main vibrational direction (grey arrow), for the cross-section (**left side**) and the longitudinal section (**right side**) of a pipe wall due to quasi-longitudinal waves (*n=0*)

Approximation for non-dimensional quasi-longitudinal wave numbers κ_l derived by Pavic [ref 20] (see footnote 132):

$$\kappa_l = k_l a \approx \zeta_l \Omega \; ; \quad \zeta_l = (1 + \Delta)^{1/2}$$
$$\Delta = v^2 (\psi - 1) / \left[(\psi - 1)(1 - v^2) + 2\eta + v^2 \right]$$
$$\psi = (c_{l,s} / c_f)^2$$
$$\eta = (\rho_f / \rho_s)(a / h)$$

(I.9)

Torsional waves (n=0)

These are free torsional waves causing purely tangential motions.

Figure I-5 Mode shape and main vibrational direction (grey arrow), for the cross-section (**left side**) and the longitudinal section (**right side**) of a pipe wall due to torsional waves (*n=0*)

Approximation for non-dimensional torsional wave numbers κ_t derived by Pavic [ref 20] (see footnote 132):

$$\kappa_t = k_t a \approx \zeta_t \Omega \; ; \quad \zeta_t = \left[2 / (1 - v) \right]^{1/2}$$

(I.10)

First-order flexural or beam-bending waves (n=1)

These are free flexural waves causing flexural motions of the pipe, corresponding with flexural waves in a slender beam. The pipe cross-section remains undeformed.

Figure I-6 Mode shape without (black lines) and with (grey lines) deformation and main vibrational directions (grey arrows), for the cross-section (**left side**) and the longitudinal section (**right side**) of a pipe wall due to flexural waves with *n=1*
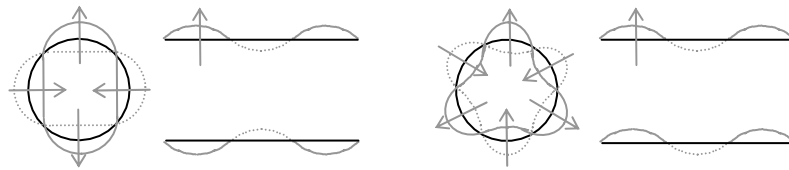
Approximation for non-dimensional flexural wave numbers κ_b derived by Pavic [ref 20] (see footnote 132):

$$\kappa_b = k_b a \approx \zeta_b \Omega \; ; \quad \zeta_b = (2+\eta)^{1/4}$$
$$\eta = (\rho_f / \rho_s)(a/h)$$

<div align="right">(I.11)</div>

Due to the effects of transverse shear and rotatory inertia waves with real and imaginary wave numbers occur at somewhat higher frequencies, see the wave number equation for higher-order flexural waves below and section I.2.1.

Higher-order flexural waves (n≥2)

These are free flexural waves around the pipe circumference causing 'lobar' mode shapes, so the pipe cross-sections deforms. The number *2n* corresponds with the number of nodes that occur on the pipe circumference. For each type of higher-order flexural waves real and imaginary wave numbers exist above the so-called 'cut-on' frequency, as for modes with *n=1*. Below the cut-on frequency a complex wave number exists.

Figure I-7 Mode shapes without (black lines) and with (grey lines) deformation and main vibrational direction (grey arrows), for the cross-section (**left side**) and the longitudinal section (**right side**) of a pipe wall due to flexural waves with *n=2* (**left side**) and *n=3* (**right side**)

First-order approximation for non-dimensional wave numbers κ_{nm} for waves with circumferential mode numbers *n>0*, derived by De Jong [ref 25] (see footnote 132):

$$\kappa_{nm}^2 = (k_{nm}a)^2 =$$

$$= \sqrt{\frac{n^2(1+n^2+2n\mu)\Omega^2 - n^4(1-n^2)^2\beta^2}{1-\nu^2}} \pm \frac{(\frac{3}{2}+n^2+2n\mu)\Omega^2 - n^2(1-n^2)^2\beta^2}{1-\nu^2} + \ldots$$

<div align="right">(I.12)</div>

$$\mu = \frac{\rho_f A_f}{\rho_s A_s}$$

234

where A_f and A_s represent the cross-sectional areas of the pipe fluid and pipe wall respectively.

Approximation for cut-on frequencies Ω_{cut-on}, derived by various authors, among which De Jong [ref 25] and Pavic [ref 20]:

$$\Omega^2_{cut-on} \approx \beta^2 \frac{n^2(n^2-1)^2}{1+n^2+2n\mu} \tag{I.13}$$

I.2.1 Real, imaginary and complex wave numbers

As shown above waves with real, imaginary and complex wave numbers can occur in pipes. Real wave numbers represent travelling waves and determine the energy flow along pipes with a length to diameter ratio greater than one. Imaginary wave numbers represent evanescent nearfields. Complex wave numbers represent travelling waves with decaying amplitudes [ref 25]. Imaginary and complex wave numbers may be important in case of energy flow along short pipes [ref 55]. Imaginary wave numbers also determine the vibrational behaviour of pipes near discontinuities [ref 25].[133]

In this study wave numbers have only been calculated to test the validity of the assumptions concerning modal properties of characteristic physical system elements such as relatively long straight pipe elements within pipe systems. This is the reason why real wave numbers have been applied, where necessary in chapter 4. Nevertheless, imaginary and complex wave numbers might be important in the energy transmission through discontinuities in pipe systems such as pipe bends, pipe clamps and short pipe coupling elements.

I.2.2 Propagation velocity of quasi-longitudinal waves in PVC pipe walls

One of the unknown parameters in the formulas in the previous section is the propagation velocity of quasi-longitudinal waves $c_{l,s}$ in plastic pipe walls. Data for plastics generally

---

[133] Both evanescent waves and travelling waves with decaying amplitudes decay along the pipe axis with a factor $exp(-k^i_{nm}z)$ [ref 25], where z represents the distance from a discontinuity.

For an air-filled plastic pipe with an outer pipe radius of 55 mm and a pipe wall thickness of 3,8 mm, i.e. a practical wastewater pipe, some calculations of the amplitude reduction have been done. The amplitude of first-order flexural waves at distances of 0,15 m and 0,5 m from a discontinuity is reduced to 60% (for 0,15 m) and 18% (for 0,5 m) at 125 Hz, 50% and 10% at 250 Hz and 38% and 4% at 500 Hz. The amplitude of second-order flexural waves is reduced to 21% (for 0,15 m) and 1% (for 0,5 m) at 500 Hz. Based on these results the influence of discontinuities on the vibro-acoustic behaviour of connected straight pipes in wastewater pipe systems is expected to be small, however at small distances not negligible.

concern flat plates and not shells, although it is not clear to which extent this causes differences.

$c_{l,s}$ has been derived from several time records of 1/8" accelerometers at two different axial positions on an open PVC pipe and the accelerometer spacing, see Figure I-8. For this purpose the pipe wall has been excited at one end by a hammer in the axial direction. The measurement equipment is described in appendix V.
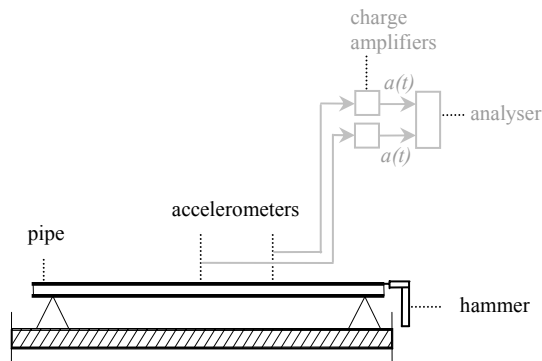

Figure I-8   Experimental set-up for the determination of the propagation velocity of quasi-longitudinal waves in a PVC pipe wall of 3,8 mm thickness and an outer shell radius of 55 mm

This has resulted in a mean value for $c_{l,s}$ of 1400 m/s.

For a pipe of the same material and with the same thickness and diameter cut-on frequencies have been calculated with the obtained value for $c_{l,s}$. After that cut-on frequencies have been determined from the point admittance of a pipe ring, i.e. a pipe piece that is short enough to avoid axial modes. The point admittance has been determined from force and acceleration measurements with an impedance head that was mounted between the pipe ring and a shaker, see Figure I-9 and Figure I-10. The measurement equipment is described in appendix V.
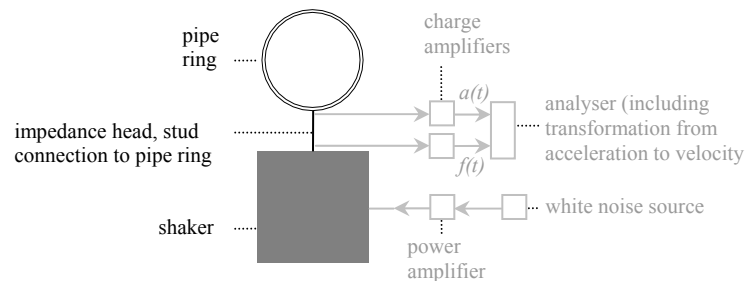
Figure I-9 Experimental set-up for the determination of cut-on frequencies for an air-filled PVC pipe with 3,8 mm wall thickness and an outer shell radius of 55 mm
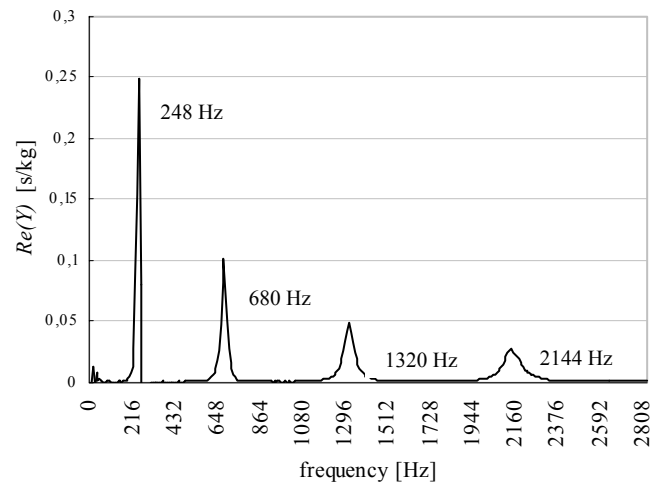

Figure I-10 Real part of the point admittance $Re(Y)$ for a PVC pipe ring, length 35 mm, with 3,8 mm wall thickness and an outer shell radius of 55 mm

By fitting the predicted values for the cut-on frequencies to the values that have been derived from the measurements with equation *(I.13)*, the mean value for $c_{l,s}$ has been altered to 1470 m/s. This value has been applied in this study.

For pure PVC (without plasticizer) Cremer and Heckl give values for the modulus of elasticity between about $2,5 \cdot 10^9$ N/m^2 and $3,5 \cdot 10^9$ N/m^2, for temperatures between 5^{0}C and 50^{0}C [ref 12]. From these values and the density of the PVC applied in this study (about 1393 kg/m^3) values for $c_{l,s}$ between about 1340 m/s and 1585 m/s have been estimated. The obtained value for $c_{l,s}$ falls within this range.

I.2.3   Real dispersion curves for practical water supply and wastewater pipes

For practical air- and water-filled water supply and wastewater pipes real non-dimensional dispersion curves have been calculated with the analytical approximations derived by Pavic [ref 20], De Jong [ref 25] and Norton [ref 6]. The calculation results are presented in Figure I-11 to Figure I-13.
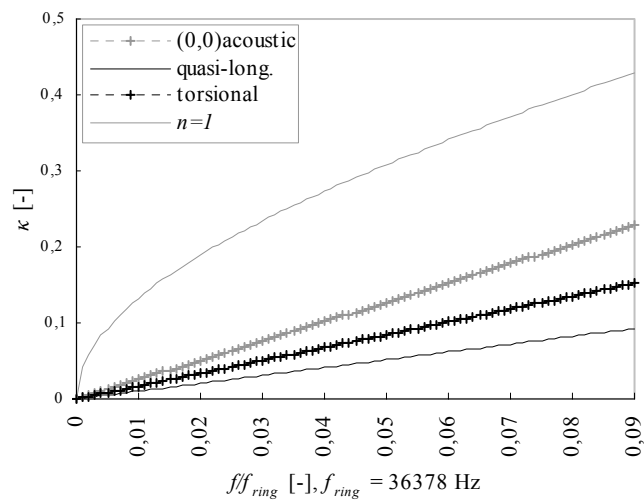
Figure I-11   Real non-dimensional dispersion curves for water-filled brass pipes with 2 mm wall thickness and an outer shell radius of 15 mm
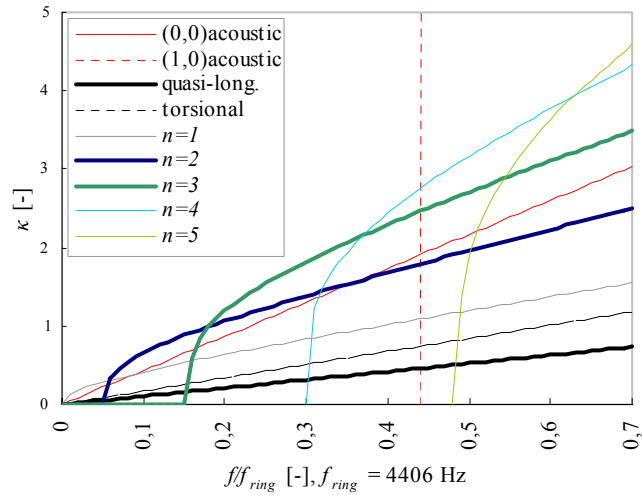
Figure I-12   Real non-dimensional dispersion curves for <u>air-filled PVC pipes</u> with 3,8 mm wall thickness and an outer shell radius of 55 mm
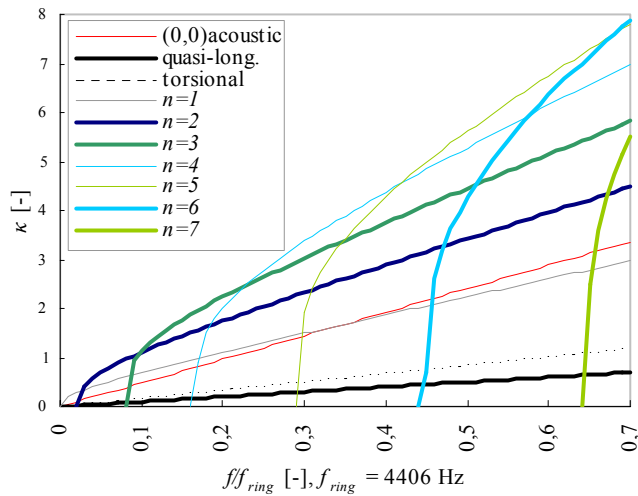
Figure I-13   Real non-dimensional dispersion curves for <u>water-filled PVC pipes</u> with 3,8 mm wall thickness and an outer shell radius of 55 mm

Figure I-11 to Figure I-13 illustrate that the pipe dimensions, pipe wall material and pipe fluid determine which types of free structural and fluid waves can propagate in a pipe within the frequency range of interest. The figures show the cut-on frequencies of higher-

order flexural, structural modes in the pipe wall and higher-order acoustic modes in the pipe fluid.

Generally only free structural waves with $n=0$ and $n=1$ can propagate in practical brass water supply pipes. In practical plastic wastewater pipes with relatively small diameters, i.e. about 40 mm, free structural waves with $n=0$ up to 4 can propagate (not shown in the figures). In practical plastic wastewater pipes with relatively large diameters, i.e. about 100 mm, free structural waves with $n=0$ up to 6 can propagate.

For water-filled pipes the wave number values are lower for quasi-longitudinal waves, compared to air-filled pipes. On the other hand, the values are higher for acoustic, first- and higher-order flexural waves. The cut-on frequencies for higher-order acoustic waves are higher in case of water-filled pipes. On the other hand, the cut-on frequencies are lower for higher-order flexural waves. Since there is no interaction between torsional and acoustic waves, for torsional waves the values are equal.

Apart from the above, the figures show wave number coincidence frequencies. At these frequencies the structural waves in the pipe wall and the acoustic waves in the pipe fluid have equal wave numbers. However, the acoustically determined frequency for wave number matching differs slightly from the structural natural frequency. There is exact spatial coupling, but no exact frequency coupling. Both are needed for complete coincidence [ref 6]. There is no exact frequency coupling, because only the acoustic waves in finite pipes, i.e. travelling waves, exhibit continuous variation of axial wave number. Structural waves in finite pipes have axial standing waves with discrete axial wave number values.

Norton [ref 6] states that turbulent flow in a pipe causes broadband internal (higher-order) acoustic waves and that the vibrational response of the pipe wall due to the internal acoustic waves, and hence the externally radiated sound power, are predominantly determined by coincidences between structural waves in the pipe wall and higher-order acoustic waves in the pipe fluid. So for the given examples coincidences can only occur for the air-filled PVC pipe above 1900 Hz.

I.3 Amplitude ratios for different types of free waves

The three-dimensional motion of the pipe wall per structural mode *(n,m)* can be described by the ratios of the amplitudes of pipe wall displacement that are given in the following equations [ref 20]:

$$\frac{U_{nm}}{W_{nm}} = \frac{(L_{12}L_{23} - L_{13}L_{22})}{(L_{11}L_{22} - L_{12}L_{21})} \qquad (I.14)$$

$$\frac{V_{nm}}{W_{nm}} = \frac{(L_{21}L_{13} - L_{11}L_{23})}{(L_{11}L_{22} - L_{12}L_{21})} \qquad (I.15)$$

In this study the elements of the *[L]*-matrix given in equation *(I.3)* have been applied.

I.3.1 Amplitude ratios for practical water supply and wastewater pipes

For practical air- and water-filled water supply and wastewater pipes amplitude ratios for pipe wall displacement have been calculated. The calculation results are presented in Figure I-14 to Figure I-22.
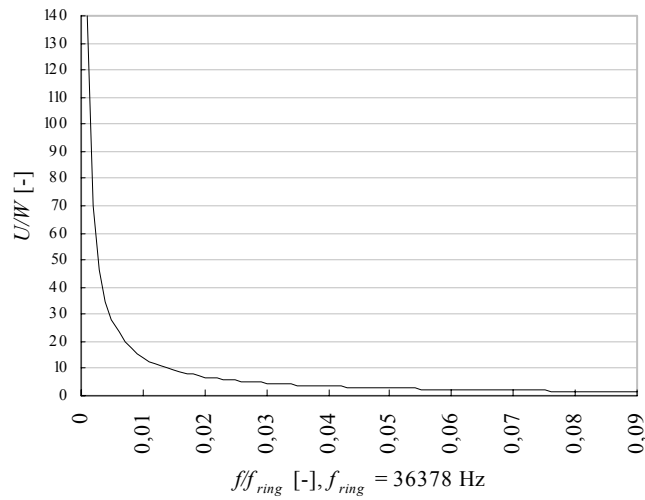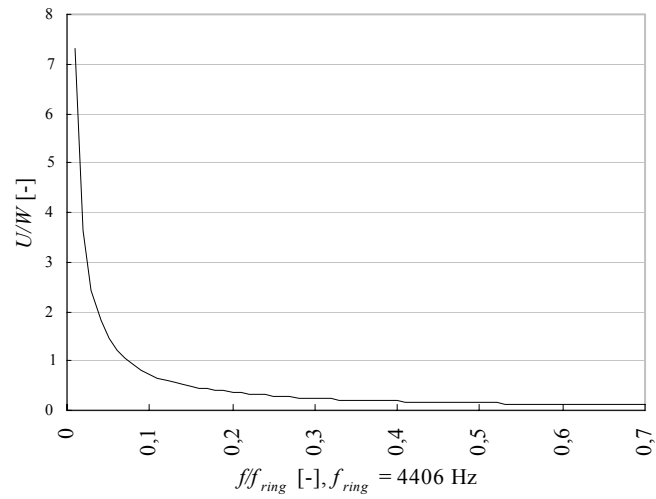

Figure I-14 Amplitude ratios for pipe wall displacement for <u>acoustic waves</u> in <u>water-filled brass pipes</u> with 2 mm wall thickness and an outer shell radius of 15 mm
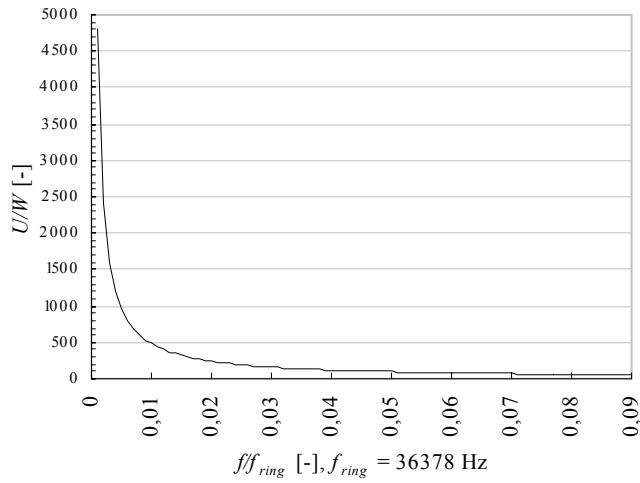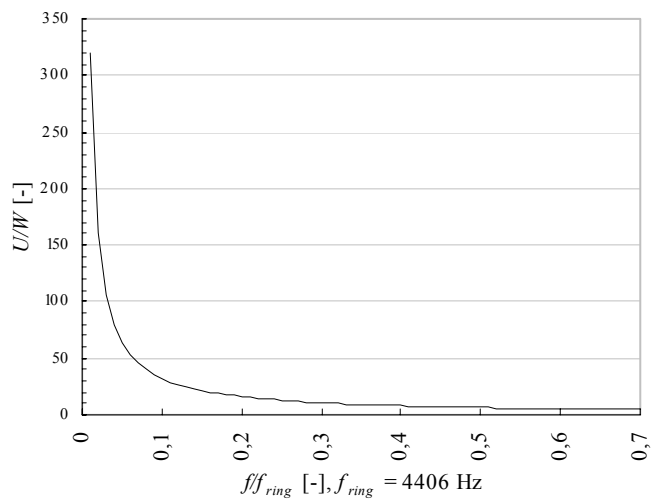
Figure I-15 Amplitude ratios for pipe wall displacement for <u>quasi-longitudinal waves</u> in <u>water-filled brass pipes</u> with 2 mm wall thickness and an outer shell radius of 15 mm
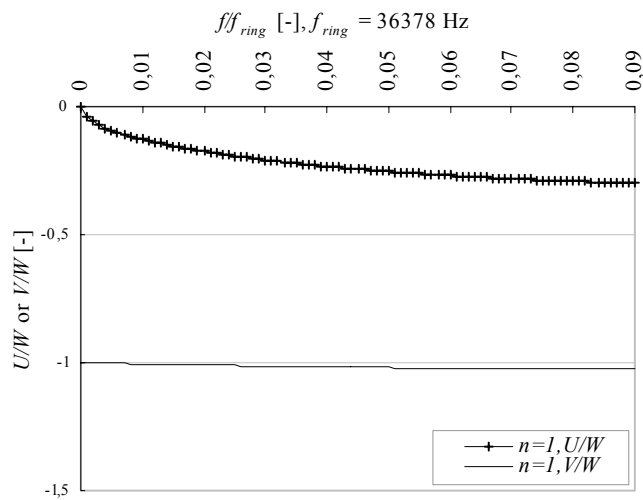
Figure I-16 Amplitude ratios for pipe wall displacement for waves with <u>n=1</u> in <u>water-filled brass pipes</u> with 2 mm wall thickness and an outer shell radius of 15 mm

242

Figure I-17 Amplitude ratios for pipe wall displacement for <u>acoustic waves</u> in <u>air-filled PVC pipes</u> with 3,8 mm wall thickness and an outer shell radius of 55 mm

Figure I-18 Amplitude ratios for pipe wall displacement for <u>quasi-longitudinal waves</u> in <u>air-filled PVC pipes</u> with 3,8 mm wall thickness and an outer shell radius of 55 mm

Figure I-19 Amplitude ratios for pipe wall displacement for waves with $n{\geq}1$ in <u>air-filled PVC pipes</u> with 3,8 mm wall thickness and an outer shell radius of 55 mm
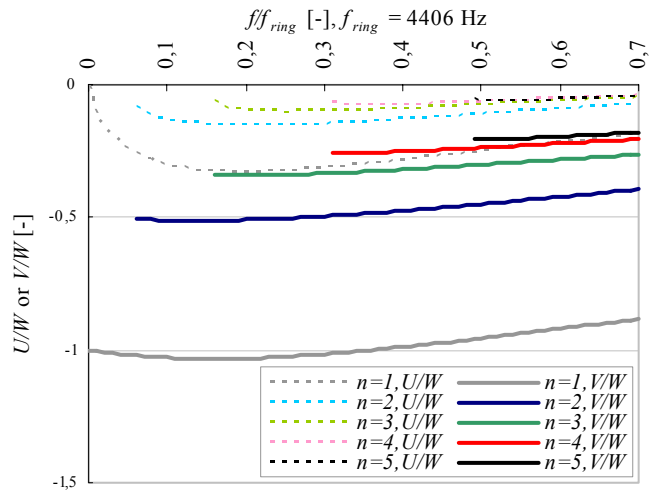

Figure I-20 Amplitude ratios for pipe wall displacement for <u>acoustic waves</u> in <u>water-filled PVC pipes</u> with 3,8 mm wall thickness and an outer shell radius of 55 mm
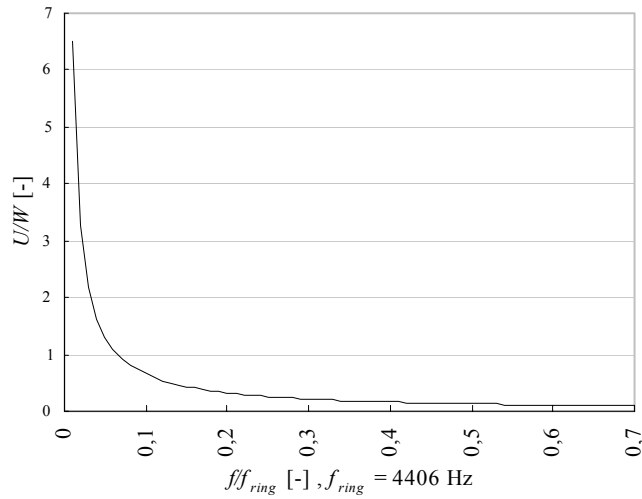
Figure I-21 Amplitude ratios for pipe wall displacement for <u>quasi-longitudinal waves</u> in <u>water-filled PVC pipes</u> with 3,8 mm wall thickness and an outer shell radius of 55 mm
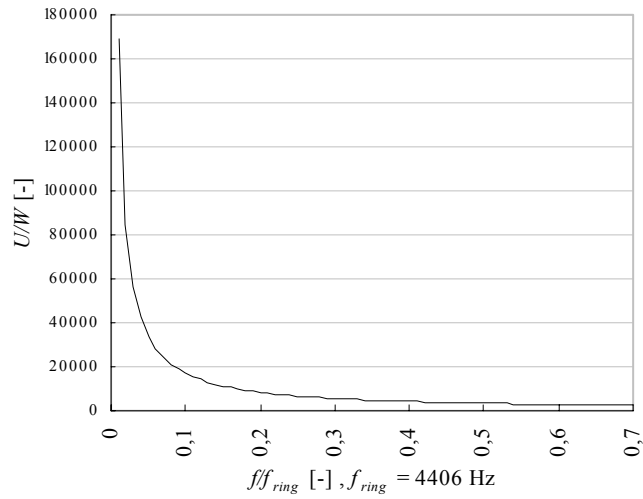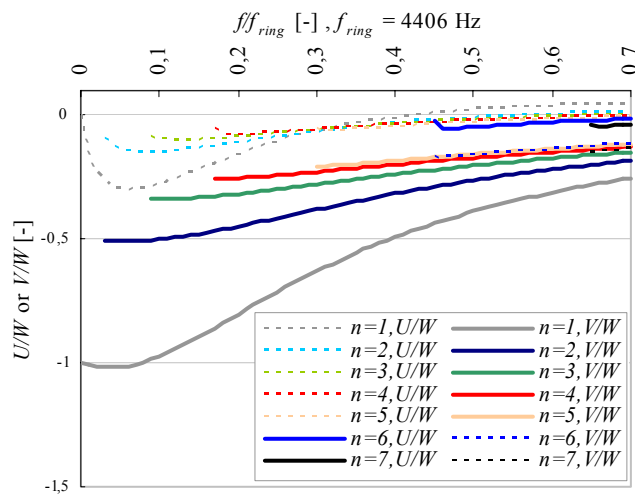

Figure I-22 Amplitude ratios for pipe wall displacement for waves with <u>$n \geq 1$</u> in <u>water-filled PVC pipes</u> with 3,8 mm wall thickness and an outer shell radius of 55 mm

Figure I-17 and Figure I-20 show that the main vibrational direction of acoustic waves is axial at low frequencies for the wastewater pipes considered. Radial vibrations start to

dominate above the frequency where the non-dimensional fluid wave number κ_a exceeds Poisson's ratio ν. Figure I-14 shows that for the water supply pipe considered (brass pipe with a relatively small diameter) the vibrations are mainly axial in the entire frequency range of interest.

Figure I-15 and Figure I-21 illustrate that the main vibrational direction of quasi-longitudinal waves is axial for practical water-filled brass water supply and plastic wastewater pipes. Figure I-18 shows that the quasi-longitudinal waves cause primarily axial vibrations up to approximately 1300 Hz for the considered air-filled plastic wastewater pipe with an outer shell radius of 55 mm.[134] Above this frequency radial vibrations become important.

For the first-order flexural waves the amplitudes of the radial and tangential vibrational components are approximately equal and larger than the amplitudes of the axial vibrational component. For the higher-order flexural waves the vibrations are more radial than tangential. This is more clearly visible at increasing circumferential mode number n. The amplitudes of the radial and tangential vibrational components are larger than the amplitudes of the axial vibrational component.

Leissa [ref 14] has described the three-dimensional motions of the pipe wall in more detail. Per structural mode *(n,m)* a shell can vibrate in three different frequencies. These frequencies correspond to the three eigenvalues, i.e. solutions, of the dispersion equation. Usually the lowest, i.e. fundamental, frequency is associated with a motion that is primarily radial, the second frequency with a motion that is primarily axial and the third frequency with a motion that is primarily tangential. This is described in more detail in [ref 14], based on calculation results of Bozich [ref 56]. For different *R/h*-ratios, Bozich has plotted the three vibrational frequencies versus *l/mR*, where *l* is the pipe length, *m* the axial mode number and *R* the pipe radius. Furthermore, Bozich has determined whether the vibrations are primarily radial, axial or tangential. The figures plotted in [ref 14] are included in Figure I-23 and Figure I-24.

---

[134] The ratio of axial displacement to radial displacement is at least 10.
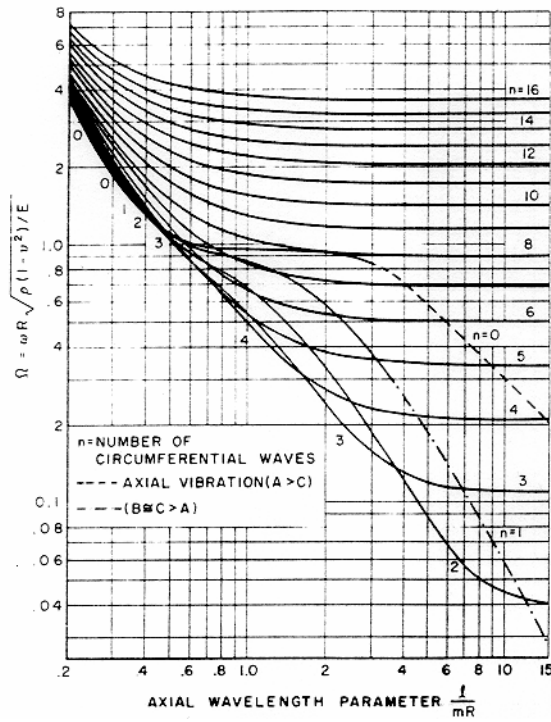
Figure I-23 Variation of the <u>non-dimensional fundamental frequency</u> Ω with l/mR according to the Flügge theory, ν=0,3, R/h=20 (as plotted in [ref 14] after [ref 56]); axial, tangential and radial vibrations denoted by A, B and C respectively; primarily radial vibrations printed as solid lines
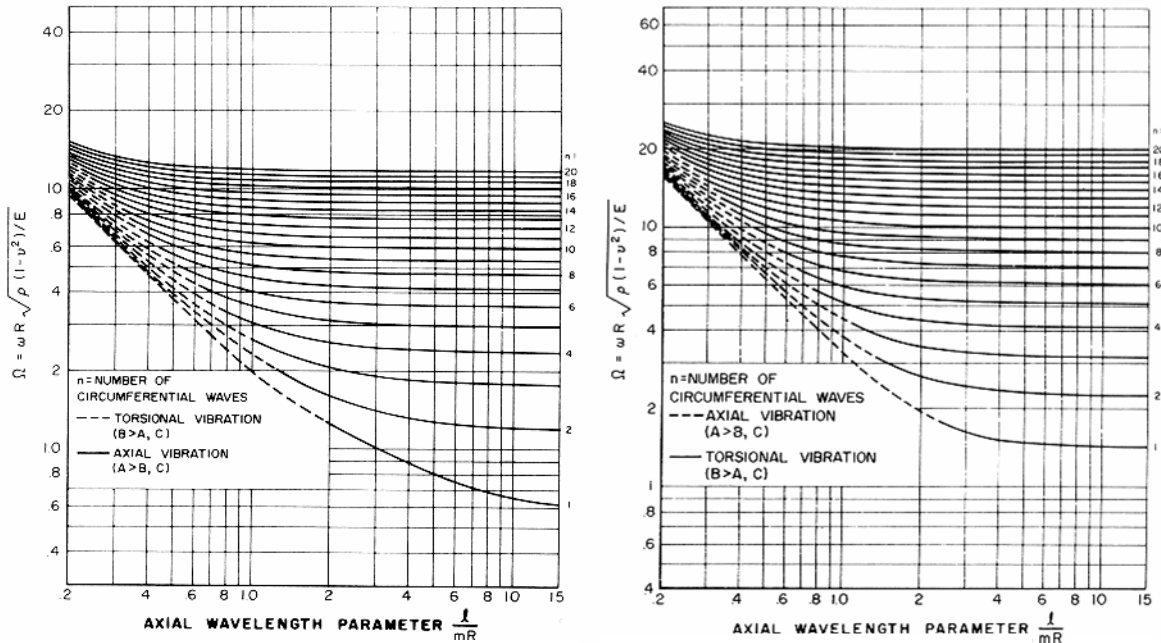
Figure I-24 Variation of the <u>non-dimensional second</u> (**left**) <u>and third</u> (**right**) <u>vibrational frequencies</u> Ω with l/mR, according to the Flügge theory, ν=0,3, R/h=20 to 5000 (as plotted in [ref 14] after [ref 56]); axial, tangential and radial vibrations denoted by A, B and C respectively

In this thesis only the vibro-acoustic behaviour of frequencies up to 2818 Hz (upper frequency of the 1/3-octave band with centre frequency 2500 Hz) is studied. For the plastic pipes studied this frequency equals $0,6\Omega$, for the brass pipes $0,08\Omega$. So, for practical water supply and wastewater pipes in buildings, the second (from $0,6\Omega$) and third (from about $1,5\Omega$) frequencies (see Figure I-24) fall out of the frequency range of interest.

For relatively long pipes ($l/mR{\geq}\pi$) the calculation results in Figure I-23 correspond to the results given in Figure I-14 to Figure I-22. For relatively short pipes ($l/mR{\leq}\pi$) the vibrations are primarily radial for all circumferential mode numbers n.

Figure I-24 illustrates that the vibrations of the second frequencies are primarily axial for relatively long pipes and primarily tangential for relatively short pipes. The l/mR-criterion varies with the circumferential mode number n (l/mR=2 for n=1 and l/mR=0,7 for n=4).

Figure I-24 illustrates that the vibrations of the third frequencies are primarily tangential for relatively long pipes and primarily axial for relatively short pipes. The l/mR-criterion corresponds to the criterion described for the second frequencies.

248

APPENDIX II

FEM MODELLING OF PIPES

The vibro-acoustic behaviour of pipes has been studied with the Finite Element Method (FEM). For this purpose some straight air- and water-filled plastic and steel pipes have been modelled in the FEM computer program Ansys version 5.4 [ref 37]. The FEM studies were focused on the determination of the natural frequencies of pipes within the frequency range of interest.

This appendix gives a short explanation of the modelling and the determination of the natural frequencies. For a more detailed description of the FEM studies the reader is referred to [ref 36].

II.1   Model elements

In order to be able to study the vibro-acoustic behaviour of pipes in an appropriate way, the model elements need to meet the following requirements:

- three-dimensional elements are needed. The reason for this is that there are modes around the pipe circumference and axial modes. The natural frequencies corresponding to different combinations of circumferential mode numbers n and axial mode numbers m are calculated;
- the element nodes can rotate. The reason for this is that rotations in the pipe are caused by wave propagation. Elements with mid-side nodes have to be excluded, because they cannot rotate;
- the elements have an elastic behaviour. This is important because both the pipe wall and the pipe fluid exhibit a linear, elastic behaviour, see appendix I;
- the modal analysis and fluid-structure interaction functions of Ansys 5.4 can be applied to the elements.

In Ansys 5.4 there are three different elements for the pipe wall that meet the requirements. These elements are called SOLID72 (element shape: tetrahedron), SOLID73 (element shape: hexahedron) and SHELL63 (element shape: hexahedron).

The SHELL63-elements exhibit a plate-like vibrational behaviour, which requires less computational time. They have to be defined on a surface, in this case the pipe fluid. Ansys 5.4 considers the surface to be the middle surface of the pipe wall. So the pipe in the

model has a lower weight than the real pipe, which could cause a (frequency-dependent) shift in the natural frequencies. This is a disadvantage of SHELL63-elements.

In Ansys 5.4 there is only one element for the pipe fluid that meets the requirements. This element is called FLUID30 (element shape: hexahedron).
There are other fluid elements in Ansys 5.4. However, these elements cannot handle fluid-structure interactions. Since it is not recommended to mix different fluid elements, FLUID30 has been applied for the entire pipe fluid.
In the models the fluid is divided into two parts: a layer of fluid elements that are in contact with the pipe wall (model option "structure present") and fluid elements inside the contact layer (model option "structure absent").

II.2 Model size

The ambient air has not been modelled, because it is assumed that the influence of the ambient air on the pipe vibrations can be neglected.

Since the mode shapes of the first- and higher-order flexural modes are not axi-symmetric, modelling only a part of the pipe cross-section (to reduce storage and computational time) is not possible.

The FEM models have been limited to a pipe length of 1 m because of the required storage and computational time.

II.3 Meshing

The Ansys 5.4 manual [ref 37] gives several guidelines for model meshing. This section describes only the guidelines that are important in this study.

Ansys 5.4 provides two meshing techniques: mapping, which results in hexahedrons, and free meshing, which results in tetrahedrons or pyramids. The mapping technique has been applied, because it gives more accurate calculation results and because this is the meshing technique that is strongly recommended by Ansys 5.4 for elements without mid-side nodes. Therefore modelling with SOLID72-elements (element shape: tetrahedron) has not been investigated further.

In order to avoid sudden jumps in pressure, stresses etc. no large variations in element size are allowed.

The elements need to have regular proportions. Therefore, the length-to-width ratio, i.e. aspect ratio, is preferred to be smaller than 3 and certainly than 5.

Each element in a curved surface should not span an angle larger than 15 degrees.

The thickness of the contact layer, i.e. layer of fluid elements between the pipe wall and other fluid elements in the pipe, should be large enough to avoid being overlapped by radial displacements of the pipe wall.

The maximum element length l_{max} should be smaller than a quarter, preferably one-sixth, of the shortest wavelength λ_{min} that could occur within the frequency range of interest:

$$l_{max} \le \frac{\lambda_{min}}{4} \le \frac{c_{min}(f_{max})}{4 f_{max}} \qquad (II.1)$$

where $c_{min}(f_{max})$ is the propagation velocity of the wave type with the shortest wavelength at the upper frequency of the frequency range of interest f_{max}.

Based upon the guidelines several straight, air- and water-filled, plastic and steel pipes consisting of SOLID73- or SHELL63-elements for the pipe wall and FLUID30-elements for the pipe fluid have been meshed.
24 pipe wall elements have been applied over the pipe circumference. This implies that the modelling is appropriate for modes with circumferential mode number $n=4$, possibly up to $n=6$ (n is the number of flexural wavelengths that fit on the circumference of the pipe). 50 pipe wall elements have been applied over the pipe length. This implies that the modelling is appropriate for modes with axial mode number $m=25$, which corresponds to 12,5 wavelengths on the length of the pipe.
Figure II-1 shows the mesh for a 1 m long air-filled PE pipe with SOLID73- and FLUID30-elements.
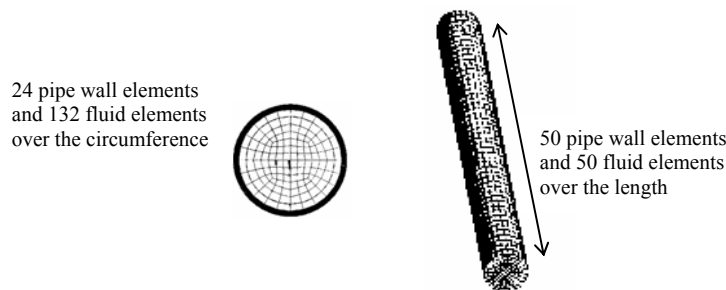
Figure II-1 Mesh over cross-section (**left side**) and longitudinal section (**right side**) for an Ansys 5.4 model of an air-filled PE pipe; pipe wall consisting of SOLID73-elements, pipe fluid consisting of FLUID30-elements; pipe length 1,0 m, pipe wall thickness 5 mm, pipe mean shell radius 50 mm

II.4   Boundary conditions

The modelled pipe was assumed to be part of a pipe with infinite length. In order to provide that each calculated mode had an integer value for the axial mode number m, a node, i.e. 'zero' displacement, or an anti-node, i.e. maximum displacement, needed to occur at both pipe ends. For this purpose the following boundary conditions appeared to be appropriate: translation of the pipe ends along the pipe axis blocked and rotation of the pipe ends around the axes orthogonal to the pipe axis blocked.

In the FEM studies the influence of several boundary conditions has been investigated:

- radial support: at the pipe ends only radial translation is constrained;
- complete clamping: at the pipe ends all degrees-of-freedom are blocked;
- reduced clamping: complete clamping at the pipe ends, except on mounting studs[135] with 7 mm diameter;
- shear diaphragm (SD): only free longitudinal translation at the pipe ends;
- stud clamping: complete clamping on mounting studs with 7 mm diameter.

II.5   Determination of natural frequencies

The natural frequencies are solutions for the eigenvalue equation, which results from the equations of motion after filling-in the general description for free, harmonic vibrations.

---

[135] At each pipe end a mounting stud with 7 mm diameter was introduced (non axi-symmetric boundary condition).

Ansys 5.4 has four different mode extraction methods using different algorithms (see [ref 37] for a full description).

Since this thesis concerns a fluid-structure interaction problem with unsymmetrical matrices, the unsymmetrical algorithm, which is based on the Lanczos algorithm, has been applied.

II.6   Results

For a PVC pipe the calculated natural frequencies for the various boundary conditions are shown for acoustic modes [136] and $n \geq 1$ in Figure II-2 to Figure II-4, together with natural frequencies determined from the analytical approximations in appendix I (see footnote 50 about the applied values for the propagation velocity of quasi-longitudinal waves in and density of PVC).
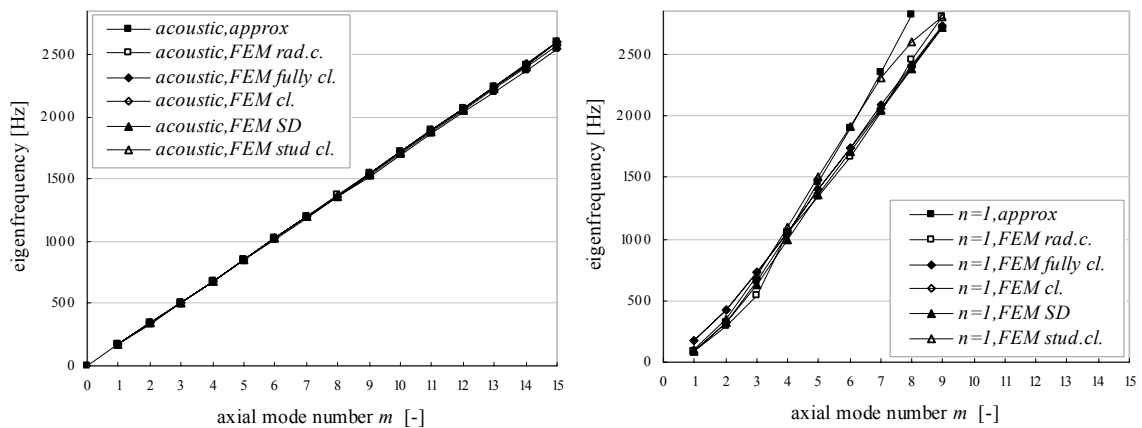
Figure II-2   Natural frequencies for acoustic modes (**left side**) and modes with circumferential mode number _n=1_ (**right side**) in an air-filled PVC pipe with 3,8 mm wall thickness, mean shell radius 53 mm and pipe length 1,0 m; calculations from FEM for various boundary conditions (see section II.4 for a description) and from approximations

---

[136] For quasi-longitudinal and torsional modes the natural frequencies for the various boundary conditions and from the approximations are almost equal (see section 4.2.2.4). This is why they are not presented here.
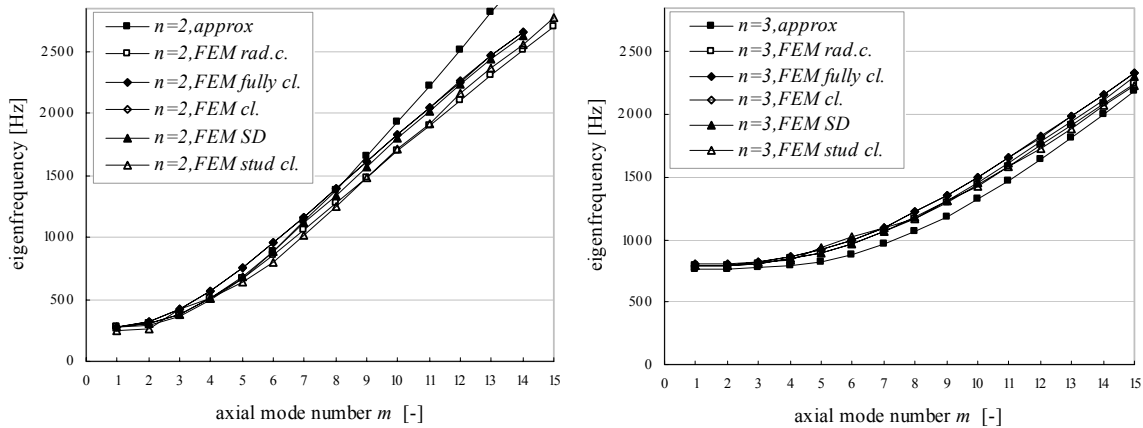
Figure II-3 Natural frequencies for modes with circumferential mode number <u>*n*=2</u> (**left side**) and <u>*n*=3</u> (**right side**) in an air-filled PVC pipe with 3,8 mm wall thickness, mean shell radius 53 mm and pipe length 1,0 m; calculations from <u>FEM for various boundary conditions</u> (see section II.4 for a description) and from <u>approximations</u>
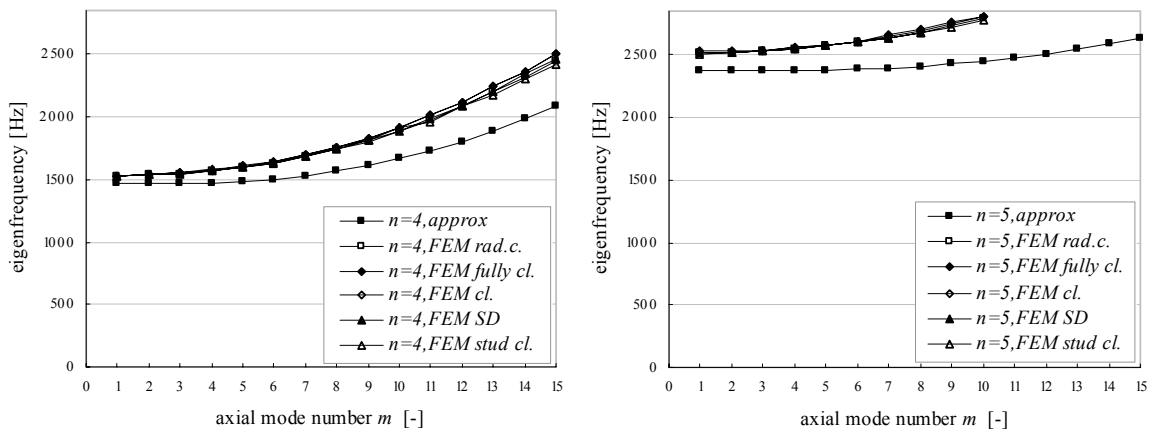
Figure II-4 Natural frequencies for modes with circumferential mode number <u>*n*=4</u> (**left side**) and <u>*n*=5</u> (**right side**) in an air-filled PVC pipe with 3,8 mm wall thickness, mean shell radius 53 mm and pipe length 1,0 m; calculations from <u>FEM for various boundary conditions</u> (see section II.4 for a descriptions) and from <u>approximations</u>

254

The (relative) difference[137] in natural frequency is small for the various boundary conditions, i.e. generally smaller than 10% with some exceptions for $n=1$ and $n=2$. The differences are larger between the FEM results and the results obtained from the approximations (differences up to 30% for $n=1$, up to 14% for $n=5$). Because the relative differences do not become larger with increasing circumferential mode number n, it is not clear whether a larger number of elements over the pipe circumference in the FEM models would have given better results. Generally speaking, the results from the approximations correspond best with the FEM results for boundary condition "stud clamping" (mean difference 10%, differences generally smaller than 15%, some exceptions up to 20%). The results are described in more detail in [ref 36].

---

[137] Relative differences have been calculated, as the ratio of two values multiplied by 100% and then minus 100%.

APPENDIX III
VIBRO-ACOUSTIC BEHAVIOUR OF PLATES

The purpose of this appendix is to give a brief outline of the modelling of the vibro-acoustic behaviour of single, homogeneous plates, as far as necessary for the understanding of the main text of this thesis. The vibro-acoustic behaviour of single, homogeneous plates is described in detail in many textbooks and other publications. Widely known are the textbooks of Cremer and Heckl [ref 12] and Fahy [ref 13].

Theories concerning the vibro-acoustic behaviour of single, homogeneous plates are often developed under the following assumptions [ref 12]:
- within the frequency range of interest the structures are supposed to be 'thin'. This is the case if the plate thickness h is small compared to the flexural wavelength, i.e. $h < \lambda_{b,s}/6$ [ref 12]. Thus, the frequency f_{upper} up to which 'thin' plate theories can be applied is

$$f_{upper} = \frac{c_{b,s}}{6h} \approx \frac{c_{l,s}}{20h} \qquad (III.1)$$

where $c_{b,s}$ and $c_{l,s}$ are the propagation (phase) velocities of flexural waves and quasi-longitudinal waves respectively.

For practical, single, concrete or brick plates this means that 'thin' plate theories are applicable up to a frequency of at least 500 Hz[138]. For the plates considered in this thesis 'thin' plate theories are not valid in an important part of the frequency range of interest.
Above the upper frequency limit, the effects of shear deformation and rotatory inertia have to be included. This results in smaller phase velocities and smaller group velocities of the flexural waves (see hereafter in this appendix). Above the upper frequency limit the difference between the corrected and non-corrected phase and group velocities becomes more than 10%.
- although most practical plates are not fully homogeneous and isotropic, they are supposed to behave as homogeneous, isotropic and elastic structures within the frequency

---

[138] For calcium-silicate structures with a thickness of 100 mm and 200 mm the frequency limits are approximately 1300 Hz and 650 Hz respectively. For a concrete structure with a thickness of 300 mm the frequency limit is approximately 580 Hz.

range of interest. For example, think of brick walls, consisting of two materials: the brick stones and the cement joints.

III.1   Dispersion curves

In practical plates in buildings three types of free waves can exist. This section gives the wave number-frequency relationships for these types of free waves, derived by Cremer and Heckl [ref 12] for 'thin', single, homogeneous, isotropic plates. For flexural waves in 'thick' plates, an approximation for the corrected flexural phase velocity from Rindel [ref 85] is given.

In-plane quasi-longitudinal waves

These are free quasi-longitudinal waves with vibrations mainly in the direction of wave propagation, parallel to the structure surface. There is a small cross-sectional contraction, which causes vibrations perpendicular to the structure surface. This contraction is represented by Poisson's ratio v.
Equation for quasi-longitudinal wave numbers k_l [ref 12]:

$$k_l = \frac{2\pi f}{c_{l,s}} = \frac{2\pi f}{\sqrt{\dfrac{E_s}{\rho_s(1-v^2)}}} \qquad (III.2)$$

where E_s and ρ_s are the Young's modulus of elasticity and the density of the plate material respectively.

In-plane shear waves

These are free shear waves with vibrations perpendicular to the direction of wave propagation, parallel to the structure surface.
Equation for shear wave numbers k_t [ref 12]:

$$k_t = \frac{2\pi f}{c_{t,s}} = \frac{2\pi f}{\sqrt{\dfrac{G_s}{\rho_s}}} = \frac{2\pi f}{\sqrt{\dfrac{E_s}{2\rho_s(1+v)}}} \qquad (III.3)$$

where G_s and $c_{t,s}$ are the shear modulus of elasticity and the propagation velocity of shear waves respectively.

Flexural waves in 'thin' plates

These are free flexural waves causing flexural, i.e. bending, vibrations, which are mainly perpendicular to the structure surface.

Equation for flexural wave numbers k_b in 'thin' plates [ref 12]:

$$k_b = \frac{2\pi f}{c_{b,s}} = \frac{2\pi f}{\sqrt[4]{\frac{B}{m''}}\sqrt{2\pi f}} = \frac{\sqrt{2\pi f}}{\sqrt{\beta c_{l,s}}}$$

$$B = \frac{I E_s}{(1 - v^2)} = \frac{h^3 E_s}{12(1 - v^2)} \qquad (III.4)$$

$$m'' = \rho_s h$$

$$\beta = \frac{h}{\sqrt{12}}$$

where $c_{b,s}$ is the propagation velocity of flexural waves in 'thin' plates. B is the bending stiffness, I is the moment of inertia per unit width and m'' is the mass per unit surface area for flat plates.

Flexural waves in 'thick' plates

Rindel gives the following approximation for the corrected flexural phase velocity in 'thick' plates [ref 85]:

$$\frac{1}{c_{b,s}'^3} \approx \frac{1}{c_{b,s}^3} + \frac{1}{\gamma^3 c_{t,s}^3}$$

$$\gamma = \frac{c_{b,s}'}{c_{t,s}} \qquad (III.5)$$

Rindel gives the value of γ as 1 [ref 85]. But Craik [ref 4] states that using the values of γ derived by Mindlin for different values of Poisson's ratio [ref 86] ensures the correct values for the flexural phase velocity at high frequencies. In this thesis γ=0,689 for Poisson's ratio 0,2 is applied.

The corrected flexural phase velocity should be applied in equation *(III.4)* to calculate flexural wave numbers k'_b in 'thick' plates.

APPENDIX IV
ACOUSTIC COUPLING BETWEEN SYSTEM ELEMENTS

In this appendix, acoustic transmission paths between pipe system elements and plates and between different pipe system elements are discussed. The example of a practical situation that has been used in chapter 3 for the illustration of the application of SEA, is also used in this appendix.

This appendix does not primarily deal with sound radiation from pipe system elements and plates to rooms. Nevertheless, these types of acoustic couplings are part of the acoustic transmission paths discussed.

IV.1   Acoustic coupling between a pipe and a plate

Figure IV-1 illustrates the structural and acoustic couplings between a pipe and a plate, respectively via a clamp (blue lines) and via a room (green lines), for the example in Figure 3-1 in this thesis. There are also acoustic couplings between the pipe fluid and respectively the pipe wall and the room.
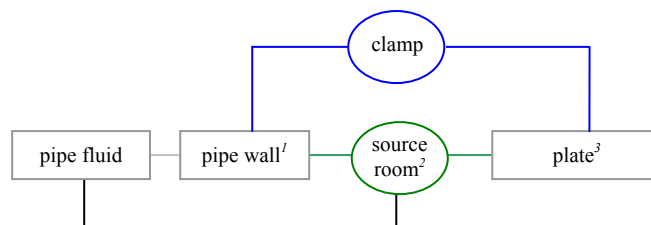
Figure IV-1 Structural and acoustic couplings for the connection pipe – plate in Figure 3-1

The plate is set into vibration due to a combination of structural and acoustic couplings or due to one of the two.

The relative importance of structural and acoustic couplings depends on the dimensions and materials of pipe, plate, clamps and room or shaft, on the distance between pipe and plate, i.e. clamp length, and on frequency[139].

It is difficult to predict the coupling loss factors and therefore energy flows between pipes and plates due to structural and acoustic couplings properly. For structural couplings this is explained in section 3.2.3.2. For acoustic couplings this is explained in the following sections.

IV.1.1 'Sub-model'

To illustrate the difficulty of predicting coupling loss factors for acoustic couplings between pipes and plates, the system part in Figure IV-1 will be analysed.

The energy flow between a pipe and a plate due to acoustic coupling can be calculated by means of a representation of this system part as a 'sub-model' existing of three subsystems: the pipe (subsystem *1*), the plate (subsystem *3*) and the acoustic volume (subsystem *2*) between pipe and plate, e.g. a room or shaft.

Coupling loss factors representing the acoustic couplings between the pipe and the acoustic volume respectively the acoustic volume and the plate and damping loss factors (without the radiation part) for the three subsystems are needed to solve the power balance equations corresponding to this 'sub-model':

$$\Pi_{i,in} = 2\pi f \eta_{ii} E_i + \sum_{\substack{j=1 \\ j \neq i}}^{3} 2\pi f \left(\eta_{ij} E_i - \eta_{ji} E_j \right)$$

$$i = 2,3 \qquad \Rightarrow \Pi_{i,in} = 0 \qquad\qquad (IV.1)$$

$$i = 1 \cap j = 3 \qquad \Rightarrow \eta_{ij} = \eta_{ji} = 0$$

Suppose that for a certain situation the input power to the pipe and the pipe energy are known from measurements[140].

For some pipe materials and most plates theoretical damping loss factor values are available. Damping loss factors can also be derived from decay rate measurements, see section 5.2.1. However, in that case radiation is included, which is only acceptable if the

---

[139] For example, for a pipe with a relatively small diameter, which is coupled rigidly to a plate in a large shaft, the vibrational energy from pipe to plate may be mainly transmitted through structural couplings. For a pipe with a relatively large diameter, which is coupled closely to a plate with sound reducing clamps in a small shaft, the acoustic transmission path may be the most important one.

[140] This section concerns the estimation of the contribution of sound radiation from the pipe to the plate to the energy level of the plate, so any input power and corresponding energy can be applied in the calculations.

losses due to radiation are negligibly small compared to the losses due to material damping. Otherwise, errors are introduced. The damping loss factor of the acoustic volume can be derived from the reverberation time of the acoustic volume. The reverberation time can either be calculated from the volume, surface areas and sound absorption coefficients of the surfaces (see footnote 34), or derived from measurements relatively easy.

The coupling loss factors η_{13} and η_{31} equal zero, because there is no or a negligible small direct acoustic coupling between the pipe and the plate in this case[141]. When 'reciprocity relationship' *(2.7)* is applied, only the coupling loss factors η_{12} and η_{23} are needed, which represent the acoustic coupling from the pipe to the acoustic volume and from the acoustic volume to the plate respectively. In case of application of the 'reciprocity relationship' also the modal densities of the three subsystems are needed. These can either be calculated or derived from measurements relatively easy, see chapter 4. Formulas for the coupling loss factors η_{12} and η_{23} are given below.

When the parameters mentioned above are known, equation *(IV.1)* results in three equations with two unknowns: E_2 and E_3, i.e. the energy levels of respectively the acoustic volume and the plate.

The coupling loss factors for the acoustic couplings from a pipe to an acoustic volume and from an acoustic volume to a plate are given in sections IV.1.2 and IV.1.3 respectively.

IV.1.2   Acoustic coupling from a pipe to an acoustic volume

The coupling loss factor $\eta_{i,rad}$ or η_{io}, representing the sound radiation from a structure i to an acoustic volume o can be written as (see [ref 12] for example)

$$\eta_{i,rad} = \eta_{io} = \frac{\rho_o c_o \sigma_i}{2\pi f m_i^{''}} \qquad (IV.2)$$

where ρ_o and c_o are the density of and the propagation velocity of sound in the acoustic volume respectively. σ_i and $m_i^{''}$ represent the radiation efficiency and the surface mass of the structure respectively.

Equation *(IV.2)* gives the coupling loss factor for sound radiation from one side of the structure only. In practical situations structures are coupled to two acoustic volumes: one at

---

[141] These coupling loss factors could represent the structural coupling between a pipe and a plate, e.g. due to a pipe clamp. This section only concerns acoustic coupling.

each side. In case of similar acoustic volumes at both sides of a structure, the loss factor corresponding to the total sound radiation from the structure is twice the loss factor calculated with equation *(IV.2)*.

Sound can be radiated from pipes due to three types of pipe wall motions, see [ref 6], so basically there are three types of radiation efficiencies for pipes resulting in three different coupling loss factors. In case of internal flow disturbances, pipe flow noise is caused mainly by radiation due to resonant modes in the pipe wall, see [ref 6]. Therefore, this section focuses on this type of sound radiation.

In the literature different approximations for radiation efficiencies are given, see for example [ref 12], [ref 52], [ref 6]. From the approximate expressions for radiation efficiencies given by Cremer and Heckl [ref 12], coupling loss factors for sound radiation due to resonant modes in the pipe wall of a wastewater pipe have been computed with equation *(IV.2)* and are shown in Figure IV-2.
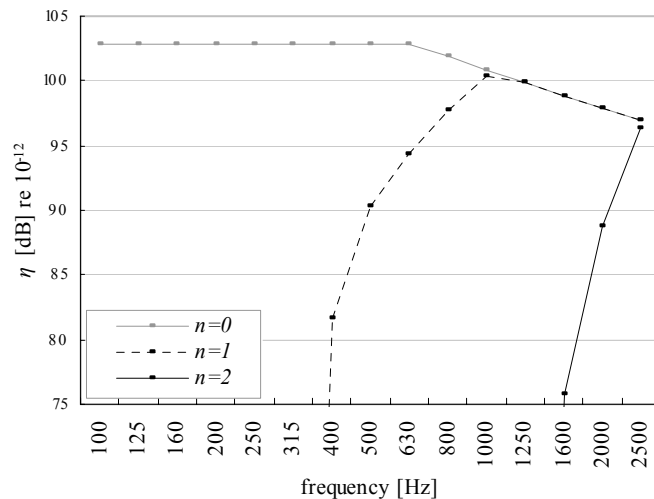
Figure IV-2 Coupling loss factors η for sound radiation from resonant modes in the pipe wall of a PVC wastewater pipe to an air-filled acoustic volume (calculated values for centre frequencies of 1/3-octave bands are presented); results are for $n=0$ modes, $n=1$ modes (first-order flexural modes) and $n=2$ modes (second-order flexural modes) in the pipe wall; external pipe diameter 110 mm, pipe wall thickness 3,8 mm

Figure IV-2 shows different coupling loss factors for different types of modes. Despite the relatively high loss factors below 1000 Hz for modes with $n=0$, sound radiation due to these modes is expected to be small, because of a less effective excitation of these modes

(only due to plane waves in the pipe fluid and perhaps a very little contribution by quasi-longitudinal modes in the pipe wall[142]) compared to the excitation of modes with $n \geq 1$ (direct excitation of a large number of modes in the pipe wall). Therefore, for the pipe considered, sound radiation due to modes in the pipe wall becomes important from about 1000 Hz, which corresponds to the frequency at which the propagation velocity of first-order flexural waves equals the propagation velocity of sound in air.

IV.1.3 Acoustic coupling from an acoustic volume to a plate

The coupling loss factor representing the acoustic coupling from an acoustic volume o to a plate i can be derived from the coupling loss factor in the opposite direction, as defined in equation *(IV.2)*, and the modal densities of the acoustic volume[143] and the plate[144] by application of the 'reciprocity relationship'. This results in the following definition:

$$\eta_{oi} = \frac{\rho_o S_i f_{c,i} \sigma_i}{\dfrac{8 \pi f^3 m_i'' V_o'}{c_o^2} + \dfrac{2 \pi f^2 m_i'' S_o'}{2 c_o} + \dfrac{2 f m_i'' L_o'}{8}} \qquad (IV.3)$$

where $f_{c,i}$ represents the critical frequency.[145]

Several textbooks contain analytical expressions for the sound radiation efficiency of finite plates, see for example [ref 4], [ref 5], [ref 12], [ref 13].

---

[142] Quasi-longitudinal modes can radiate sound too. Compared to the sound radiation of flexural modes, the sound radiation of quasi-longitudinal modes is very small. This is due to the small amplitudes of quasi-longitudinal modes in the radial vibrational direction.

[143] The following relationship for the modal density of an acoustic volume o provided by Fahy [ref 9] has been applied in order to obtain equation *(IV.3)*:
$n_o = (4 \pi f^2 V_o'/c_o^3) + (\pi f S_o'/2 c_o^2) + (L_o'/8 c_o)$
where V_o', S_o' and L_o' are respectively the volume, the total surface area and the total length of all edges of the acoustic volume.

[144] Relationships for the modal density of thin plates are given in section 4.4.2.1. The following relationship for the modal density of a plate i [ref 4], [ref 5] has been applied in order to obtain equation *(IV.3)*:
$n_i = \pi S_i f_{c,i}/c_o^2$

[145] At the critical frequency the flexural wavelength in the structure and the wavelength in the ambient medium are equal. The critical frequency of a structure i can be written as [ref 12]
$f_{c,i} = c_o^2/(1,8 c_{l,i} h_i)$
where $c_{l,i}$ represents the propagation velocity of quasi-longitudinal waves in and h_i the thickness of the plate.

The formula[146] for the radiation efficiency from Lyon and DeJong [ref 4] has been applied in order to calculate coupling loss factors for the acoustic coupling from acoustic volumes to plates with equation *(IV.3)*. Only flexural modes within the structure are included (see footnote 142). The results are shown in Figure IV-3.
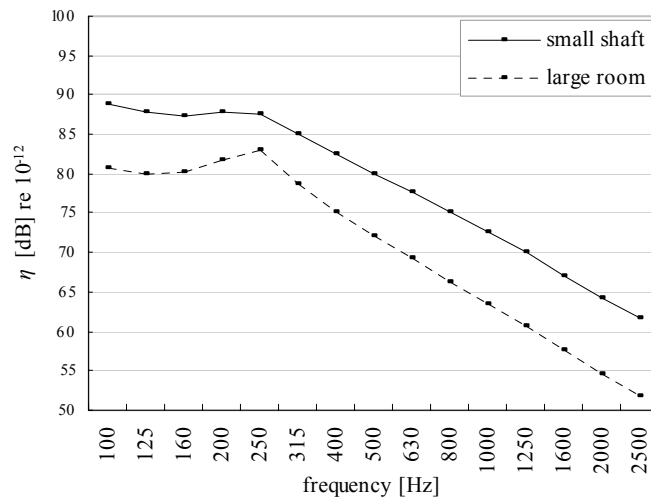
Figure IV-3 Coupling loss factors η for the acoustic coupling from an air-filled acoustic volume to a calcium-silicate plate (calculated values for centre frequencies of 1/3-octave bands are presented); **small shaft**, plate dimensions 0,5x3,4x0,1 m^3 and acoustic volume dimensions 0,5x0,3x3,4 m^3; **large room**, plate dimensions 4,4x3,4x0,1 m^3 and acoustic volume dimensions 4,4x3,4x3,4 m^3

Equation *(IV.3)* and Figure IV-3 illustrate that the modal properties of the acoustic volume determine the coupling loss factor from an acoustic volume to a plate, and therefore the energy flow between a pipe and a plate. The coupling loss factors for small shafts are higher than for large shafts. In addition, also the damping loss factors of pipe, plate and acoustic volume are of influence for the energy flow between a pipe and a plate. The damping loss factor of the acoustic volume is related to the reverberation time[147] and therefore to the room acoustic features of the acoustic volume. When the distance between

---

[146] This formula is a curve fit for the radiation efficiencies in three frequency ranges: below, at and above the critical frequency. The curve fit is valid for simply supported plates with uniform thickness and density, radiating into free space, and for the case of light fluid loading [ref 4]. Some clamping at real edges will increase the radiation efficiency below the critical frequency by a factor of 2 [ref 5].

[147] The damping loss factor η_{oo} of an acoustic volume o is given by [ref 4]:

$\eta_{oo} = 2,2/(fT_o)$

where T_o is the reverberation time of the acoustic volume.

a pipe and a plate is relatively large, i.e. at least 0,5 m to 1 m, the 'sub-model' could be applied to predict the energy flow due to acoustic coupling between pipes and plates. However, in building practice the distance between pipes and plates is so small that it is not clear to which extent the modal properties and room acoustic features of the acoustic volume are relevant. The 'sub-model' supposes a more or less uniform (i.e. diffuse) sound field in the acoustic volume and a more or less uniform (i.e. diffuse) excitation of the plate. This will not be valid for a pipe in a relatively large acoustic volume, and that is mounted closely to the plate. Then the plate is located in the direct sound field of the pipe. Modelling the pipe as a line source to the plate would probably be more correct. In that case the 'sub-model' is not applicable. Introduction of coupling loss factors that represent the acoustic coupling between pipe and plate without (specified) interaction of the acoustic volume, and with that a two subsystem 'sub-model'[148] would be more appropriate:

$$\Pi_{i,in} = 2\pi f \eta_{il} E_i + \sum_{\substack{j=1,3 \\ j \neq i}} 2\pi f (\eta_{ij} E_i - \eta_{ji} E_j)$$

$$i = 3 \qquad \Rightarrow \Pi_{i,in} = 0 \qquad\qquad (IV.4)$$

As illustrated in this section, it is difficult to predict the coupling loss factors and therefore energy flows between pipes and plates due to acoustic couplings properly.

In this thesis, structural coupling and acoustic coupling are characterized together by one coupling loss factor per transmission direction. In the experimental set-ups in this thesis, it has been determined that the contribution of acoustic coupling to the coupling loss factors for characteristic clamps is negligibly small (see sections 5.4.3 and 5.6.4).


IV.2   Acoustic coupling between different pipe system elements

Figure IV-4 illustrates the structural (red lines) and acoustic (green and grey lines) couplings between pipe system elements, for the example in Figure 3-1 in this thesis. Structural couplings are couplings of the pipe walls of different pipe system elements. Two types of acoustic couplings can be distinguished, either via the pipe fluid or/and via the ambient medium, i.e. a room or shaft.

---

[148] In equation *(IV.4)* the numbers of the subsystems correspond to the numbers in equation *(IV.1)* and in Figure IV-1. In this case subsystem *2* is not included in the 'sub-model'. Therefore, in equation *(IV.4)* subsystem *2* is lacking.
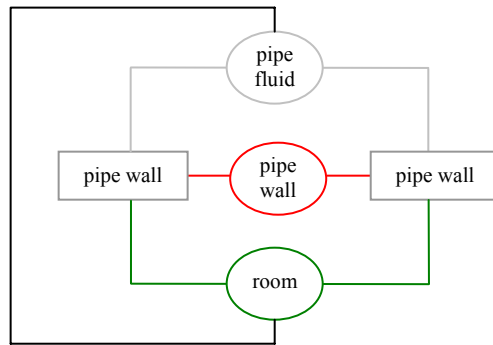
Figure IV-4 Structural and acoustic couplings between pipe system elements in Figure 3-1

A pipe system element is set into vibration due to a combination of structural and acoustic couplings or due to one of the two. The relative importance of structural and acoustic couplings depends on the dimensions and materials of the pipe system elements and their couplings, the characteristics of the ambient medium, e.g. free field or a small reverberant room, the type of pipe fluid, e.g. air or water, and on frequency[149].

In this thesis, structural coupling and acoustic coupling are characterized together by one coupling loss factor per transmission direction. In the experimental set-ups in this thesis, it has been determined that the contribution of acoustic coupling to the coupling loss factors for characteristic discontinuities is negligibly small (see sections 5.5.3 and 5.6.4).

---

[149] For example, for air-filled pipe system elements with relatively small diameters, which are coupled rigidly to each other, vibrational energy may be mainly transmitted via couplings of the pipe walls of the elements. For pipe system elements with relatively large diameters, water-filled pipe system elements and flexible couplings the transmission path via the pipe fluid, and possibly via the ambient medium, may be the most important one, particularly in case of small, reverberant shafts.

APPENDIX V

MEASUREMENT EQUIPMENT USED IN THIS STUDY

In this appendix, the measurement equipment used in this study is described.

In this study, the analysis of all measurements (except for decay times, see section 5.3) was done with an eight channel FFT analyser, type 2035 from Brüel & Kjær (B&K), with two 25 kHz input modules (each input module contains four channels), type 3023 from B&K (B&K Multichannel Analysis System, type 3350).

Measurements aimed at the determination of the point admittance of or input power to pipes were done with an impedance head (with spherical point contact to the pipe), type 8001 from B&K, mounted with a drive-rod (Ø 3,5 mm) on a shaker.

Measurements aimed at the determination of the point admittance of pipe system joints were done with an impedance hammer (with spherical point contact), type 8202 from B&K. The excitation force was detected by the force transducer (from B&K, type 8200) of the impedance hammer. Accelerations were detected with an accelerometer, type 4344 from B&K. The accelerometer was mounted with bees wax on the inner surface of the joint, on the opposite side from the excitation position.

Measurements aimed at the determination of the point admittance of or input power to plates were done either with an impedance hammer (see above) or with a force transducer (with spherical point contact to the plate), type 8200 from B&K, mounted with a drive-rod (Ø 3,5 mm) on a shaker. In both case accelerations were detected with an accelerometer, type 4370 from B&K. The accelerometer was mounted with a magnet on a 2 mm thick steel plate (Ø 23 mm), that was glued on the plate with cement glue, on the opposite side from the force transducer.

Measurements aimed at the determination of the vibrational energy of pipes were performed with accelerometers, type 4506 (3D-accelerometers) from B&K, that were powered by the analyser. The accelerometers were placed in matching holders from B&K, that were glued on small plastic elements that on their turn were glued on the pipe. The plastic elements had a straight side and a side following the curvature of the pipe.

Measurements aimed at the determination of the vibrational energy of plates were performed with accelerometers, type 4370 or type 4366 from B&K. The accelerometers

were mounted with magnets on 2 mm thick steel plates (Ø 23 mm) that were glued on the plate with cement glue.

During all measurements amplifiers, type 2626 from B&K for force signals, and type 2635 from B&K for acceleration signals (except for signals from 3D-accelerometers, see above) have been used.

Different shakers (type 4809 from B&K and an unknown fabricate) were used, in combination with precision noise generator, type 8057A from HP, and with different power amplifiers (type 2706 from B&K and type 2125 MB from MB Electronics respectively).

APPENDIX VI
# ACCURACY OF DETERMINATION METHODS FOR PARAMETERS

In this study, the accuracy of two determination methods for parameters has been investigated to some extent. The results are described in this appendix.

VI.1   Repeatability of damping and coupling loss factors obtained with PIM

This section gives some insight in the accuracy of the damping and coupling loss factors obtained with PIM in the first experimental set-up (see section 5.4). In section 5.4.2, it has been mentioned that the measurements have been done for two excitation positions and ten response positions on both the pipe and plate. In order to include possible differences in loss factors due to differences in installation of a pipe system, the pipe has been removed and replaced between the measurement series with the different excitation positions. By doing so, the possible influence of changes in the tightness of the clamp has been included, although it has to be mentioned that the pipe has been re-installed by the same person.
Figure VI-1 to Figure VI-4 show the loss factors obtained from the two measurement series. Also the mean values of the two series are shown (these values were also shown in Figure 5-11 in section 5.4.3).
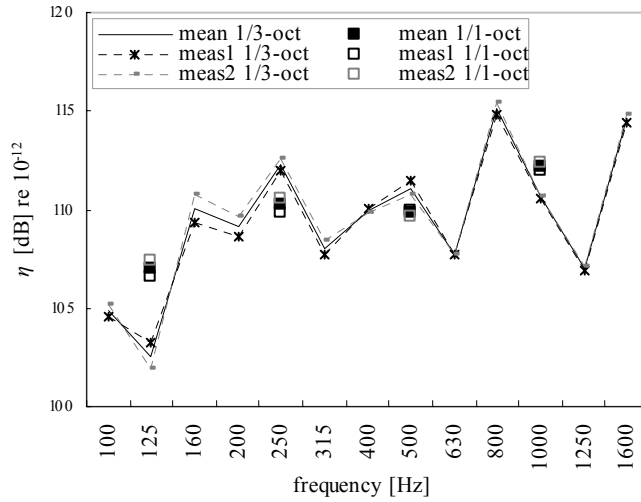
Figure VI-1 <u>Damping loss factors</u> η in (1/3-)octave bands for a <u>straight pipe</u> (subsystem *1*) determined with PIM in laboratory set-up 1. The values are determined from two measurement series with different excitation positions, respectively before after re-clamping the pipe on the plate. Also the averaged values of these two series are given.
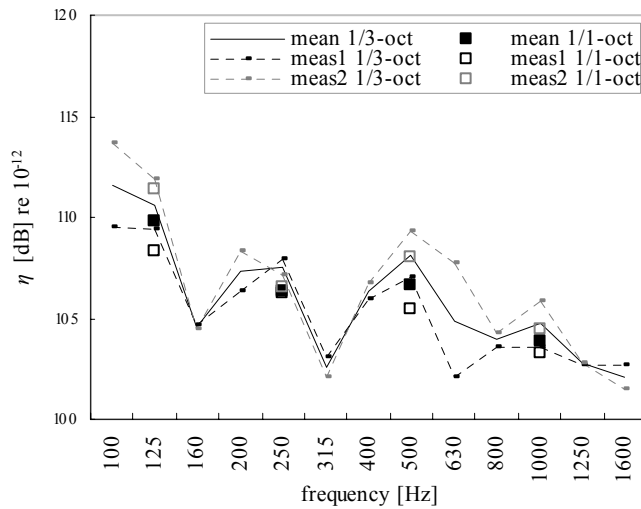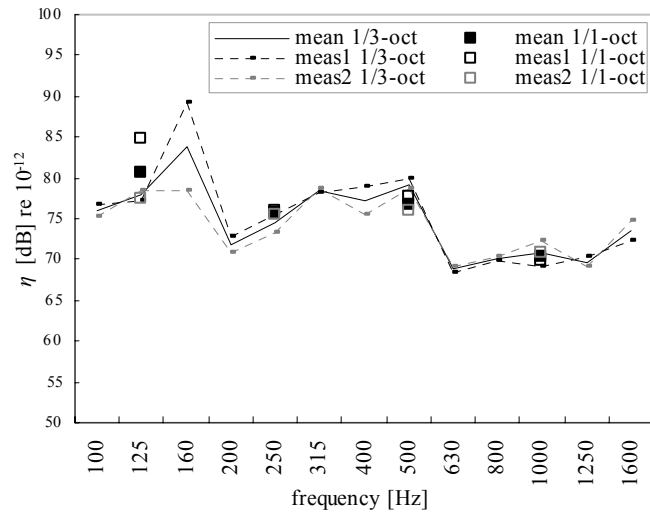

Figure VI-2 <u>Damping loss factors</u> η in (1/3-)octave bands for a <u>plate</u> (subsystem *2*) determined with PIM in laboratory set-up 1. The values are determined from two measurement series with different excitation positions, respectively before and after re-clamping the pipe on the plate. Also the averaged values of these two series are given.
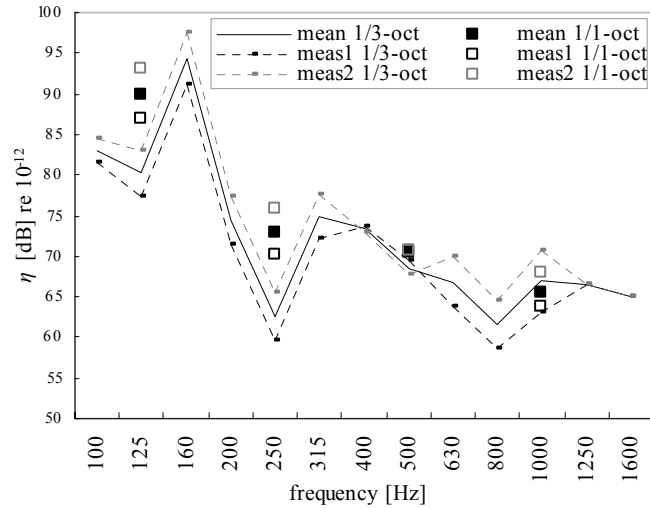
Figure VI-3 <u>Coupling loss factors</u> η in (1/3-)octave bands representing the <u>energy transmission from pipe</u> (subsystem *1*) <u>to plate</u> (subsystem *2*) via a pipe clamp, determined with PIM in laboratory set-up 1. The values are determined from two measurement series with different excitation positions, respectively before and after reclamping the pipe on the plate. Also the averaged values of these two series are given.

Figure VI-4 <u>Coupling loss factors</u> η in (1/3-)octave bands representing the <u>energy transmission from plate</u> (subsystem *2*) <u>to pipe</u> (subsystem *1*) via a pipe clamp, determined with PIM in laboratory set-up 1. The values are determined from two measurement series with different excitation positions, respectivly before and after reclamping the pipe on the plate. Also the averaged values of these two series are given.
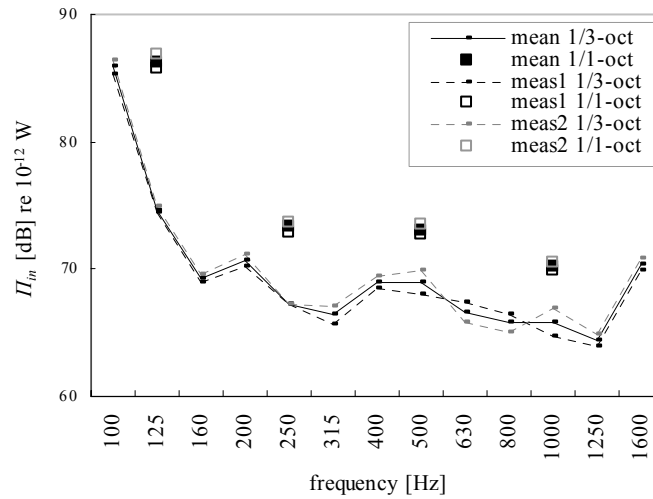
For octave bands, Figure VI-1 to Figure VI-4 generally show differences between the mean values and the values obtained from the two measurements of 1 dB at most for damping loss factors and of 3 dB at most for coupling loss factors. The results in 1/3-octave bands show larger differences. The repeatability of the applied determination method seems to be quite good, although averaging over more excitation positions might be desirable.

VI.2   Repeatability of maximum equivalent input powers

This section gives some insight in the accuracy of the maximum (max hold values per octave band, time constant 1 s) equivalent input powers for toilet flushing obtained in the third experimental set-up (see section 6.3). Two measurement series with toilet flushing have been done. In order to include possible differences in input powers due to differences in installation of a pipe system, the pipe system has been re-installed between the measurement series. By doing so, the possible influence of changes in the tightness of the clamp and in connecting pipe system parts has been included, although it has to be mentioned that the pipe system has been re-installed by the same person.

Figure VI-5 shows the maximum equivalent input powers obtained from the two measurement series. Also the mean values of the two series are shown (these values were also shown in Figure 6-2 in section 6.3.3).

Figure VI-5 Maximum equivalent input power Π_{in} in (1/3-)octave bands due to toilet flushing determined in laboratory set-up 3 from the responses of the middle vertical pipe (subsystem *2*). The values are determined from two measurement series, respectively before and after re-clamping the pipe on a plate. Also the averaged values of these two series are given.

For (1/3-)octave bands, Figure VI-5 shows differences between the mean values and the values obtained from the two measurements of 1 dB at most. The repeatability of the applied determination method seems to be very good, specifically considering the fact that it concerns a transient source. The good repeatability results are expected to follow directly from the fact that max hold values are applied for the source characterization.

REFERENCES

[ref 1]   Bouwbesluit, Ministerie van Volkshuisvesting, Ruimtelijke Ordening en Milieubeheer, 2003

[ref 2]   NPR 5075, Geluidwering in woongebouwen – Sanitaire toestellen en installaties voor de aan- en afvoer van water, Nederlands Normalisatie Instituut, 1991

[ref 3]   Inquiries noise annoyance

[ref 4]   Lyon, R.H. and R.G. DeJong, Theory and application of Statistical Energy Analysis, second edition, 1995

[ref 5]   Craik, R.J.M., Sound transmission through buildings using Statistical Energy Analysis, 1996

[ref 6]   Norton, M.P., Fundamentals of noise and vibration analysis for engineers, digital reprint, 2001 (first edition 1989)

[ref 7]   De Langhe, K., High frequency vibrations: contributions to experimental and computational SEA parameter identification techniques, PhD-thesis, Katholieke Universiteit Leuven (Belgium), 1996

[ref 8]   Hodges, C.H. and J. Woodhouse, Theories of noise and vibration in complex structures, Reports on Progress in Physics, 49, 107-70, 1986

[ref 9]   Fahy, F.J., Statistical energy analysis, chapter 7 in Noise and vibration, edited by R.G. White and J.G. Walker, Ellis Horwood, 1982

[ref 10] Fahy, F.J. and D. Yao, Power flow between non-conservatively coupled oscillators, Journal of Sound and Vibration, 114(1), pp. 1-11, 1987

[ref 11] Sun, J.C. and R.S. Ming, Distributive relationships of dissipated energy by coupling damping in non-conservatively coupled structures, Proceedings of Internoise 88, Avignon, France, pp. 323-326, 1988

[ref 12] Cremer, L. and M. Heckl, Structure-borne sound, translated and revised version by E.E. Ungar, 1988

[ref 13] Fahy, F.J., Sound and structural vibration – radiation, transmission and response, 1985

[ref 14] Leissa, A.W., Vibration of shells, second edition, 1993

[ref 15] Leissa, A.W., Vibration of plates, 1993

[ref 16] Fuller, C.R., The effects of wall discontinuities on the propagation of flexural waves in cylindrical shells, Journal of Sound and Vibration, 75(2), pp. 207-228, 1981

[ref 17] Fuller, C.R. and F.J. Fahy, Characteristics of wave propagation and energy distributions in cylindrical elastic shells filled with fluid, Journal of Sound and Vibration, 81(4), pp. 501-518, 1982

[ref 18] El-Raheb, M., Vibrations of three-dimensional pipe systems with acoustic coupling, Journal of Sound and Vibration, 78(1), pp. 39-67, 1981

[ref 19] Pavic, G., Vibrational energy flow in elastic circular cylindrical shells, Journal of Sound and Vibration, 142(2), pp. 293-310, 1990

[ref 20] Pavic, G., Vibroacoustical energy flow through straight pipes, Journal of Sound and Vibration, 154(3), pp. 411-429, 1992

[ref 21] Finnveden, S., Simplified equations of motion for the radial-axial vibrations of fluid filled pipes, Journal of Sound and Vibration, 208(5), pp. 685-703, 1997

[ref 22] Finnveden, S., Spectral Finite Element Analysis of the vibration of straight fluid-filled pipes with flanges, Journal of Sound and Vibration, 199(1), pp. 125-154, 1997

[ref 23] Finnveden, S., Formulas for modal density and for input power from mechanical and fluid point sources in fluid filled pipes, Journal of Sound and Vibration, 208(5), pp. 705-728, 1997

[ref 24] De Jong, C.A.F. and J.W. Verheij, Measurement of energy flow along pipes, Proceedings of the Second international congress on recent developments in air- and structure-borne sound and vibration, Auburn University, USA, March 4-6, pp. 577-584, 1992

[ref 25] De Jong, C.A.F., Analysis of pulsations and vibrations in fluid-filled pipe systems, PhD-thesis, Technische Universiteit Eindhoven and TNO Institute of Applied Physics (The Netherlands), 1994

[ref 26] Verheij, J.W., Multi-path sound transfer from resiliently mounted shipboard machinery, PhD-thesis, Technische Hogeschool Delft and Institute of Applied Physics TNO-TH (The Netherlands), 1982

278

[ref 27] Verheij, J.W., Measurements of structure-borne wave intensity on lightly damped pipes, Noise control engineering journal, pp. 69-76, September-October, 1990

[ref 28] Fulford, R.A. and B.M. Gibbs, Structure-borne sound power and source characterisation in multi-point-connected systems, part 1: case studies for assumed force distributions, Journal of Sound and Vibration, 204(4), pp. 659-677, 1997

[ref 29] Gibbs, B.M. and B.A.T. Petersson, Measurement and characterisation of sources of structure-borne sound, Proceedings of Internoise 96, Liverpool, pp. 1307-1311, 1996

[ref 30] Petersson, B.A.T. and B.M. Gibbs, Some common characteristics of multi-point and component structure-borne sound sources, Proceedings of Internoise 96, Liverpool, pp. 1319-1323, 1996

[ref 31] Gibbs, B.M., Machine bases as structure-borne sound sources, Proceedings of the Fifth international congress on sound and vibration, Adelaide, Australia, december 15-18, pp. 2359-2373, 1997

[ref 32] Janssens, M.H.A., C.M. Langeveld and J.W. Verheij, Theoretical and experimental study of a generalized pseudo-forces method for source characterization, Proceedings of the Fifth international congress on sound and vibration, Adelaide, Australia, december 15-18, pp. 1547-1553, 1997

[ref 33] Moorhouse, A.T., J.M. Mondot and B.M. Gibbs, Source descriptors for structure-borne sound sources, Proceedings of the Fifth international congress on sound and vibration, Adelaide, Australia, december 15-18, pp. 2449-2456, 1997

[ref 34] Sas, P. (editor), Advanced techniques in applied and numerical acoustics, Seminar notes of ISAAC8, Leuven, Belgium, 1997

[ref 35] EN 14366, Acoustics - Laboratory measurement of noise from wastewater installations, 2004

[ref 36] Vilquin, T., Vibration transmission through water supply systems to building construction - part 2: numerical simulation, Master's thesis, Université Catholique de Louvain (Belgium) and Technische Universiteit Eindhoven (The Netherlands), 1999

[ref 37] Swanson Analysis Systems, Ansys user's manual, version 5.0, 1994 and version 5.4 (internet), 1999

[ref 38] Bosmans, I., Analytical modelling of structure-borne sound transmission and modal interaction at complex plate junctions, PhD-thesis, Katholieke Universiteit Leuven (Belgium), 1998

[ref 39] Hopkins, C., Structure-borne sound transmission between coupled plates, PhD-thesis, 2000

[ref 40] Leppington, F.G., E.G. Broadbent and K.H. Heron, The acoustic radiation efficiency of rectangular panels, Proceedings of the Royal Society of London, A382, pp. 245-271, 1982

[ref 41] Maidanik, G., Response of ribbed panels to reverberant acoustic fields, Journal of the Acoustical Society of America, 34, pp. 809-826, 1962

[ref 42] Kuttruff, H., Room acoustics, 1979

[ref 43] Gerretsen, E., Admittantiemetingen aan een houten en een betonnen vloer – vergelijking van meet- en verwerkingsmethodieken, TPD-HAG-RPT-900093, TNO Institute of Applied Physics, 1990

[ref 44] Verheij, J.W., Inverse and reciprocity methods for machinery noise source characterization and sound path quantification, part 2: transmission paths, International Journal of Acoustics and Vibration, vol. 2, no. 3, pp. 103-112, 1997

[ref 45] ISO 10848, Acoustics – Laboratory measurement of the flanking transmission of airborne and impact noise between adjoining rooms, Part 1-4, 2005

[ref 46] Gerretsen, E., Industrielawaai in gebouwen – admittantie voor verschillende aanstootvormen, TPD-memo 741 nr. 1, TNO Institute of Applied Physics, 1975

[ref 47] Schroeder, M.R., New method of measuring reverberation time, Journal of the Acoustical Society of America, vol. 37, no. 3, pp. 409-412, 1965

[ref 48] Smith, P.W. Jr., Statistical models of coupled dynamical systems and the transition from weak to strong coupling, Journal of the Acoustical Society of America, 65, pp. 695-698, 1979

[ref 49] Newland, D.E., Calculation of power flow between coupled oscillators, Journal of Sound and Vibration, 3, pp. 262-276, 1966

[ref 50] Newland, D.E., Power flow between a class of coupled oscillators, Journal of the Acoustical Society of America, 43, pp. 553-559, 1968

[ref 51] Scheffer, W.J.H., Het ontwerpen van sanitaire installaties, 1990

[ref 52] Junger, M.C. and D. Feit, Sound, structures and their interaction, M.I.T. Press, 1972

[ref 53] Norton, M.P. and M.K. Bull, Mechanisms of the generation of external acoustic radiation from pipes due to internal flow disturbances, Journal of Sound and Vibration, 94(1), pp. 105-146, 1984

[ref 54] NEN 1070, Geluidwering in gebouwen – specificatie en beoordeling van de kwaliteit, 1999

[ref 55] Bobrovnitskii, Y.I., On the energy flow in evanescent waves, Journal of Sound and Vibration, 152(1), pp. 175-176, 1992

[ref 56] Bozich, W.F., The vibration and buckling characteristics of cylindrical shells under axial load and external pressure, AFFDL-TR-67-28, 1967

[ref 57] Hall, D.E., Basic acoustics, 1987

[ref 58] Leissa, A.W., The free vibration of rectangular plates, Journal of Sound and Vibration, 31(3), pp. 257-293, 1973

[ref 59] Bies, D.A. and S. Hamid, In-situ determination of loss and coupling loss factors by the power injection method, Journal of Sound and Vibration, 70(2), pp. 187-204, 1980

[ref 60] Clarkson, B.L. and R.J. Pope, Experimental determination of modal densities and loss factors of flat plates and cylinders, Journal of Sound and Vibration, 77(4), pp. 535-549, 1981

[ref 61] Brown, K.T. and M.P. Norton, Some comments on the experimental determination of modal densities and loss factors for statistical energy analysis, Journal of Sound and Vibration, 102(4), pp. 588-594, 1985

[ref 62] Norton, M.P. and R. Greenhalgh, On the estimation of loss factors in lightly damped pipeline systems: some measurement techniques and their limitations, Journal of Sound and Vibration, 105(3), pp. 397-423, 1986

[ref 63] Rennison, D.C. and M.K. Bull, On the modal density and damping of cylindrical pipes, Journal of Sound and Vibration, 54(1), pp. 39-53, 1977

[ref 64] Manning, J.E. and G. Maidanik, Radiation properties of cylindrical shells, Journal of the Acoustical Society of America, 36, pp. 1691-1698, 1964

[ref 65] Stimpson, G. and N. Lalor, Practical noise modeling of car body structures using energy flow analysis, Proceedings of Internoise 91, pp. 1233-1236, 1991

[ref 66] Brüel & Kjær, type 7841, copyright Acoustics Engineering, software module DIRAC 2.7 build 1356, 2002

[ref 67] Schroeder, M.R., Integrated impulse method measuring sound decay without impulses, Journal of the Acoustical Society of America, 66, pp. 497-500, 1979

[ref 68] Crocker, M.J. and A.J. Price, Damping in plates (Letter to the editor), Journal of Sound and Vibration, 9(3), pp. 501-505, 1969

[ref 69] Fahy, F.J., Reply to the letter to the editor "Damping in plates" by M.J. Crocker and A.J. Price, Journal of Sound and Vibration, 9(3), pp. 506-508, 1969

[ref 70] Ranky, M.F. and B.L Clarkson, Frequency average loss factors of plates and shells, Journal of Sound and Vibration, 89(3), pp. 309-323, 1983

[ref 71] Meier, A., Bestimmung von Schalldämm-Massen unter Berücksichtigung des Verlustfaktors, Proceedings of DAGA 98, Zürich, March 1998

[ref 72] Meier, A. and A. Schmitz, Application of total loss factor measurements for the determination of sound insulation, Building Acoustics, 6(2), pp. 71-84, 1999

[ref 73] Wijngaard, J., Parameters voor de akoestische modelvorming van een leidingsysteem voor sanitair – Met gebruikmaking van Statistical Energy Analysis en de Power Injection Method, Master's thesis, Technische Universiteit Eindhoven (The Netherlands), 2003

[ref 74] Persoon, S.A., Geluidvoortplanting door leidingsystemen – Experimenteel onderzoek, Master's thesis, Technische Universiteit Eindhoven (The Netherlands), 1999

[ref 75] Gerretsen, E., Constructiegeluid in gebouwen – Modelvorming in de bouwakoestiek, lecture notes, Technische Universiteit Eindhoven (The Netherlands), 2001 February

[ref 76] EN 12354, Building Acoustics – Estimation of acoustic performance of buildings from the performance of products – Part 1: Airborne sound insulation between rooms, 2000

[ref 77] EN 12354, Building Acoustics – Estimation of acoustic performance of buildings from the performance of products – Part 2: Impact sound insulation between rooms, 2000

[ref 78] ISO 3822, Acoustics, laboratory tests on noise emission from appliances and equipment used in water supply installations, 1999

[ref 79] Soedel, W., Vibrations of shells and plates, 1981

[ref 80] Fégeant, O., Vibratory Power Transmission to a Reinforced Cylindrical Shell Structure, Acta Acustica united with Acustica, Vol. 89 (2003), pp. 263-272, 2003

[ref 81] Brüel & Kjær, user's manual Multichannel Analysis System, type 3350

[ref 82] Langley, R.S., Mid and high-frequency vibration analysis of structures with uncertain properties, Proceedings of the Eleventh International Congress on Sound and Vibration, St. Petersburg, Russia, 5-8 July 2004, pp. 3-19, 2004

[ref 83] Fahy, F.J., An introduction to Statistical Energy Analysis, Seminar notes of ISAAC5, 1994

[ref 84] Möser, M., M. Heckl and K.-H. Ginters, Zur Schallausbreitung in flüssigkeitsgefüllten kreiszylindrischen Rohren, Acustica 60, pp. 34-44, 1986

[ref 85] Rindel, J.H., Dispersion and absorption of structure-borne sound in acoustically thick plates, Applied Acoustics, 41, pp. 97-111, 1994

[ref 86] Mindlin, R.D., Influence of rotatory inertia and shear on flexural motion of isotropic, elastic plates, Journal of Applied Mechanics, pp. 31-38, 1951

[ref 87] Koopman, A., Martin, H.J. and C.M.J. Siebesma, Characterization of structure-borne sound sources in dwellings, Proceedings of Internoise 94, Yokohama (Japan), pp. 637-640, 1994

[ref 88] Koopman, A., Characterization of structure-borne sound sources by classification and equivalence, Proceedings of Internoise 96, Liverpool, pp. 1331-1334, 1996

[ref 89] Gerretsen, E., Development and use of prediction models in building acoustics as in EN 12354, Proceedings of Forum Acusticum Budapest, 2005

[ref 90] Alber, T.H., Fischer, H.-M. and B. Gibbs, Approach to describe valves as sound sources for fluid- and structure-borne sound, Proceedings of Forum Acusticum Budapest, 2005

[ref 91] Späh, M.M., Fischer, H.-M. and B. Gibbs, New laboratory for the measurement of structure-borne sound power of sanitary installations, Proceedings of Forum Acusticum Budapest, 2005

[ref 92] prEN 12354-5, Building Acoustics – Estimation of acoustic performance of buildings from the performance of elements – Part 5: Sound levels due to service equipment, 2005 September

[ref 93] Villot, M. and C. Guigou-Carter, Laboratory characterization and field prediction of whirlpool bath noise, Proceedings of Forum Acusticum Budapest, 2005

[ref 94] Qi, N. and B. Gibbs, Structure-borne power from machines in buildings: Prediction of installed power from laboratory measurements, Proceedings of Forum Acusticum Budapest, 2005

[ref 95] Scholl, W., About a test facility for installation noise in wooden houses, Proceedings of Forum Acusticum Budapest, 2005

THANKS

This work is finished!

While looking back to a period in which I have learned so much, about acoustics, about time management (or not?), about taking decisions and about people (including myself), I want to thank everyone who contributed to the completion of this thesis, in particular:

Eddy Gerretsen and Heiko Martin,
for your supervision, for your enthusiastic support, for giving me complete freedom in this research and for never having doubts about my ability to finish this work

Barry Gibbs, Gerrit Vermeir and Martin de Wit,
for taking the time to read this thesis and giving your approval

Jan Verheij,
for your valuable comments on draft versions of this thesis

Sara Persoon, Welmoed Siebesma, Thomas Vilquin, and Jan Wijngaard,
the students who participated in this project, for your contribution to this work

Constant Hak, Raymond Jöris, Jan van de Kerkhof, Frans-Karel van Wely (†) and the students working in "HET LAB" during the years I spent there,
for assisting with my experiments, for the discussions about everything except this work, for the fun and for the coffee

Renz van Luxemburg,
for your support, for arranging the combination of this research with working at TNO and for being a very pleasant and inspiring colleague

TNO, especially Eddy Gerretsen, Aart de Geus, Arnold Koopman, Ger Kusters, Geert-Jan van Oosterhout, Cor Pernot and Marcel van Vliet,
for your support, related to this study and/or to my work at TNO

Truus,	Maarten,	Patricia,
for 'picking a date'	for your support	for your special
to finish this work	by email	attention by phone

Anneke, Juul, Pieter and Juliette,
for always believing in me and telling me so

Paul,
for being there and for putting things into perspective

Time to travel further …

CURRICULUM VITAE

Susanne Bron-van der Jagt

November 19, 1970   Born in Wageningen, The Netherlands

1983 - 1989   Education at pre-university level (Gymnasium β)
Final examination in June 1989

1989 - 1995   Study at the faculty of Architecture, Building and Planning of Technische Universiteit Eindhoven
Specialisation in building physics
Master's thesis on prediction and measurement of direct and flanking sound transmission in residential buildings
Graduation in June 1995

1995 - 1996   Consultant in the fields of building physics, acoustics and fire safety at Cauberg-Huygen

1996 - 2002   PhD student (part-time, research on the topic of the present thesis), in the group of Building Physics and Systems of the faculty of Architecture, Building and Planning of Technische Universiteit Eindhoven
Various (scientific) articles and contributions to conferences on the topic of the present thesis

1996 - now   Researcher and consultant in the field of sound and vibration (especially building acoustics) at TNO (Netherlands Organisation for Applied Scientific Research)
Various (scientific) articles and contributions to conferences and seminars related to modelling and experimental work on (flanking) sound transmission through lightweight building structures